Advanced Modeling and Simulation of Integrated Gasification Combined Cycle Power Plants with CO_2-capture

Von der Fakultät für Maschinenbau, Verfahrens- und Energietechnik

der Technischen Universität Bergakademie Freiberg

genehmigte

Dissertation

zur Erlangung des akademischen Grades

Doktor-Ingenieur

(Dr.-Ing)

vorgelegt

von Dipl.-Ing. Mathias Rieger

geboren am 23.04.1978 in Hoyerswerda

Gutachter: Prof. Dr.-Ing. Bernd Meyer, Freiberg

Prof. Dr.-Ing. Michael Beckmann, Dresden

Tag der Verleihung: 17.04.2014

Versicherung

Hiermit versichere ich, dass ich die vorliegende Arbeit ohne unzulässige Hilfe Dritter und ohne Benutzung anderer als der angegebenen Hilfsmittel angefertigt habe; die aus fremden Quellen direkt oder indirekt übernommenen Gedanken sind als solche kenntlich gemacht.

Bei der Auswahl und Auswertung des Materials sowie bei der Herstellung des Manuskripts habe ich Unterstützungsleistungen von folgenden Personen erhalten:

Prof. Dr.-Ing Bernd Meyer (Betreuer)

Dr. Ing. Karsten Riedl (Berechnung der GuD-Investitionskosten; Appendix I5)

Weitere Personen waren an der Abfassung der vorliegenden Arbeit nicht beteiligt. Die Hilfe eines Promotionsberaters habe ich nicht in Anspruch genommen. Weitere Personen haben von mir keine geldwerten Leistungen für Arbeiten erhalten, die nicht als solche kenntlich gemacht worden sind.

Die Arbeit wurde bisher weder im Inland noch im Ausland in gleicher oder ähnlicher Form einer anderen Prüfungsbehörde vorgelegt.

Ort, Datum Dipl.-Ing. Mathias Rieger

Danksagung

An dieser Stelle möchte ich all denen danken, die mich auf vielfältige Weise während meiner Zeit am Institut für Energieverfahrenstechnik- und Chemieingenieurwesen der TU Bergakademie Freiberg unterstützten.

Besonders danken möchte ich Herrn Prof. Dr.-Ing. Bernd Meyer für die Betreuung meiner Dissertation. Das in mich und meine Arbeitsweise gesetzte Vertrauen sowie die fortwährende Unterstützung bei der Bewältigung neuer Herausforderungen haben meine persönliche und berufliche Entwicklung äußerst positiv beeinflusst.

Herrn Prof. Dr.-Ing. Michael Beckmann danke ich für die Übernahme des Zweitgutachtens.

Meinen ehemaligen Arbeitskollegen Hardy Rauchfuß, Robert Pardemann und Martin Gräbner danke ich für wertvolle Hinweise und die jederzeit kollegiale und freundschaftliche Zusammenarbeit.

Meinen lieben Eltern danke ich für die immerwährende und selbstlose Unterstützung. Die Leistung meiner Eltern kann nicht mit Dankesworten aufgewogen werden – sie wird mir bestes Beispiel sein, für die Erziehung unserer eigenen Kinder.

Meiner lieben Ehefrau Franziska danke ich für die vielfältige Unterstützung, das Verständnis für meine Arbeit und nicht zuletzt ihre Geduld mit mir.

Table of contents

List of figures

List of tables

List of abbreviations

AGR	Acid gas removal
$A_{heating\ surface}$	Heat transfer area of the HRSG heating surfaces
ASU	Air separation unit
BFW	Boiler feed water
C	Carbon content (ultimate analysis)
CapEx	Capital expenditures
CC-IGCC	IGCC with Carbon Capture
CCPP	Combined cycle power plant
CCR	Carbon conversion ratio
Cl	Chlorine content (ultimate analysis)
CO	Carbon monoxide
CO_2	Carbon dioxide
CoE	Cost of electricity
$CoE_{CC\text{-}IGCC}$	Cost of electricity for a CC-IGCC (including the costs of CO_2-avoidance)
CoE_{conv}	Cost of electricity for a conventional steam power plant (including the costs of CO_2-avoidance)
COORIVA	Project name for the federal funded German research project investigating CO_2-reduction through integrated gasification and capture
CoP	ConocoPhillips
COP	Coefficient of performance for the refrigeration plant at the AGR
COS	Carbonyl sulfide
CO-shift	Carbon monoxide conversion
c_p	Specific heat capacity

CPRH	Condensate preheater
CRR	Carbon retention rate
CSC	Convective syngas cooler
DGAN	Diluent gaseous nitrogen
$\Delta H_{25°C}$	Standard enthalpy of reaction
Δp_{comb}	Pressure loss due to the gas turbines combustion chamber
Δp_{comb}	Pressure loss due to the gas turbines combustion chamber at reference (design) conditions
Δt_m	Mean logarithmic temperature difference
Eco	Economizer
EPRI	Electric Power Research Institute
$\dot{e}_{H_2O}$	Specific exergy flow of the wet gas
$\dot{E}_{chem}$	Chemical exergy flow
$\dot{E}_{coal}$	Exergy flow the coal
$\dot{e}_{dry}$	Specific exergy flow of the dry gas
$\dot{E}_{overall}$	Overall exergy flow
$\dot{E}_{thm}$	Thermomechanical exergy flow
GAN	Gaseous nitrogen
GE	General Electric
GE-Q	GE gasifier with full water quench
GE-R	GE gasifier with radiant cooler and water quench
GE-RC	GE gasifier with radiant cooler and convective syngas cooler
GOX	Gaseous oxygen
GSP	Gaskombinat Schwarze Pumpe
H	Hydrogen content (ultimate analysis)

h	Specific enthalpy
h_0	Specific enthalpy at reference state
H_2	Hydrogen
H_2S	Hydrogen sulfide
HCL	Hydrogen chloride
HCN	Hydrogen cyanide
HHV	Higher heating value
HP GAN	High pressure gaseous nitrogen
HP	High pressure
HP-BFW	High pressure boiler feed water
HPC	High pressure column
HP-steam	High pressure steam
HRSG	Heat recovery steam generator
η	Electrical efficiency (net)
$\eta_{ex,gasifier}$	Exergetic efficiency of the coal gasifier
IEA	International Energy Agency
IGCC	Integrated Gasification Combined Cycle
IP- BFW	Intermediate pressure boiler feed water
IP	Intermediate pressure
IP-steam	Intermediate pressure steam
k	Heat transfer coefficient
$K_{ASU,air}$	Specific air integration
$K_{ASU,DGAN}$	Specific DGAN demand
$K_{ASU,HP\ GAN}$	Specific HP GAN demand
$K_{ASU,LP\ GAN}$	Specific LP GAN demand
$L_{air,int}$	Level of air integration

LHV	Lower heating value
LHV_{coal}	Lower heating value of coal
LP- BFW	Low pressure boiler feed water
LP GAN	Low pressure gaseous nitrogen
LP	Low pressure
LPC	Low pressure column
LP-steam	Low pressure steam
MAC	Main air compressor (of the ASU)
MeOH	Methanol
MHE	Main heat exchanger
MIT	Massachusetts Institute of Technology
$\dot{m}$	Mass flow rate
$\dot{m}_{H_2O}$	Mass flow rate of the wet gas
$\dot{m}_{coal}$	Mass flow rate of coal
$\dot{m}_{compr,ref.}$	Compressor mass flow at reference (design) conditions
$\dot{m}_{compr}$	Compressor mass flow
N	Nitrogen content (ultimate analysis)
N_2	Nitrogen
NETL	National Energy Technology Laboratory
NH_3	Ammonia
NOx	Nitrogen oxides
$\dot{n}$	Molar flow rate
$\dot{n}_{H_2}$	Molar flow of H_2 in the raw gas at the interface between gasifier and CO-shift
$\dot{n}_{H_2O}$	Molar flow of H_2O in the raw gas at the interface between gasifier and CO-shift

$\dot{n}_{carbon,coal}$	Molar flow rate of carbon (coal input)
$\dot{n}_{carbon,unconverted}$	Molar flow rate of unconverted carbon (gasifier output)
$\dot{n}_{CO,converted\ gas}$	Molar flow rate of carbon monoxide in the converted gas (downstream CO-shift)
$\dot{n}_{CO,raw\ gas}$	Molar flow rate of carbon monoxide in the raw gas (upstream CO-shift)
$\dot{n}_{CO}$	Molar flow of CO in the raw gas at the interface between gasifier and CO-shift
$\dot{n}_{dry}$	Molar flow rate of the dry gas
O	Oxygen content (ultimate analysis)
OPC	Overall project costs
OpEx	Operational expenditures
p	Pressure
p_0	Pressure at reference state
$P_{el,aux}$	Electrical auxiliary load
$P_{ASU,aux}$	Electrical auxiliary load for the ASU
$P_{ASU,spec}$	Specific electrical auxiliary load for the ASU
$P_{aux,AGR/SRU/TGT}$	Total electrical auxiliary load for the AGR, the SRU and the TGT process
$P_{aux,CO2-compression}$	Electrical auxiliary load for the CO_2-compressor
$P_{aux,refrigaration\ plant}$	Electrical auxiliary load for the refrigeration plant (AGR)
$P_{gas\ turbine,ref.}$	Gas turbine power output (gross) at reference (design) conditions
$P_{gas\ turbine}$	Gas turbine power output (gross)
$p_{reactor}$	Pressure in the gasification reactor

PRENFLO	Pressurized entrained flow
π_{turb}	Pressure ratio of the gas turbines turbine section
$\pi_{turb,ref}$	Pressure ratio of the gas turbines turbine section at reference (design) conditions
$\dot{Q}$	Heat flow
$Q_{cooling\ screen}$	Heat flow through the gasifiers cooling screen
$\dot{Q}_{coal,LHV}$	Heat flow of coal based on the LHV
$\dot{Q}_{evaporator,refrigeration\ plant}$	Heat flow at the evaporator of the refrigeration plant (AGR)
R	Universal gas constant
RC	Radiant cooler
s	Specific entropy
S	Sulfur
s_0	Specific entropy at reference state
SCGP	Shell Coal Gasification Process
$Slurry_{H2O\ frac}$	Water faction within the coal/water slurry
SO_2	Sulfur dioxide
SRU	Sulfur recovery unit
$\Sigma\ \dot{E}_{effort}$	Sum of exergy efforts
$\Sigma\ \dot{E}_{loss}$	Sum of exergy losses
t	Temperature
t_0	Temperature at reference state
$t_{blade,ref.}$	Blade (surface) temperature at reference (design) conditions
t_{blade}	Blade (surface) temperature
TGT	Tail gas treatment

$t_{hot\ gas,ref.}$	Hot gas temperature before cooling air admixture at reference (design) conditions
$t_{hot\ gas}$	Hot gas temperature before cooling air admixture
TIT	Turbine inlet temperature
$TIT_{ref.}$	Turbine inlet temperature at reference (design) conditions
$t_{reactor}$	Temperature in the gasification reactor
$V_{exhaust\ gas}$	Volumetric flow of exhaust gas that is not fed to the gasification reactor
$V_{HP\ GAN}$	Volumetric flow of HP GAN
$V_{LP\ GAN}$	Volumetric flow of LP GAN
$\dot{V}_{H_2+CO}$	Volumetric flow of H_2 and CO
$\dot{V}_{air,ASU}$	Air demand (volumetric flow) of the ASU
$\dot{V}_{DGAN}$	Demand of DGAN (volumetric flow)
$\dot{V}_{GOX}$	Volumetric flow of GOX
$\dot{V}_{GOX}$	Volumetric flow of GOX produced by the ASU
$\dot{V}_{GT\ extr.air}$	Volumetric flow of extraction air from the gas turbine
$\dot{V}_{HP\ GAN}$	Demand of HP GAN (volumetric flow)
$\dot{V}_{LP\ GAN}$	Demand of LP GAN (volumetric flow)

1 Motivation and objective

Integrated Gasification Combined Cycle (IGCC) power plants with CO_2-capture are widely expected as the silver bullet towards CO_2-lean power generation and the combined chemical and energetic utilization of fossil fuels [24; 34; 52].

Despite of often published thermodynamic benefits (higher efficiency than conventional pulverized coal fired power plants) and technological advantages (almost zero-emission of carbon dioxide, particles and mercury-, sulfur-, chlorine- or bromine compounds, etc.) IGCC could not yet be established on the power generation market.

Nevertheless, IGCC power plants with Carbon Capture (CC-IGCC) offer a promising alternative for a considerable reduction of greenhouse gas emissions.

The complex correlations within and between the individual sub-processes and their impact on plant operation, performance and economics are so far inadequately described and partially misunderstood or even underestimated.

A lot of international studies do not show more than an assembly of calculation results with a superficial description of individual sub-processes and for the most part an overall concept optimization is missing.

The objective of this thesis is an extensive description of the correlations in some of the most crucial sub-processes for hard coal fired CC-IGCC and their influence on overall plant operation, performance and economics.

The development and description of simulation models for CC-IGCC sub-processes will clarify the most important coherences. The generated findings point out thermodynamic and economic potentials as well as operational limits and therefore provide the basis for future concept optimization and engineering development directions.

The derived conclusions and evaluations are helpful and necessary both for engineering companies and electric utilities either for technological and operational purposes or for investment and strategy decisions.

2 Literature survey

Fossil fuels and especially coals are broadly anticipated to play a dominant role within the future power generation market worldwide [3; 30]. CO_2-emmissions that are inherently connected with conventional coal usage and their potential influence on the global climate are the key factor for the development of coal based CO_2-lean power generation concepts. In this context CC-IGCC power plants are considered to be a promising alternative.

A great number of international studies investigated the expected IGCC-performance and IGCC-economics. The objective of the present literature survey is the analysis and assessment of study results for CC-IGCC.

2.1 Plant performance and economics of CC-IGCC

Performance data for CC-IGCC concepts are extracted from Holt (2000) [24], Holt (2002) [25], Chen and Rubin [6], Chiesa et al. [7], Cormos [8], Descamps et al. [9], Gräbner et al. [20], Huang et al. [29], IEA [31], Katzer [34], Klara and Plunkett [36], Kunze and Spliethoff [39], Martelli et al. [43] and NETL (2002-2010) [45-47].

Fig. 1 shows the efficiency of the investigated IGCC-concepts allocated to four industrial coal gasifier types as there are:

- The Shell Coal Gasification Process (SCGP),
- The Siemens gasifier,
- The ConocoPillips (CoP) gasifier and
- The General Electric (GE) gasifier.

The latter type is commercially available in three configurations:

- With full water quench (GE-Q),
- With radiant cooler and convective syngas cooler (GE-RC) and
- With radiant cooler and water quench (GE-R).

Referring to this, distinctions are also made in the figure.

Moreover, Fig. 1 provides some information about the coal-feedstock for which the different IGCC-concepts have been developed. These coals can all be classified as bituminous. The coal moisture content varies between 5 and 13 % and the lower heating value between 25 and 30 MJ/kg. Therefore the concepts are comparable.

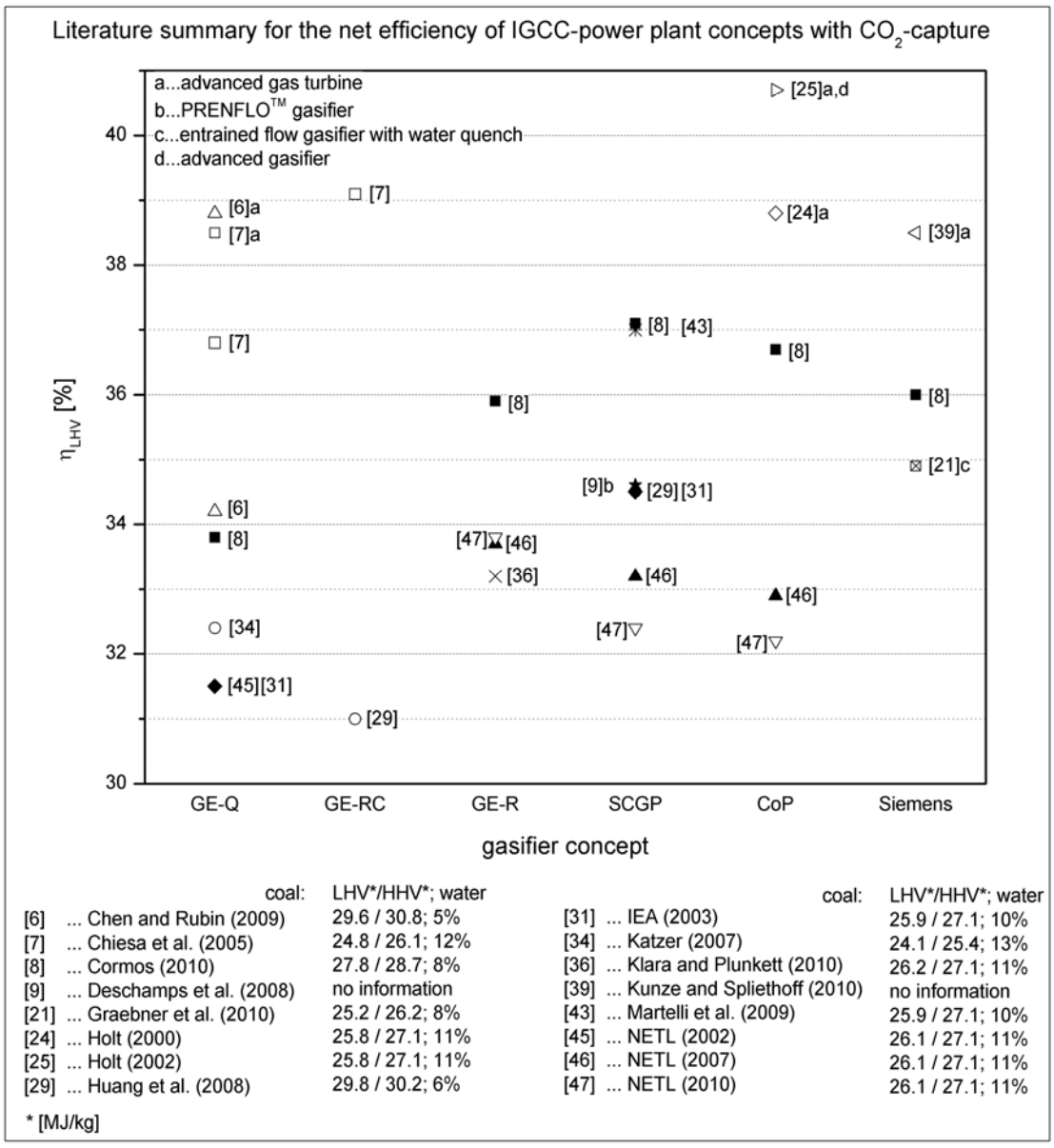

		coal:	LHV*/HHV*; water
[6]	... Chen and Rubin (2009)		29.6 / 30.8; 5%
[7]	... Chiesa et al. (2005)		24.8 / 26.1; 12%
[8]	... Cormos (2010)		27.8 / 28.7; 8%
[9]	... Deschamps et al. (2008)		no information
[21]	... Graebner et al. (2010)		25.2 / 26.2; 8%
[24]	... Holt (2000)		25.8 / 27.1; 11%
[25]	... Holt (2002)		25.8 / 27.1; 11%
[29]	... Huang et al. (2008)		29.8 / 30.2; 6%
[31]	... IEA (2003)		25.9 / 27.1; 10%
[34]	... Katzer (2007)		24.1 / 25.4; 13%
[36]	... Klara and Plunkett (2010)		26.2 / 27.1; 11%
[39]	... Kunze and Spliethoff (2010)		no information
[43]	... Martelli et al. (2009)		25.9 / 27.1; 10%
[45]	... NETL (2002)		26.1 / 27.1; 11%
[46]	... NETL (2007)		26.1 / 27.1; 11%
[47]	... NETL (2010)		26.1 / 27.1; 11%

* [MJ/kg]

Fig. 1 Literature summary for the net efficiency of IGCC-power plant concepts with CO_2-capture

As it can be seen in Fig. 1 there is a high fluctuation for the expected net efficiency even for IGCC-concepts with the same gasifier type.

For a few selected studies, Table 1 provides some explanation where the observed performance differences arise from.

Table 1 Major differences between some selected studies

study	Chiesa et al. [7]	Huang et al. [29]	Cormos [8]	NETL(2010) [47]
Gasifier type	GE-RC	GE-RC	CoP	CoP
Gas turbine power [MW]	294	286	334	2 x 232
IGCC Gross output [MW]	503	523	528	704
Auxiliary load [MW]	120	129	115	190
IGCC Net output [MW]	383	394	414	514
Coal Input [MW (LHV-based)]	978	1271	1127	1577
IGCC Gross efficiency [% (LHV based)]	51.4	41.2	46.9	44.6
IGCC Net efficiency [% (LHV based)]	39.1	31.0	36.7	32.6
Gas turbine efficiency [%] a)	39	39	39	39
Gas turbine fuel [MW] b)	753	733	856	2 x 595
Efficiency of fuel gas generation [MW] c)	77	58	76	75

a) assumed gas turbine efficiency

b) calculated as follows: Gas turbine power / Assumed gas turbine efficiency

c) calculated as follows: Gas turbine fuel / Coal input

By comparing the study results of Chiesa et al. [7] and Huang et al. [29], both investigating an almost identical IGCC-concept based on the GE-RC, the following can be noted: Although the gas turbine power output and the selected technologies are approximately the same, the efficiency of the gas generation part (conversion of coal to gas turbine fuel) differs by about 20 %-points when for both concepts the

same gas turbine efficiency is assumed. This fact indicates that both studies use greatly different modeling assumptions for the gas generation part.

In contrast, the studies conducted by Cormos [8] and NETL (2010) [47], both investigating an IGCC-concept based on the CoP gasifier, seem to use almost the same modeling assumptions for it (as there is no big difference at the efficiency of the gas generation part). However, the net-performance difference of about 4 %-points is due to disparities at the auxiliary load calculation and at the chosen gas turbine class (F-class and G-class).

With respect to a comparison of all four major gasifier types, only the study conducted by Cormos [8] can be considered. Therein CC-IGCC concepts are investigated for all mentioned gasifiers on a common basis, so that a realistic technology comparison can be conducted. According to this study, the highest net efficiency can be achieved using the SCGP followed by the CoP gasifier: However, a fairly high difference to the absolute performance data provided by the engineering based studies as for instance IEA [31], Gräbner et al. [20] or the NETL-studies [45-47] is noted. Moreover, the mentioned NETL-studies identify an IGCC-concept based on the GE-R as superior to a concept with CoP gasifier or SCGP.

The economic analysis of CC-IGCC concepts (Table 2) shows a quite diverse pattern.

Table 2 Literature summary for the cost of electricity of CC-IGCC

Gasifier type	Cost of electricity (CoE)	Published	Reference
GE-Q	60 $/MWh	2002	[45]
GE-Q	56 €/MWh	2003	[31]
GE-Q	96 $/MWh	2009	[6]
GE-RC	69 $/MWh	2008	[29]
GE-R	103 $/MWh	2007	[46]
GE-R	106 $/MWh	2010	[36]
GE-R	106 $/MWh	2010	[47]
SCGP	63 €/MWh	2003	[31]
SCGP	110 $/MWh	2007	[46]
SCGP	68 $/MWh	2008	[29]
SCGP	97 $/MWh	2009	[43]
SCGP	119 $/MWh	2010	[47]
CoP	56 $/MWh	2000	[24]
CoP	106 $/MWh	2007	[46]
CoP	110 $/MWh	2010	[47]

As shown in Table 2, the cost of electricity (CoE) for a CC-IGCC was assumed to be in the range of about 60 $/MWh in the years between 2000 and 2003. At the end of this decade, the CoE was almost doubled up to more than 105 $/MWh.

For example, the CoE for a CC-IGCC based on the CoP gasifier varies greatly from 56 $/MWh [24] in the year 2000 to 110 $/MWh [47] ten years later.

This increase is mainly caused by three facts, which can be illustrated by a comparison of the two last-mentioned studies (in each case for the IGCC based on the CoP gasifier):

1. The tremendous rise of capital costs of more than 140 %
2. The increase of fuel cost by about 30 %
3. The reduction of the expected net efficiency by about 8 %-points

2.2 Optimization approaches for IGCC

Most of the optimization approaches for IGCC-concepts were focused on the investigation of the integration influence between the gas turbine and the air separation unit (ASU). The technological need for ASU-integration is described in detail by Smith [57] or Farina and Bressan [13].

In general, it has to be distinguished between air- and nitrogen integration. The level of air integration stands for the amount of gas turbine extraction air in relation to the air demand of the ASU. A level of 50 % means that half of the ASUs air demand is extracted as compressed air out of the gas turbine. The remaining 50 % have to be compressed by the main air compressor (MAC) of the ASU. The nitrogen that is generated at the ASU can be admixed to the hydrogen rich gas for the purpose of NOx-reduction and to stabilize combustion. Hence, the amount of admixed nitrogen in relation to the produced nitrogen flow is expressed by the level of nitrogen integration.

Fig. 2 summarizes the relative efficiency for IGCC-concepts dependent on the level of air integration for different nitrogen integration rates.

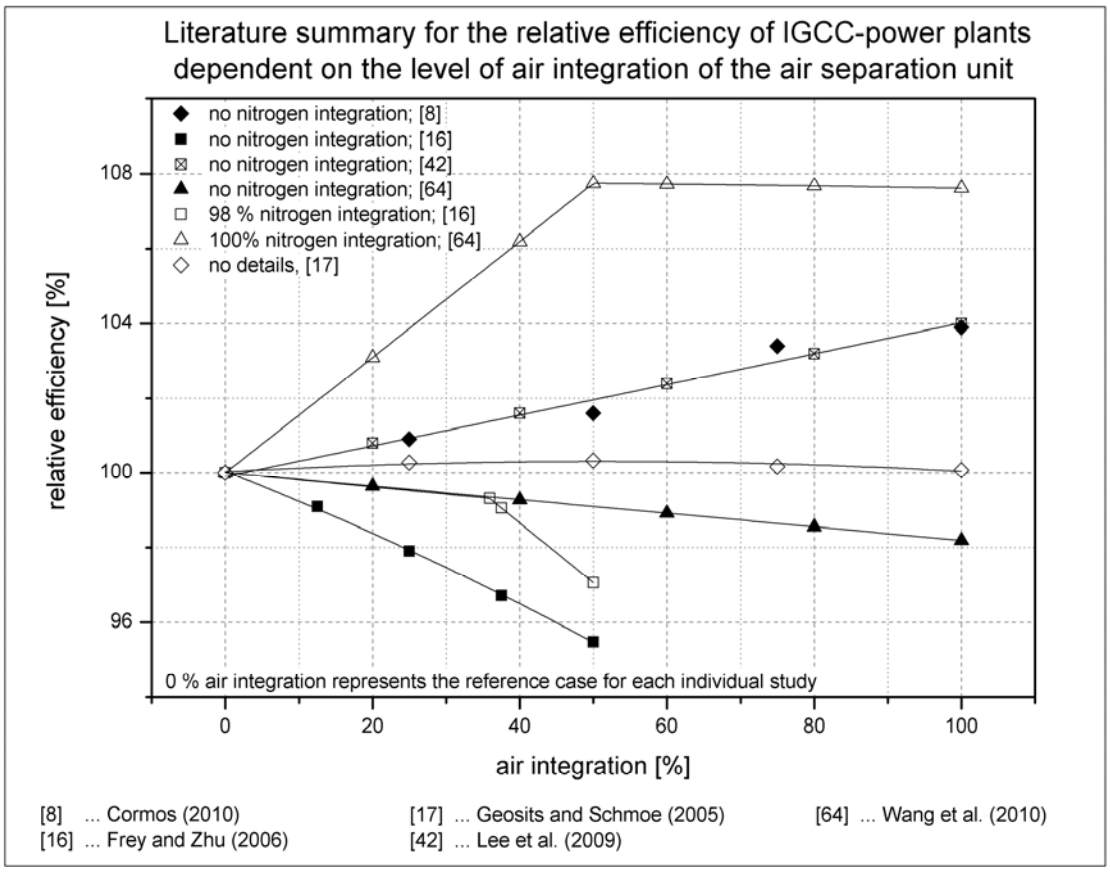

Fig. 2 Literature summary for the relative efficiency of IGCC-power plants dependent on the level of air integration of the air separation unit

Each of the considered studies gives a clear statement concerning the relation between the efficiency and the level of air integration. However, taken a general view (Fig. 2), these results are partly opposed to each other. Therefore, some of the studies shall be analyzed in more detail:

1. <u>Different air-integration ratios; cases without nitrogen integration</u>

   Frey and Zhu [16] and Wang et al. [64] for instance conclude that the maximum IGCC-efficiency appears at zero air integration and falls at increasing air extraction rates. The gradient of the relative efficiency is in both cases almost linear, but with a quite different slope.

   Frey and Zhu [16] investigated different integration options for an IGCC without carbon capture, based on the GE-RC. At decreasing air extraction rates, the compressor inlet flow of the gas turbine was reduced in order to keep the turbines exhaust gas flow constant. For the ASU, two different pressure levels (5 bar and 10-15 bar) were investigated. The highest IGCC-efficiencies were

always achieved with the low pressure ASU. It was found that air compression in the MAC is more efficient than in the gas turbines compressor since the latter requires air expansion down to the ASUs operating pressure.

The study conducted by Wang et al. [64] almost used the same approach, but only a low-pressure ASU and not a high-pressure ASU was considered. External air compression in the MAC was also found more efficient than in the gas turbine compressor; however the differences between full and zero air integration were not as broad as found by Frey and Zhu [16].

In contrast to the above summarized articles, Cormos [8] for example published directly opposed characteristics. The author investigated different air integration levels for an IGCC with carbon capture, based on the Siemens gasifier. Within this study, it was found that the IGCC-efficiency reaches its maximum at 100 % air integration and falls almost linear with decreasing air integration ratios. The quite low auxiliary load of the ASU indicates that excess nitrogen was not admixed to the hydrogen rich fuel before combustion in the gas turbine.

As expected, the gas turbine power output increases at falling air integration levels. But surprisingly, the steam turbine power output falls at an increasing gas turbine output. This is not typical for combined cycle processes – an explanation for this behavior would have been helpful, but was not provided by the author. Moreover, it is not clear, why the power output of the air expander (which expands the gas turbine extraction air to the required ASU operating pressure) keeps at a constant value at different air extraction rates.

2. <u>Different air-integration ratios; cases with full nitrogen integration</u>

   Frey and Zhu [16] and Wang et al. [64] also investigated the impact of air integration to the IGCC efficiency at full nitrogen integration levels.

   Frey and Zhu [16] came to the result that the highest IGCC-efficiency again can be achieved at zero air integration. In contrast to the analysis without nitrogen integration, the concepts with a high pressure ASU are always found superior to those with a low-pressure ASU. This is a consequence of the higher product (essentially nitrogen) pressure which can be achieved at ASUs that operate at an elevated pressure. The higher product pressure reduces the pressure ratio for nitrogen compression and therefore the specific work for compression.

Wang et al. [64] identifies a slight efficiency maximum at a level of 50 % air integration upon a sharp efficiency increase between zero and 50 % air-side integration. Unfortunately, this study only presents the results – an explanation is missing, so that one can only speculate about the reasons of this behavior: The gas turbine power output has a clear maximum at 50 % air integration and decreases with almost the same slope to both sides of this value. The decrease of gas turbine power in the range between 50 and 100 % air integration is due to the decreasing flow through the turbine. The reason for power decrease beneath 50 % air integration is not clear. If the gas turbine would have reached its maximum flow or mechanical limit, a constant power output from 50 % down to zero air integration would have been expected.

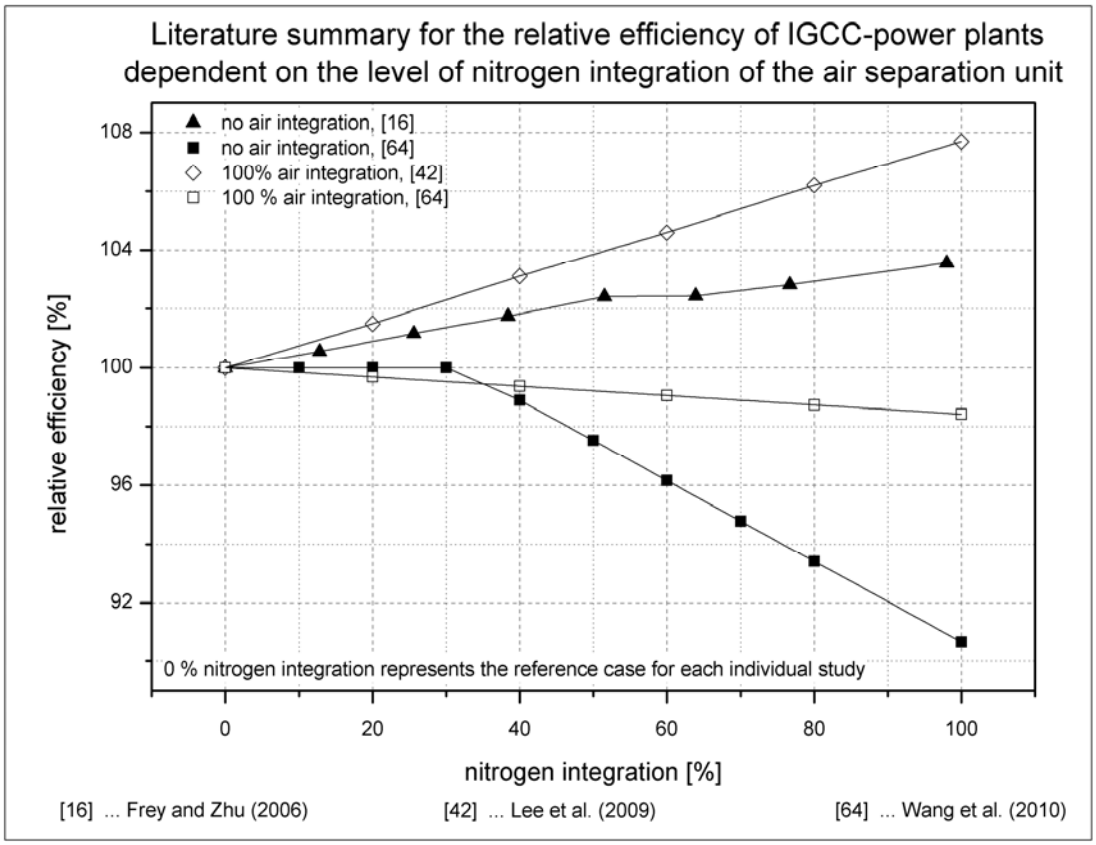

Fig. 3 Literature summary for the relative efficiency of IGCC power plants dependent on the level of nitrogen integration of the air separation unit

3. Different nitrogen-integration ratios; cases without air integration

   Again Frey and Zhu [16] and Wang et al. [64] investigated these scenarios and got to opposed results: The former study claims that the highest efficiency can be expected at full nitrogen integration. Due to the application of two different ASU pressure-concepts, the following could be observed:

   Elevated-pressure ASUs are superior to conventional low-pressure ASUs when the level of nitrogen integration exceeds the 50 % line. The change of the ASU pressure-concept is indicated by the discontinuity of the respective graph in Fig. 3.

   In contrast, Wang et al. [64] reports an almost constant efficiency between zero and 30 % nitrogen integration. From there on a sharp efficiency decrease with a steady slope is shown for increasing nitrogen integration rates. The used gas turbine has its power maximum at 30 % nitrogen integration. Again, the gas turbine power output decreases with almost the same slope to both sides of the maximum. Same as mentioned above, the missing background information for the gas turbines operating behavior complicates the confirmability of the results.

4. Different nitrogen-integration ratios; cases with full air integration

   The publications of Lee et al. [42] and Wang et al. [64] present contradictory results.

   Wang et al. [64] reports a slight maximum at zero nitrogen integration and a small efficiency decrease with a rising nitrogen integration rate. The gas turbine power output increases continuously over the complete range. So it is assumed, that the gas turbine does not reach its full capacity with the given 100 % air integration.

   The analysis presented by Lee et al. [42] stands out due to the sophisticated modeling of the gas turbines operating behavior. Amongst others, this is achieved by using a compressor map and the consideration of the compressor surge margin as well as the firing temperature. So the authors came to the result that the IGCC-power output increases more rapidly than the fuel consumption at increasing nitrogen integration rates. Consequently, the IGCC-efficiency increases in this direction, too.

A few studies investigate the CO_2-capture rate as an optimization parameter. Chen and Rubin [6] report that a CO_2-capture rate of 90 % yields to the lowest costs of CO_2-avoidance. Descamps et al. [9] vary the CO_2-capture rate for a CC-IGCC between 80 and 98 % and identify the highest efficiency at 80 % CO_2-capture, which is reported to be 7.5 % higher than the efficiency at 98 % CO_2-capture.

An IGCC concept with 60 % CO_2-capture is compared to an IGCC-concept with 80 % CO_2-capture by Ordorica-Garcia et al. [49], where an efficiency advantage of about 4.5 % and an advantage for the CoE of about 6.5 % are found for the IGCC with 60 % CO_2-capture.

Future technologies as processes with ion transport membranes, hot gas clean up, advanced gas turbines, advanced gasifiers and others that are not defined as proven technology are disregarded in the literature survey, since the state of the art technology will most likely provide the basis for the first of its kind CC-IGCC application.

2.3 Critical review

As the literature data presented in Chapter 2.1 and 2.2 show either high fluctuation (efficiency, CoE) or even contrary behavior (air and nitrogen integration) a concluding assessment of CC-IGCC concepts and optimization approaches seems not possible yet.

Moreover, for some study results a high level of uncertainty is assumed since the evolutionary history of them cannot be reconstructed [4; 6; 29; 64].

The extensive studies conducted by the International Energy Agency (IEA) [31], the Electric Power Research Institute (EPRI) [24; 25] and the National Energy Technology Laboratory (NETL) [45; 46] have room for improvement as process modeling is inadequately described. Consequently, the calculation results are hard to reconstruct. For this reason the cause determination for the observed data fluctuation is hindered or even not possible. Also for Bohm et al. [2], Chen et al. [6], Gräbner et al. [20], Kim et al. [35], Lee et al. [41] and Martelli et al. [43] results assessment and concept comparison suffer from the low level of modeling details provided.

The study “The future of coal” [34] prepared by the well-known Massachusetts Institute of Technology (MIT) reports a fairly big lack of knowledge with regard to process modeling tools and defines this as a major problem for a reliable assessment of complex power generation cycles as CC-IGCC. Furthermore, therein an “urgent need to develop modeling and simulation capability and tools” (ibid, p. 103) is stated, as the basis for secure concept comparison.

The literature review for IGCC optimization scenarios reveals a very diverse picture. In the following some shortcomings and doubts about the investigated studies concerning the ASU-integration aspect are pointed out:

- According to Smith [57], the maximum hydrogen content within the gas turbine fuel can be realized at 45-50 vol. % which means that fuel gas dilution below this value is not required. As a consequence the investigations conducted by Frey and Zhu [16], Farina and Bressan [13], Lee et al. [42] and Maurstad [44] concerning the effect of nitrogen dilution have become obsolete.
- Spliethoff [58] claims that air “integration of 100 % will always yield the maximum efficiency” (ibid, p. 612) since the “better compression efficiency of the gas turbine helps to reduce the energy demand for the compression as a whole” (ibid, p. 611). In contrast to the gas turbine compressor, the main air compressor (MAC) of the ASU operates with intercooling and pressurizes the air only to the necessary pressure level. Hence, the compression efficiency within the MAC should be superior to the gas turbine compression.
- Within the summary of the federal funded German COORIVA-project, Gräbner et al. [20] mentioned that the maximum IGCC-efficiency is reached at full air and nitrogen integration. Unfortunately, modeling and simulation details which could have been used to prove this statement are not published.
- Incomprehensible conclusions are found in Emun et al. [10] as there is stated that increasing nitrogen dilution, yields to growth of thermal efficiency, ”due to a decrease in the slurry (coal) requirement, as more N_2 is used to drive the turbine” (ibid, p. 335).
- Wang et al. [64] also presents only calculation results. Explanations of the essential gas turbine characteristics as well as information about modeling details

fail to appear. Consequently, the reader is forced to speculate about the reasons for the presented results.

- In accordance with Geosits and Schmoe [17] the maximum IGCC-efficiency can be reached at 50 % air integration. However, no details and boundary conditions are presented to prove this statement, but it is mentioned that the generated findings are "likely to change with improving gasification plant, ASU and gas turbine performance and, therefore, should be evaluated for each project." (ibid, p. 3).

At this point it has to be mentioned that the publications of Frey and Zhu [16] and Lee et al. [42] present some good approaches that are taken into consideration within this thesis. In detail, these approaches are the investigation of different ASU- pressure levels and the sophisticated modeling of the gas turbines operating behavior.

Literature reviewed in terms of the optimum CO_2-capture rate showed the following weak points:

- The carbon monoxide conversion rate (CO-conversion rate) within the carbon monoxide shift (CO-shift) cycle is varied in Descamps et al. [9] by a change of intermediate pressure (IP) steam supply to the CO-shift in order to investigate different CO_2-capture rates. The mentioned approach is not realistic, as the reduction of IP-steam supply primarily causes the catalyst to overheat.
- There are reasonable doubts about the results found by Ordorica-Garcia et al. [49] as the calculated auxiliary load share of the acid gas removal (AGR) system differs greatly from the AGR auxiliary load share presented within the extensive engineering-based studies as [20] or [31].

To sum it up, it can be stated that proper process description, modeling and simulation are often missing within the reviewed literature. Very diverse results have been found so that clear tendencies could not be derived.

3 Thesis outline

As a consequence of the literature review, the development and proper description of sophisticated process modeling tools for the major CC-IGCC sub-processes are defined as one of the main tasks of this thesis.

More precisely, simulation models for the gasification process, the ASU, the carbon monoxide conversion (CO-shift) cycle, the AGR unit with CO_2-compression, the sulfur recovery unit (SRU), the tail gas treatment (TGT) process, the gas turbine and the water steam cycle of the combined cycle power plant (CCPP) are developed.

Special emphasis is laid on the substantial description of global coherences in order to clarify the correlations within and between the individual sub-processes. So, the simulation models are used for instance to investigate the influence of integration between the gas turbine and the ASU for a CC-IGCC.

Furthermore, CC-IGCC concept routes for four types of industrial coal gasifiers (CoP gasifier, GE-R, SCGP and Siemens gasifier) are designed and simulated using the developed process calculation models, so that a comprehensible technology and concept assessment can be conducted. The results of the thermodynamic calculations provide the basis for an economic evaluation and the analysis of critical points.

The generated findings represent the starting point for CC-IGCC concept optimization. Thereby different optimization scenarios are investigated so that amongst others the thermodynamic and economic influence of the CO_2-capture rate is clarified.

Finally, the generated knowledge yields to the development of an advanced gasification based power plant configuration which improves the economic results.

4 Modeling and Simulation of sub processes for CC-IGCC

In this chapter the main sub-processes of CC-IGCC power plants are investigated in detail. For a given overall CC-IGCC configuration, the individual processes are described and the thermodynamic and technical correlations are clarified extensively. Sophisticated process simulation models are developed and implemented for the simulation of selected scenarios. The generated results are in turn the basis for a performance assessment and an illustration of the operating behavior.

4.1 Basis CC-IGCC configuration

The basis configuration for the investigated CC-IGCC concepts includes the typical components which are necessary to achieve approximately 90 % CO_2-capture by using a hard coal fed gasification process.

The chosen process arrangement (simplified expressed in Fig. 4) is briefly described in the following. References therefore can be found in [31] or [21].

A deepening investigation of the sub-processes is given in the subsequent chapters.

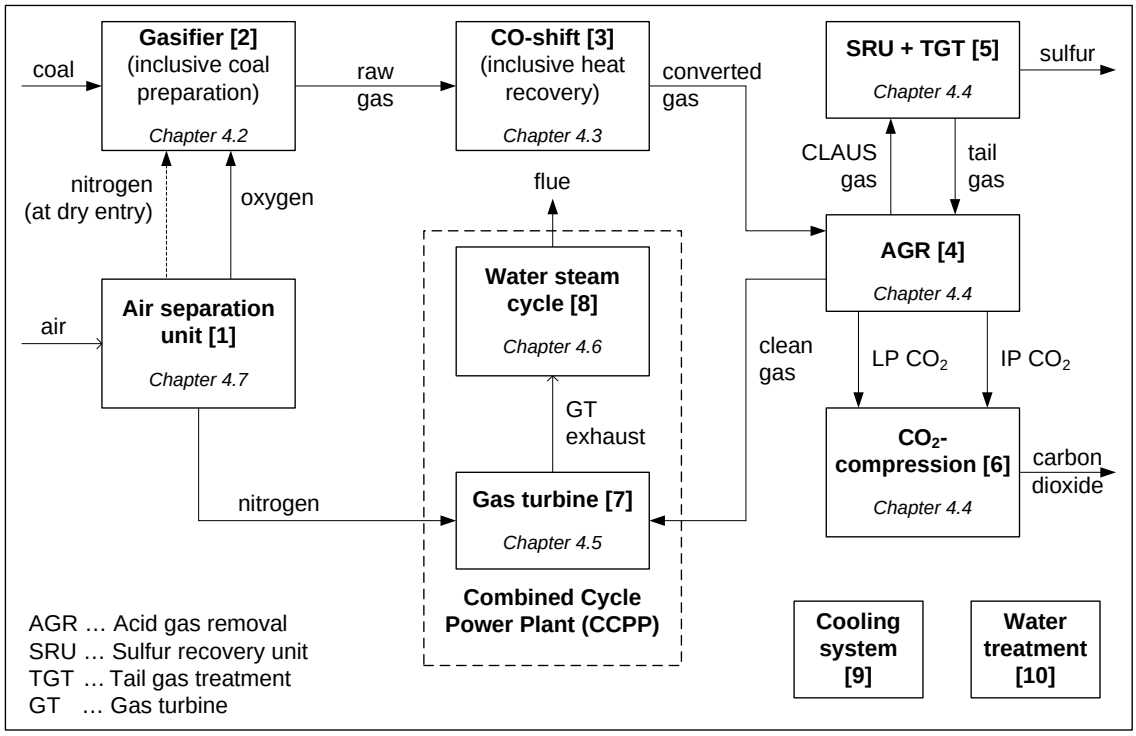

Fig. 4 General process arrangement for the investigated CC-IGCC

The individual concepts for the four different types of gasifiers somewhat differ however the general layout displays a lot of similarities.

For the gasification processes with a dry entry system (SCGP and Siemens gasifier) the coal feedstock is first grinded, dried and pneumatically pressurized while for the remaining (GE-R and CoP gasifier) a coal/water slurry is prepared and pressurized after coal pulverization. The individual coal gasification processes mainly differ in matters of reactor cooling and raw gas cooling.

Downstream gasification, the generated raw gas enters the two stage (sour gas) CO-shift unit where the main part of the carbon monoxide is catalytic converted with steam to carbon dioxide and hydrogen. As the concept with sour gas shift has been found advantageous compared to the sweet shift concept [31], the former has been chosen. A good portion of the released reaction heat is recovered for internal use as for instance steam generation, quench water preheating or clean gas saturation. The CO-shift cycles also vary depending on the gasification process as the generated raw gases contain different amounts of steam.

Leaving the CO-shift cycle, the converted gas enters the AGR which is a physical absorption unit using methanol as solvent. Hence, the selected AGR-system should show similar characteristics as the industrial Rectisol® process. While the separated CO_2 is compressed to the desired pressure, the sulfur containing components (mostly H_2S and COS) are converted to elementary sulfur within the SRU. For sulfur recovery the CLAUS-process running on oxygen-enriched air has been chosen. The remaining tail gas is treated in the TGT-unit and recycled back to the AGR.

The clean, dry and hydrogen-rich gas escaping the AGR is then diluted with excess nitrogen from the ASU and saturated with steam using low temperature heat from the CO-shift cycle. Nitrogen and steam dilution are necessary operational measures in order to realize secure combustion in the gas turbine with low emissions of nitrogen oxides (NOx).

Finally, the conditioned fuel gas is preheated within the water steam cycle of the CCPP and burned in the gas turbine for electricity generation purposes. The gas turbine exhaust is used for steam generation in the heat recovery steam generator (HRSG) of the water steam cycle before it is discharged to the ambient. The generated steam is used in a steam turbine for additional electricity production. Moreo-

ver, the water steam cycle of the CCPP usually features a couple of interfaces to other sub-processes as it operates for instance as heat source (e.g. for solvent regeneration within the AGR) or as a supplier of process streams (e.g. gasification agent for the gasifier).

The ASU acts not directly within the process chain but supplies necessary process media as gaseous oxygen (GOX) to the gasification process and to the SRU. Furthermore, it also delivers high pressure gaseous nitrogen (HP GAN) and low pressure gaseous nitrogen (LP GAN) for the pneumatic coal feeding system as well as diluent gaseous nitrogen (DGAN) for dilution of the hydrogen rich fuel gas.

The cooling system and the water treatment section are not investigated in detail but are considered for the sake of completeness.

According to Fig. 4 each subsystem has been numbered in order to advance clarity for the interface configuration.

In anticipation of the flow schemes presented in the following chapters, the nomenclature for the process streams between the individual sub-processes is explained in Appendix A.

4.2 Coal gasification system

In the following, four types of industrial coal gasifiers (GE-R, CoP gasifier, SCGP, and Siemens gasifier) are investigated in detail. Simulation models for the individual gasification processes are developed based on fundamental system descriptions. It should be mentioned that the presented process schemes and models do not exactly reflect the industrial processes. A couple of assumptions and simplifications have been defined in order to realize a comparative study.

More detailed information concerning the gasification systems can be found in [19; 22; 54] where especially the boundary conditions for process modeling and simulation are taken from.

4.2.1 The Shell Coal Gasification Process

The Shell Coal Gasification Process (SCGP) and the very similar PRENFLO (Pressurized Entrained Flow) process are oxygen blown entrained flow gasification processes with a dry entry system. Between 2002 and 2008 both processes were jointly merchandized by Shell and Uhde as SCGP. At the moment, both processes are again competing on the market [26].

As illustrated in Fig. 5 the SCGP can be described as follows: Raw coal is grinded and dried before pressurization (typically with nitrogen) in a lock hopper system. The gasification agents (GOX and steam) are introduced to the pressurized coal close to the burner entry in the reactor. Usually four burners are applied in an opposite arrangement in order to realize steady fuel supply and ignition as well as an enhanced particle residence time through recirculation within the reactor [19].

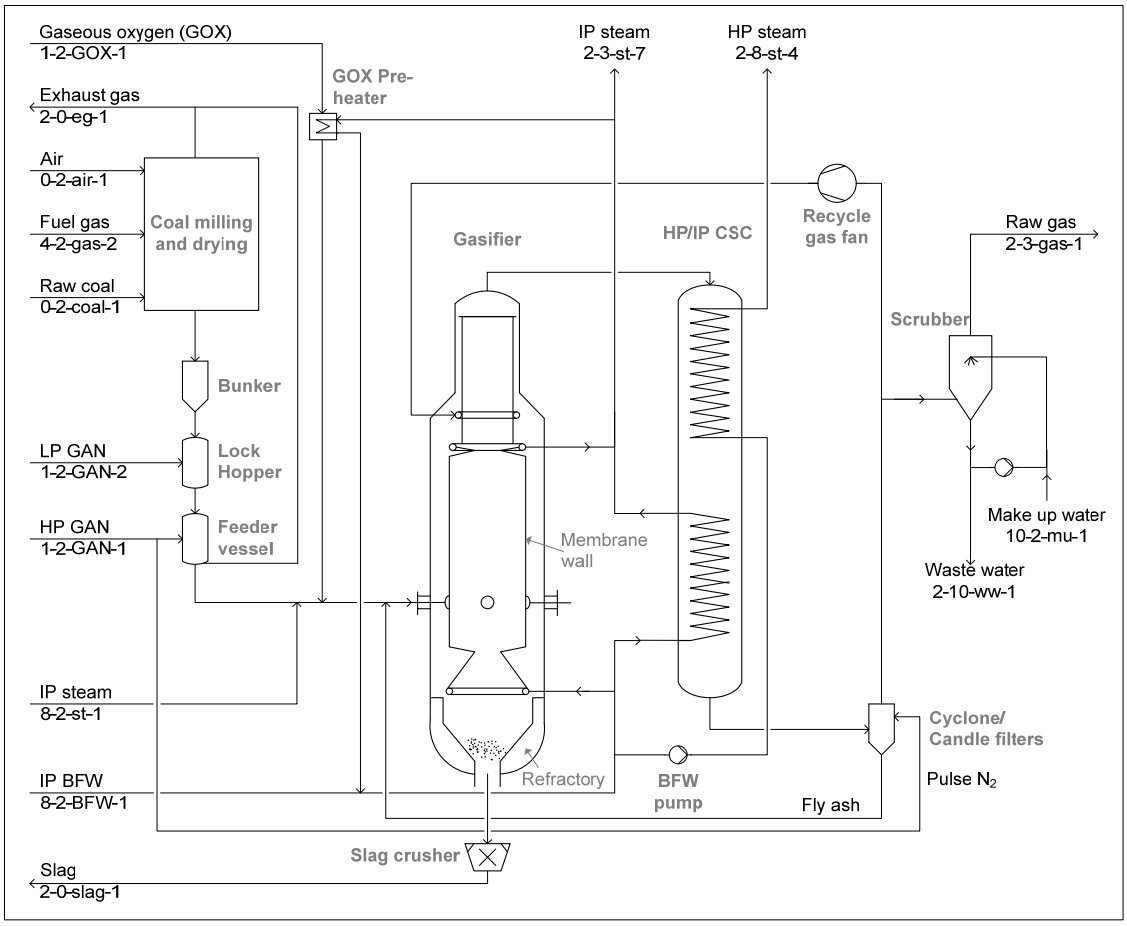

Fig. 5 Process flow scheme of the SCGP according to [19; 22]

Coal gasification takes place at reactor temperatures between 1400 and 1700 °C and reactor pressures of 30 to 41 bar. The gasification reactor itself is designed as a vertical cylindrical pressure vessel with an integrated membrane wall. The refractory lined membrane wall which protects the pressure vessel from direct radiation and liquid slag exposure is designed as heating surface for IP-steam generation. Through heat removal by the cooled membrane wall a solid slag layer is established at the reactor surface and acts as a thermal barrier. Upon the solid layer a liquid slag film flows down through a centric hole and drops into a water bath. In here the slag immediately granulates to a glassy material before it is discharged through a lock hopper system which is often supported by a slag crusher unit [22; 26; 54].

The generated raw gas flows upwards and drags some of the molten slag along. A cold recycle gas is introduced immediately above the reactor in order to solidify the molten slag before entering the heat recovery system. The amount and the temperature of the recycle gas are adjusted to ensure complete slag consolidation. Depending on the coal and ash properties, the raw gas temperature behind the gas quench varies between 700 and 900 °C while the amount of recycle gas is typically in the same range as the amount of raw gas leaving the overall gasification system [19].

Downstream the cold gas quench, the raw gas enters the convective syngas cooler (CSC) which is typically designed as a water tube boiler. Depending on the individual application, the CSC may contain economizer, evaporator and superheater surfaces. However, for the cause of simplicity and economics frequently only evaporator surfaces are applied. Generation of high pressure steam (HP-steam) and intermediate pressure steam (IP-steam) takes place in order to cool the raw gas down to approximately 250 °C. The generated IP-steam is sent to the downstream CO-shift cycle as necessary reaction partner and temperature moderator. The saturated HP-steam is superheated and expanded within the water/steam cycle of CCPP.

Adjacent the CSC, fly ash removal is realized by a cyclone (for bulk removal) and ceramic candle filters (for fine removal). At low ash contents in the coal (< 8 ma.-%) a fly ash recycle has to be applied to guarantee a sufficient slag layer on the membrane wall [11]. The same has to be established when insufficient gasification

enlarges the carbon content within the fly ash. Downstream fly ash removal, the recycle gas for the gas quench is extracted and recompressed in the quench gas fan. Final removal of soluble trace compounds as NH_3, HCN or HCl is realized by a water wash unit.

The produced raw gas normally consists mainly of carbon monoxide (about 60 mol. %) and hydrogen (about 30 mol. %) and is virtually free of higher hydrocarbons [22]. Typical for the SCGP are carbon conversion ratios of more than 98 % and cold gas efficiencies between 80 and 83 % whereby the two parameters are defined as follows:

$$\text{Carbon Conversion Ratio} = \text{CCR} = 1 - \frac{\dot{n}_{\text{carbon,unconverted}}}{\dot{n}_{\text{carbon, coal}}} \quad (1)$$

$$\text{Cold Gas Efficiency} = \frac{\dot{m}_{\text{raw gas}}\ \text{LHV}_{\text{raw gas}}}{\dot{m}_{\text{coal}}\ \text{LHV}_{\text{coal}}} \quad (2)$$

The overall thermal efficiency which considers the chemical as well as the recovered thermal energy is specified to about 95 % where the appeared losses according to [54] are made up as follows:

- 0.8 to 2 % heat loss due to reactor wall losses and slag discharge,
- 0.2 to 1 % due to unconverted carbon,
- 2 % heat loss at the heat recovery steam generators.

4.2.2 The Siemens gasifier

The Siemens gasifier was originally designed for salty brown coal under the name GSP (Gaskombinat Schwarze Pumpe) process in East Germany in the 1980s. The developed flow scheme for the subsequent process description is shown in Fig. 6.

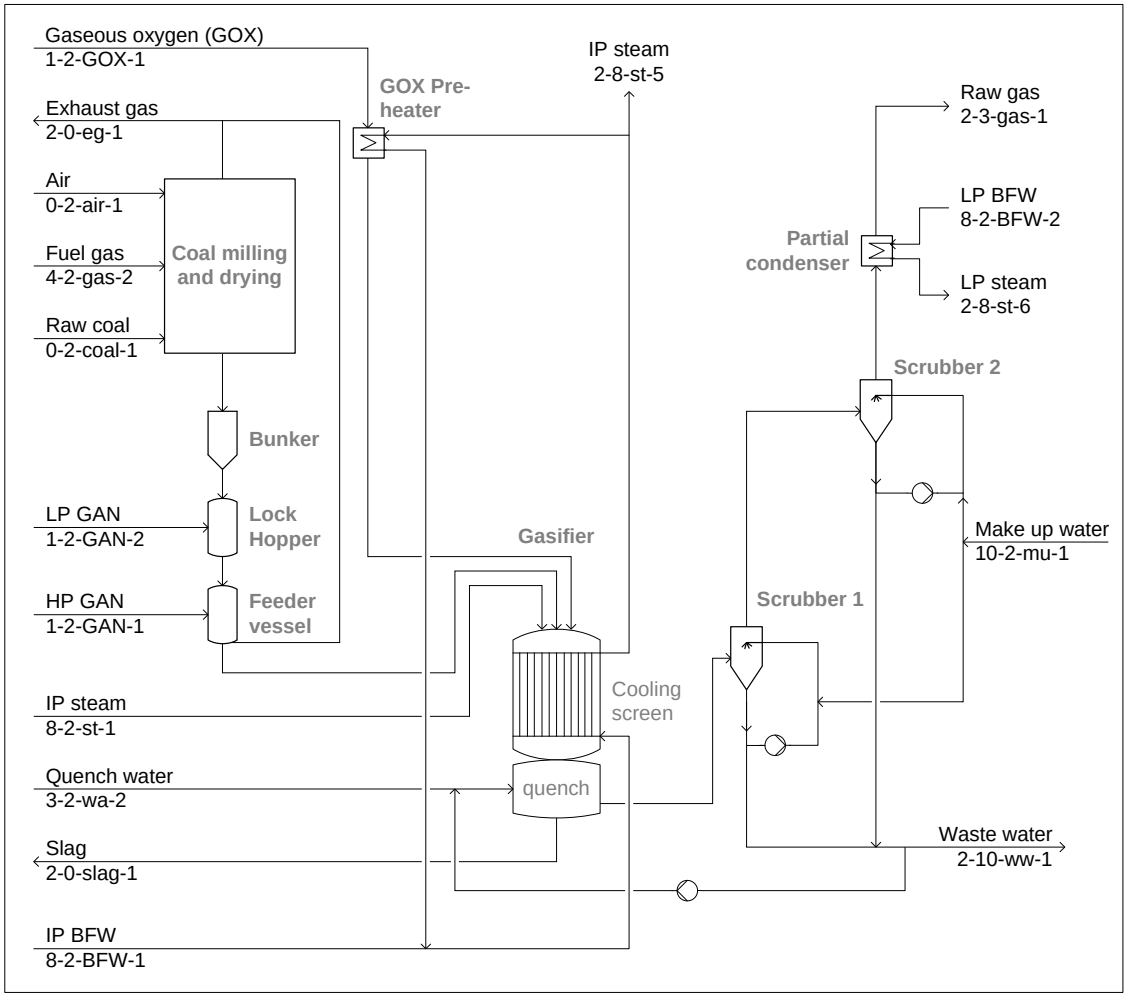

Fig. 6 Process flow scheme of the Siemens gasifier according to [19; 54]

Such as the SCGP, the Siemens gasifier also features a dry coal entry system with a milling and drying section and a pneumatic feeding system. In contrast to the SCGP, the burners are placed at the top of the reactor so that the direction of flow is inverted. Up to a thermal input of 500 MW one centrally arranged burner that combines the ignition and pilot flame with the coal dust nozzles is applied. At higher thermal input rates a four-burner-design will be applied so that a central pilot and ignition burner is surrounded by three coal dust nozzles arranged in a 120 ° offset pattern [54].

The reactor itself is offered in two different designs: The reactor design with cooling screen similar to the membrane wall of the SCGP is applied for coals that contain a sufficient amount of mineral matter so that an adequate slag layer can be established as thermal barrier at the cooling screen. In contrast, a refractory lined reactor design is applied for feedstock with low mineral contents. The design with a cooling screen is preferred whenever possible since it has demonstrated long term successful operation at high availability rates [54]. Therefore, the refractory design is not considered in the following since the observed feedstock contains a sufficient amount of mineral matter.

Caused by the original design feedstock (salty brown coal) the application of a convective syngas cooler was a priori excluded since salt deposits on the heating surfaces would occur. Different water quench designs were investigated. Of these, one configuration has proved reliable operation where the quench water nozzles are annularly placed in one single or multiple levels. The quench area is completely free of installed equipment in order to avoid fine slag disposal. The granulated slag is discharged by a lock hopper system similar the SCGP [54]. The quench water is supplied at a temperature of about 200 °C [21] in order to increase the steam content within the quenched raw gas. The high steam content in turn is advantageous since it avoids or reduces the steam demand for the downstream CO-shift.

The saturated raw gas which leaves the quench section at temperatures between 170 and 240 °C is routed to a series of two Venturi scrubbers where soluble trace compounds and fine particles are removed. Downstream the scrubbers a partial condenser cools the raw gas by a few centigrade. Thereby the volatile salt particles will be enclosed in the condensed vapor droplets before the raw gas leaves to the downstream processes [54].

The operating conditions within the reaction chamber and the raw gas composition at the outlet of the gasification zone are very similar to the SCGP. It has to be mentioned, that the reaction chamber can be operated at approximately 50 K lower temperature than at the SCGP (at the same boundary conditions). This difference is due to the concurrent flow direction of gas and slag which compensates a part of the heat losses.

Due to the water quench a partial conversion of carbon monoxide and water to hydrogen and carbon dioxide is reported by Schingnitz and Görz [53] so that the final raw gas composition should be slightly different compared to the SCGP.

4.2.3 The ConocoPhillips gasifier

The ConocoPhillips (CoP) process is a two-stage entrained flow gasifier where the feedstock is introduced to the reactor as coal/water slurry. So far, the CoP technology has been realized only once in the Wabash River IGCC power plant (Indiana/USA). Compared to a dry entry system, the slurry feed is on the one hand mainly beneficial through its less complexity (no lock hoppers and coal dryers) and the unproblematic feedstock pressurization up to 80 bar [22; 54]. On the other hand a higher oxygen demand has to be accepted compared to a dry entry system, since the additional slurry water fraction has to be evaporated and heated up to reactor temperature.

According to Fig. 7 the process can be described as follows: The raw coal is grinded by the addition of water to the same particle size as necessary for pulverized coal combustion power plants. The coal/water suspension features a coal fraction of about 50 to 70 ma. %. In any case the lowest possible water content has to be aspired in order to minimize the heat load necessary for water evaporation within the reactor [54]. A slurry composition of about 65 ma. % coal and 35 ma. % water counts as typical for the CoP gasifier. Originally a slurry split of 70 % to the first stage and 30 % to the second stage was envisioned [19].

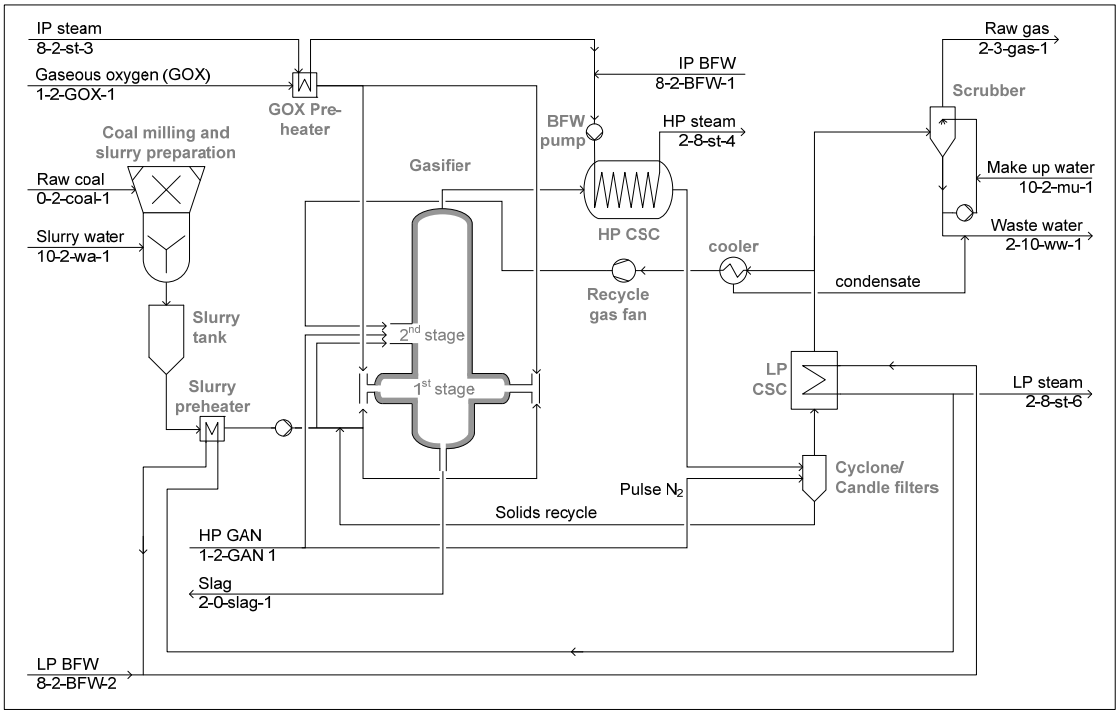

Fig. 7 Process flow scheme of the CoP gasifier according to [22; 26; 63]

After pressurization by the slurry pump the suspension is indirectly preheated with steam and fed together with oxygen to the first stage of the reactor. Here, the partial oxidization takes place at temperatures between 1320 and 1500 °C considering the ash melting behavior of the individual coal. The two burners are placed within the horizontal cylindrical vessels in an opposite arrangement. The chosen layout of the first stage enables efficient mixing of the reaction partners so that a high carbon conversion can be realized [19; 26; 63].

The reactor itself is completely refractory lined and can be operated at pressures up to 41 bar. The coal ash accumulates as liquid slag at the reactor wall of the first stage and is continuously discharged (lock hopper free) after granulation in a water bath. Carbon particles which are discharged through the water bath are fed back to the slurry preparation after sedimentation [26; 63].

At the second stage of the reactor the remaining coal/water slurry (without oxygen) is brought into the upwards flowing hot raw gas. Through water evaporation and endothermic reactions the raw gas cools down to about 1000 to 1050 °C. The second stage therefore acts as a so called chemical quench which is a unique feature of the CoP gasifier. Due to the chemical quench the generated raw gas contains unconverted carbon and ash. The amount of unconverted carbon increases with a

decreasing coal reactivity. Therefore the actual slurry split ratio of 70/30 % has been changed to 80/20 % since the CoP gasifier at the Wabash River IGCC is operated on low reactive petrol coke. A higher feed ratio to the second stage would in fact require an additional cyclone in front of the convective syngas cooler (CSC) [19].

To ensure the desired quench effect the raw gas passes a residence vessel downstream the reactor [19]. Thereafter the particle loaded gas is cooled down to about 350 to 400 °C in the CSC which is designed as a vertical fire tube boiler. The generated saturated HP-steam is sent to the CCPP for steam superheating and expansion.

Downstream the CSC, final dust removal takes place in cyclone and candle filters achieving separation ratios of 99.9. The separated carbon and fly ash is pneumatically recycled (with nitrogen or syngas) to the first stage slurry [22; 26; 63]. The almost dust free raw gas is further cooled down in a low temperature heat recovery section for low pressure steam (LP-steam) generation. The generated LP-steam is also routed to the CCPP for superheating and expansion. Downstream the LP-CSC approximately 20 % of the raw gas are recycled back to the second stage of the gasification reactor to adjust the desired temperature. The remaining raw gas is finally directed to a water wash for removal of soluble trace compounds [46].

Due to the slurry entry and the chemical quench the raw gas might contain considerable amounts of the undesirable components carbon dioxide (about 16 mol. %) and methane (about 4.5 mol. %), respectively [46]. On the other hand, these disadvantages are partly compensated by an improved oxygen consumption and cold gas efficiency. In fact, the cold gas efficiency is specified to values between 70 and 80 %. Further enhancement can be achieved through an increased slurry feed ratio to the second stage as described and analyzed by Gräbner [19].

4.2.4 The General Electric coal gasifier

The General Electric coal gasification process is characterized by a completely refractory lined entrained flow reactor where the feedstock is handled as coal/water slurry. In general, GE offers three technologies which mainly differ in methods of raw gas cooling:

- The GE gasifier with a full water quench (GE-Q)
- The GE gasifier with a radiant and a convective syngas cooler (GE-RC)
- The GE gasifier with a radiant cooler and a water quench (GE-R)

The latter one combines the reliable water quench with a highly efficient heat recovery so that an acceptable performance penalty and a superior availability (compared to the GE-RC layout) shall be achieved. Therewith it is expected to overcome the problems with fly ash deposits in the convective coolers as observed at the GE-RC in the Tampa Electric Polk Power Station IGCC [28].

In fact, the GE-R is the chosen technology for the Edwardsport IGCC which was supposed to start commercial operation in 2012 [66]. For this reason, the technology with radiant cooler and water quench is exclusively pursued within this thesis for process description as well as for modeling and simulation of the GE gasifier.

According to Fig. 8 the GE-R technology can be described as follows:

The slurry preparation proceeds in an analog manner as at the CoP technology with a specified solid fraction of about 65 to 74 % [54].

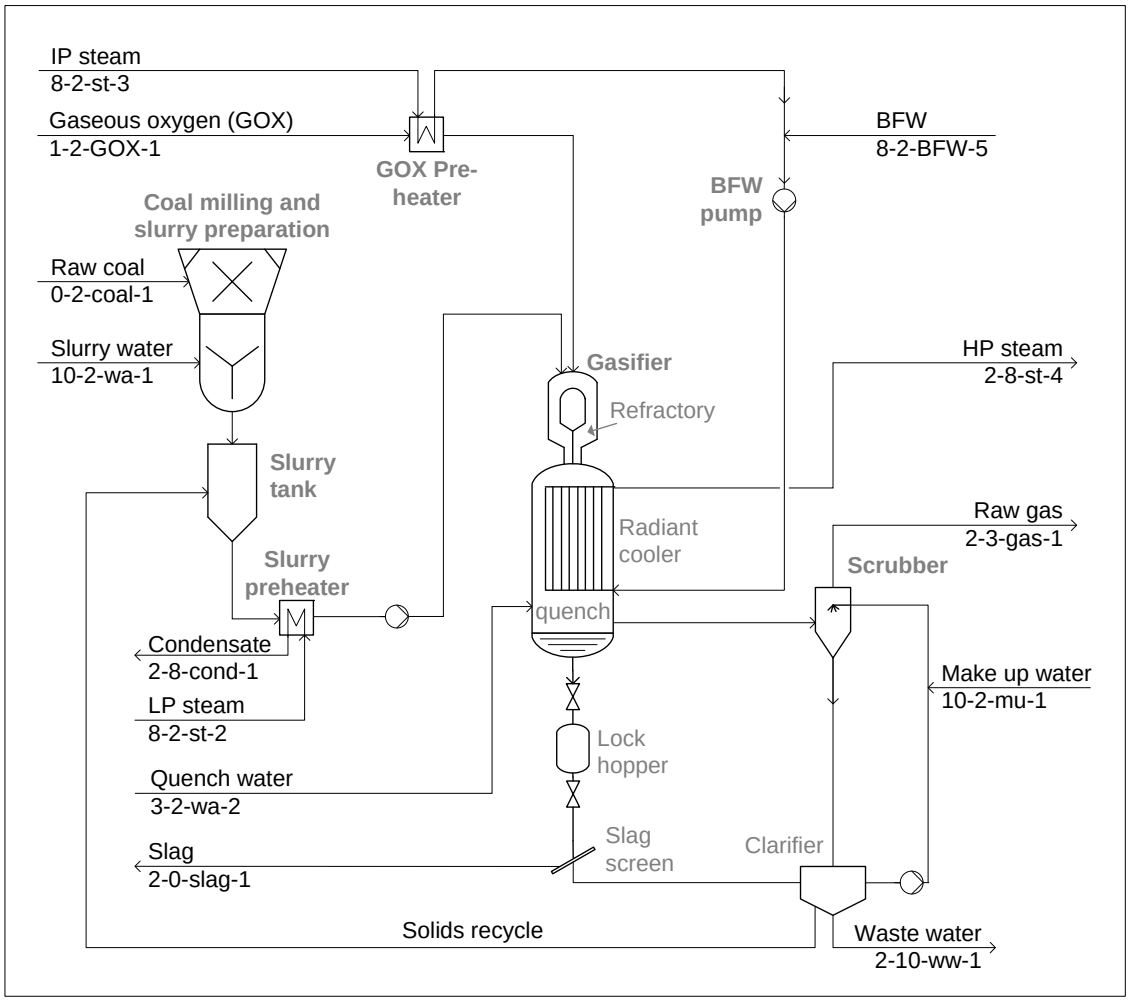

Fig. 8 Process flow scheme of the GE-R according to [22; 26; 54]

After preheating, the slurry suspension and gaseous oxygen are introduced at the top of the reactor so that a downward flow direction is set up. The molten slag accumulates at the reactor wall and drops down in a water bath which is placed underneath the radiant cooler (RC). The duct between the reactor and the RC is designed in a way that a contact between molten slag and the heating surfaces of the RC is avoided.

As the hot raw gas still contains sticky and corrosive slag droplets it has to be cooled down in the RC to a temperature at which the slag loses its adhesive character [54]. Intermediate pressure boiler feed water (BFW) extracted from the CCPP is pressurized and fed to the RC where saturated HP-steam is generated through heat exchange with the hot raw gas. Downstream the RC the raw gas is quenched until complete saturation using preheated quench water.

As reported by Gräbner [19] only partial carbon conversion of about 90 % per cycle can be achieved at the given boundary conditions. Therefore the unconverted carbon has to be separated from the granulated slag and then fed back to the slurry tank. Thus, an overall carbon conversion ratio similar to the other discussed gasification processes can be achieved.

Finally, the raw gas is routed to a scrubber unit for the removal of soluble trace components and fine particles before it leaves the gasification unit to the CO-shift.

Due to the slurry entry the generated raw gas contains considerable amounts of carbon dioxide. This fact and the low carbon conversion are the reasons for a relatively low cold gas efficiency which is expected in the lower 70 % area [19].

4.2.5 Modeling and Simulation of the gasification processes

A typical world market coal was selected as feedstock for the comparative investigation. Table 3 shows the appropriate coal analysis.

Table 3 Coal analysis (retrieved from [37])

Parameter	Unit	Value	Parameter	Unit	Value
Proximate analysis					
Fixed carbon	ma. %	50.15	Moisture	ma. %	5.50
Volatile matter	ma. %	36.98	Ash	ma. %	7.37
Ultimate analysis					
C	ma. %	72.35	Cl	ma. %	0.05
H	ma. %	4.97	S	ma. %	2.84
O	ma. %	5.56	Moisture	ma. %	5.50
N	ma. %	1.36	Ash	ma. %	7.37
Heating value (according to DULONG)					
LHV	MJ/kg	29.888	HHV	MJ/kg	31.107

The process simulation models were developed according to the above discussed process schemes and descriptions.

The characteristic parameters for the coal preparation and feeding process as well as the electrical auxiliary load strongly depend on the properties of the individual feed stock and the chosen systems and machineries. Since this approach demands a lot of manufacturer know-how and experiences, it was decided to use literature data in order to receive the same basis for the process evaluation. Table 4 shows the corresponding parameters and their related literature sources.

Table 4 Specific parameters for the coal preparation and feeding process

Parameter	Unit	CoP	GE-R	SCGP	Siemens
$P_{el,\ aux}$	kWh/t_{coal}	30[a)] [46]	21 [46]	43[a)] [21]	26 [21]
$V_{LP\ GAN}$	Sm^3/Sm^3 GOX	-		0.16 [21]	
$V_{HP\ GAN}$	Sm^3/Sm^3 GOX	-		0.30 [21]	
$V_{exhaust\ gas}$	% of input GAN	-		83 [31]	
$Slurry_{H2O-frac}$	ma. %	35 [19]		-	
a) … auxiliary load for recycle gas fan included					

Table 5 shows the defined boundary conditions for process simulation. The reactor pressures of the SCGP, the Siemens gasifier and the CoP gasifier were selected in order to supply a gas turbine fuel at an adequate pressure level. At the same time the chosen pressure represents the upper end of the nowadays technical possible level [22]. Since the GE gasification process has been found more competitive at higher pressures [31], an elevated gasifier pressure was selected. The gasification temperatures were defined in order to keep a sufficient distance to the flow temperature (about 1300 °C [37]) of the coal ash. The heat losses have been selected in accordance to Gräbner [19].

Table 5 Boundary conditions for simulation of the coal gasification process

Parameter	Unit	CoP	GE-R	SCGP	Siemens
$p_{reactor}$	bar	40	60	40	40
$t_{reactor}$	°C	1450[b)]/1000[c)]	1450	1450	1450
CCR	%	99[b)]/42[c)]	90	99.5	99.5
Wall loss	% of coal heat input	0.5	1.2	1.0	1.0
$Q_{cooling\ screen}$		-	-	2.0	2.0
b) … 1st stage; c) … 2nd stage					

The reactors itself are simulated by setting the reaction equations and the appropriate temperature approaches to the equilibrium state (refer to Appendix C2) which were retrieved from Gräbner [19]. The defined carbon conversion ratios and the reactor temperatures are adjusted by the oxygen flow. For the processes with a dry entry system, the moderator steam flow represents an additional parameter to conform the overall heat balance. Some assumptions that have not been mentioned up to now are considered below.

At the SCGP, about 57 % of the raw gas is recycled so that a temperature of 825 °C is adjusted at the entry of the CSC. Saturated HP-steam is generated by raw gas cooling assuming a pinch point of 88 K and 2 % heat loss within the CSC. Final raw gas cooling down to 274 °C is realized by IP-steam generation with an IP pinch point of 10 K. The Pinch point of the HP-CSC was found in order to provide enough heat to generate the necessary amount of IP-steam required at the downstream CO-shift. The pulse gas flow for the ceramic candle filters is fixed at 0.5 % of the raw gas flow (in accordance to Gräbner [19]).

For the CSC of the CoP gasifier the pinch points were selected to 10 K both for the high and the low pressure steam generator. Concerning the heat loss and the pulse gas demand, the same conditions were defined as at the SCGP. About 21 % of the raw gas is extracted downstream the LP-CSC and recycled back to the second gasifier stage after cooling down to 30 °C.

Due to the water excess within the raw gas (caused by the slurry entry) and the realized residence time within the reactor, the gas composition at the GE-R matches to an equilibrium temperature far below the actual reactor temperature [19]. This temperature has been determined by Gräbner [19] to about 993 °C. It is used in the simulation model for calculation of the final raw gas composition by an additional equilibrium reactor. Adjacent, the hot raw gas is cooled in the RSC down to 816 °C by HP-steam generation before final water quench cooling down to complete saturation takes place (in accordance to Gräbner [19]).

The developed CHEMCAD flow sheets and the individual heat and material balances for the simulation cases can be found in the Appendixes B2 to B9. For the calculation of the thermodynamic properties the Soave-Redlich-Kwong equation of state was used.

Fig. 9 shows the calculated raw gas composition for the four different gasifier concepts. As expected, the raw gas of the processes with a dry feed system is very similar. There are only slight differences at the carbon dioxide and nitrogen content due to the partial CO-conversion during the water quench and the pulse gas for the candle filters respectively. The raw gases of the processes with slurry entry look similar whereas the methane content at the CoP case marks the slight difference. The noticeable methane content is caused by the relatively low reaction temperature (about 1000 °C) prevailing at the second gasifier stage of the CoP gasifier. Since the methane will slip through the CO-shift unit and the AGR as well, higher CO_2-emissions are expected at the IGCC concept with a CoP gasifier.

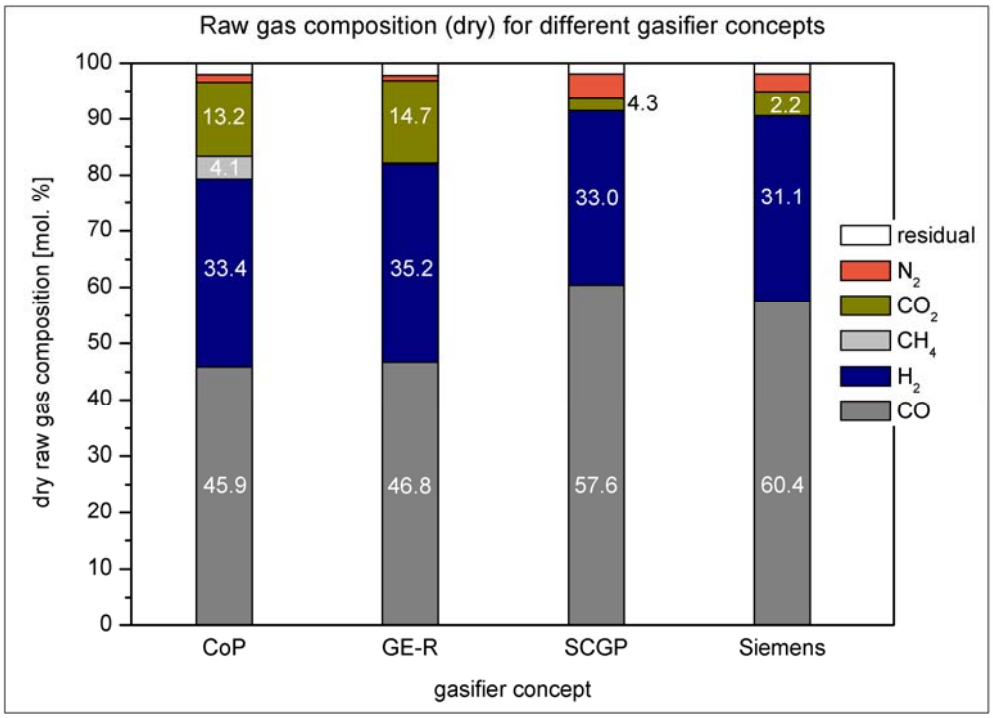

Fig. 9 Raw gas composition (dry) for different gasifier concepts

For evaluation and comparison of the different gasification processes the following parameters have been defined:

$$\text{GOX demand} = \frac{\dot{V}_{GOX}}{\dot{Q}_{coal,LHV}} \qquad \left[\frac{Sm^3\ GOX}{GJ\ coal}\right] \qquad (3)$$

$$\text{Syngas yield} = \frac{\dot{V}_{H_2+CO}}{\dot{Q}_{coal,LHV}} \qquad \left[\frac{Sm^3\ H_2+CO}{GJ\ coal}\right] \qquad (4)$$

$$H_2 \text{ to CO ratio} = \frac{H_2}{CO} = \frac{\dot{n}_{H_2}}{\dot{n}_{CO}} \qquad [-] \qquad (5)$$

$$\text{Steam to CO ratio} = \frac{H_2O}{CO} = \frac{\dot{n}_{H_2O}}{\dot{n}_{CO}} \qquad [-] \qquad (6)$$

The above mentioned parameters are visualized in Fig. 10 for a comparison of the different gasifier concepts.

The GAN-demand for the different processes was not visualized here, since it is an input parameter for the simulation as shown in Table 4.

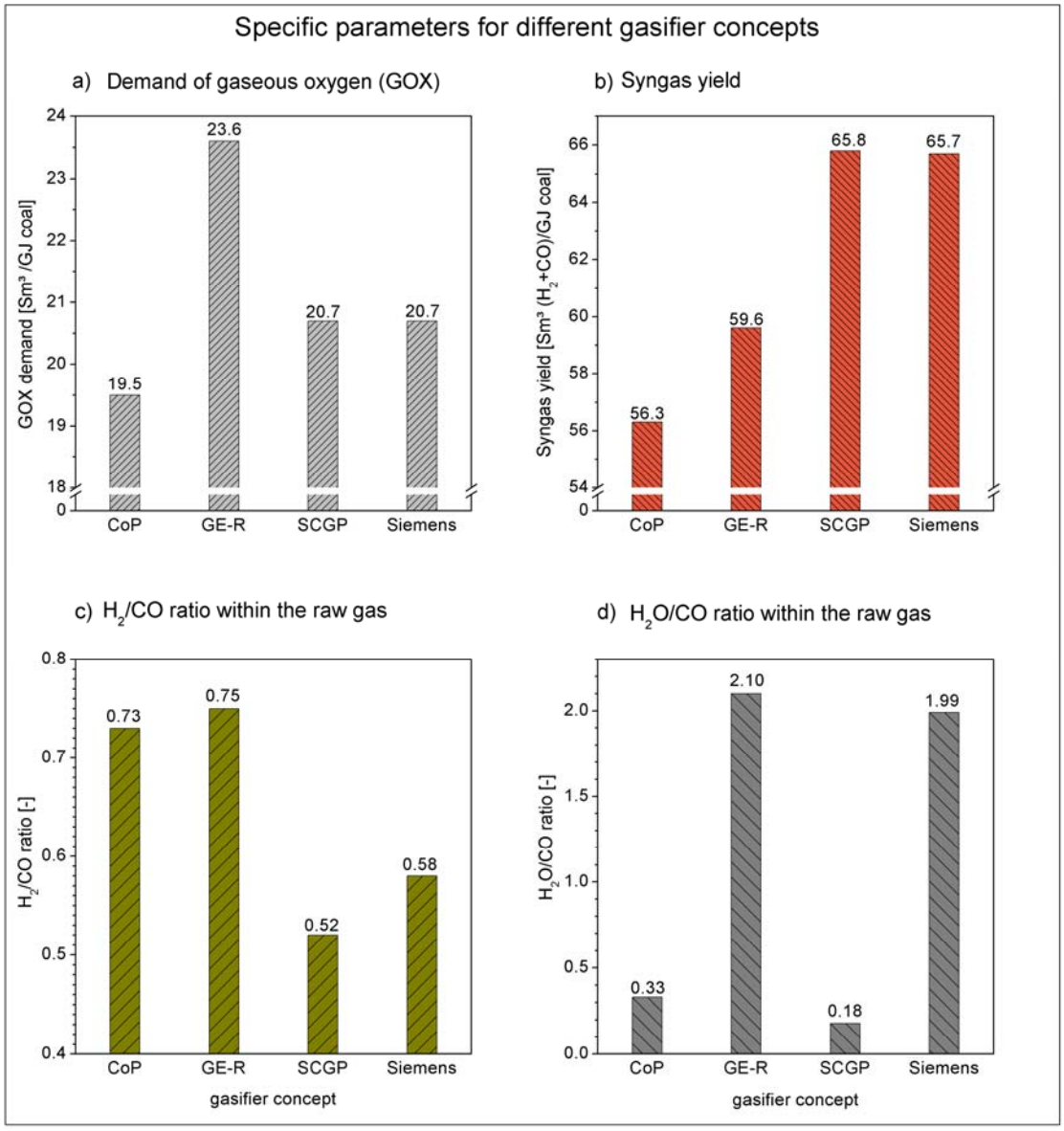

Fig. 10 Specific parameters for different gasifier concepts

The second gasifier stage at the CoP process, where no additional oxygen is required for coal gasification, overcompensates the drawback of the slurry entry so that the CoP gasifier exhibits the lowest specific oxygen demand (refer to Fig. 10a). The very similar gasification principle of the Siemens gasifier and the SCGP yields to the same specific oxygen demand which is roughly 6 % higher than at the CoP gasifier. In contrast, the GE-R shows a 14 % higher oxygen demand compared to the Siemens gasifier and the SCGP and a 21 % higher demand as the CoP gasifier,

all caused by the incomplete carbon conversion per pass combined with the slurry entry system.

Since the carbon monoxide and hydrogen fraction within the raw gas accumulates to more than 90 mol. % at the Siemens gasifier and the SCGP (refer to Fig. 10a), the syngas yield shows the highest values out of the four concepts (refer to Fig. 10b). Due to the higher carbon dioxide content within the raw gas the syngas yield at the GE-R is 9 % lower than at the aforementioned concepts. The CoP concept shows an additional reduction of the parameter by about 5 % caused by the methane fraction which does not appear at the other three principles.

The hydrogen to carbon monoxide ratio of the raw gas shows a value of about 3:4 for the gasifiers with slurry entry and about 1:2 for the gasifiers with a dry entry system (refer to Fig. 10c). As a consequence the necessary carbon monoxide conversion is higher for the latter ones when a common chemical synthesis would be considered as downstream process.

The steam to carbon monoxide ratio illustrated in Fig. 10d indicates a high steam content for the raw gasses of the water quench gasifiers (GE-R and Siemens gasifier) and a relatively low steam content for the gasifiers with dry raw gas cooling (CoP gasifier and SCGP). Consequently, the last mentioned gasifiers will require additional steam as reaction partner and temperature moderator at the downstream CO-shift while the raw gas out of the GE-R and Siemens gasifier contains probably enough of it.

The cold gas efficiency is presented in Table 6 for the observed gasifier concepts. As expected the concepts with a dry entry system show superior values compared to the gasifiers with a slurry entry system. However, the chemical quench at the CoP gasifier yields to a noticeable improvement compared to the GE-R process.

Table 6 Cold gas efficiency for the different gasification processes

Gasifier	CoP	GE-R	SCGP	Siemens
Cold gas efficiency	78.7 %	72.7 %	80.5 %	80.1 %

4.2.6 Exergetic analysis of the gasification processes

The fundamentals of exergetic analyses are extensively described by Fratzscher et al. [15]. According to their remarks, the exergy of process streams has to be calculated under consideration of:

- The thermomechanical exergy (as an expression of temperature and pressure differences between the individual state and a reference state),
- The chemical exergy (as an expression of the reaction potential compared to the pure environmental components), and
- The concentration exergy (as an expression of differences between the composition of the individual process stream and the ambient).

The concentration exergy is not included at the presented analysis, since the concentration difference to the ambient is not considered as a useful benefit.

The reference state for all exergy calculations has been set to 25 °C and 1.01325 bar. The ambient air has been defined to contain 78.1 mol. % of nitrogen, 21 mol. % of oxygen and 0.9 mol. % of argon.

Hence, the overall exergy of process streams is calculated as

$$\dot{E}_{overall} = \dot{E}_{thm} + \dot{E}_{chem} \quad . \tag{7}$$

The thermomechanical exergy is regarded as a mixture of a dry and a water phase so that it can be calculated as follows:

$$\dot{E}_{thm} = \dot{n}_{dry}\, \dot{e}_{dry} + \dot{m}_{H_2O}\, \dot{e}_{H_2O} \tag{8}$$

where

$$\dot{e}_{dry} = c_p\big|_{t_0}^{t} (t - t_0) - T_0 \left(c_p\big|_{t_0}^{t} \ln\frac{T}{T_0} - R \ln\frac{p}{p_0} \right) \qquad \left[\frac{kJ}{kmol}\right] \tag{9}$$

$$\dot{e}_{H_2O} = h - h_0 - T_0 (s - s_0) \; . \qquad \left[\frac{kJ}{kg}\right] \tag{10}$$

The chemical exergy of the gaseous process streams is calculated using the molar reaction exergy of the pure components according to equation (11). Those and the related method of calculation are excellent described by Gräbner [19].

$$\dot{E}_{chem} = \dot{n}_{dry} \sum_i (x_i \, \dot{e}_i) \, . \qquad (11)$$

Finally, the exergy of coal is calculated through the following statistical formula that has been proposed by Baehr [1]:

$$\dot{E}_{coal} = \dot{m}_{coal} \, 0.967 \, LHV_{coal} + 2.389 \, . \qquad \text{(LHV in MJ/kg)} \qquad (12)$$

The exergetic efficiency has been defined as evaluation criteria between the four gasifier concepts according to the following:

$$\eta_{ex,gasifier} = 1 - \frac{\Sigma \, \dot{E}_{loss}}{\Sigma \, \dot{E}_{effort}} \, . \qquad (13)$$

The exergy loss is calculated as the difference between incoming and outgoing exergy streams.

The four different gasification processes are evaluated considering all interface streams to and from the individual process according to the appropriate flow schemes (Fig. 5 to Fig. 8) and to the heat and material balances (Appendixes B3, B5, B7, B9).

Fig. 11 shows the calculated exergetic efficiencies for the four different gasifier concepts. As the generated raw gas and the recovered heat (steam generation) represent the only benefit out of the gasification processes, the individual exergy shares of the raw gas and the heat recovery system are pointed out in the graphic below. Moreover, the chemical raw gas exergy as well as the thermomechanical raw gas exergy (consisting of the dry phase and the water phase) are related to the overall exergy effort.

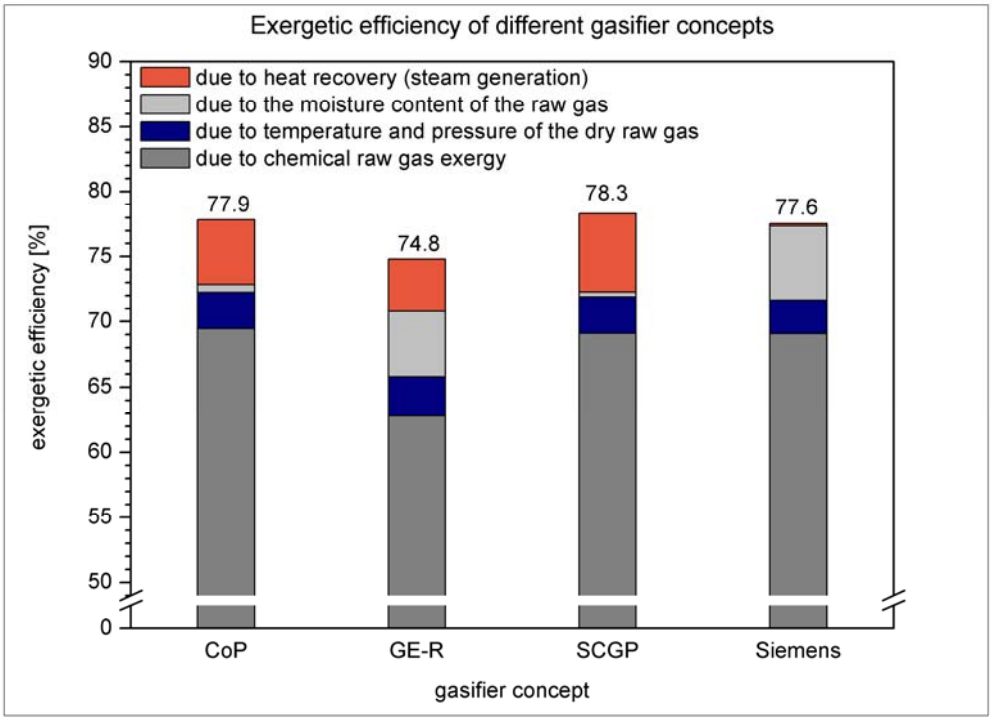

Fig. 11 Exergetic efficiency of different gasifier concepts

As it can be seen the chemical raw gas exergy is almost even at the CoP gasifier, the Siemens gasifier and the SCGP. Only the GE-R shows a chemical raw gas exergy that is about 10 % lower than that of the aforementioned concepts.

Since the raw gas pressure and the raw gas temperature after gas cooling are within the same range at all concepts, the share of the thermomechanical exergy of the dry raw gas is also nearly equal. Due to the water quench at the GE-R and the Siemens gasifier, the thermomechanical exergy fraction of the raw gas increases in comparison to the remaining two concepts.

Caused by the raw gas heat recovery system at the CoP gasifier and the SCGP, a considerable exergy amount is transferred to the generated steam. Therefore the exergetic efficiency reaches a slightly better value as the Siemens gasifier. The radiant cooler in combination with the water quench at the GE-R is responsible for the highest exergy recovery out of the four concepts so that the overall efficiency drawback to the other three concepts is reduced to roughly 4 %.

4.3 Carbon monoxide shift

Within a CC-IGCC the carbon monoxides shift (CO-shift) cycle represents the subsequent process step downstream the gasification system. The intention of the CO-shift is to convert the carbon monoxide contained in the raw gas to hydrogen and carbon dioxide according to the following equilibrium reaction:

$$CO + H_2O \leftrightarrow H_2 + CO_2 \qquad \Delta H_{25°C} \approx -41\ \text{kJ/mol} \qquad (14)$$

The catalytic reaction takes place in one single or in a series of adiabatic reactors (normally two or three) whereas the individual number of reactors depends on the maximum allowable carbon monoxide slip. Fig. 12 visualizes the temperature profile and the carbon monoxide content for a three-stage CO-shift using a typical raw gas from an entrained flow coal gasifier.

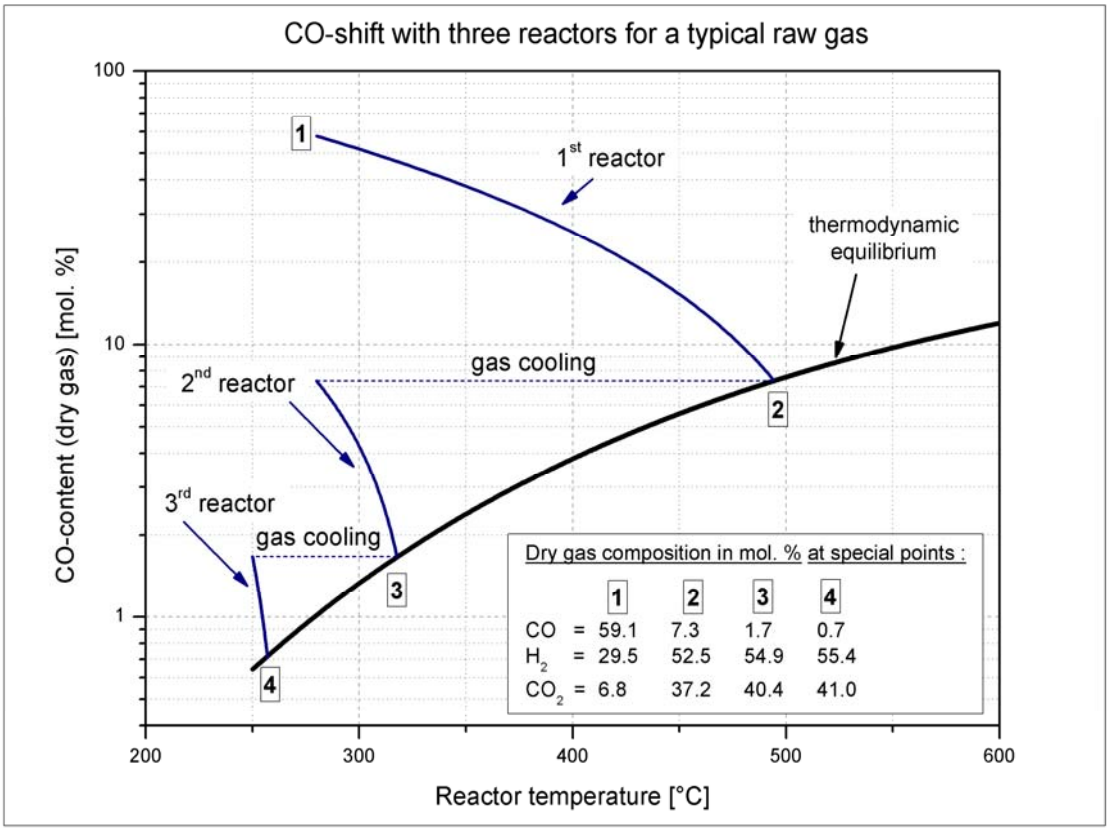

Fig. 12 CO-shift with three reactors for a typical raw gas

As illustrated, the first reactor realizes the lion's share of CO-conversion. However, due to the sharp temperature increase within the reactor bed, the minimum reachable CO-content in the first reactor is limited by the thermodynamic equilibrium to relatively high values. On the other hand, the third reactor just slightly reduces the

carbon monoxide slip, so that for a CC-IGCC a two reactor configuration with intercoolers in between typically delivers acceptable carbon monoxide conversion ratios so that an overall CO_2-cature rate of about 90 % can be realized. Therefore a two-stage configuration has been chosen for the investigated CC-IGCC concepts.

The above mentioned CO-conversion ratio is defined as follows:

$$\text{CO-conversion ratio} = \left(1 - \frac{\dot{n}_{\text{CO, converted gas}}}{\dot{n}_{\text{CO, raw gas}}}\right) * 100 \qquad (15)$$

The catalysts for the raw gas shift consist mainly of cobalt and molybdenum and attain their full activity only when enough sulfur compounds (100 to 1500 ppm) are present in the feed gas. The catalysts favor also the parallel conversion of carbonyl sulfide (COS) to hydrogen sulfide (H_2S) so that the COS content in the shifted gas reaches low levels close to the thermodynamic equilibrium [60]. Occasionally, also a catalyst guard bed for Cl^- and HCN is applied. Further information to raw gas shift catalysts, operating conditions and experiences are provided by Frank [14].

The maximum process temperature is influenced by the temperature resistance of the catalyst in order to avoid catalyst sintering. For this reason the feed gas has to contain enough steam for temperature moderation, especially at high carbon monoxide contents. At the same time, the feed gas temperature to the reactor has to be determined so that a sufficient margin to the saturation temperature is given and the catalyst activity is high enough to promote the reaction.

The above described fundamentals have been used to develop CO-shift cycles for the CC-IGCC concepts based on the four different gasifiers. Thereby the following requirements have to be considered:

- High carbon monoxide conversion rates,
- Efficient heat recovery (steam generation; quench water preheating),
- Saturation of the clean and diluted fuel gas.

In the following the layout and the performance of the developed cycles are described in detail.

4.3.1 CO-shift cycle for the Siemens gasifier and the GE-R

As the raw gases of the Siemens gasifier and the GE-R already contain a sufficient amount of steam, the released reaction heat can be used to a good portion for steam generation. Concurrently a large amount of quench water has to be preheated up to 200 °C in order to realize a high vapor pressure within the raw gas at the gasifier outlet. The process flow scheme for the CO-shift of the CC-IGCC with Siemens gasifier is presented in Fig. 13.

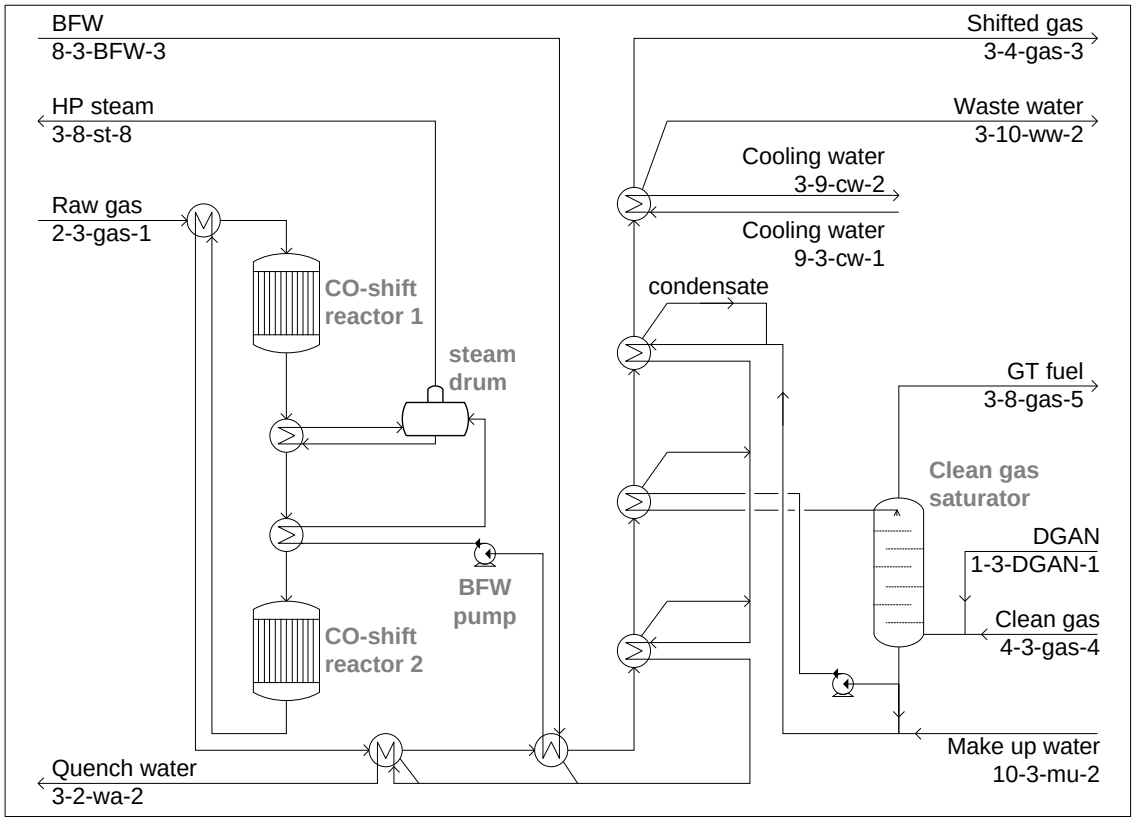

Fig. 13 CO-shift cycle for a CC-IGCC with Siemens gasifier

The incoming raw gas is first preheated to 280 °C against the converted gas leaving the second CO-shift reactor at about 320 °C. The hot exhaust of the first CO-shift reactor is cooled down in two consecutive gas/water heat exchangers. Thus, the high temperature heat is recovered through preheating and evaporating of high pressure boiler feed water (HP-BFW) which is then sent as saturated steam to the combined cycle. The temperature differences between the HP-BFW and the hot gas are adjusted in order to realize a feed gas temperature to the second CO-shift reactor of again 280 °C.

The low temperature heat is recovered within a series of gas/water heat exchangers in which the quench water and the BFW are preheated and the heat losses of the clean gas saturator are compensated. The process condensate contributes a big portion to the required amount of quench water so that only minor amounts of make up water are necessary. After final gas cooling the converted gas leaves to the AGR and the discharged condensate to the waste water treatment in order to avoid undesired accumulations within the process.

Typically, part of the raw gas can be bypassed to the first reactor for the purpose of process control. Since this is not within the scope of this thesis, the raw gas bypass was not considered.

The requirements and boundary conditions of the CO-shift cycle for the CC-IGCC with GE-R are very similar to the case with Siemens gasifier. The only exception is due to the necessary clean gas expansion in front of the clean gas saturator. Hence, an additional heat exchanger (for clean gas heating) and an expansion turbine are added to the cycle. The corresponding process flow diagram can be found in Appendix C1.

4.3.2 CO-shift cycle for the SCGP and the CoP gasifier

Due to the dry gas cooling system at the SCGP and the CoP gasifier, the corresponding raw gases contain only minor amounts of steam (refer to Fig. 10d). Consequently the raw gas has to be moisturized in order to achieve acceptable CO-conversion rates. The so called cooler/saturator cycle with additional external steam supply is a common CO-shift application for “dry” raw gases so that it is chosen for the aforementioned gasifiers. For both gasifier types the same CO-shift layout is used with the only difference that the external steam at the SCGP case is delivered by the convective syngas cooler while the water/steam cycle of the CCPP supplies the steam at the case with CoP gasifier.

According to the developed layout for a raw gas generated by the SCGP (Fig. 14; Appendix C2 shows the corresponding process flow diagram for the CoP case) a good portion of the released reaction heat is transferred to an internal water flow which is used in a saturator to moisturize the incoming raw gas. Thus the H_2O/CO ratio in the gas is raised to about 1.3. Additionally, external IP-steam is mixed to the raw gas leaving the saturator for the purposes of CO-conversion enhancement

and temperature moderation within the first CO-shift reactor. The additional steam has to be introduced right after the saturator so that the mixture can be pre-heated to the desired temperature. The hot exhaust of reactor 1 is initially cooled in a feed/effluent heat exchanger and subsequently in a gas/water heat exchanger against the circulating water flow so that the same feed gas temperature as at the first CO-shift reactor can be realized. The circulating flow rate is adjusted in order to achieve a water inlet temperature to the saturator of 230 °C. The exhaust of the second CO-shift reactor is used to preheat the circulating water before it is cooled and dehumidified in a direct cooler. The bottom product of the saturator becomes the top feed of the direct cooler after exchanging heat to the clean gas saturator cycle and the cooling water. Downstream the direct cooler, the most part of the remaining steam in the converted gas is condensed and discharged before the gas leaves to the acid gas removal section.

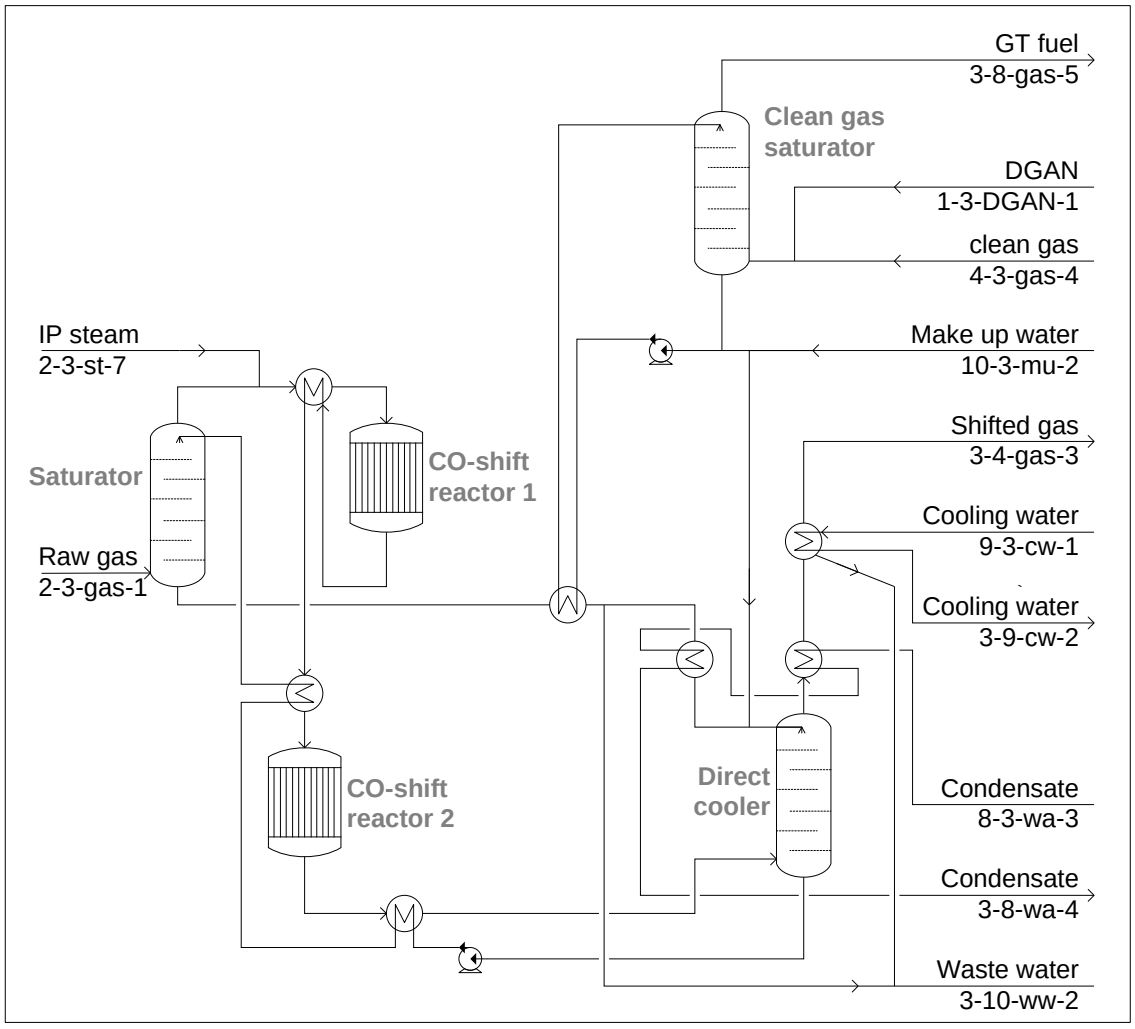

Fig. 14 CO-shift cycle for a CC-IGCC with SCGP gasifier

4.3.3 Modeling and Simulation of the CO-shift cycle

The process simulation models for the CO-shift cycle were developed in CHEMCAD according to the above described flow schemes and descriptions. Same as at the gasifier simulations, the Soave-Redlich-Kwong equation of state is used for the calculation of the thermodynamic properties. Table 7 provides the typical temperature bandwidth and the approach to the thermodynamic equilibrium for raw gas shift catalysts as well as the chosen boundary conditions for process simulation.

Table 7 Significant process parameters for raw gas shift catalysts

Parameter	Unit	Literature data	Reference	Chosen
$t_{Reactor\ inlet}$	°C	200 … 290	[14; 60]	280
$t_{Reactor\ outlet}$	°C	< 500	[60]	< 500
Equilibrium approach	K	0[a] … 40[b]	[60]	20
a) Start of run; b) End of run				

The simulation results and the corresponding CHEMCAD flow sheets are presented in the Appendixes C3 to C10.

As mentioned before, the reactor temperature and the CO-conversion rate are the most crucial parameters during the process. Since both strongly depend on the steam content within the raw gas, calculations for different H_2O/CO ratios have been performed. The individual influence is clarified in Fig. 15 for the four different raw gases.

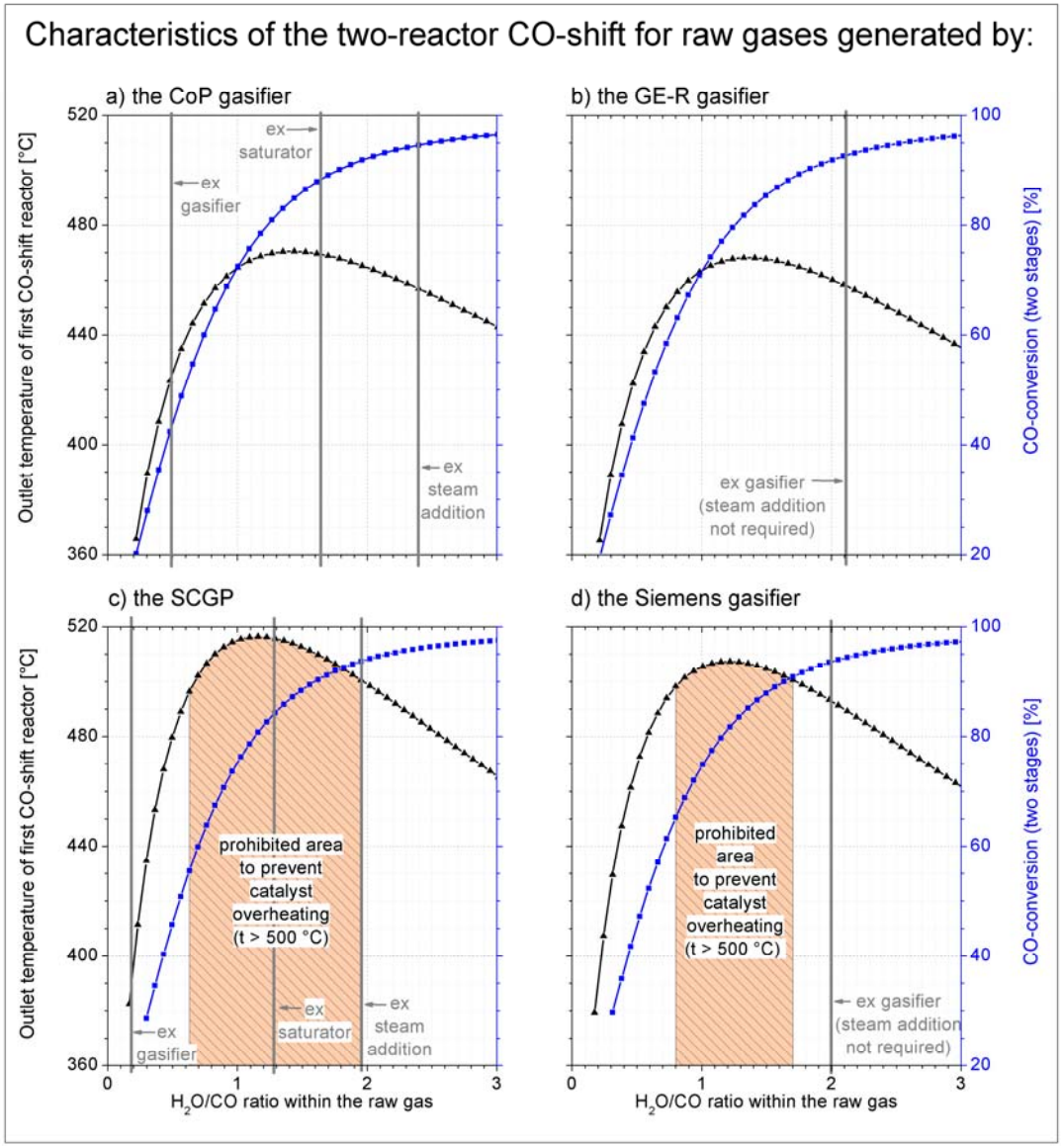

Fig. 15 Characteristics of the two-reactor CO-shift for different raw gases

As illustrated, the water content within the raw gases of the GE and the Siemens gasifier is already high enough to achieve comparable CO-conversion rates and to avoid process temperatures of more than 500 °C. For the other two raw gases the steam content has to be raised by internal steam generation (saturator) and external steam addition so that the same level of CO-conversion can be reached. While at the SCGP case steam addition is also necessary for temperature moderation, no temperature restrictions are expected at the CoP case due to the lower CO-content within the raw gas leaving the gasifier (refer to Fig. 9).

Finally the composition of the gas leaving the CO-shift cycle to the AGR is provided in Table 8. Due to the almost same CO-conversion rate, the gas composition varies only slightly between the four concepts. Due to the final cooling step, the converted gases are almost free of steam/water.

Table 8 Gas composition after the CO-shift cycle

Compo-nent	Unit	CoP	GE-R	SCGP	Siemens
H_2	mol. %	53.4	54.7	55.9	56.4
CO	mol. %	2.0	2.4	2.4	2.4
CO_2	mol. %	39.3	40.5	37.5	37.8
Residual	mol. %	5.3	2.4	4.2	3.4

4.4 Acid gas removal, CO_2-compression and sulfur recovery

Physical absorption processes are widely considered as the preferred method for acid gas removal in a CC-IGCC [20; 24; 31; 45; 46]. Hence, the acid gas removal unit investigated in this thesis follows the principle of physical absorption. A process simulation model based on the industrial Rectisol® technology is developed and used to investigate the influence of different boundary conditions.

The Rectisol® process using methanol (MeOH) as solvent is chosen due to its superior technical characteristics compared to other absorption processes. Kohl and Nielsen [38] mention the following amenities of the Rectisol® process:

- The considerably higher solubility of acid gases due to possible operating temperatures of less than -60 °C ,
- “the demonstrated ability to separate troublesome impurities that are produced in the gasification of coal or heavy oil, including hydrogen cyanide, aromatics, organic sulfur compounds, and gum-forming hydrocarbons” (p. 1215),
- “The ability to achieve very sharp separations, with H_2S concentrations of typically 0.1 ppm and CO_2 concentrations of just a few ppm in the treated gas” (p. 1216),

- A low solvent viscosity even at extreme operating temperatures so that mass and heat transfer are not significantly impaired,
- The supply of dry and essentially sulfur free carbon dioxide,
- And the generation of a concentrated H_2S-stream suitable for a conventional CLAUS-plant.

To get access to the full technical potential, a relative complex process flow scheme is necessary. This and the need of low level refrigeration leads to high plant costs so that the Rectisol® technology is mostly applied at difficult gas treating conditions where other processes are not possible [38].

As the separated CO_2 leaves the Rectisol® process essentially free of water and sulfur, it is pressurized without further pretreatment in a multistage compressor.

The CLAUS-process operated with oxygen enriched air is chosen for sulfur recovery. The remaining sulfur dioxide containing tail gas is hydrogenated (using hydrogen extracted from the AGR) to hydrogen sulfide and recycled back to the AGR.

In the following the mentioned processes and the developed simulation models are described in detail. The fundamentals of gas purification are not enlarged herein. The interested reader is therefore referred to [38; 60; 65]. The developed process flow schemes take into account the information provided by [23; 38; 48; 60].

4.4.1 Selective acid gas removal and CO_2-compression

According to Fig. 16 the developed acid gas removal process can be described as follows: At first, the feed gas (a mixture of the shifted gas and the tail gas from the TGT unit) is cooled against the products in a gas/gas heat exchanger (HE1) before it is externally cooled (in Ch1) to about 5 °C with cooling energy delivered by the refrigeration plant. To avoid freezing of the contained water, a minor amount of methanol is added to the feed gas before it enters the second heat exchanger (HE2). There it is cooled to sub-zero temperatures (typically between minus 20 and minus 30 °C) until it enters the pre-wash stage located at the bottom of the absorption column. Here the feed gas is exposed to a small quantity of cold, CO_2-loaded solvent so that troublesome impurities as water, benzene, HCN, NH_3, naphthalene and part of the sulfur compounds are absorbed and further routed to the $MeOH/H_2O$ column.

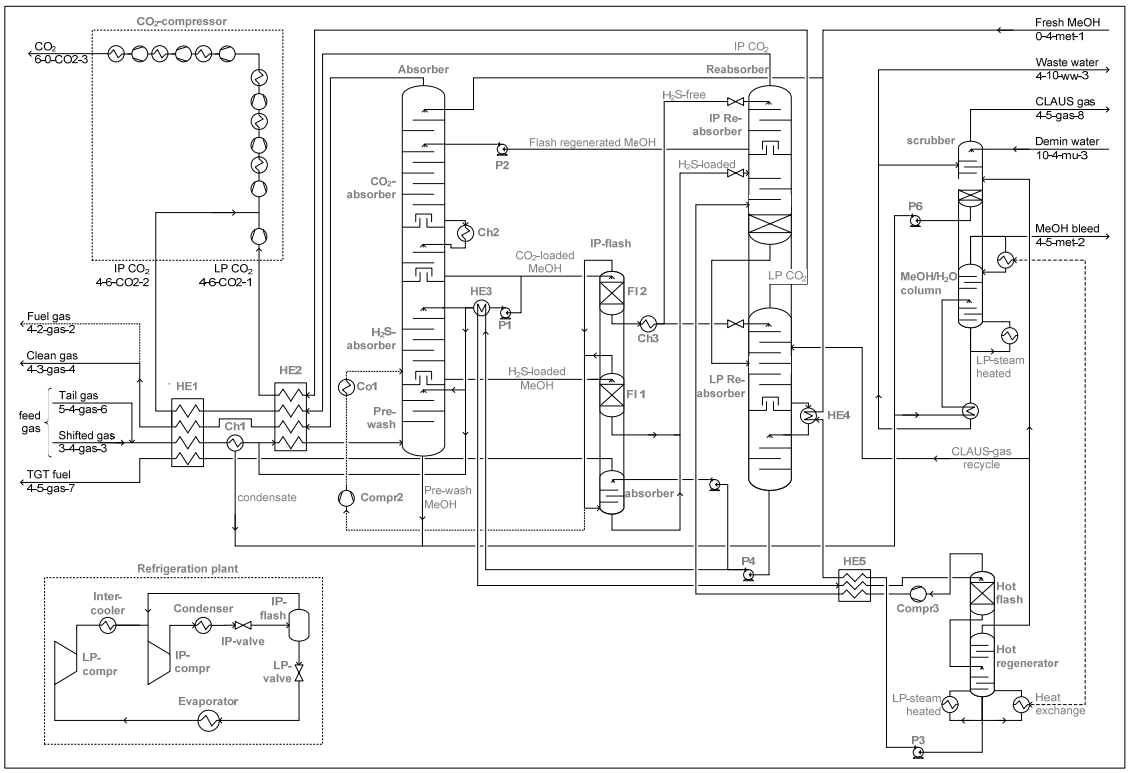

Fig. 16 Flow scheme for the AGR unit with refrigeration plant and CO_2-compressor

The pretreated feed gas flows upwards to the H_2S-absorption level where it is also faced to the cold and CO_2-loaded methanol. Sulfur compounds as H_2S and residual COS are primarily and almost completely removed due to the good solvent selectivity caused by the already high CO_2-content. Adjacent, the sulfur free gas runs up to the CO_2-absorption section where it is charged with methanol at different grades of purity. While flash regenerated methanol is introduced within the upper third of the column, ultra-pure solvent out of the hot regenerator purifies the gas to its required CO_2-content at the top of the absorption column. The released heat of absorption causes the solvent temperature to increase and therefore the absorption capacity to decrease. Consequently, an intercooler (Ch2) has been placed in the lower third of the column in order to enhance the absorbable amount of CO_2. Ammonia acts as the cooling agent provided by the refrigeration plant. The cold, desulfurized and CO_2-lean gas leaves the AGR after heat exchange (in HE2 and HE1) for clean gas dilution and saturation to the CO-shift unit.

The CO_2-loaded methanol leaving the CO_2-absorber is split so that one part acts as the solvent for the H_2S-absorber and the pre-wash stage as already explained. In-

ternal cooling is realized (in HE3) for the purpose of absorption capacity enhancement. The remaining CO_2-loaded solvent is depressurized in the upper part of the IP-flash column (Fl 2) in order to release valuable gases. The same is done with the H_2S-loaded solvent leaving the H_2S-absorber in the lower part of the IP-flash column (Fl 1). The valuable gases can either be recompressed (Compr2), water cooled (in Co1) and recycled to the H_2S-absorber or used for hydrogenation in the TGT process. In the latter case further treatment is necessary (in the absorber) in order to reabsorb the also released CO_2. Depending on the operating pressure of the system, stepwise flashing and recompression might be advantageous in order to optimize the auxiliary load consumption.

The H_2S-loaded solvent streams are throttled and fed to the lower section of the IP-reabsorber where a part of the contained CO_2 is released. As also some of the contained H_2S desorbs out of the solvent, the H_2S-free methanol is introduced to the top of the reabsorber after external recooling (Ch3) through the refrigeration plant. There it reabsorbs the released sulfur compounds and therefore keeps the CO_2 essentially sulfur free. Flash regenerated methanol is extracted at the upper part of the IP-reabsorber and sent as solvent to the CO_2-absorber. Thus, energy can be saved at the hot regenerator as not the full solvent stream has to be hot regenerated. The bottom product of the IP-reabsorber is throttled and fed to the lower section of the LP-reabsorber where the remaining CO_2 is finally released at the top. Reabsorption of the released sulfur compounds is realized in the same way as described for the IP-reabsorber. The released IP- and LP-CO_2 is first used for feed gas cooling (in HE1 and HE2) before it is pressurized in an intercooled multi-stage compressor (cooled with cooling water) up to supercritical conditions (100 bar, 30 °C).

The deep temperatures appearing at the desorption process are used to cool the hot regenerated solvent (in HE4) to its lowest process temperature before entering the CO_2-absorber.

The flash regenerated solvent leaving the LP-reabsorber still contains a high amount of carbon dioxide and nearly all sulfur compounds that were brought in with the feed gas. As a consequence the cold solvent has to be heated in order to decrease its absorption capacity for the contained acid gases. In a first step, the solvent exchanges heat (in HE3) to the CO_2-loaded stream entering the H_2S-

absorber and the pre-wash stage before it is heated to about 70 °C against the hot regenerated methanol and some volatile gases (in HE5). During this heat exchange the most part of the contained acid gases already desorb so that they can be recompressed and recycled after a slight pressure reduction within the hot flash. This recycling is one possible measure to provide a concentrated H_2S-stream suitable for a conventional CLAUS-process.

Final solvent purification takes place in the hot regenerator which is heated with LP-steam from the combined cycle and with condensing heat from the $MeOH/H_2O$ column. The hot regenerated solvent leaves at the bottom of the column and is cooled to deep temperatures as already described. One part of the hot regenerator's top product (CLAUS-gas recycle) is routed back to the reabsorber for acid gas enrichment. The remaining is fed to a scrubber where the contained methanol is washed out using demineralized water and process condensate so that the CLAUS-gas reaches its final quality. The methanol containing water streams are fed to the $MeOH/H_2O$ column where they are thermally separated so that a methanol rich gas can be withdrawn at the top of the column. The liquid bottom product is send to the water treatment section while the discharged gas is burned at the SRU.

The deep temperature cooling load (for Ch1, Ch2, and Ch3) is provided by a refrigeration plant based on the vapor-compression technology.

Ammonia as the chosen refrigeration agent is compressed in a multistage compressor with intercooling up to about 10 bar. The upper process pressure is determined by the cooling water temperature at the condenser. After ammonia condensation and heat removal to the cooling water, the process pressure is reduced in two steps. The lower process pressure has to be defined so that the ammonia evaporates at a temperature lower than required for internal recooling in Ch1, Ch2, and Ch3.

The necessary ammonia flow is found depending on the required cooling load after the process pressures and temperature differences are fixed.

4.4.2 Sulfur recovery and tail gas treatment

As mentioned above, the CLAUS-process operated with oxygen enriched air and a hydrogenation process are chosen for sulfur recovery and tail gas treatment, respectively.

Fig. 17 shows the developed flow scheme for the corresponding processes.

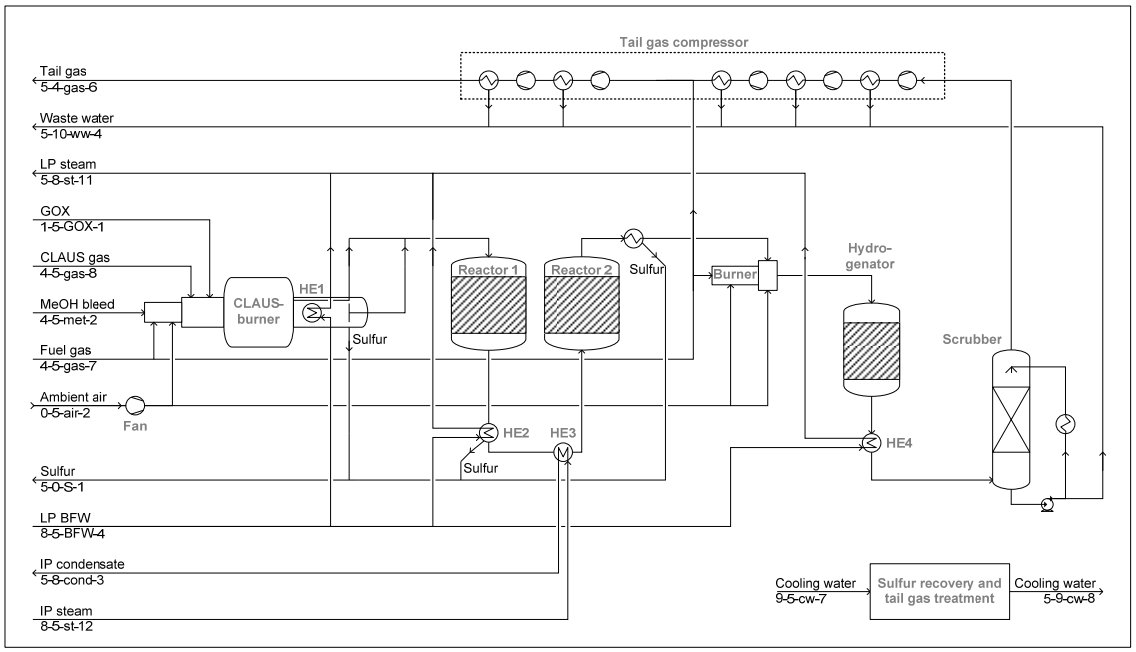

Fig. 17 Flow scheme for the sulfur recovery unit and the tail gas treatment plant

The modeled CLAUS-process consists of a thermal stage (CLAUS-burner) and two consecutive catalytic stages with intercoolers in between. According to Schreiner [55] a maximum desulfurization rate of 95 % for the CLAUS-process itself can be expected. Furthermore, Schreiner [55] mentioned that the overall sulfur recovery rate (which comprises the AGR, the SRU and the TGT process) can be as high as 99.8 % when the treated tail gas is recirculated back to the AGR.

The methanol discharge from the AGR unit is incinerated with ambient air at very high temperatures in the central muffle of the CLAUS-burner. The CLAUS-gas itself reacts with oxygen at temperatures between 950 and 1200 °C according to the following gross reaction:

$$10\ H_2S + 5\ O_2 \rightarrow 2\ H_2S + SO_2 + 7\ S + 8\ H_2O\ . \qquad (16)$$

The stoichiometry given by Schreiner [55] clarifies that about 70 % of the contained hydrogen sulfide is converted to elementary sulfur already in the thermal stage. Leaving the CLAUS-oven, the hot flue gas is cooled below the sulfur condensing temperature so that the liquid sulfur can be discharged. Gas cooling is realized in a heat recovery steam generator (HE1) using boiler feed water extracted from the combined cycle plant. A part of the hot gas is passed by the steam generator and used to adjust the inlet temperature to the first catalytic reactor by mixing with the cooled gas. Further sulfur recovery takes place in two catalytic fixed bed reactors where the remaining hydrogen sulfide and sulfur dioxide are converted according to the following:

$$2\,H_2S + SO_2 \rightarrow 3\,S + 2\,H_2O. \tag{17}$$

Carbonyl sulfides and carbon disulfides which are primarily generated at the thermal stage are effectively hydrolyzed at temperatures of about 350 °C in the first catalytic reactor [55]. Heat recovery and sulfur removal is realized in the same manner as explained for the thermal stage (in HE2 and HE3). The tail gas is indirectly heated by IP-steam condensation in front of the second catalytic rector to avoid catalyst wetting.

Due to an incomplete H_2S-conversion (caused by the limiting thermodynamic equilibrium) and practical restrictions occurring at the sulfur condensation process (sulfur nebula, [55]) the remaining tail gas still contains considerable amounts of hydrogen sulfide and sulfur dioxide. Therefore the tail gas is first heated by a burner to about 200 °C and then fed to the hydrogenation reactor where the following reaction is promoted by a cobalt-molybdenum catalyst:

$$SO_2 + 3\,H_2 \rightarrow H_2S + 2\,H_2O. \tag{18}$$

Additionally, the contained sulfur vapor is also hydrogenated while the carbon sulfides (COS, CS_2) are hydrolyzed so that the remaining tail gas essentially contains only hydrogen sulfide as sulfur compound. The necessary hydrogen for the hydro-

genation process is supplied by the fuel gas extracted from the AGR. Finally, the contained water is separated from the tail gas in a scrubber unit and during the recompression process in the intercooled compressor.

4.4.3 Modeling and Simulation of acid gas removal and treatment

The simulation model for the AGR process was developed in CHEMCAD according to the above described flow scheme and description. The thermodynamic properties were calculated taking into account the work of Chang et al. [5] that extends the Soave-Redlich-Kwong equation of state to methanol systems with light gases and/or water. The implemented absorption behavior of gases in methanol (visualized in Fig. 18 for the key gas components) builds the basis for process simulation.

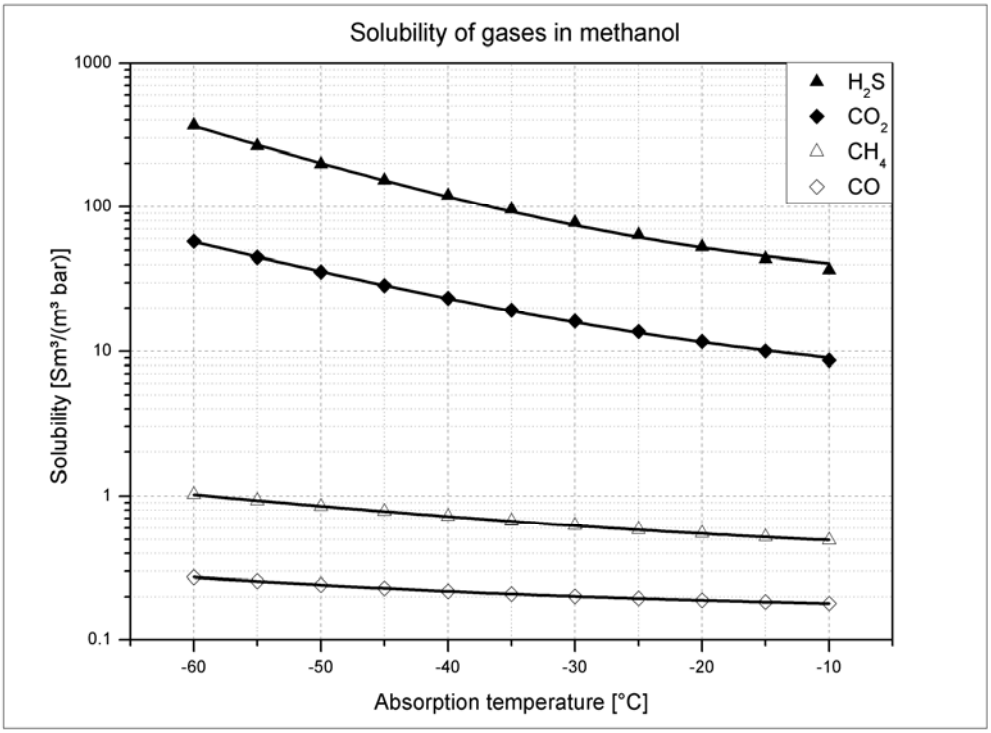

Fig. 18 Calculated solubility of gases in methanol

As an initial examination, the influence of the CO_2-partial pressure in the feed gas is investigated in order to illustrate the characteristic performance of the AGR process. Therefore calculations are performed using a typical feed gas at different operating pressures. Specific parameters are introduced for the auxiliary load and the regenerator steam demand as evaluation criteria. Table 9 shows the boundary conditions that are defined in order to generate comparable results.

Table 9 Boundary conditions for AGR process simulation

Parameter	Value
Sulfur compounds within clean gas	< 0.1 ppm(v)
Sulfur compounds within CLAUS-gas	≈ 62 mol. %
Sulfur compounds within removed CO_2	< 12 ppm(v)
CO-content within removed CO_2	≈ 250 ppm(v)

Only a few simulation parameters have to be adjusted in order to comply with the above given boundary conditions. While the amount of LP-steam for the hot regenerator is responsible for the clean gas sulfur content, the CLAUS-gas recycle rate is used to regulate the sulfur content within the CLAUS-gas. The CO_2-quality regarding the sulfur compounds is influenced by the split ratio of the CO_2-loaded methanol leaving the CO_2-absorber and the split ratio of the H_2S-free solvent to the IP-flash. Since the amount of co-absorbed carbon monoxide increases at higher operating pressures, the chosen IP-flash pressure level strongly affects the CO-content within the captured CO_2. Therefore it was also found advantageous to realize a staged IP-flash expansion (and recompression of the valuable gases) at higher operating pressures. Table 10 shows the adjusted simulation parameters for the different investigated operating pressures.

Table 10 Parameter adjustment for AGR process simulation

CO_2-partial pressure in feed gas	9.5 bar	13.5 bar	19 bar	28.5 bar
Ratio of CO_2-loaded MeOH (out of CO_2-absorber) to the H_2S-absorber	45 %	45 %	45 %	40 %
Ratio of H_2S-free solvent (out of Fl2) to the IP Reabsorber	60 %	60 %	70 %	72 %
CLAUS-gas recycle rate	42 %	30 %	18 %	0 %
(staged) IP-flash level [bar]	8.8	11.8	27/15	49/31/20

The calculation results for the partial pressure study visualized in Fig. 19a and b show an increase of the specific auxiliary load consumption and the specific steam demand at falling CO_2-partial pressures in the feed gas.

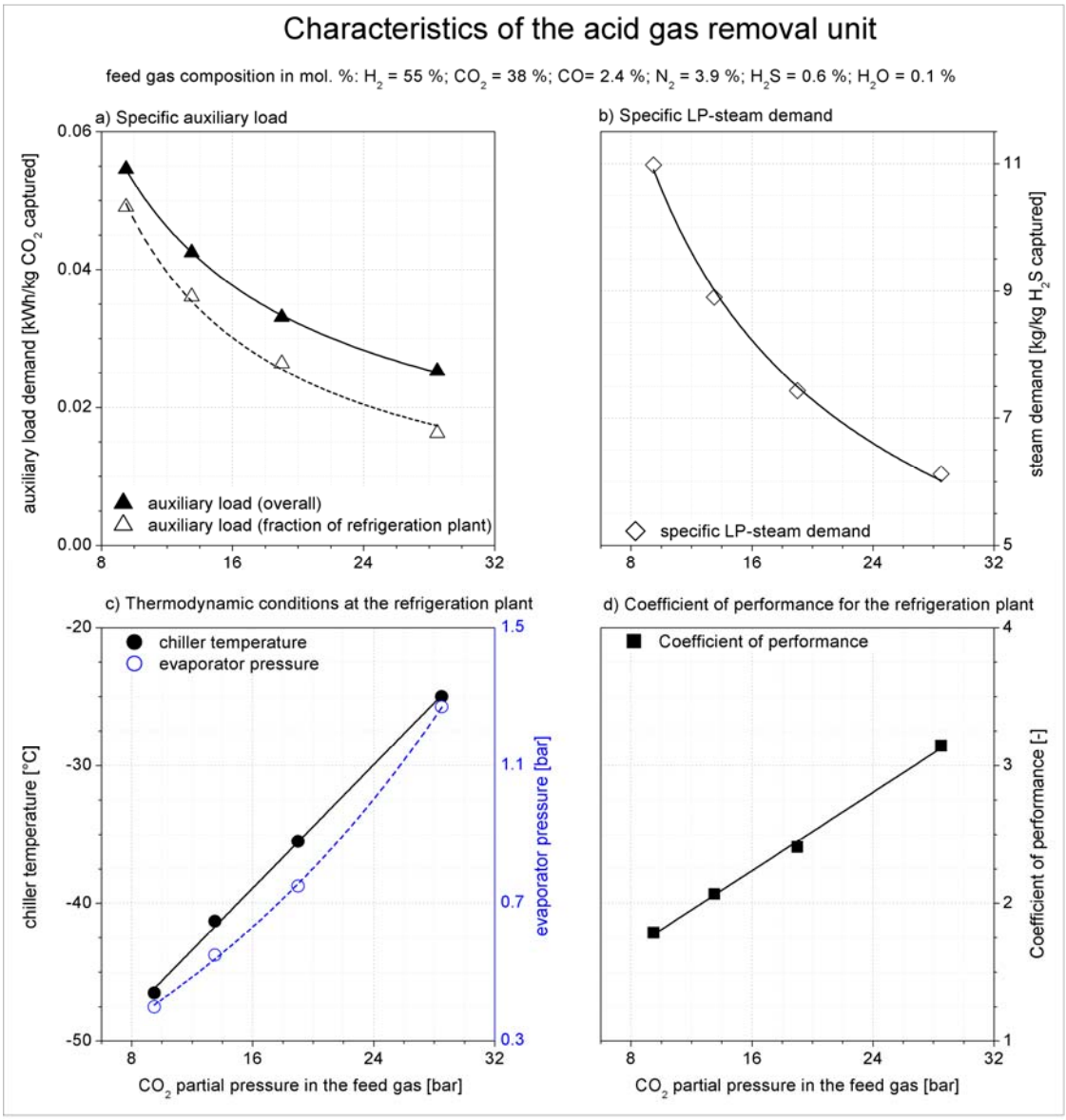

Fig. 19 Characteristics of the acid gas removal unit

The curve progression for these parameters can be well expressed by a power function so that the results are in good agreement with the information provided by Prelipceanu et al. [51] for an industrial Rectisol® process.

In addition, Fig. 19a shows that the auxiliary load fraction caused by the refrigeration plant decreases at higher CO_2-partial pressures. This is caused by a reduced

solvent flow (as a consequence of higher solubility rates; cf. Fig. 18) and by the enhanced coefficient of performance (COP) for the refrigeration process.

The latter one stands for the quality of the refrigeration plant and is defined as follows:

$$\text{Coefficient of performance} = \text{COP} = \frac{\dot{Q}_{\text{evaporator,refrigaration plant}}}{P_{\text{aux,refrigaration plant}}}. \qquad (19)$$

The COP typically rises at increasing evaporator temperatures (evaporator pressures) as the pressure ratio for vapor compression decreases. As a consequence of the higher acid gas solubility, the necessary chiller temperature can be reduced at increasing CO_2-partial pressures. Hence, the evaporator temperature (evaporator pressure) of the refrigeration plant can also be increased which yields to an enhanced COP (cf. Fig. 19c and d) and finally to a declining auxiliary load share for the refrigeration plant.

Further investigations showed that neither the CO/CO_2-rate within the feed gas nor the CO_2-capture rate influence the specific auxiliary load and the specific steam demand as long as the CO_2-partial pressure and the above mentioned boundary conditions (cf. Table 9) are kept constant.

Finally the AGR process including CO_2-compression and the SRU and TGT process are simulated for the shifted gases that are originally generated by the four different gasifier types. Since the feed gas composition differs only slightly (cf. Table 8), major distinctions between the individual concepts may only occur due to the higher feed gas pressure of the gas generated by the GE-R. The corresponding calculation results are summarized in Table 11.

Table 11 AGR calculation results for different feed gases

CC-IGCC based on gasifier:		CoP	GE-R	SCGP	Siemens
CO_2-partial pressure	bar	14.1	22.9	13.4	13.4
CO_2-capture rate			99 %		
$P_{aux,AGR/SRU/TGT}$	kWh/ kg CO_2	0.042	0.034	0.043	0.043
$P_{aux,CO2\text{-}compression}$	kWh/ kg CO_2	0,081	0,070	0,081	0,081
Clean gas: H_2-content	mol. %	87.7	91.7	89.2	90.4
Clean gas CO-content	mol. %	3.3	4.0	3.9	3.8
Clean gas CO_2-content	mol. %	0.5	0.5	0.5	0.5
Clean gas CH_4-content	mol. %	4.5	0.3	0	0
Clean gas (N_2+Ar)-content	mol. %	4.0	3.5	6.4	5.3

As expected, the higher CO_2-partial pressure favors the feed gas generated by the GE-R with regard to the specific auxiliary load. Moreover, the higher operating pressure allows an elevated reabsorber pressure so that the CO_2- compression can start at an enhanced level. Hence, the specific auxiliary load for the CO_2-compressor is also improved in comparison with the other three gases that have almost the same CO_2-partial pressure. The detailed results and modeling assumptions can be found in the Appendixes D1 – D15.

4.5 Gas turbine

The lion's share of electric power production in a CC-IGCC is realized by the gas turbine as part of the combined cycle power plant. The gas turbine process itself can be expressed by the Joule- or Brayton-cycle. The thermodynamic fundamentals are commonly known and described (e.g. [40]) so that they are not reiterated herein.

A hydrogen-rich gas as it is generated in a CC-IGCC has a much smaller volumetric calorific value and a much lower density than natural gas for which power plant gas turbines are designed for. Therefore, the combustion is characterized by significantly higher stoichiometric flame temperatures and a much higher risk of pre-ignition and flashback. Hence, the NOx emissions will exceed the natural gas values and the increased volumetric fuel flow rate will require modifications at the gas turbine fuel handling system. Operational measures as fuel gas dilution (with steam and/or nitrogen from the ASU) reduce the adiabatic flame temperature (and hence the NOx emissions) as well as the flame speed and consequently also the risk of pre-ignition and flashback [57].

On the other hand, fuel gas dilution yields to a mass flow mismatch between the compressor and the turbine section. Consequently, the gas turbine power output will increase (and may reach the mechanical limit) and compressor surge problems can occur (caused by the enlarged pressure ratio). As a result, compressor mass flow reduction realized by the variable inlet guide vanes and/or air extraction for the ASU may avoid these problems [57].

The presented investigations focus on the challenges that arise when a common power plant gas turbine is fired with hydrogen-rich fuel instead of natural gas. Therefore, a generic gas turbine simulation model was developed and used to study the influence of different boundary conditions to gas turbine performance and operation.

4.5.1 Modeling of the gas turbine process

Reliable gas turbine performance calculations require the consideration of turbine and combustion chamber cooling as well as the limitations that are caused by this. The generic gas turbine program is based on a turbine cooling model presented by Horlock et al. [27] and developed in CHEMCAD. The thermodynamic properties are calculated using the Soave-Redlich-Kwong equation of state.

As indicated in Fig. 20, gas turbine cooling is considered so that the required cooling air flow is completely extracted after the last compressor stage and introduced to the hot gas in front of the first turbine vane. This simplification is commonly accepted and yields to the standardized turbine inlet temperature (TIT; T9 in Fig. 20) [32] which is the decisive factor for the gas turbines level of technology.

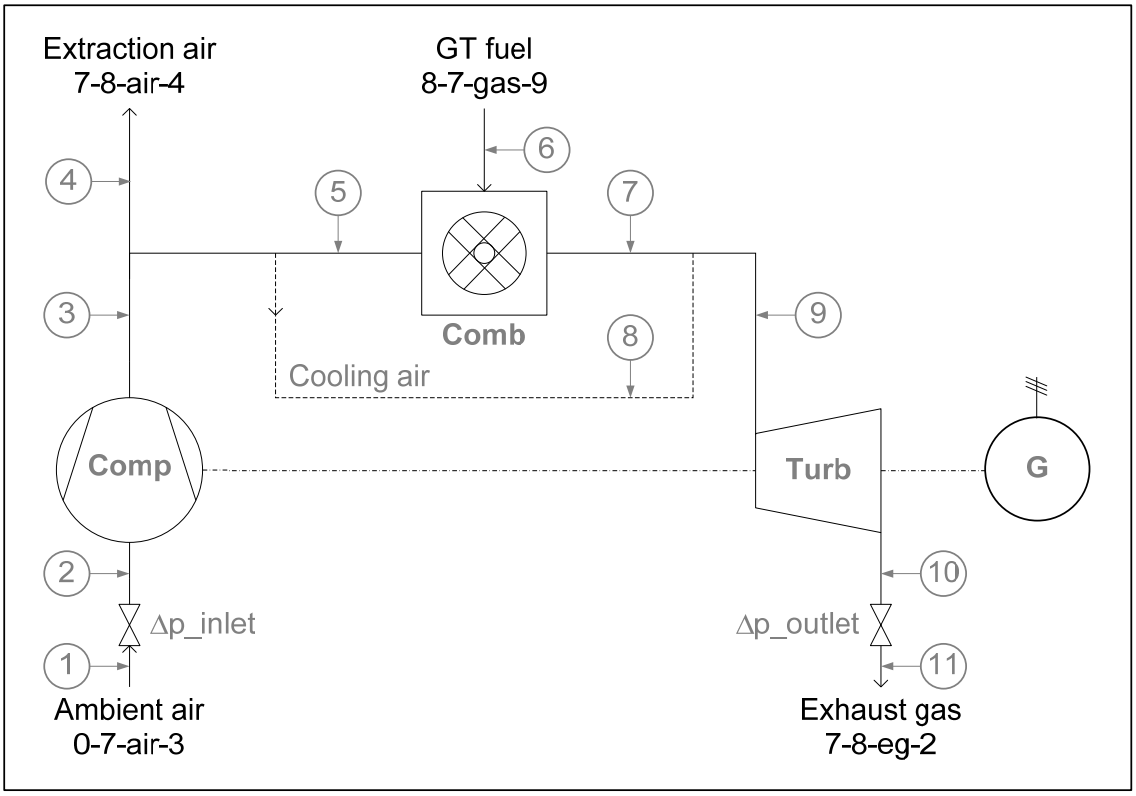

Fig. 20 Flow scheme for the gas turbine in a CC-IGCC

The applied cooling model uses a semi-empirical formula for an estimation of the required cooling air fraction to avoid turbine material overheating. The derivation of this equation is extensively described by Horlock et al. [27].Therein two essential effects of turbine cooling are carried out:

- The reduction of gas stagnation temperature at the entry to the first turbine row and
- A pressure loss resulting from mixing the cooling air to the hot gas.

The aerodynamic losses that are expressed by the latter one yield to a degradation of the polytropic expansion efficiency in contrast to a not cooled turbine.

Jonsson et al. [33] presented an application of the mentioned cooling model to a commercially available gas turbine for the purpose of performance predictions for novel cycles. The developed generic model is based on the therein described approach. Specific modeling parameters have been adjusted so that the calculated gas turbine performance matches with published performance data [56] for the Siemens gas turbine SGT5-4000F. Detailed information for this reference point calculation with natural gas fuel can be found in Appendix E1.

In contrast to Jonsson et al. [33], the gas turbine model shall not be used for design point calculations but for off-design calculations with hydrogen-rich fuel. Therefore the model has to be extended so that the turbines swallowing capacity, which affects the inlet pressure to the turbine section at non-design conditions, can be reproduced. According to Traupel [59], the turbine inlet pressure for a fixed gas turbine only depends on the particular turbine mass flow and the turbine inlet temperature so that the following equation can be applied:

$$p_9 = \frac{\dot{m}_9}{\dot{m}_{9,ref}} \sqrt{\frac{T_9}{T_{9,ref}}} \sqrt{\frac{1-\pi_{turb,ref}^2}{1-\pi_{turb}^2}} \; p_{9,ref} \tag{20}$$

The reference parameters correspond to the natural gas reference case discussed above. They are summarized in Appendix E2.

The available cooling air flow is fixed by the turbine design (reference). Hence, the cooling air fraction only depends on the compressor end pressure and the losses in the cooling air ducts. Pardemann [50] therefore suggests and verifies a simplified method to estimate the cooling air flow for off design calculations as follows:

$$\dot{m}_8 = \sqrt{\frac{\Delta p_{comb}}{\Delta p_{comb,ref}}}\ \dot{m}_{8,ref} \tag{21}$$

Implementing these correlations qualifies the generic model for off-design performance calculations and for blade temperature predictions.

4.5.2 Gas turbine process simulation

As mentioned above, fuel gas dilution and compressor air extraction are most likely necessary in a CC-IGCC because of the difficulties of hydrogen combustion. Hence, the generic model is used in a first step to investigate the principle behavior of some crucial gas turbine parameters at different fuel gas dilution and compressor air extraction rates. In this context, the blade temperature, the gas turbine power output and the compressor pressure ratio have been calculated at different turbine inlet temperatures.

Fig. 21 shows the relative deviation of these parameters from the reference values at natural gas operation for four different compressor air extraction rates. The compressor inlet flow has been kept constant at the reference value to suppose full load operation. The calculations are performed with the purified fuel gas originally generated by the Siemens gasifier (cf. Table 8) assuming steam (maximum 10 mol. %) and nitrogen dilution in order to adjust a fuel gas hydrogen content between 45 and 90 mol. %.

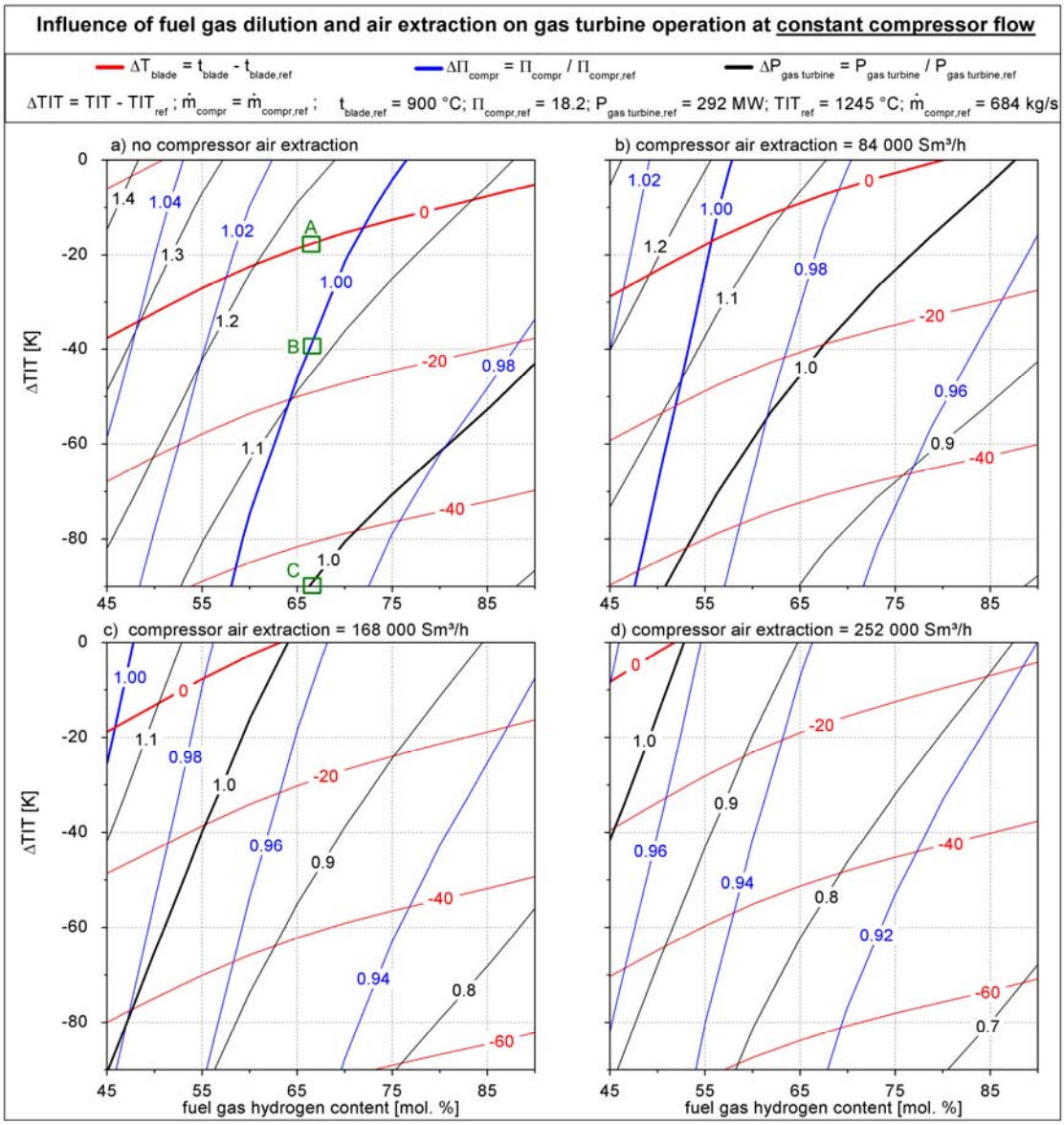

Fig. 21 Influence of fuel gas dilution and air extraction on gas turbine operation at constant compressor flow

Considering the results presented in Fig. 21 the following can be noticed:

- For a constant TIT, the blade temperature, the compressor pressure ratio and the gas turbine power output increase at rising fuel gas dilution rates (decreasing fuel gas hydrogen content).
- Without compressor air extraction and TIT-reduction, the aforementioned gas turbine parameters are significantly higher than at reference conditions (natural gas fuel).

- Without compressor air extraction, the TIT has to be drastically reduced in order not to exceed the reference values. For clarification refer to Fig. 21a – assuming a possible fuel gas hydrogen content of 67 mol. %:
  - The TIT has to be reduced by about 18 K in order not to exceed the reference blade temperature (point A),
  - the TIT has to be reduced by about 39 K in order not to exceed the reference compressor pressure ratio (point B),
  - the TIT has to be reduced by about 90 K in order not to exceed the reference gas turbine power output (point C),
- Compressor air extraction reduces the necessary TIT-reduction to reach the same values for compressor pressure ratio, power output and blade temperature as at reference conditions.

The observed behavior is a consequence of the increased hot gas flow through the turbine section in comparison to the natural gas reference case. The enlarged hot gas flow yields to an increase of the compressor pressure ratio, the gas turbine power output and the blade temperature. The increase of the blade temperature is a consequence of the almost unchanged cooling air flow in relation to the design (reference) value. As mentioned above, the cooling air flow is limited through the turbine design. An increased hot gas flow and an unchanged cooling air flow inevitably involve an increase of the blade temperature.

Concluding it can be stated that the IGCC-performance would suffer from the tremendous TIT-reduction that is necessary when the gas turbine is operated according to the assumed principle.

For this reason, compressor mass flow reduction is identified as an additional operational measure. In this way, the hot gas flow through the turbine section is reduced so that the crucial gas turbine parameters can be kept at an acceptable level. As indicated above, compressor flow control can be technically realized by the variable inlet guide vane at the entry of the compressor.

Assuming the same boundary conditions, the influence of fuel gas dilution and air extraction on gas turbine operation is investigated again but now considering the compressor part load, too. The compressor mass flow is chosen to control the gas turbine power output so that the reference value may not be exceeded. The hot gas temperature (T7 in Fig. 20) that can be adjusted via the individual fuel mass flow

also acts as a variable but for blade temperature control and TIT control. For all three temperatures the maximum is defined at the reference value (natural gas). Fig. 22 illustrates the corresponding results.

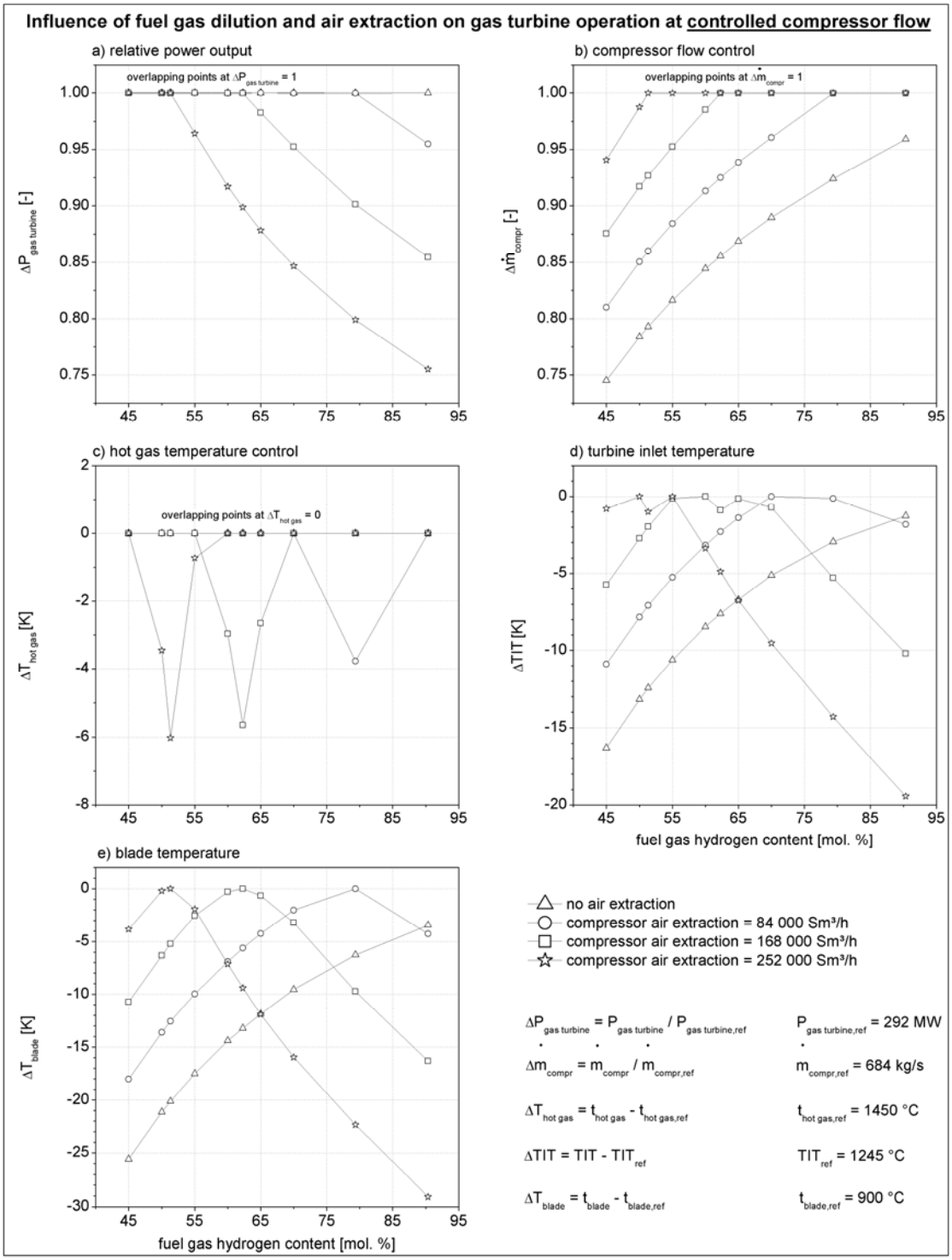

Fig. 22 Influence of fuel gas dilution and air extraction on gas turbine operation at controlled compressor flow

As shown, the compressor has to be operated in part load for the complete possible fuel gas hydrogen range when air extraction is not applied and the gas turbine power output must not exceed the reference value. Due to the reduced hot gas flow, the blade temperature and the TIT are always below the reference value although the hot gas temperature is kept at the maximum.

In the case of 84 000 Sm^3 extraction air, the compressor mass flow has to be reduced for power output control at fuel gas hydrogen contents below 79 mol. %. Additionally, the hot gas temperature has to be derated at this corner point to avoid a higher blade temperature as at reference conditions. Below this hydrogen content, the hot gas temperature can be kept at the maximum as the blade temperature and the TIT stay below the reference. This behavior is also caused by the decreasing hot gas flow.

The behavior at the other two air extraction rates is similar to the latter one with the difference that the compressor flow has to be reduced only at fuel gas hydrogen contents below 62 mol. % (at 168 000 Sm^3/h extraction air) and 51 mol. % (at 252 000 Sm^3/h extraction air), respectively. For both cases, the hot gas temperature has to be derated at the individual corner point by about 6 K in order to keep the blade temperature within the limit. Furthermore, a slight hot gas temperature reduction is necessary within the corner point area to avoid a higher TIT as at reference conditions.

In general it can be noticed, that the highest blade temperature is achieved at that fuel gas hydrogen content where the gas turbines mechanical limit is reached and its compressor is barely operated at full load flow. The highest TIT is also obtained within the area of this corner point and its maximum shifts with decreasing air extraction rates to higher hydrogen contents. The gas turbine efficiency is not illustrated as it makes only sense to consider it in one context with the ASU auxiliary load. Nevertheless, the range where a high TIT is achieved indicates an optimal gas turbine performance. The influence to the overall IGCC performance will be clarified in one of the subsequent chapters.

In a continuative investigation, the gas turbine model and the generated findings are used to carry on the comparison of the IGCC cycles that are based on the four different gasifier types.

Therefore the individual gases are conditioned so that a fuel gas hydrogen content of 45 mol. % is adjusted (described in previous chapters). Nowadays this value represents the upper limit for the fuel gas hydrogen content of advanced power plant gas turbines (cf. Gräbner [21] and Smith [57]).

Gas turbine operation is simulated considering compressor air extraction of 252 000 Sm^3/h for all cases.

Same as above, the compressor mass flow and the hot gas temperature are used to control the power output and the TIT, respectively so that the reference values are reached (power output) or not exceeded (temperatures).

Table 12 summarizes some calculation results.

The complete heat and material balances as well as the CHEMCAD flow schemes can be found in Appendixes E3 to E7.

Table 12 Gas turbine calculation results for different fuel gases

Parameter	Unit	CoP	GE-R	SCGP	Siemens
$\Delta m_{compressor}$	%	99	94	94	94
$\Delta T_{hot\ gas}$	K	-3	0	0	0
ΔTIT	K	0	0	-1	-1
ΔT_{blade}	K	0	-3	-4	-4

As it can be seen, gas turbine operation is very similar for all of the investigated concepts. The sole noticeable difference is observed at the CoP case where the compressor mass flow has to be derated only by about one percent compared to the reference value (instead of 6 % at the other cases). This is caused by the fact that the fuel gas generated by the CoP gasifier contains a considerable amount of methane which in turn involves a higher LHV than at the other three cases. As a consequence the necessary fuel gas mass flow decreases so that the compressor inlet mass flow can be enlarged to reach the reference power output of 292 MW. The higher blade temperature at the CoP case is again caused by the augmented hot gas flow.

4.6 The water-/steam cycle

The water-/steam cycle of the CCPP represents the final major sub process within the direct IGCC process chain. It is powered by the gas turbine exhaust gas and connected to all of the upstream processes.

Fig. 23 shows the developed flow scheme for the water-/steam cycle of the CC-IGCC. The mayor elements are the heat recovery steam generator (HRSG) and the steam turbine with condenser. Cooling water heat removal is realized by a conventional wet cooling tower which however is not part of the further investigation. The HRSG has three different pressure levels (HP, IP, LP) with one reheat stage and represents therefore the state of the art design for CCPPs driven by advanced F-class gas turbines [21]. Consequently, the steam turbine is characterized by a high pressure section, an intermediate pressure section and a low pressure section.

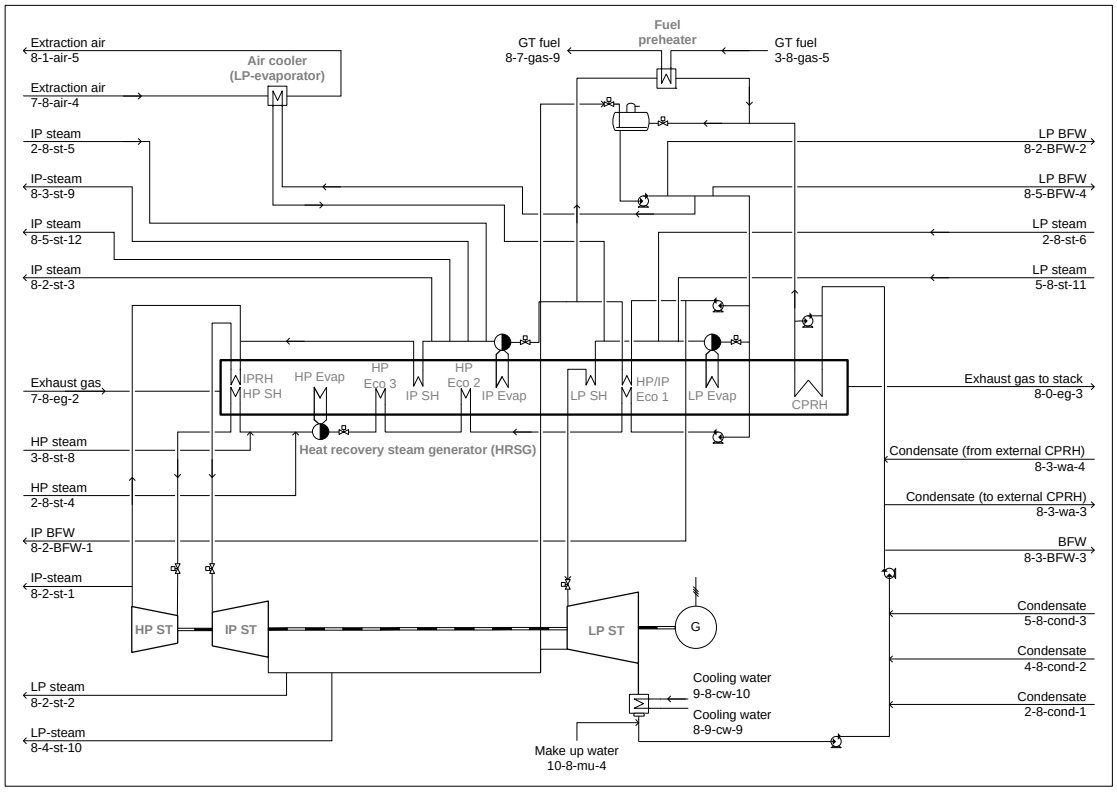

Fig. 23 Flow scheme for the water-/steam cycle in a CC-IGCC

The arrangement of the HRSG heating surfaces is a result of thermodynamic simulations aiming at exergy loss minimization. Each pressure level contains economizer, evaporator and superheater segments which are individually placed so that they fit optimally to the temperature range of the exhaust gas.

As indicated above, the water-/steam cycle serves the heat demand of the up-stream processes via numerous interfaces. At the same time, it also acts as the supplier of boiler feed water and superheater for saturated steam which is generated for instance at the raw gas cooling section. Furthermore, fuel gas preheating and cooling of the air that is extracted from the gas turbines compressor are realized within the cycle.

4.6.1 Modeling and simulation of the water-/steam cycle

A process simulation model is developed in CHEMCAD according to the above given flow sheet. The thermodynamic properties for all gaseous process streams are calculated by the use of the Soave-Redlich-Kwong equation of state. Water and steam properties are considered corresponding to international standards.

Water-/steam cycle simulations for CCPPs are common practice in the power plant business. The ambitious part is always the design of the HRSG. This in turn is profoundly affected by the chosen temperature differences at the individual pinch points and approach points. These temperature definitions and the basics of HRSG design are perfectly described by Lechner [40].

The Q,t - diagram of the HRSG is predestinated to explain the process of boiler design. Fig. 24a shows one of a HRSG in a conventional, natural gas fired CCPP.

For a given exhaust gas flow and a chosen HP evaporator pressure, boiler design takes place as follows:

- First, the temperature difference at the pinch point of the HP evaporator and the temperature difference between the gas turbines exhaust gas and the temperature of live steam and reheat steam have to be chosen.
- Once this is done, the amount of heat available for HP evaporation, superheating and reheating is fixed.
- Then, heat balance calculations give the HP steam flow as soon as the grade of sub cooling at the HP evaporator inlet is chosen. The necessary HP feed water is preheated in staged heating surfaces so that it enters the steam drum just slightly sub cooled.
- The producible amounts of IP and LP steam are achieved in the same way.

As it can be seen in Fig. 24a, the HP path consumes the lion's share of the exhaust gas energy. The other two pressure levels are subordinated and preserve only that heat which is not required at the HP level. Nevertheless, they are necessary in order to minimize the exhaust gas losses. The quantity of IP steam and LP steam is directly influenced by the temperature difference at the HP pinch point. It can only be augmented by an increase of the HP pinch point which however goes at the expense of efficiency.

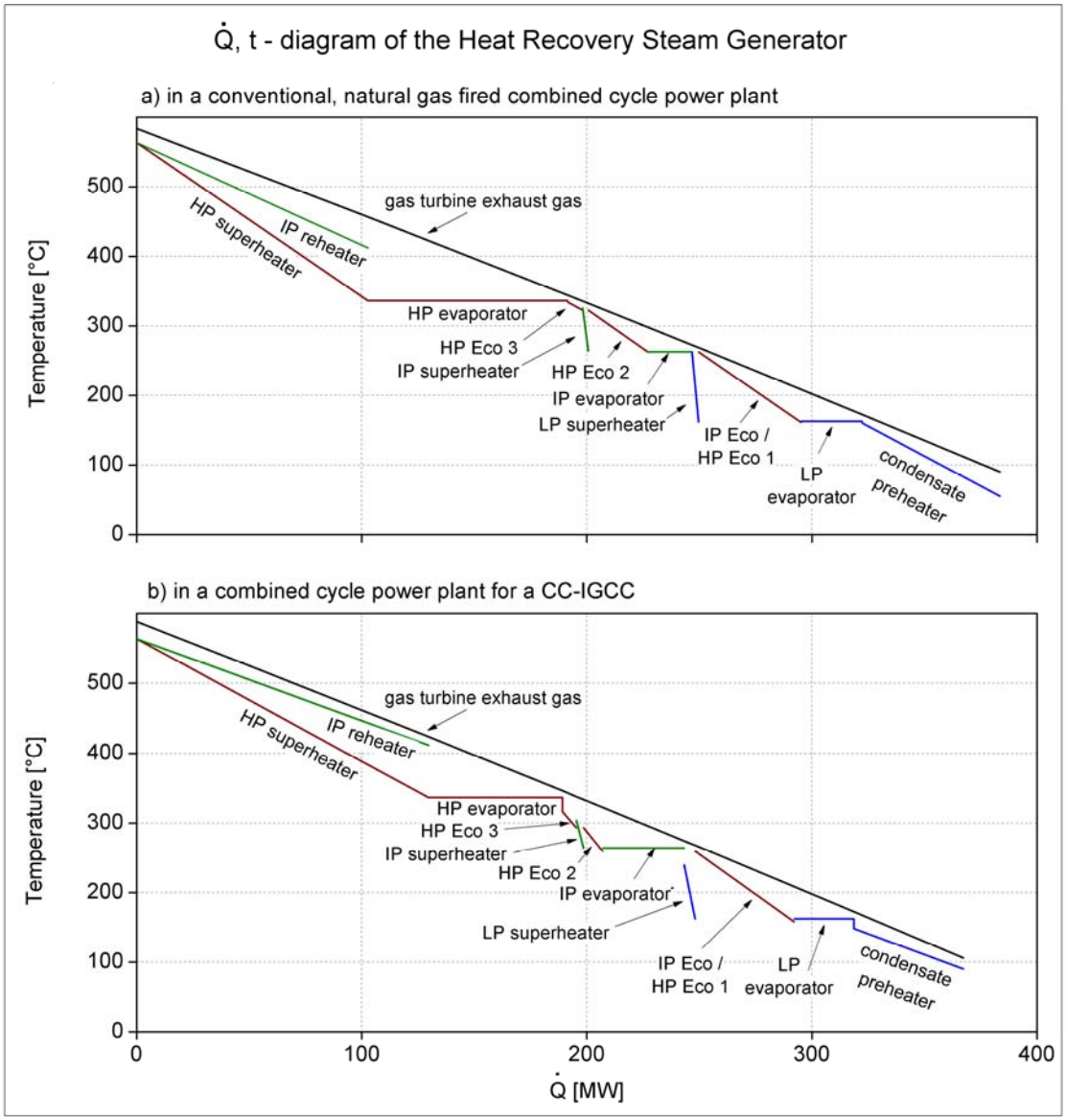

Fig. 24 Q,t – diagram of the heat recovery steam generator

Although HRSG design for a CC-IGCC follows the same principles, the Q,t – diagram looks somewhat different. Fig. 24b shows the diagram for the concept based on the SCGP. As it can be seen, the superheater and the IP reheater consume about 30 %

more exhaust gas energy as at the conventional HRSG. At the same time, the heat flow to the HP evaporator is reduced by this amount. This is caused by the additional steam flow received from the CSC which has to be superheated in the HRSG. Consequently, less energy remains for the HP evaporator and the therein generated steam flow decreases. Hence, the heat demand of the HP economizers 2 and 3 also drops, which in turn shifts more exhaust gas energy to the IP evaporator. This process yields to an increased flow of IP steam and feed water so that the HP/IP economizer and the LP evaporator consume about the same exhaust gas energy as at the conventional case. Since the boiler feed water for the CSC is warmed within the condensate preheater (CPRH), the overall condensate flow is markedly increased in comparison to the conventional HRSG. A part of the condensate is externally preheated within the CO-shift cycle as shown in Fig. 14.

With regard to the temperature differences, especially the IP reheater and the CPRH show considerably lower values in comparison to the conventional HRSG. This again is a result of the mass flow mismatch caused by the strong integration of the water-/steam cycle with the upstream processes.

As the temperature differences and the transferred heat strongly affect the heating surface area, a comparison of the four CC-IGCC concepts is conducted. Therefore, the individual water-/steam cycles are simulated considering all interfaces to the other processes. The heating surface areas are calculated according to the following:

$$A_{\text{heating surface}} = \frac{\dot{Q}}{k\ \Delta t_m} \tag{22}$$

where k represents the heat transfer coefficient and Δt_m the mean logarithmic temperature difference. In accordance to VDI-Wärmeatlas [61] a value of 50 W/m^2K seems to be a good approximation for the heat transfer coefficient. For the purpose of concept comparison, this k-value is kept constant for all heating surfaces and all compared concepts.

Fig. 25 shows the calculated heating surface areas for the different CC-IGCC concepts in comparison to a conventional HRSG. As supposed, the HP superheater and

the IP reheater are significantly larger and the HP evaporator and HP economizer considerably smaller than at the reference boiler. As a result, the IP evaporator and IP economizer surfaces are sized larger. The heating surface areas for the IP superheater, the LP evaporator and the CPRH just slightly differ from the reference. All in all, the GE-R case shows the highest deviations as the water-/steam cycle has to handle the largest amount of saturated HP steam (generated at the RSC and at the CO-shift as well).

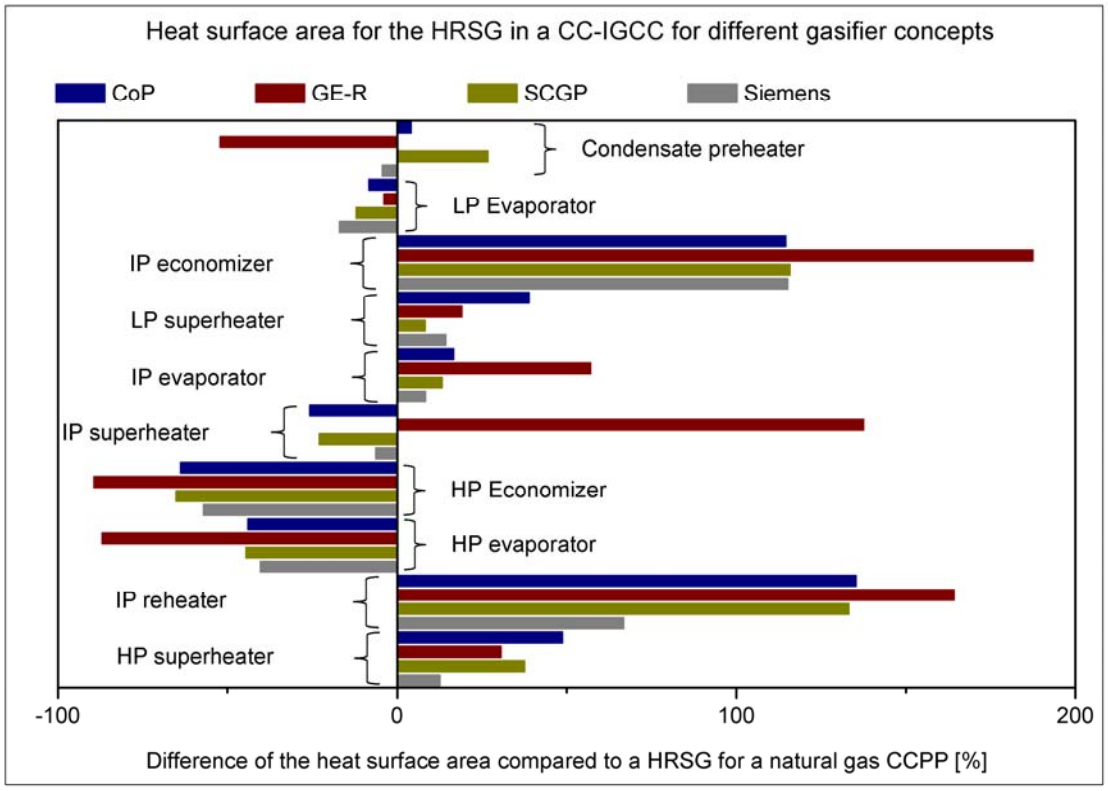

Fig. 25 Heat surface area for the HRSG in a CC-IGCC

The overall results are helpful, especially when CCPP operation on back up fuel (natural gas) has to be considered. For natural gas operation, the heating surfaces are either too small (e.g. the HP evaporator) or too large (e.g. the IP reheater) which in fact entails efficiency penalties, caused for instance by a required water injection to the superheated steam. A detailed economic analysis based on the planned operating regime (expected operating hours on coal and natural gas as well as the corresponding fuel prices) is necessary to optimize the HRSG-design. As a result the design of the individual heating surfaces might be adjusted. However, this analysis goes beyond the scope of the presented investigation.

At the end, the performance results of the water-/steam cycle simulations are summarized in Table 13. In accordance to [21], the auxiliary load of the combined cycle process is estimated to be 2.2 % of the CCPPs gross power output. The boundary conditions, the CHEMCAD flow schemes and the heat and material balances for the individual cycles can be found in the Appendixes F1 to F9.

Table 13 Performance results of water-/steam cycle simulation

Parameter	Unit	CoP	GE-R	SCGP	Siemens
$P_{steam\ turbine,\ gross}$	MW	175.1	200.7	176.7	169.4
$P_{CCPP,\ aux}$	MW	10.3	10.8	10.3	10.2

4.7 Air separation unit

Since the air separation unit is the by far biggest auxiliary load consumer of a CC-IGCC, special interest is laid on its process description as well as on modeling and simulation in order to detect optimization potential. As already mentioned, the ASU not only supplies oxygen to the gasifier and the SRU but also nitrogen to the pneumatic coal feeding system (only for the SCGP and Siemens gasifiers) and for fuel gas dilution purposes. The considerable amounts of the diluent nitrogen as well as the need for gas turbine air integration are responsible for special boundary conditions compared to a conventional ASU for chemical processes. Conventional units usually are designed for quite low operating pressures (approximately 5-6 bar). For CC-IGCC, an elevated pressure concept might be superior.

In the following the cryogenic air separation process is described based on a common ASU flow sheet applying the classical double-column arrangement. Building on that, a process simulation model is developed and used for simulation of a wide range of operating scenarios. The specific auxiliary load consumption is calculated and illustrated dependent on the level of air and nitrogen integration. Based on that, a decision can be made if a low or an elevated pressure ASU should be applied.

The sophisticated three-column distillation ASU which is supposed to be energetically advantageous at operating pressures higher than 12 bar [21] is not considered, since there is only one reference unit operating worldwide (AVESTA, Finland). Therefore, this technology does not represent the state of the art. Moreover, this configuration is much more complex and inflexible to load changes (ibid, page 77-78 in AP2001) so that it is rather not qualified for nowadays electricity grid requirements.

4.7.1 Fundamentals of air separation and process description

The subsequently described process represents one out of a multiplicity of possible configurations [21]. It is used to clarify the fundamental coherences while it is not claimed that the chosen process represents the optimum configuration for each CC-IGCC.

Referring to Fig. 26 a conventional cryogenic air separation process can be described as follows: First, the ambient air is compressed in the Main Air Compressor (MAC) and then cooled and purified from dust, water, carbon dioxide, and other unwanted impurities.

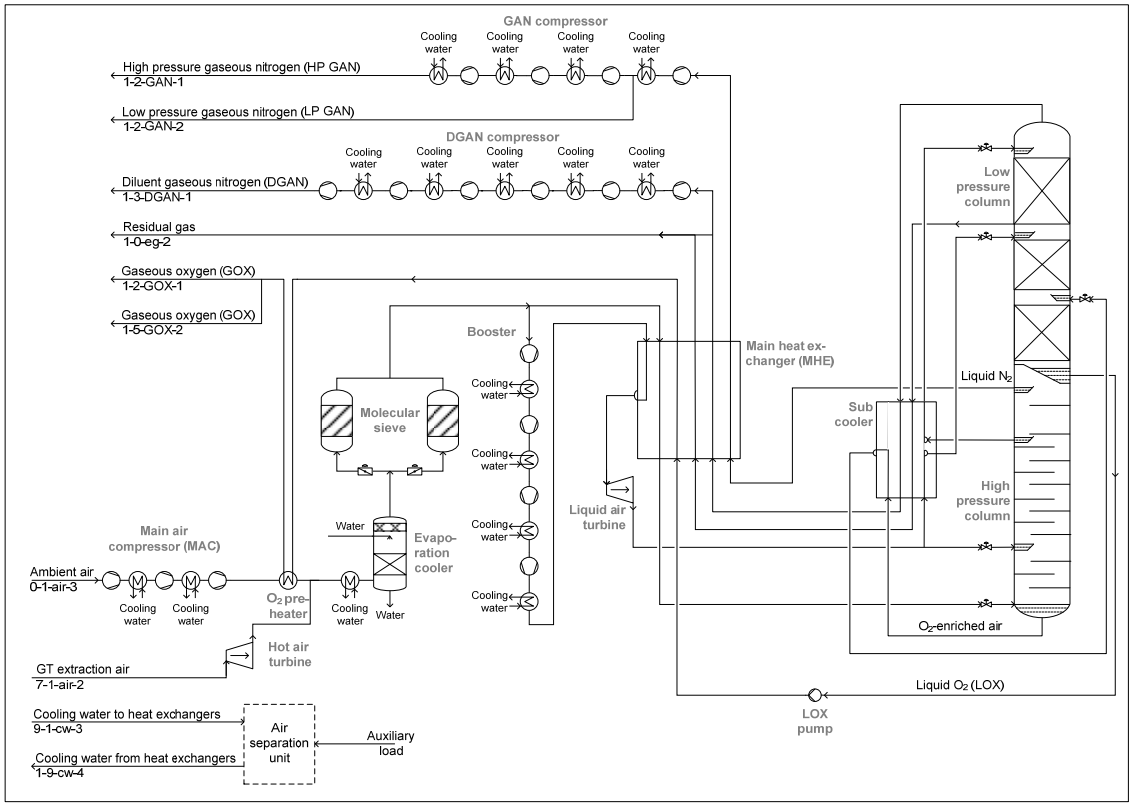

Fig. 26 Process flow diagram of the low pressure air separation unit

In case of gas turbine air integration a part or all of the required air is extracted from the gas turbine. As air extraction takes place downstream the gas turbine compressor, the extracted air needs to be expanded (due to the higher pressure level of common gas turbines) in the hot air turbine to the required operating pressure of the ASU.

Thereafter, one part of the air is cooled down close to its condensing temperature (ca. 1 K superheated) within the main heat exchanger (MHE) before it is fed to the last stage of the high pressure distillation column (lower column). The remaining part of the air is compressed up to approximately 70 bar in a booster unit with intercoolers, then liquefied within the MHE and depressurized in the liquid air turbine for energy recovery and concurrent sub cooling. Subsequently, the liquid air is split so that one part is throttled (by taking advantage of the Joule-Thomson-effect) and fed to the lower column. The remaining liquid is sub cooled, throttled and fed to the low pressure distillation column (upper column).

The split-distribution of gaseous and liquid air as well as the specific feed and extraction stages are optimization parameters that are individually found in order to compensate the heat losses and fulfill the energy balance.

Within the high pressure column the pre-separation of air takes place. Due to the fact that the evaporation temperature of nitrogen is lower than that of oxygen (argon is in between), an oxygen-enriched liquid (about 35 mol. %) accumulates at the bottom while a nitrogen-rich vapor rises to the top of the column. After liquefaction within the condenser of the high pressure column, one part of the nitrogen-rich stream can be extracted as an ultraclean product. Another part is used as reflux for the lower column while the remaining is sub cooled and fed as reflux to the upper column.

The oxygen-enriched stream leaving the high pressure column is sub cooled, throttled and fed to the low pressure column where the final separation takes place. So, the oxygen product with its desired purity is distilled at the bottom of the upper column and subsequently pumped to the required pressure before it is evaporated in the MHE.

At the top of the upper column diluent gaseous nitrogen (DGAN) and a few stages below a residual gas can be taken off. The individual amount of the latter one affects the DGAN-purity and is therefore used for DGAN purity-adjustment, especially at higher operating pressures of the ASU.

Pure liquid nitrogen is extracted at the top of the lower column before it is evaporated in the MHE. After compression to the required pressure levels it is used as gaseous nitrogen (GAN) for the coal preparation and feeding process.

Inside the distillation column an intensive contact between liquid and vapor is realized where both intend to reach the equilibrium state. To achieve this, the rising vapor needs to lower its oxygen content which is realized by partial condensation of oxygen. The released condensing enthalpy yields to an evaporation of nitrogen out of the liquid phase so that the liquid also approaches its equilibrium condition.

Fig. 27 shows the equilibrium composition of boiling oxygen-nitrogen mixtures at different pressure levels. The equilibrium data are an integral part of the database implemented in CHEMCAD. As it can be seen, the dew point curve and the bubble point curve approach each other at rising operating pressures. Hence, air separa-

tion at higher pressures is hampered and requires a higher number of separation stages as well as a higher reflux ratio.

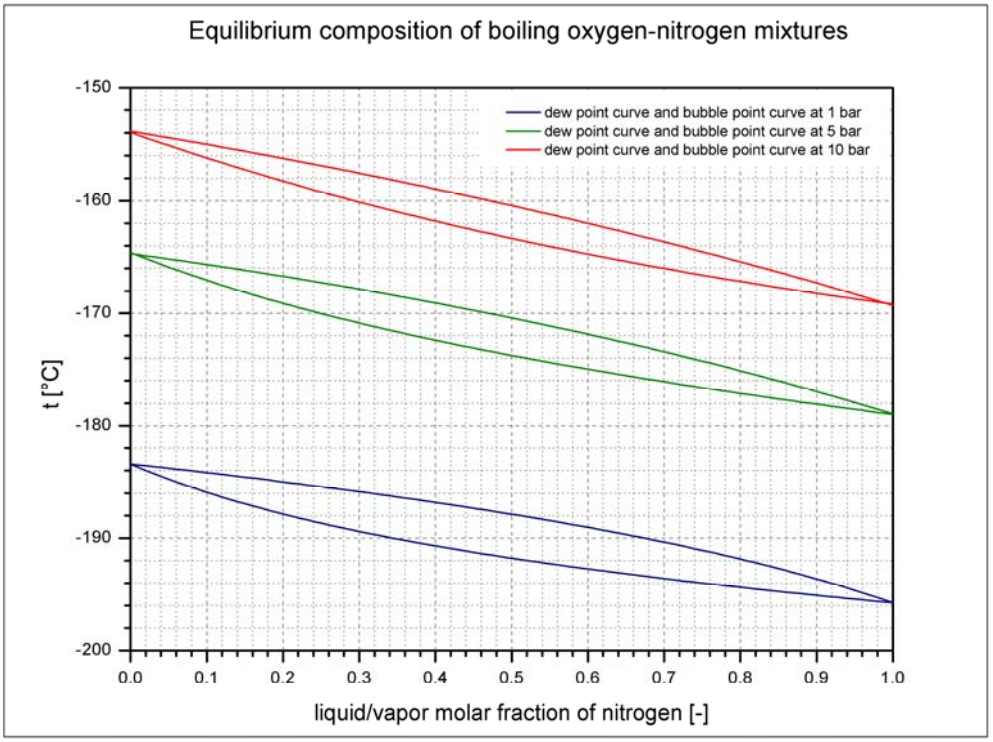

Fig. 27 Equilibrium composition of boiling oxygen-nitrogen mixtures

The pressure difference between the upper and the lower distillation column is a fundamental factor which significantly influences the operating conditions of the ASU. is the pressure level is determined so that the nitrogen vapor at the top of the lower column condensates at a slightly higher temperature (2 … 3 K) as the temperature of boiling oxygen at the bottom of the upper column. In doing so, the released condensing enthalpy can be transferred to the upper column and realize the heat supply for evaporation. As a consequence, the upper and the lower column are thermally coupled which means that the condenser of the lower column acts as the reboiler of the upper one. The determination of pressure levels for the high and low pressure column is visualized for two different examples in Fig. 28.

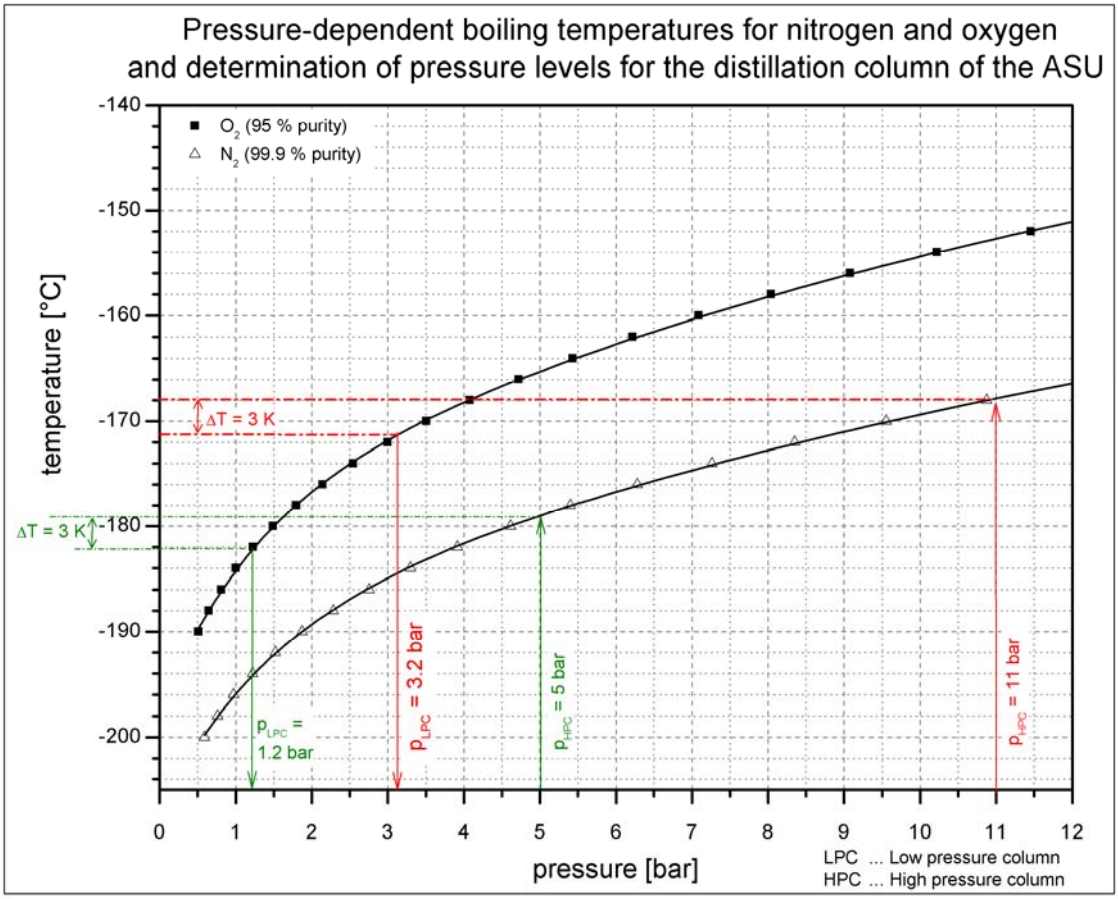

Fig. 28 Pressure-dependent boiling temperatures for nitrogen and oxygen and determination of pressure levels for the distillation column of the ASU

As it can be seen the evaporation temperatures of oxygen and nitrogen depart from each other with rising pressures. Therefore the necessary pressure difference (pressure loss) between upper and lower column increases at higher operating pressures. Fig. 28 illustrates an increase of pressure loss from roughly 4 bar to approximately 8 bar when the operating pressure in the lower column is increased from 5 to 11 bar. Consequently the compression energy for the MAC increases at higher column pressures. Nevertheless an elevated pressure ASU might be superior (especially at high DGAN-demands) since the pressure ratio for DGAN-compression is considerable reduced compared to a conventional low pressure concept.

4.7.2 ASU simulation models

For ASU simulation, two different models are developed in CHEMCAD. While the first model is used for the simulation of a low pressure concept, the second is used to simulate an elevated pressure one. Both models adopt a similar configuration and differ only in detail.

The simulation model for the low pressure concept is based on the process arrangement (Fig. 26) and the description given in 4.7.1.

For the elevated pressure concept, the differences result from the higher distillation pressure and influence the necessary compressor and column stages as well as the compensation of heat losses. To enhance the oxygen yield, a part or the compressed DGAN is recycled, liquefied and used as reflux for the lower column. Therefore the air supply to the lower column is omitted. Table 14 summarizes the main differences between the low and the elevated pressure concept.

Table 14 Main differences between the developed ASU-models

Component	Low pressure ASU	Elevated pressure ASU
MAC	3 stages (to 5.8 bar)	4 stages (to 12 bar)
Hot air turbine	Expansion to 5.8 bar	Expansion to 12 bar
Lower column	35 theoretical stages	45 theoretical stages
	5.1 bar pressure	11.3 bar pressure
Upper column	25 theoretical stages	45 theoretical stages
	1.3 bar pressure	3.5 bar pressure
GAN compressor	4 stages	3 stages
DGAN compressor	6 stages	4 stages
Residual gas expander	No (not possible)	Yes (from 3 to 1 bar)

The process flow diagram for the elevated pressure concept can be found in Appendix G1. The developed CHEMCAD flow sheets for the low pressure ASU and the elevated pressure ASU are shown in the Appendixes G2 and G3.

The developed process models simulate an interconnection of turbo machineries, heat exchangers and distillation columns. The first two elements are simply specified by setting the efficiency and the pressure ratio and the temperature differences respectively. The distillation columns are calculated using the principle of equilibrium stage. That is to say, that the equilibrium state for each component (air can be considered as a mixture of nitrogen, oxygen and argon) at each stage is calculated by solving the so called MESH-equations (MESH: Material balance, Equilibrium condition, Summation condition, Heat balance) [18]. The equilibrium stage is also known as the theoretical stage since the practical necessary number of stages is achieved by considering the stage efficiency. Cubic equations are proved for calculation of vapor-liquid equilibriums. Out of these equations, the Peng-Robinson equation of state delivers reliable data especially at very low temperatures and is therefore preferred for the calculation of cryogenic processes. Hence, it has been chosen for the calculation of thermodynamic properties. Special care has to be taken for the placement of the feed and extraction stages of the distillation columns. A steady curve progression for the vapor and liquid composition indicates the correct position of the feed streams, as the compositions of the feed streams have to coincide with the vapor or liquid composition at the corresponding column stage. In Fig. 29 the vapor and liquid compositions inside the upper column are illustrated for the low pressure concept as an example. The steady curve progression indicates the correct placement of the feed streams.

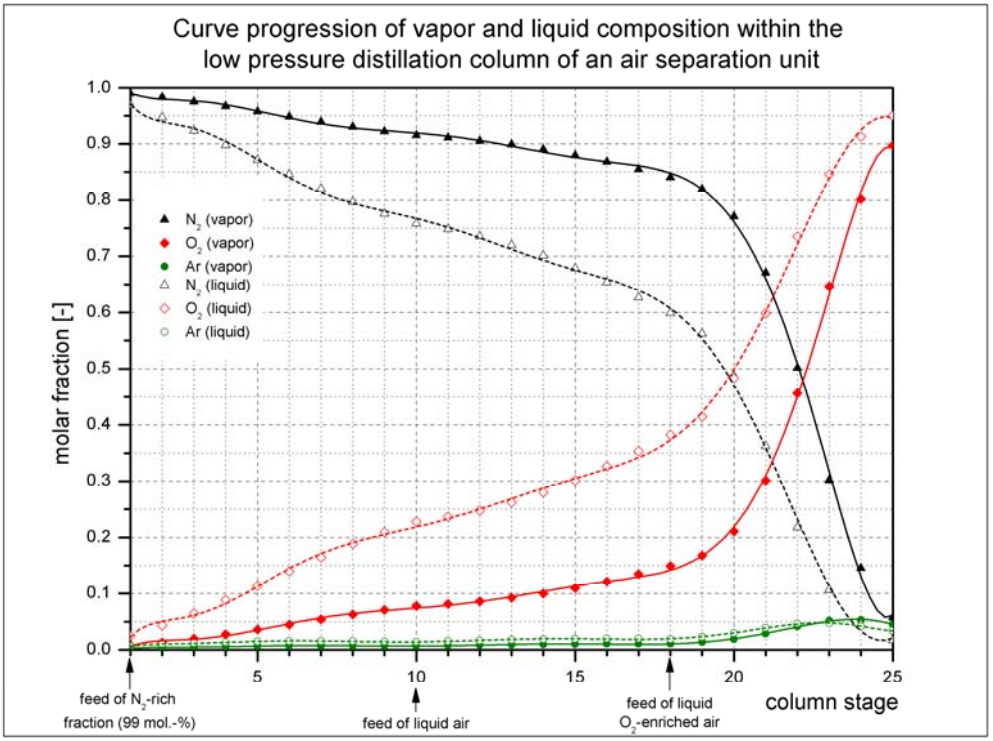

Fig. 29 Vapor and liquid composition inside the low pressure column of the ASU

4.7.3 Simulation of ASU operating scenarios

The auxiliary load for an ASU within a CC-IGCC mainly depends on the level of air integration and the DGAN demand for fuel gas dilution. Therefore, the developed ASU models are used for simulations covering a widespread operating area for these two factors. The following parameters are defined for process assessment:

Specific auxiliary load: $$P_{ASU,spec} = \frac{P_{ASU,aux}}{\dot{V}_{GOX}} \quad \left[\frac{kWh}{Sm^3GOX}\right] \tag{23}$$

Level of air integration: $$= \frac{\dot{V}_{GT\ extr.\ air}}{\dot{V}_{air,ASU}} \quad [\%] \tag{24}$$

Specific air integration: $$K_{ASU,air} = \frac{\dot{V}_{GT\ extr.\ air}}{\dot{V}_{GOX}} \quad \left[\frac{Sm^3 extr.air}{Sm^3GOX}\right] \tag{25}$$

Specific DGAN demand: $$K_{ASU,DGAN} = \frac{\dot{V}_{DGAN}}{\dot{V}_{GOX}} \quad \left[\frac{Sm^3\ DGAN}{Sm^3\ GOX}\right] \tag{26}$$

Specific HP GAN demand: $$K_{ASU,HP\ GAN} = \frac{\dot{V}_{HP\ GAN}}{\dot{V}_{GOX}} \quad \left[\frac{Sm^3\ HP\ GAN}{Sm^3\ GOX}\right] \tag{27}$$

Specific LP GAN demand: $$K_{ASU,LP\ GAN} = \frac{\dot{V}_{LP\ GAN}}{\dot{V}_{GOX}} \quad \left[\frac{Sm^3\ LP\ GAN}{Sm^3\ GOX}\right] \tag{28}$$

The air demand for the separation process and the available amount of DGAN slightly vary for the different ASU operating pressures. Hence, the levels of air and nitrogen integration are ambiguous parameters when comparing air separation units since they stand for different absolute amounts of extraction air and DGAN. Therefore, the aforementioned parameters $K_{ASU,air}$ and $K_{ASU,DGAN}$ are introduced as alternative expressions.

For ASU processes that have to supply GAN for the coal preparation and feeding process, the GOX-specific HP and LP GAN demand have to be considered as well.

The GAN and DGAN demands are not physically influenced by the amount of GOX. They are only referred to the amount of GOX in order to simplify concept assessment.

A series of simulations have been conducted for various air integration levels and specific DGAN demands, both for the low pressure and the elevated pressure concept as well. The calculations were carried out for an ASU that produces oxygen and nitrogen for a dry feed entrained flow gasification process in a CC-IGCC power plant. The underlying boundary conditions are summarized in Table 15.

Table 15 Boundary conditions for ASU simulation

Stream	Parameter	Value
GOX	Purity	95 mol. %
	Conditions	50 bar; 60 °C
HP GAN	Purity	< 0.1 mol. % O_2
	Conditions	70 bar; 70 °C
	$K_{ASU,HP\ GAN}$	0.30 Sm^3 HP GAN/Sm^3 GOX
LP GAN	Purity	< 0.1 mol. % O_2
	Conditions	> 9 bar (extraction at suitable stage); 30 °C
	$K_{ASU,LP\ GAN}$	0.16 Sm^3 LP GAN/Sm^3 GOX
DGAN	Purity	< 1 mol. % O_2
	Conditions	34 bar; ≈ 100 °C (as received after last stage)
Ambient air	Conditions	15 °C, 1013.25 mbar, 60 % relative humidity
	Composition	77.316 mol. % N_2, 20.735 mol. % O_2, 1.009 mol. % H_2O, 0.907 mol. % Ar, 0.033 mol. % CO_2
GT extraction air	Conditions	16 bar; 170 °C
	Composition	Same as ambient air

The specific demands of HP GAN and LP GAN are chosen in accordance to Gräbner et al. [21] and therefore represent typical values for a dry feed entrained flow gasification process in a CC-IGCC.

Fig. 30 exemplifies the calculated auxiliary load distribution for four comparable operating points.

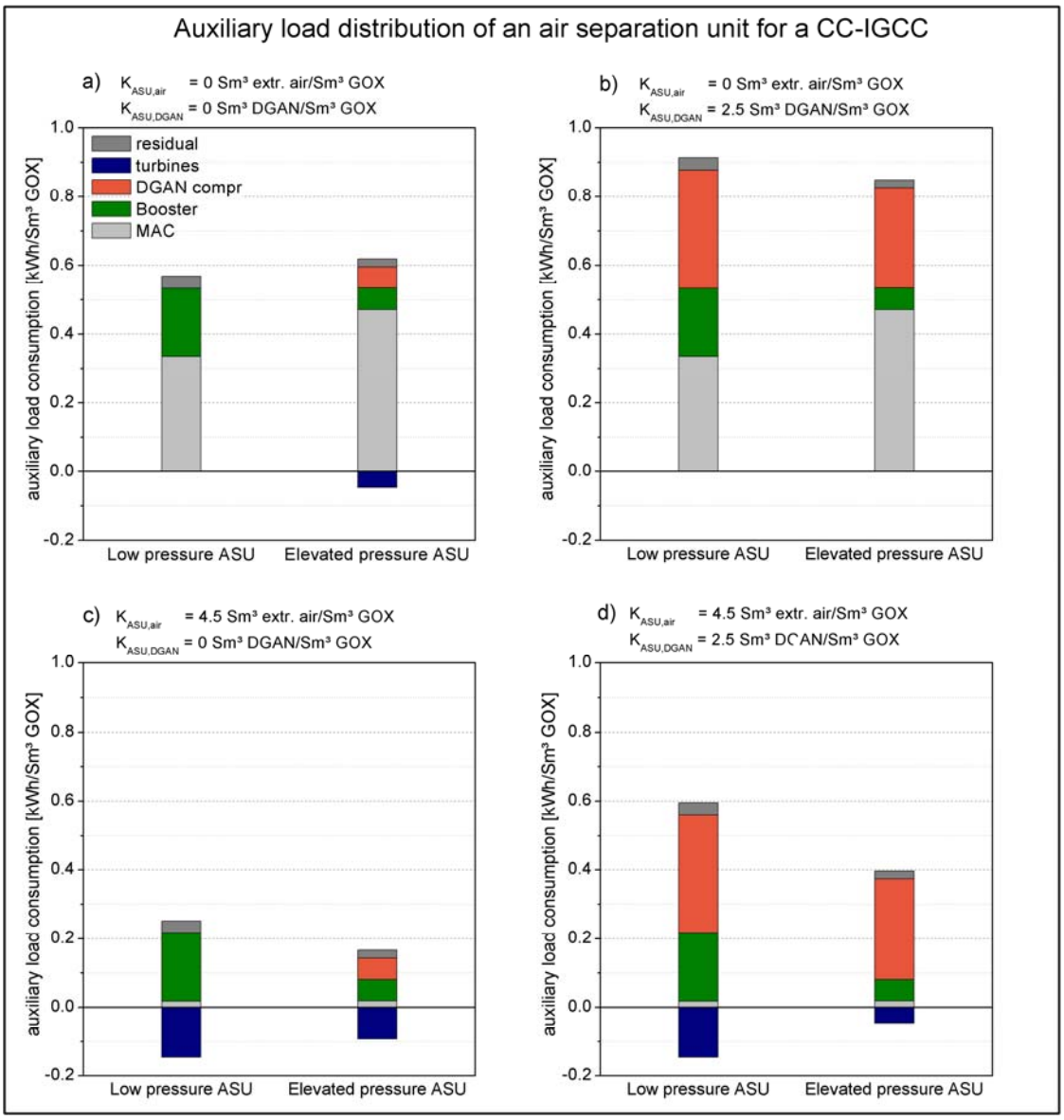

Fig. 30 Auxiliary load distribution of air separation units for a CC-IGCC

As illustrated, the MAC and the booster consume the main part of the necessary auxiliary load when extraction air is not used and DGAN is not required (Fig. 30a). Although DGAN is not necessary, auxiliary load induced by the DGAN compressor is shown at the elevated pressure concept. This is due to the nitrogen recycle as it is explained in Chapter 4.7.2.

At the elevated pressure concept, energy can be recovered by the residual gas expander since the remaining nitrogen occurs at about 3 bar. As a consequence both pressure concepts end up at an equal level for the specific auxiliary load.

If a high amount of extraction air is used and DGAN is still not required (Fig. 30c), the booster and the DGAN-compressor (only at the elevated pressure concept) will become the major auxiliary load consumer. At this case a considerable amount of energy can be recovered by the hot air turbine which expands the extraction air to the operating pressure of the lower column. For this operating point the elevated pressure concept has already been superior to the low pressure one which is mainly caused by the lower pressure ratio for the booster.

As it can be seen in Fig. 30b and Fig. 30d, a high DGAN demand clearly favors the elevated pressure concept. The lower pressure ratio for DGAN compression is responsible for the auxiliary load advantage. Additionally it has to be mentioned that at these high DGAN demands the residual nitrogen cannot be used at the expansion turbine since it is needed to regenerate the molecular sieves.

The overall calculation results are presented in Fig. 31.

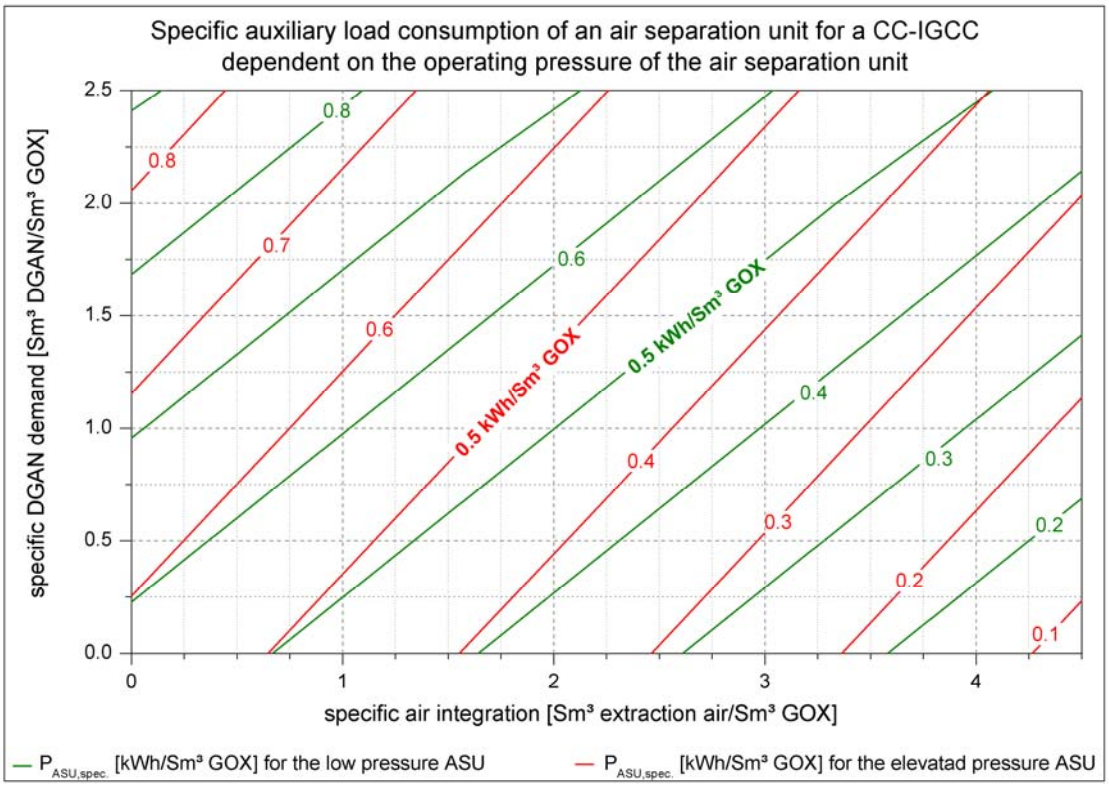

Fig. 31 Specific auxiliary load consumption of an air separation unit for a CC-IGCC dependent on the operating pressure of the air separation unit

The tabulated calculation results can be found in Appendix G4. For the given boundary conditions, the elevated pressure concept is superior or at least equivalent to the low pressure concept within the entire operating range. Therefore the low pressure concept will not be considered for further investigations.

The auxiliary load for the simulated air separation units can be calculated using equation (29). The corresponding coefficients are summarized in Table 16.

$$P_{ASU,spec} = Z + A * K_{ASU,air} + B * K_{ASU,DGAN} \qquad \left[\frac{kWh}{Sm^3 GOX}\right] \qquad (29)$$

where A, B and Z are simple coefficients.

Table 16 Coefficients for calculation of the specific ASU auxiliary load

Coefficient	Unit	Low pressure ASU	Elevated pressure ASU
Z	kWh/Sm^3 GOX	0.56654	0.57189
A	kWh/Sm^3 GOX	-0.10236	-0.11061
B	kWh/Sm^3 DGAN	0.13809	0.11103

Based on the previous examinations and findings, the ASUs auxiliary load was calculated for the CC-IGCC with the four different gasifier types. Table 17 summarizes the individual boundary conditions and the received simulation results.

Table 17 ASU simulation results for the CC-IGCC based on different gasifiers

Demand & supply	Unit	CoP	GE-R	SCGP	Siemens
GOX	10^3 Sm^3/h	74.9	97.2	78.5	78.5
DGAN	10^3 Sm^3/h	165.7	171.5	202.1	195.4
GAN (HP+LP)	10^3 Sm^3/h	1.6	0	38.8	35.5
Extraction air	10^3 Sm^3/h		251.7		
Results					
Air demand	10^3 Sm^3/h	357.3	449.9	371.4	368.3
Specific air demand	Sm^3/Sm^3 GOX	4.77	4.63	4.73	4.69
$L_{air,int}$	%	70	56	68	68
$K_{ASU,air}$	Sm^3/Sm^3 GOX	3.4	2.6	3.2	3.2
$P_{ASU,aux}$	MW	29.2	39.9	40.1	38.7
$P_{ASU,spec}$	kWh/Sm^3 GOX	0.39	0.41	0.51	0.49

As shown in Table 17, the ASU for the IGCC power plant with a CoP gasifier requires the least specific auxiliary load closely followed by the GE-R case. This difference is due to the slightly higher DGAN demand and the higher GOX pressure for the GE-R. The other two cases are characterized by a roughly 25 % higher specific auxiliary load. In turn this is a consequence of the GAN extractions which are not necessary (or at least at a minor amount) for the GE-R and the CoP gasifier. These extractions out of the high pressure column reduce the available reflux to the low pressure column. The losses can only be outbalanced by the mentioned nitrogen recycle which in fact is responsible for the higher specific auxiliary load. The minor differences between the SCGP and the Siemens case are caused by the slightly higher DGAN and GAN demand at the CC-IGCC with SCGP.

The heat and material balances for the discussed concepts is provided in the Appendixes G5 – G8.

5 Thermodynamic evaluation of IGCC-concepts

Within this chapter, selected IGCC-concepts are evaluated with respect to their thermodynamic performance. Therefore, the developed process simulation models are used to analyze the thermodynamic behavior of different IGCC configurations.

In the first part, a comparative benchmark of the CC-IGCC concepts based on the four different gasifier types is accomplished. Subsequently, a study is conducted to clarify the effects of integration between the gas turbine and the ASU on the overall IGCC performance. The chapter closes with a survey analyzing the performance and the CO_2-emissions of IGCC-concepts designed for different carbon retention rates (CRR).

5.1 Benchmark of CC-IGCCs with different gasifiers

One central goal of this thesis is a comprehensible evaluation of CC-IGCC concepts based on four industrial coal gasifiers. The overall concept arrangement and the individual sub-processes have already been extensively described in Chapter 4.

The simulation results and the thermodynamic analysis for each of the IGCC sub-processes are presented there as well. Therefore, the results only have to be summarized in the following.

Table 18 shows the most important performance results for the four different concepts. The thermal heat input to the gasifier is adjusted, so that the gas turbine generates 292 MW which at the same time represents the defined mechanical shaft limit.

Table 18 Performance summary for CC-IGCC concepts

Parameter	Unit	CoP	GE-R	SCGP	Siemens
$P_{gas\ turbine}$	MW	292.0	292.0	292.0	292.0
$P_{steam\ turbine}$	MW	175.1	200.7	176.7	169.4
$P_{expansion\ turbine}$	MW	-	3.3	-	-
$P_{IGCC,gross}$	MW	467.1	496.1	468.7	461.4
$P_{auxiliary\ load}$	MW	88.4	98.3	103.2	99.4
$P_{IGCC,net}$	MW	378.7	397.8	365.5	362.0
Q_{coal}	MW	1049.1	1129.0	1035.1	1037.8
$\eta_{IGCC,gross}$	%	44.5	43.9	45.3	44.5
$\eta_{IGCC,net}$	%	36.1	35.2	35.3	34.9

The steam turbine power output at the GE-R-concept is about 12 to 15 % higher than at the other three configurations. This is mainly caused by the concurrent HP-steam generation in the radiant cooler and in the CO-shift cycle. At the other concepts this kind of heat recovery is only possible either at the gasifier (SCGP and CoP gasifier) or at the heat recovery section of the CO-shift cycle (Siemens gasifier). Hence, the CC-IGCC with GE-R also shows the highest net power output which is roughly 5 % higher than at the CoP-IGCC and 9 to 10 % higher than at the configurations based on the other two gasifiers.

The best net efficiency is expected for the concept with CoP gasifier which exhibits a clear advantage over the other three configurations. Despite of its significantly better gross efficiency, the SCGP-concept only reaches a net efficiency which lies about 0.8 %-points below the leading value. Fig. 32 illustrates this behavior.

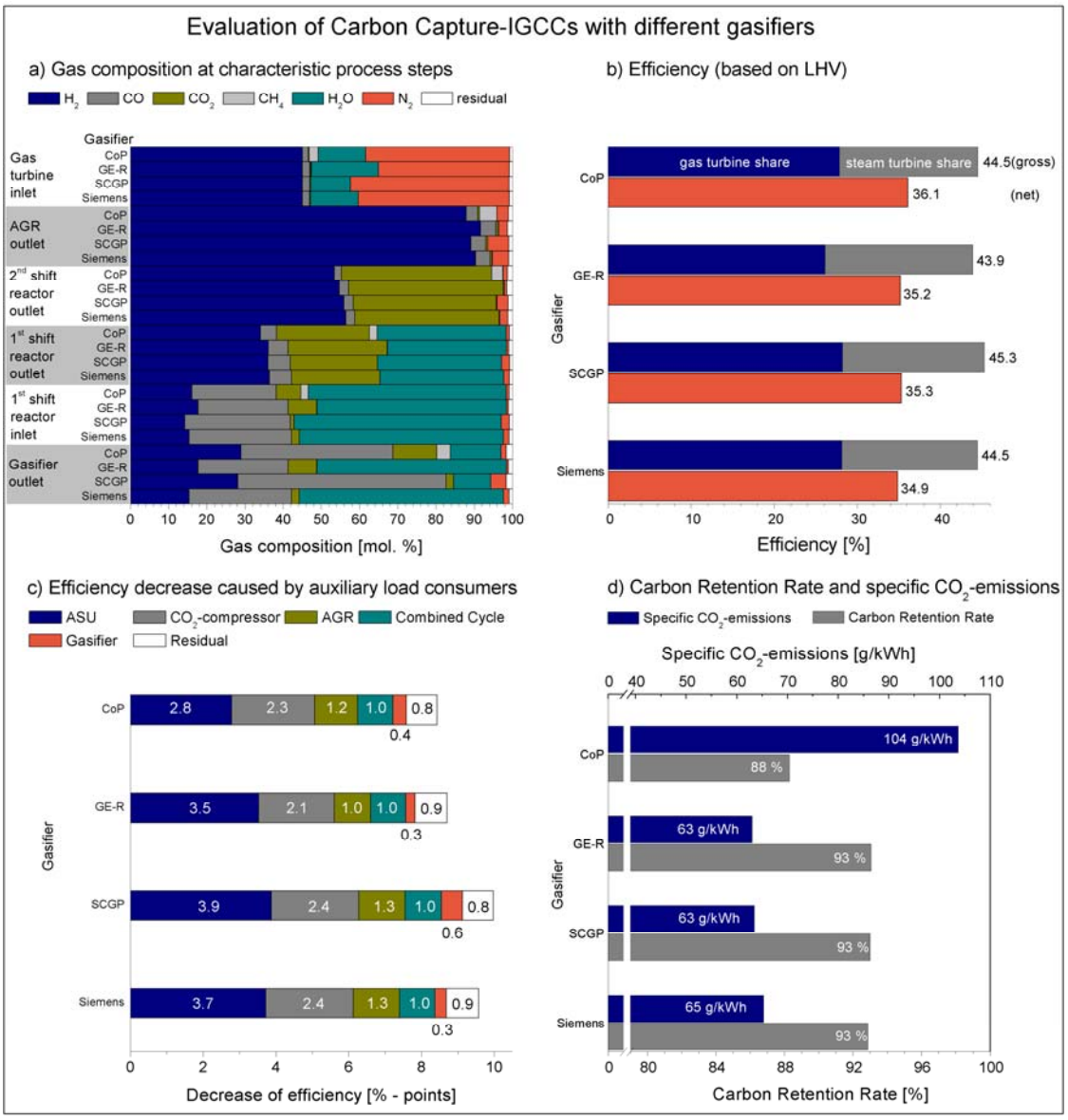

Fig. 32 Evaluation of CC-IGCCs based on different gasifier concepts

As seen in Fig. 32c, the markedly lower auxiliary load fraction for the CoP-IGCC is the reason for the highest of all net efficiencies. This is mainly due to the lower share for the ASU which in turn is achieved by the significant lower demand of gaseous nitrogen for the gasification process (as explained in Chapter 4.7.3).

The concept with GE-R also shows a clearly lower auxiliary load fraction in comparison with the SCGP-concept so that the net efficiency for both configurations ends up at the same level. In spite of a 14 % higher oxygen demand compared to the SCGP, the ASU for the GE-R consumes a lower auxiliary load share. This again is due to the missing demand of gaseous nitrogen for the coal feeding process. Additionally, the higher operating pressure at the GE-R concept results in a lower auxil-

iary load for the AGR and the CO_2-compressor so that the efficiency gap to the SCGP- and the Siemens-configuration is reduced or even compensated.

The Siemens-IGCC shows a similar auxiliary load distribution in comparison with the SCGP case. The slightly different auxiliary load fractions for the ASU and the gasifier are caused by the different demand of gaseous nitrogen (GAN and DGAN) and the necessary power for the quench gas recycle compressor at the SCGP. As a consequence the Siemens-IGCC shows the weakest of all net efficiencies. However there is only a small distance to the efficiencies of the CC-IGCC with SCGP and GE-R.

An exergetic analysis for the overall IGCC-concepts is conducted according to the fundamentals described in chapter 4.2.6. The results are provided inTable 19.

The analysis identifies the gasifier and the gas turbine as the main cause for exergy destruction. These losses are inevitable since they are caused by the irreversibility of chemical fuel conversion. While the other sub-processes contribute only minor exergy losses, the water-/steam cycle is responsible for the third largest amount of exergy destruction. This is basically owed to the necessary temperature differences in the HRSG and the irreversibility of energy conversion within the steam turbine.

Table 19 Exergy losses related to the exergy input to the CC-IGCC

IGCC sub process	Unit	CoP	GE-R	SCGP	Siemens
ASU	%	2.3	2.7	2.5	2.5
Gasifier	%	22.3	25.7	22.1	22.8
CO-shift	%	3.5	2.1	3.7	2.5
AGR/SRU/TGT	%	4.4	4.2	4.3	4.3
CO_2-compressor	%	2.2	2.0	2.3	2.3
Gas turbine	%	21.1	19.7	21.4	21.4
Water-/steam cycle	%	8.3	8.7	8.5	9.4
Residual	%	0.8	0.8	0.8	0.8
Exergetic efficiency	%	35.1	34.2	34.4	34.0

The exergetic efficiency shows the same differences between the concepts as the energetic efficiency. These overall distinctions are caused by the individual ones in the particular sub-processes. The presented analysis identifies the major causes for exergy destruction and therefore provides the basis for an exergetic optimization.

Some differences between the four concepts shall be explained in more detail:

- ASU: The CC-IGCC based on the CoP gasifier shows the least exergy loss which is due to the lowest demand of GOX. In contrast, the CC-IGCC with GE-R has the highest demand of GOX which accordingly causes the highest of all exergy losses. Please also see Fig. 10a for clarification.
- Gasifier: The exergetic analysis is already provided in chapter 4.2.6.
- CO-shift: There are slight advantages for the IGCC-concepts based on the Siemens gasifier and the GE-R. On the one hand, this is due to the lower temperature differences at the heat recovery section (with steam generation). On the other hand, the missing IP-steam demand (for temperature moderation at the first CO-shift reactor) has a positive impact, too.

- AGR/SRU/TGT/CO_2-compressor: There are no noteworthy advantages for none of the four concepts.
- Gas turbine: The CC-IGCC with GE-R shows the least (relative) exergy losses. At a closer look all four concepts have almost the same absolute exergy loss at the gas turbine process. The lower relative exergy loss is caused by the fact that the concept with GE-R needs about 8 to 9 % more coal in comparison to the other concepts (due to the higher exergy loss at the gasifier).
- Water-/steam cycle: The differences between the four concepts are caused by the individual HRSG-design and the need to apply different temperature differences.

With respect to the CO_2-emissions, an equal level can be reached for the IGCC configurations based on the GE-R, the SCGP and the Siemens-gasifier (see Fig. 32d). Due to the methane content in the gas turbine fuel (see Fig. 32a), the CoP-IGCC comes out with a 60 % higher specific CO_2-emission and a five percent lower carbon retention rate (CRR). The latter one is defined as the ratio of carbon atoms in the captured CO_2 related to that in the coal.

As a conclusion of this study, a theoretical efficiency potential of about 1.6 %-points can be identified for the SCGP-IGCC when the gasifier would operate on an enhanced pressure level (like the GE-R) and without gaseous nitrogen for the coal feeding system (assuming a solid feed pump). In this case the higher operating pressure would cause the auxiliary load fraction of the CO_2-compressor and the AGR to decline, so that the values of the GE-R-case could be reached (each will bring a rise of 0.3 %-points for the net efficiency). Additionally, the ASU auxiliary load fraction would drop to the level of the CoP-case (as a consequence of the omitted gaseous nitrogen demand for the coal entry system) which would bring another 1 %-point increase of the net efficiency.

5.2 Level of integration between the gas turbine and the ASU

A further goal of this thesis is to clarify the influence of integration between the gas turbine and the air separation unit on the overall IGCC performance. The technical need for air and nitrogen integration and the impact on gas turbine operation have already been described in Chapter 4.5. The effects of different rates of air extraction and nitrogen dilution (DGAN demand) on the performance of the air separation process were demonstrated in Chapter 4.7.3. Based on these investigations, the other sub-processes of a CC-IGCC were simulated for four different air extraction rates and a range of different nitrogen dilution rates (to adjust a certain fuel gas hydrogen content). The CC-IGCC with Siemens gasifier is selected for the study. The results are presented in Fig. 33.

The operating behavior of the gas turbine as shown in Fig. 22 is decisive. The gas turbine power output (Fig. 33a) is restricted by the defined mechanical shaft limit which is kept by controlling the compressor inlet flow.

The steam turbine power output (Fig. 33b) is mainly influenced by the gas turbines exhaust gas flow which reaches its maximum for a given air extraction rate at the point where the highest blade temperature is attained. With reference to Chapter 4.5.2, this point is reached at a fuel gas hydrogen content where the gas turbine operates at the mechanical shaft limit and its compressor barely runs at full load flow. At increasing air extraction rates, the amount of steam generated in the extraction air cooler also increases, which in fact, is the cause for the absolute differences between the maxima of the steam turbine power outputs at different air extraction rates.

The trend of the plants gross efficiency (Fig. 33c) is the same as that for the gas turbines efficiency. The highest gross efficiency is logically achieved without air extraction and at the highest of the investigated nitrogen dilution rates. At the same time, this operating point requires the highest of all auxiliary loads (Fig. 33d). This is mainly caused by the necessary power for the main air compressor and the DGAN-compressor of the ASU. For a given air extraction rate, the auxiliary load fraction stays about constant within a fuel gas hydrogen range between 79 and 90 mol. %. Within this range the fuel gas is only diluted with steam so that no DGAN-compressor load is required. For lower fuel gas hydrogen contents, DGAN compression causes the auxiliary load fraction to a steady increase.

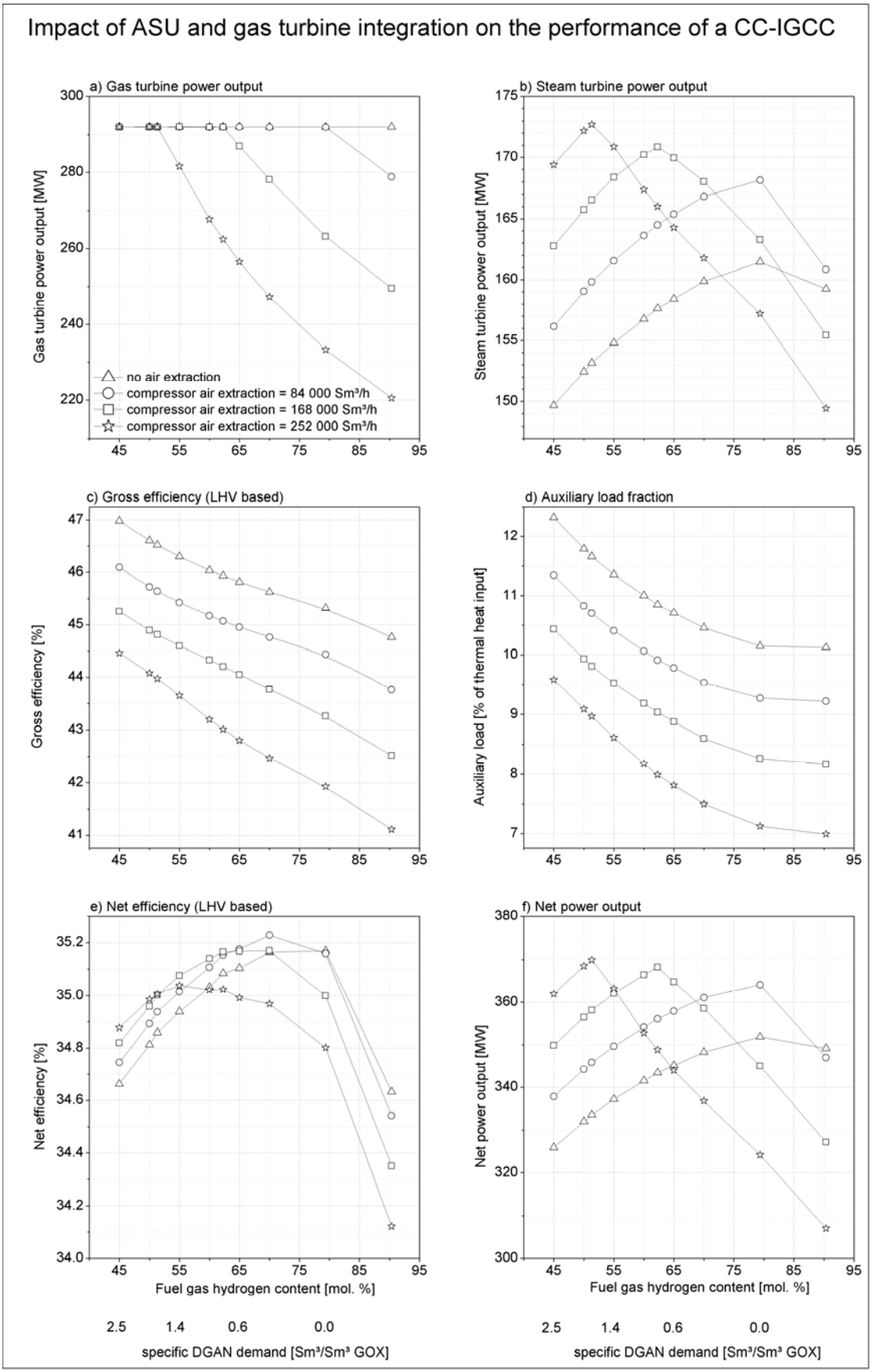

Fig. 33 Impact of ASU and gas turbine integration on the performance of a CC-IGCC

For fuel gas hydrogen contents between 45 and 65 mol. %, the resulting net efficiency (Fig. 33e) shows just a marginal difference (max. 0.2 %-points) among the various rates of compressor air extraction. Over the full fuel gas hydrogen range a slight efficiency maximum is noticed for each air extraction rate. This maximum is found at that point where the turbine inlet temperature for the individual air extraction rate reaches its maximum, too.

The net power output (Fig. 33f) follows the trend of the steam turbine power output and shows a clear optimum for each air extraction rate. This optimum also shifts to the right side of the diagram with decreasing air extraction rates. The maximum is found at that fuel gas hydrogen content where the gas turbine has already operated at the mechanical shaft limit while the compressor barely runs at full load flow. From Fig. 33f it can be concluded that a higher net power output and also a higher net efficiency could be reached at a fuel gas hydrogen content of 45 mol. % when a higher compressor air extraction rate would have been considered. However, this has not been done since compressor air extraction of 252 000 Sm^3/h gives about 7 % air integration which should not be exceeded to enable a proper start-up process of the CC-IGCC [21].

The presented investigation illustrates the influence of the level of integration between the gas turbine and the ASU on the performance of a CC-IGCC under given boundary conditions. As the generated results are based on generic process simulation models and special assumptions, they should not be considered as universally valid. The investigation should rather be comprehended as a particular case study presenting an approach to analyze and optimize the integration aspect between the gas turbine and the ASU in a CC-IGCC. Nevertheless, the following findings are stated to be valid for every other CC-IGCC application with respect to the gas turbine and ASU integration:

- The gas turbines operating behavior and limitations are decisive for the identification of the optimal level of integration between the gas turbine and the ASU.
- High levels of air integration are only thermodynamically advantageous at high levels of nitrogen integration. The thermodynamic benefit of air integration disappears as soon as higher maximum fuel gas hydrogen contents can be realized than possible with the nowadays state of the art technology.

- For a given compressor air extraction rate, the maximum of net efficiency and net power output is achieved at that nitrogen integration rate (fuel gas hydrogen content) where the gas turbine is operated at the mechanical shaft limit while its compressor barely runs at full load flow.

5.3 IGCC concepts with different carbon retention rates (CRRs)

At the end of the thermodynamic assessment, a case study was conducted to clarify the influence of different CRRs to the IGCC-performance and the specific CO_2-emissions. Therefore, four different operating scenarios were defined based on the overall configuration developed for the concept with Siemens gasifier.

The following measures were found suitable for a reduction of the CRR in a given overall configuration:

- Capture and compression of the high pressure CO_2 while the low pressure CO_2 is vented to the atmosphere; all other things are equal to the reference case,
- Reduction of the CO_2-capture rate in the AGR through a derated solvent flow,
- CO-shift cycle with just one reactor instead of two while nearly all CO_2 is captured in the AGR,
- CO-shift cycle with just one reactor instead of two with a concurrently reduced CO_2-capture rate in the AGR through a derated solvent flow.

Corresponding to the above mentioned measures, four different IGCC-cases are developed and simulated. Fig. 34 shows the generated results in comparison to the chosen reference case (IGCC-with Siemens gasifier).

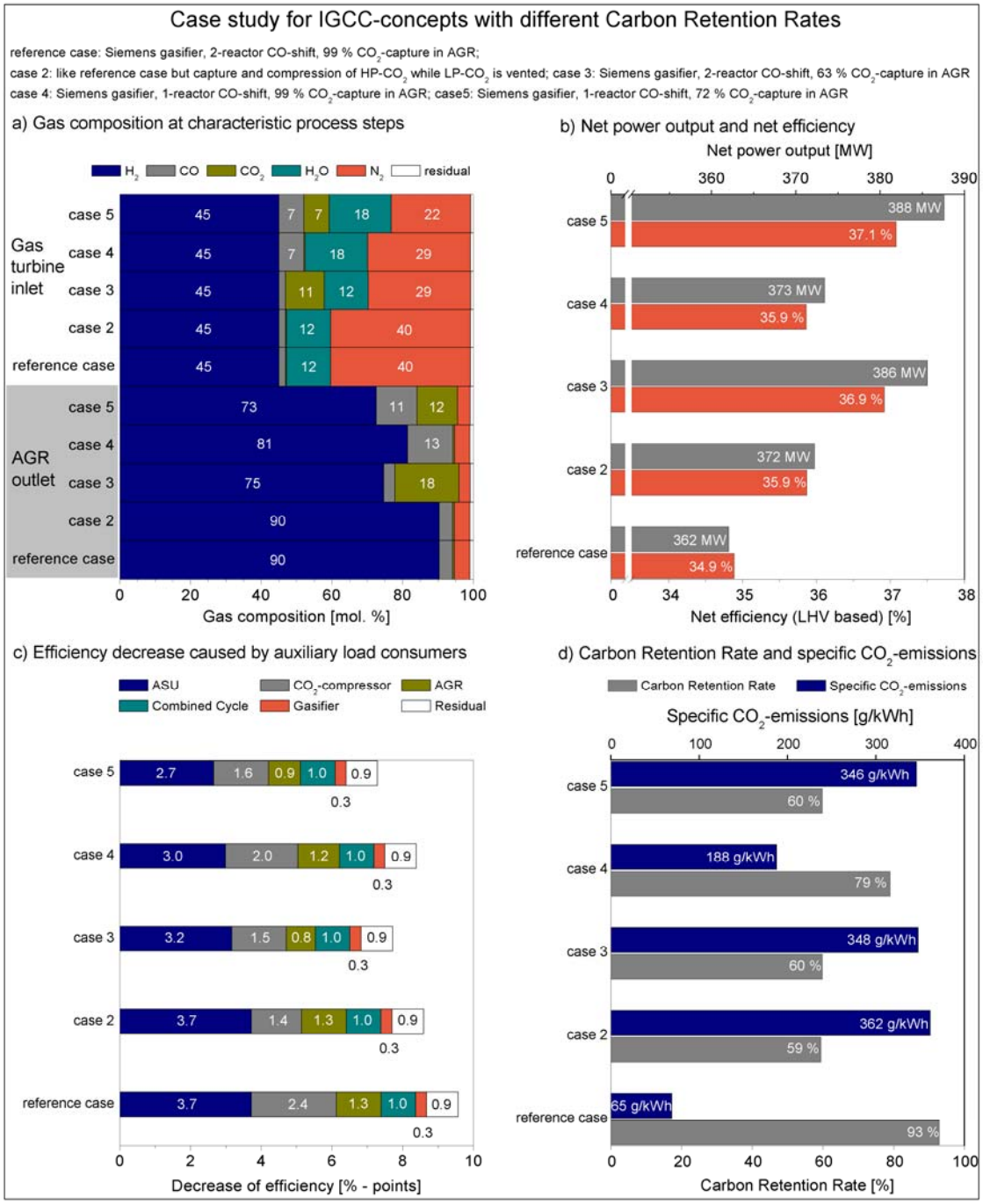

Fig. 34 Case study for IGCC-concepts with different carbon retention rates

The first measure (case 2) does not affect the main process flow since the captured CO_2 is not internally used. Hence, the gross plant performance is identical to the reference case. Venting the LP-CO_2 stream involves that only the remaining HP-CO_2 has to be compressed. Therefore, the specific auxiliary load demand as well as the absolute power consumption for the CO_2-compressor decreases in comparison to the reference case. Consequently, the net power output increases by about 10 MW

which implies a 1 %-point higher net efficiency. At the same time the CO_2-emissions increase so that a CRR of roughly 60 % is reached.

With respect to case 3, the solvent flow in the AGR is reduced so that about 18 mol. % of CO_2 remain in the clean gas. As a consequence, a CRR of about 60 % is achieved while the auxiliary load fraction for the CO_2-compressor and the AGR decrease. Additionally, the auxiliary load share for the ASU is also lowered since less nitrogen dilution is necessary to adjust a fuel gas hydrogen content of 45 mol. %. The auxiliary load savings and the different fuel gas composition are responsible for an increase of the net power output of about 24 MW and a 2 %-points efficiency enhancement, all in comparison to the reference case.

Case 4, characterized by a one-reactor CO-shift and a bulk CO_2-removal within the AGR shows nearly the same performance results as case 2 but features a clear advantage with respect to the CRR and the resulting CO_2-emissions. The better performance compared to the reference case is caused by the reduced auxiliary load for the ASU, the CO_2-compressor and the AGR. Due to the different arrangement of the CO-shift cycle (see Appendix H1 for the corresponding CHEMCAD process model), more steam can be brought in the gas turbine fuel gas. Therefore, the ASU auxiliary load fraction is actually lower than at case 3 since the nitrogen dilution rate can be reduced even more.

The last of the considered measures (case 5) can be seen as a combination of case 3 and case 4. The CRR of 60 % is achieved with a one-reactor CO-shift and a concurrent reduction of the solvent flow within the AGR. In doing so, the net efficiency and the net power output can be increased by about 2.2 %-points and 26 MW, respectively, in comparison to the reference case. The ASUs auxiliary load share brings a 1 %-point lower efficiency decrease than at the base concept. This is due to the considerable amounts of CO, CO_2 and H_2O in the fuel gas which reduce the necessary quantity of DGAN provided by the ASU. Although the specific auxiliary load demand for the AGR increases as a cause of the lower CO_2-partial pressure, the absolute value declines through the reduced solvent flow.

The previous case study illustrated the thermodynamic performance for concept alternatives with a CRR between roughly 60 and 80 %. The lower border for the CRR was chosen since it marks the level that is common for state of the art combined cycle power plants driven on natural gas. A configuration with a one-reactor CO-shift cycle and a concurrently reduced CO_2-capture rate within the AGR offers the best values for efficiency and output when aspiring 60 % carbon retention. A concept with a two-reactor CO-shift cycle and the same CRR exhibits a slightly inferior performance. A CRR of nearly 80 % is the maximum that can be achieved with a one-reactor CO-shift cycle. Capturing only the HP-CO_2 stream while the LP-CO_2 is vented to the atmosphere only makes sense when peak load capacity has to be raised in an already designed plant.

Nevertheless, a final assessment of the reviewed alternatives is only possible in coherence to an economic evaluation which will be conducted in the following chapter.

6 Economic evaluation and optimization

6.1 Economics of CC-IGCC concepts

This chapter illustrates a simplified economic analysis both for the CC-IGCC concepts based on different gasifier-types and for the conducted case study examining various CRRs. The analysis is based upon the discounted cash flow method and the procedure as it is applied by Gräbner et al. [21] to several IGCC concepts that use a world market hard coal and German lignite as feedstock.

The overall project costs (OPC) for the investigated CC-IGCC concept with Siemens gasifier are assumed to be the same as those for the hard coal fired IGCC concept with CO_2-capture in the aforementioned study (OPC = 3,450 €/kW). Hence, the OPC for the CC-IGCC with Siemens gasifier come up to 1,249 Mio € considering the net power output of 362 MW.

The individual OPC-portions originated by the main subsystems and several other capital expenditures (CapEx) are also derived from Gräbner et al. [21].

Table 20 summarizes these values.

Table 20 Overall project costs for the CC-IGCC with Siemens gasifier

Investment cost (price level 2008) for	% of OPC	Mio €
Gas generation (coal handling, gasification, water treatment)	25.0	312
Gas treatment (CO-shift/AGR/SRU/TGT)	11.5	144
CO_2-compressor	2.5	31
Combined Cycle	29.0	362
ASU	7.0	87
Infrastructure and utilities	13.0	162
Main spare parts and architect engineer (AE)	3.0	37
Miscellaneous	9.0	112
Sum	100.0	1,249

These reference data are used in combination with the individual calculation results and a few literature sources to estimate the OPC for the other three CC-IGCC concepts. The respective calculation is shown in appendix I1.

Table 21 summarizes the corresponding results.

Table 21 Overall project costs for the CC-IGCCs with different gasifiers

Investment cost for	Unit	CoP	GE-R	SCGP	Siemens
Gas generation	Mio €	335	352	419	312
Gas treatment	Mio €	137	145	144	144
CO_2-compressor	Mio €	30	34	31	31
Combined Cycle	Mio €	367	389	368	362
ASU	Mio €	84	109	87	87
Direct investment costs	Mio €	953	1,029	1,050	936
Infrastructure and utilities	Mio €	165	179	182	162
	% of OPC	13	13	13	13
Main spare parts and architect engineer	Mio €	38	42	42	37
	% of OPC	3	3	3	3
Miscellaneous	Mio €	114	124	126	112
	% of OPC	9	9	9	9
Overall project costs (OPC)	Mio €	1,271	1,373	1,400	1,249
	€/kW(net)	3,357	3,453	3,830	3,450

As it can be seen, the CC-IGCC with CoP gasifier is expected to have the lowest specific OPC while the concept based on the SCGP shows the worst specific OPC (approximately 14 % higher than at the CoP-case).

Table 22 shows the remaining boundary conditions that are necessary to calculate the cost of electricity (CoE) as the decisive evaluation parameter.

Table 22 Other boundary conditions for the economic analysis

Parameter	Value	Parameter	Value
Interest Rate	10 %	Maintenance costs	1 % of OPC
Useful life	25 a	Costs for taxes and insurances	0.5 % of OPC
Fuel costs	2.6 €/GJ	CO_2-transport and storage costs	8 €/t
Miscellaneous costs	10 % of fuel cost	CO_2-emission certificate price	30 €/t
Availability	7315 h/a (= 83.5 %)	Labor costs (60 persons x 65 000 €/a)	3.9 Mio €/a

The above provided data are chosen in accordance to Gräbner et al. [21] representing a good basis for a realistic concept assessment. In concordance to Gräbner et al. [21], the payment dates for the capital expenditures are distributed over the expected construction period of 5 years. The complete procedure for the CoE-determination is explained in the Appendixes I2 and I3.

Fig. 35a illustrates the resulting CoE for the IGCC-concepts based on the different gasifiers types. As it can be seen, the concept with CoP gasifier shows slight advantages in comparison to the concept with Siemens gasifier and this with GE-R. Although to name a clear favorite out of these three concepts seems to be daring especially when the uncertainties of cost estimation are considered. However, the concept based on the SCGP is most likely the worst economic choice out of the considered concepts since a 7 to 10 % higher CoE has to be expected.

Furthermore, Fig. 35a clarifies the dominant impact of the capital costs to the CoE. Roughly 60 % of the CoE is owed to the CapEx while the second largest cost driver (fuel) only takes responsibility for less than a quarter of the CoE. The other cost components are from minor influence.

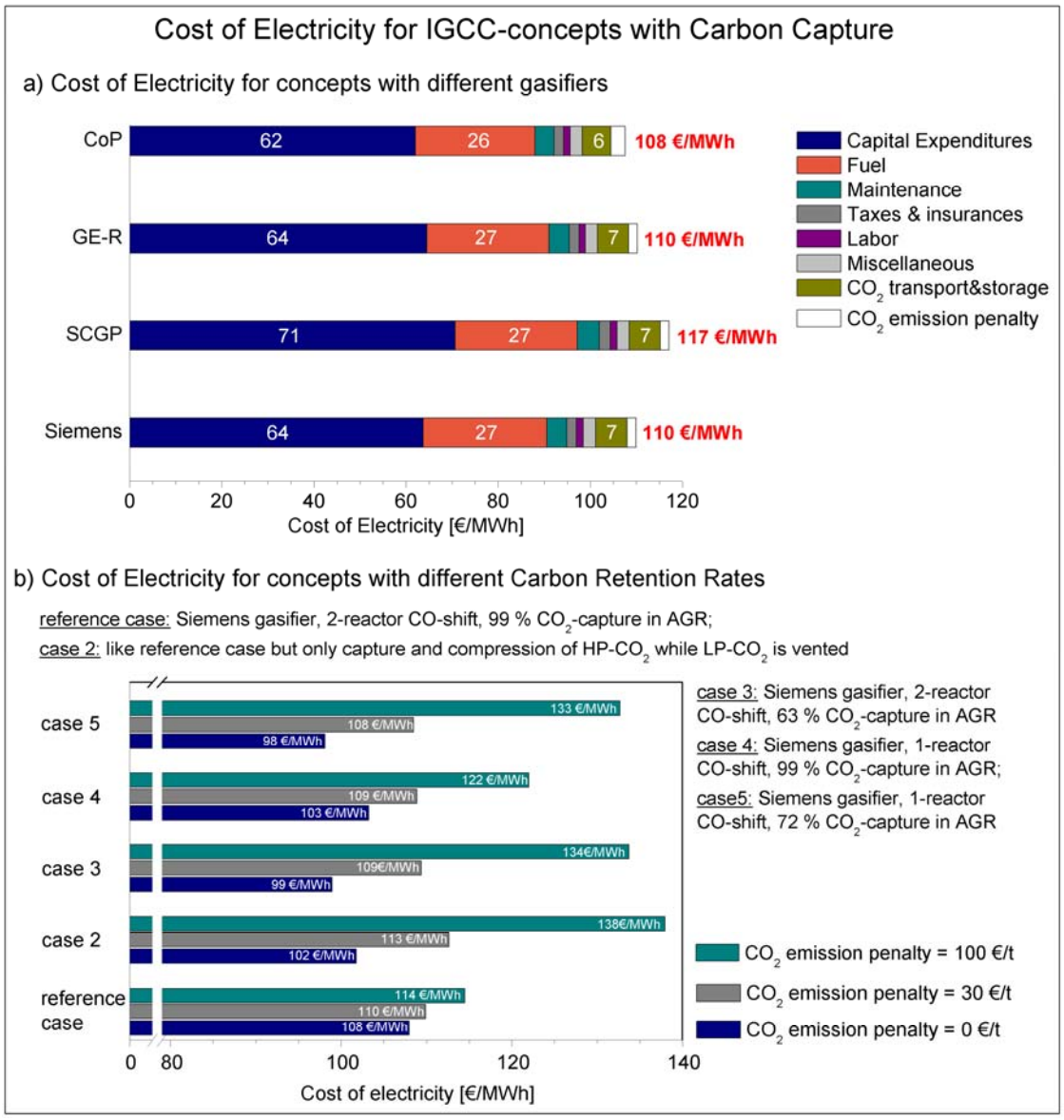

Fig. 35 Cost of electricity for IGCC-concepts with carbon capture

Fig. 35b shows the CoE for the concept alternatives with different carbon retention rates (refer to Chapter 5.3) calculated for a range of CO_2-emission penalties.

Due to the high carbon retention rate, the CoE response to a changing CO_2-emission penalty is only marginal for the reference case.

The concepts with a reduced CO_2-capture rate are only expected to be markedly advantageous if no or minor CO_2-emission penalties have to be paid. Under the given boundary conditions the break-even-price for the CO_2-emission penalty is found to be at about 30 €/t.

With respect to the results of case 3 and case 5 it can be summarized, that it does not matter if the IGCC is equipped with a one-reactor CO_2-shift or a two-reactor CO_2-shift as long as the same CRR is adjusted at the AGR. The capital costs assumed for the CRR-analysis can be found in Appendix I4.

The investigation of concept economics closes with a sensitivity study analyzing the influence of certain cost drivers to the CoE. Fig. 36 visualizes the relative CoE assuming realistic improvements (target values) for the net efficiency, the plant availability, the interest rate and the capital expenditures.

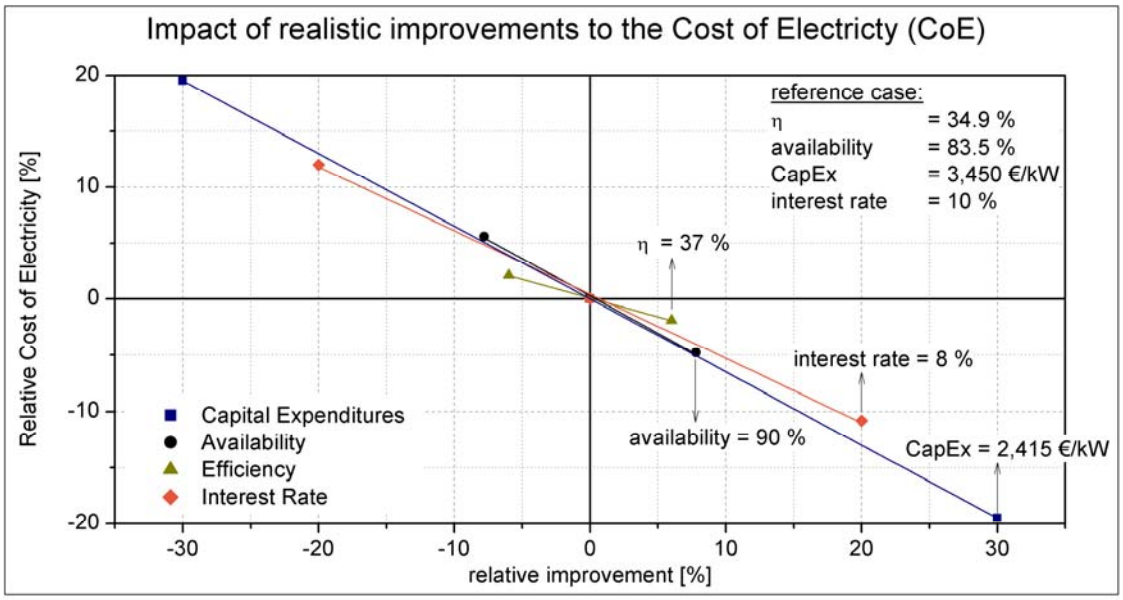

Fig. 36 Impact of realistic improvements to the cost of electricity (CoE)

The CapEx reduction promises the highest potential for CoE reduction as the underlying investment costs are provided with an uncertainty range of ± 30 % [21]. The figure also clarifies the minor influence of efficiency and availability enhancements (at least in a realistic bandwidth) to the CoE. In contrast, a 20 %lower interest rate would strongly reduce the CoE. However, the interest rate is driven by the financial market and a reduced rate would also have to be applied to competing technologies.

In the following, the cost of CO_2-avoidance is introduced as an additional evaluation parameter. The definition is:

$$\text{cost of } CO_2\text{-avoidance} = \frac{CoE_{CC\text{-}IGCC,a} - CoE_{conv,a}}{CO_2 \text{ emission}_{conv} - CO_2 \text{ emission}_{CC\text{-}IGCC}} \tag{30}$$

where

- $CoE_{CC\text{-}IGCC,a}$ is the CoE for a CC-IGCC (excluding the costs for CO_2-penalties),
- $CoE_{conv,a}$ is the CoE for a conventional steam power plant (excluding the costs for CO_2-penalties),
- CO_2 $emission_{CC\text{-}IGCC}$ are the specific CO_2-emissions for a CC-IGCC and
- CO_2 $emission_{conv}$ stands for the specific CO_2-emissions for a conventional steam power plant.

The following example shall illustrate the meaning of the cost of CO_2-avoidance. Bearing in mind the herein presented simulation results and the aforegoing economic assessment, the following is assumed:

$CoE_{CC\text{-}IGCC,a}$ = 108 €/MWh

$CoE_{conv,a}$ = 50 €/MWh

CO_2 $emission_{CC\text{-}IGCC}$ = 65 kg/MWh

CO_2 $emission_{conv}$ = 710 kg/MWh

According to equation (30) the

$$\text{cost of } CO_2\text{-avoidance} = \frac{108 - 50}{710 - 65} \; \frac{[\frac{€}{MWh}]}{[\frac{kg}{MWh}]} = 90 \frac{€}{t} \; .$$

Accordingly, the CoE including the cost of CO_2-avoidance are calculated as follows:

$$CoE_{CC\text{-}IGCC} = 108 \frac{€}{MWh} + \frac{65kg}{MWh} * \frac{90€}{t} = 114 \frac{€}{MWh}$$

$$CoE_{conv} = 50 \frac{€}{MWh} + \frac{710kg}{MWh} * \frac{90€}{t} = 114 \frac{€}{MWh} \quad .$$

Hence, the calculated cost of CO_2-avoidance gives the price for the CO_2-emission penalty that is necessary to achieve the same CoE for the CC-IGCC and the conventional steam power plant without carbon capture.

Fig. 37 illustrates the so calculated cost of CO_2-avoidance for a CC-IGCC in comparison to a conventional hard coal fired steam power plant.

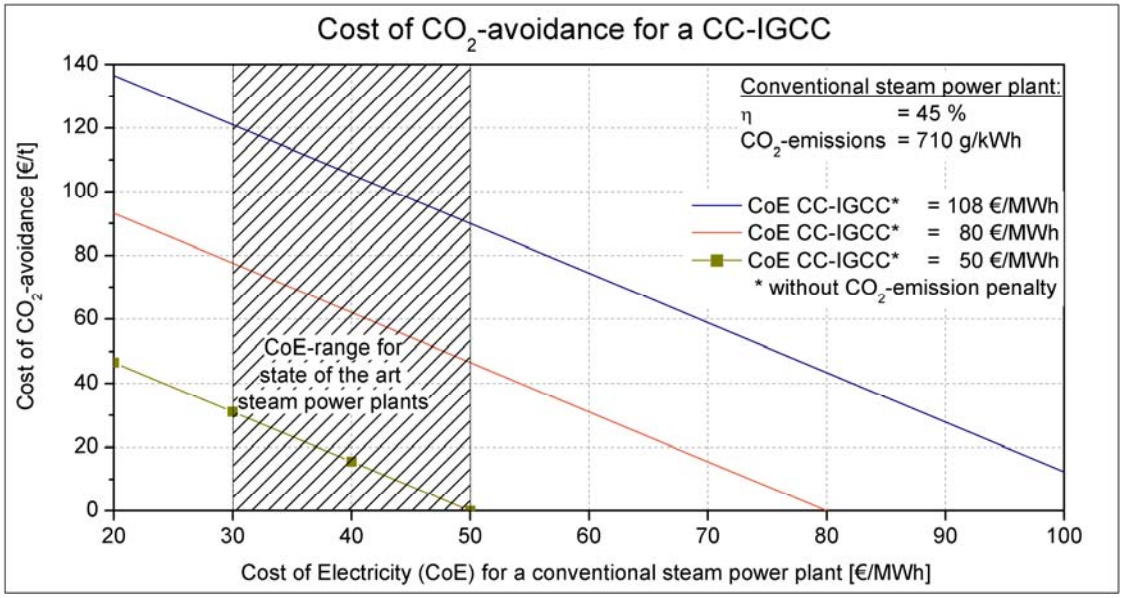

Fig. 37 Cost of CO_2-avoidance for a CC-IGCC

The shaded area in Fig. 37 provides the CoE-range for state of the art steam power plants in Germany [62]

The upper (blue) graph applies to the simulated CC-IGCC with Siemens gasifier achieving a CRR of about 93 %. The graph shows that the CO_2-emission penalty for this concept would have to assume 120 €/t (= cost of CO_2-avoidance) to be competitive with a conventional steam power plant having a CoE (without CO_2-

emission penalty) of 30 €/MWh. If this conventional steam power plant only had a CoE (without CO_2-emission penalty) of 50 €/MWh, the CO_2-emission penalty would have to assume 90 €/t in order to get CoE-parity amongst the CC-IGCC and the conventional plant.

The middle (red) graph represents a 26 % lower CoE as it would appear if the improvements for efficiency, availability and CapEx (as demonstrated in Fig. 36) could be realized. Accordingly the CO_2-emission penalty would have to be between 50 and 80 €/t to make this concept competitive to a conventional steam power plant without CO_2-capture.

The lower (green) curve in Fig. 37 shows that the CoE for a CC-IGCC has to be reduced by over 50 % (in comparison to the calculated reference value) in order to be competitive to a state of the art steam power plant without carbon capture. Only if this CoE-reduction can be achieved, the CO_2-emission penalties could range between 0 and 30 €/t. Present day prizes for the CO_2-emission certificate range between 5 and 15 €/t [12] so that CC-IGCC for power generation are today far away from economic feasibility.

Summing up, the following conclusions can be taken from of the economic analysis:

- At present day boundary conditions, CC-IGCC will only be superior to state of the art steam power plants if the prices for the CO_2-emission certificates will be markedly higher than 110 €/t or when the CoE for the CC-IGCC can be reduced by more than 50 % in comparison to the calculated values.
- The high Capital Expenditures are the key cost driver for the CoE of CC-IGCC.
- CC-IGCC based on the four investigated gasifier technologies show only a slightly different cost of electricity, especially when the distance to the CoE for state of the art steam power plants is considered.
- A reduced carbon retention rate (60 %) is only favorable (in comparison to a CRR of 93 %) at low prices for the CO_2-emission certificate. Since CC-IGCC can only be superior to present day steam power plants at high CO_2-emission certificate prices, a reduced CO_2-capture rate seems to be not an option at all.

6.2 Optimized IGCC-concept with enhanced economics

As pointed out in the latter chapter, capital cost reduction is the key to enhance the economic feasibility of a CC-IGCC. The economic analysis identified the gas generation section and the combined cycle plant as the main CapEx producers as both of them are responsible for more than 70 % of the direct investment costs.

Table 23 shows the individual shares of the direct investment costs for the five major subsystems of the CC-IGCC based on the Siemens gasifier. The provided specific costs in €/kW (gross) include the costs for "infrastructure and utilities", "main spare parts and architect engineer" and "miscellaneous" as they are originally calculated as fraction of the overall project costs.

Table 23 Capital costs of a CC-IGCC assigned to the main sub-systems

IGCC-subsystem	Capital Expenditures	
	% of direct investment costs	€/kW (gross)
Gas generation	33	902
Gas treatment	15	415
CO_2-compressor	3	90
Combined Cycle	39	1,047
ASU	9	253

As it can be seen in Table 23, the Combined Cycle is responsible for the biggest share of the capital expenditures. Moreover, the calculated specific costs were found to be markedly higher than for a conventional natural gas fired combined cycle power plant (NG CCPP). A reference calculation was carried out for a common NG CCPP using the software "Thermoflow" which includes a vendor proved cost library (see Appendix I5). The thereby achieved specific cost of 684 €/kW confirmed the assumption and showed that the Capital Expenditures for a CCPP in a CC-IGCC are roughly 50 % higher in comparison to a common NG CCPP.

These findings initiate the idea to decouple the CCPP from the upstream processes so that a standardized combined cycle power plant with considerable lower capital

expenditures can be applied. To realize this, all interfaces between the water-/steam cycle and the other sub-processes of the CC-IGCC had to be cut. At the same time it had to be investigated how the complete water and steam supply for the consuming processes can be ensured. Heat balance calculations prove that the heat recovery section of the CO-shift cycle is able to serve all water and steam consumers so that a decoupled CCPP can be realized. The modified flow sheet of the CO-shift cycle can be found in Appendix I6.

Now, process simulations will show the impact on the performance of the de-integrated power plant, henceforth called gasification combined cycle (GCC). The GCC concept is based on the Siemens gasifier since there is the lowest quantity of excess steam expected (out of the four gasifier types). The excess steam is that amount of steam generated in the CO-shift which is not necessary for the other sub-processes of the GCC. Hence, it is expanded in an additional small steam turbine for power production. Table 24 shows the performance comparison between the IGCC and the GCC both based on the Siemens gasifier.

Table 24 Performance comparison between IGCC and GCC

Parameter	Unit	IGCC	GCC
$P_{gas\ turbine}$	MW	292.0	292.0
$P_{steam\ turbine}$	MW	169.4	129.8
$P_{additional\ turbine}$	MW	-	16.9
$P_{IGCC,gross}$	MW	461.4	438.7
$P_{auxiliary\ load}$	MW	99.4	113.8
$P_{IGCC,net}$	MW	362.0	324.9
Q_{coal}	MW	1037.8	941.6
$\eta_{IGCC,gross}$	%	44.5	46.6
$\eta_{IGCC,net}$	%	34.9	34.5

As illustrated in Table 24 the net power output and the net efficiency decrease for the investigated GCC in comparison to the reference IGCC. On the one hand this behavior is caused by the omitted ASU integration (refer to Chapter 5.2) and on the other hand by the lower steam parameters at the heat recovery section of the CO-shift cycle. But as pointed out in Chapter 6.1, the achieved performance penalties will not noticeably influence the CoE.

Table 25 shows the cost of electricity for the investigated GCC concept. In addition to the reduced expenditures for the CCPP also different CapEx reduction rates are assumed for the gas island (all sub-processes except the CCPP).

Table 25 Cost of electricity (CoE) for a GCC concept

	CC-IGCC (reference)	GCC-concept		
		CapEx reduction for the gas island		
		0 %	15 %	50 %
CoE [€/MWh]	110	96	90	76
Relative CoE	100 %	88 %	82 %	69 %

The actual possible CoE-savings that can be reached by a GCC configuration with optimized CCPP costs are about 12 % in comparison to the reference IGCC.

If the GCC concept also caused CapEx reductions for the gas island (by the development of standardized sub-processes with a reduced number of interfaces), additional CoE-savings could be achieved. The CoE could be reduced by 18 % (in comparison to the reference CC-IGCC) if the CapEx for the decoupled gas island dropped by about 15 %.

The procedure of CoE-calculation is identical to the one explained in the Appendixes I1 to I3.

Concluding, the following can be noticed with respect to the investigated GCC concept:

- It is possible to decouple the CCPP from the subsequent processes without major performance penalties.
- The CoE is expected to be markedly lower than for the reference IGCC.
- It is supposed to be easier to realize CapEx-reductions for a decoupled gas island than for a highly integrated process (e.g. by standardization and reduction of the construction time)
- A GCC concept will tremendously reduce financing and risk if the decoupled, standardized gas island is erected at an existing CCPP.

7 Executive summary

Integrated Gasification Combined Cycle (IGCC) power plants are a promising alternative to conventional power generation technologies. Especially the capability to accomplish almost zero-emissions of carbon dioxide and hazardous substances is a unique feature for the IGCC-technology in a fossil fuel based power generation market. Nevertheless, IGCC power plants with Carbon Capture (CC-IGCC) could not be established on the market so far.

The complexity and the entirely different process technology of CC-IGCC are supposed to deter electric utilities from project realization. Indeed, previous descriptions of the complex correlations within and between the individual sub-processes of CC-IGCC have room for improvement. Moreover, there is a high level of uncertainty with respect to the economic feasibility of CC-IGCC.

The objective of this thesis is to provide an extensive description of the correlations in some of the most crucial sub-processes for hard coal fired CC-IGCC. For this purpose, process simulation models are developed and used to clarify the influence of certain boundary conditions on plant operation, performance and economics.

In the beginning, recent studies for IGCC-concepts are summarized. A closer look is taken to the published plant performance and the expected cost of electricity (CoE). Distinctions are made with respect to four different coal gasification technologies. These are the Shell Coal Gasification Process (SCGP), the Siemens gasifier, the ConocoPillips gasifier (CoP) and the General Electric (GE) gasifier. Moreover, different approaches for concept optimization are analyzed. Most of them investigated the influence of integration between the gas turbine and the air separation unit (ASU). A smaller number of studies proposed measures to achieve the optimum CO_2-capture rate.

The published results show a high fluctuation for the efficiency and the CoE even for IGCC-concepts with the same gasifier type. A detailed analysis is carried out for a few selected studies in order to clarify the cause for these differences. It is found that some of the studies use greatly different assumptions for process modeling

which are not adequately described. The CoE-fluctuations mainly appear as a result of different underlying costs for investment and fuel.

Each of the considered studies that investigate the influence of integration between the gas turbine and the ASU provide a clear statement for the correlation between the efficiency and the level of integration. However, the results of the individual studies are partly opposed to each other so that a clear tendency cannot be derived. The same has to be noticed for the studies investigating the optimal CO_2-capture rate. Again, a detailed analysis of selected studies is conducted in order to find the reason for the different results. Same as above, no final clarification can be derived since different assumptions are used and modeling details are rare. However, a weak point breakdown provides some basic ideas for the subsequent adaptation.

In general, the most part of the reviewed literature is criticized since the descriptions of the individual processes are often inadequate and modeling details are mostly not provided or rather given in a short deepness. Due to this lack of information, the analysis of results is hindered and general conclusions cannot be derived. Same as argued by the Massachusetts Institute of Technology [34], the lack of published modeling details is considered to be a serious handicap for reliable assessment of complex CC-IGCC.

As a consequence, the following scope of work is defined for this thesis:

- Process flow diagrams for CC-IGCC concepts based on the four above mentioned gasifier types have to be designed.
- Sophisticated process simulation models for the main sub-processes of a CC-IGCC have to be developed and applied. Moreover, a substantial description of global coherences is to be aimed at so that the correlations within and between the individual sub-processes can be clearly illustrated.
- The concepts have to be ranked on the basis of an energetic and economic assessment.
- The influence of integration between the gas turbine and the ASU, under consideration of thermodynamic and operational aspects, has to be analyzed.

- Finally, the optimal CO_2-capture rate for a CC-IGCC has to be identified.

Within the main part of this thesis, process flow diagrams for CC-IGCC concepts and sophisticated process simulation models are developed and described. The concepts based on the four gasifiers are slightly different to each other but on a common basis. The developed models proof successful simulation for the gasification processes, the CO-shift cycle, the acid gas removal unit, the sulfur recovery process, the gas turbine, the water-/steam cycle and the ASU. Based on this, the coherences within and between the mayor sub-processes are extensively discussed and described. As a consequence of the achieved high level of detail, model validation is not possible. However, the plausibility check of results does not indicate any reasonable doubts on the developed models. Beyond that, the efficiency for one comparable concept published by Gräbner et al. [20] shows conformity to the herein presented results.

The comparative benchmark of the CC-IGCC concepts based on the four different gasifier types adds up the following:

- The highest net efficiency is expected for the concept with CoP gasifier ($\eta_{IGCC,net}$ = 36.1 %).
- The concepts with the SCGP and the GE-gasifier with radiant cooler turn out to reach the same level of efficiency ($\eta_{IGCC,net}$ = 35.3 % and 35.2 %, respectively).
- The concept based on the Siemens gasifier achieves the weakest of all four efficiencies ($\eta_{IGCC,net}$ = 34.9 %). However, there is only a small distance to the two last mentioned concepts.
- All concepts but the one with CoP-gasifier can achieve CO_2-emissions as low as about 65 g/kWh which corresponds to a carbon retention rate of 93 %. Due to the methane content produced by the CoP-gasifier, this concept reaches only about 104 g/kWh (88 % carbon retention rate).
- The concept based on the SCGP is expected to be the worst economic choice under given boundary conditions. The calculated CoE is 7 to 10 % higher than at the other three concepts. However, a clear favorite technology out of these three cannot be named, since the achieved CoE are quite contiguous (108 – 110 €/MWh).

The economic analysis also clarifies the dominant impact of the investment costs. Roughly 60 % of the CoE is owed to the investment costs while the second largest cost driver (fuel) only takes the responsibility for less than a quarter of the CoE. In addition, a sensitivity study brings out that investment cost reduction promises the highest potential for CoE enhancement. On the other hand, the improvements of efficiency and availability only have a minor influence to the achievable CoE. Finally, the cost of CO_2-avoidance compared to a conventional pulverized coal power plant without CO_2-capture is calculated to be between 90 and 120 €/t of CO_2. This means, that CC-IGCC at nowadays conditions will only be superior to state of the art steam power plants if the prices for the CO_2-emission certificates will be markedly higher than 90 €/t of CO_2. Otherwise the CoE for a CC-IGCC needs to be reduced by over 50 % in order to be economic feasible at present day prices for the CO_2-emission certificates.

Furthermore, a case study illustrates the thermodynamic performance for concept alternatives with reduced CO_2-capture rates. The economic analysis shows that a reduced CO_2-capture rate is only favorable (in comparison to the reference CC-IGCC) at low prices for the CO_2-emission certificate. However, economic feasibility at the present day power generation market is also not given at all.

The analysis of the influence of integration between the gas turbine and the ASU delivers the following results:

- The gas turbines operating behavior and limitations are decisive for the identification of the optimal level of integration between the gas turbine and the ASU.
- High levels of air integration are only thermodynamically advantageous at high levels of nitrogen integration. The thermodynamic benefit of air integration disappears as soon as higher maximum fuel gas hydrogen contents can be realized than possible with the nowadays state of the art technology.

- For a given compressor air extraction rate, the maximum of net efficiency and net power output is achieved at that nitrogen integration rate (fuel gas hydrogen content) where the gas turbine is operated at the mechanical shaft limit while its compressor barely runs at full load flow.

Finally, the previous findings are used to develop an advanced plant configuration with improved economics. The idea is to decouple the combined cycle power plant (CCPP) from the upstream processes so that a standardized CCPP with considerable lower CapEx can be applied. As a consequence of de-integration, the net efficiency decreases slightly by about 0.4 %-points which however does not noticeably increase the CoE. On the other hand the CoE is expected to decrease by about 18 % through the use of standardized sub-processes. Moreover, the proposed concept is expected to be less financially venturous for a first time application of a gasification based power plant with CO_2-capture.

In summary, IGCC power plants with CO_2-capture are not found to be an economically efficient power generation technology at present day boundary conditions. The field of application is rather assumed to be the combined production of chemicals and power or the utilization of challenging coals that cannot be handled at conventional fired power plants. In this regard, the unique features of IGCC-technology can be better accentuated.

Appendix

Appendix A – Nomenclature of the process streams used in the flow schemes

The nomenclature of the process streams has to be interpreted as follows:

source process – target process – fluid – serial number.

The source and target processes were numbered as follows:

0	Battery Limits / Ambient
1	Air Separation unit (ASU)
2	Gasifier
3	CO-shift
4	Acid gas removal (AGR)
5	Sulfur recovery unit (SRU)
6	CO2-compression
7	Gas turbine
8	Water steam cycle
9	Cooling system
10	Water treatment

The following abbreviations were used for the fluids:

Coal	Coal
GOX	Gaseous oxygen
GAN	Gaseous nitrogen
DGAN	Diluent nitrogen
Gas	Flammable gas
eg	Exhaust gas
st	Steam
BFW	Boiler feed water
Slag	Slag
wa	Process water / process condensate
cond	Condensate (from clean steam)

mu	Make up water
ww	Waste water
cw	Cooling water
CO2	Carbon dioxide
met	Methanol
S	Sulfur

Example: 2-3-st-7 means:

From Gasifier – To CO-shift – Fluid: Steam – ongoing steam stream number in the overall IGCC flow scheme: 7

Appendix B1 – Deviation from the equilibrium temperatures in K

Reaction	SCGP	Siemens	GE	CoP	
				1st stage	2nd stage
$C + O_2 \leftrightarrow CO_2$	0	0	0	-150	-50
$C + CO_2 \leftrightarrow 2\ CO$	-330	-310	0	-150	-50
$CO + 3\ H_2 \leftrightarrow CH_4 + H_2O$	10	0	-320	-150	-50
$CO + H_2O \leftrightarrow H_2 + CO_2$	-280	0	0	-150	-50
$H_2 + S \leftrightarrow H_2S$	0	0	0	-150	-50
$CO + S \leftrightarrow COS$	-45	0	24	-150	-50
$N_2 + 3\ H_2 \leftrightarrow 2\ NH_3$	0	0	0	-150	-485
$N_2 + H_2 + 2\ C \leftrightarrow 2\ HCN$	0	0	0	-150	-50
$Cl_2 + H_2 \leftrightarrow 2\ HCl$	0	0	0	-150	-50

Appendix B2 – CHEMCAD-flow sheet for the model of the SCGP

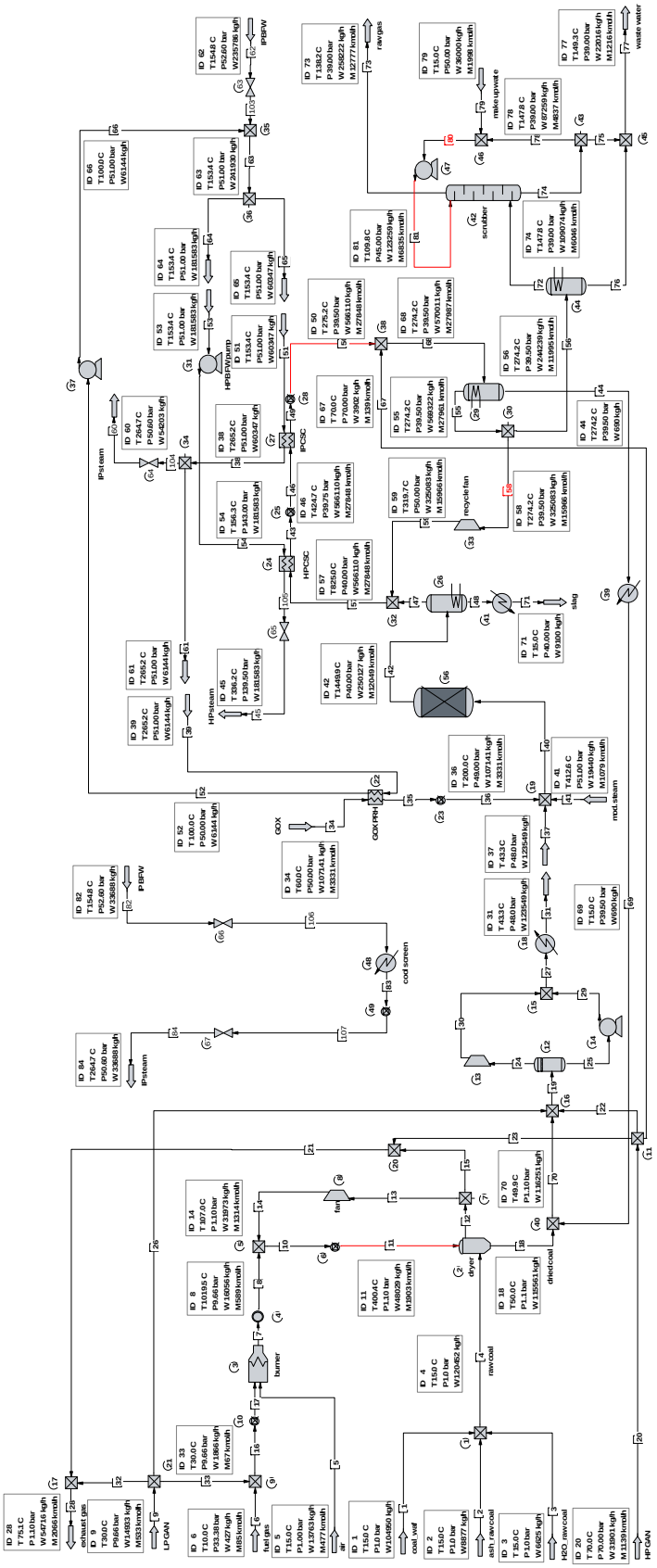

Appendix B3 – Heat and material balance for the model of the SCGP

stream ID		0-2-coal-1	0-2-air-1	1-2-GOX-1	1-2-GAN-1	1-2-GAN-2	4-2-gas-2	8-2-st-1	8-2-BFW-1	10-2-mu-1	2-0-eg-1	2-0-slag-1	2-3-gas-1	2-3-st-7	2-8-st-4	2-10-ww-1
name		raw coal	air	GOX	HP GAN	LP GAN	fuel gas	IP steam	IP BFW	make up water	exhaust gas	slag	raw gas	IP steam	HP steam	waste water
t	°C	15.0	15.0	60.0	70.0	30.0	10.0	412.6	154.8	15.0	73.8		138.2	264.7	336.2	149.3
p	bar		1.0	50.0	70.0	9.7	33.4	51.0	52.6	50.0	1.1		39.0	50.6	139.5	39.0
m	kg/s	34.634	3.957	30.807	9.173	4.294	0.123	5.590	76.091	10.351	15.733	2.616	74.248	24.924	51.167	6.330
n	kmol/s		0.137	0.958	0.327	0.153	0.024	0.310	4.224	0.575	0.594		3.674	1.384	2.840	0.350
V	Nm³/h		11,067	77,281	26,415	12,365	1,974				47,928		296,445			
LHV	kJ/kg	29,887					45,142						11,226			
HHV	kJ/kg	31,116					53,031						11,862			
h	kJ/kg		-99	22	38	3	-1,333	-12,757	-15,328	-15,919	-1,531		-4,373	-13,190	-13,324	-15,161
s	J/kgK		128	-873	-1,141	-656	-4,664	-2,729	-7,522	-9,184	4		1,634	-3,447	-4,056	-7,495
M	kg/kmol		28.85	32.16	28.02	28.02	5.02	18.01	18.01	18.01	26.49		20.21	18.01	18.01	18.10
Σ	mol %		100.00	100.00	100.00	100.00	100.00	100.00	100.00	100.00	100.00		100.00		100.00	100.00
H2	mol %						89.15				0.00		28.11			0.01
CO	mol %						3.85				0.00		54.55			0.02
CO2	mol %		0.03				0.50				0.19		1.95			0.00
N2	mol %		77.31	1.94	99.91	99.91	5.54				79.59		4.07			0.00
Ar	mol %		0.91	3.06	0.03	0.03	0.92				0.27		0.80			0.00
CH4	mol %						0.03				0.00		0.03			0.00
O2	mol %		20.74	95.00	0.06	0.06	0.00				2.91		0.00			0.00
H2O	mol %		1.01				0.00	100.00	100.00	100.00	17.05		9.67	100.00	100.00	99.32
H2S	mol %						0.00				0.00		0.76			0.01
COS	mol %						0.00				0.00		0.07			0.05
SO2	mol %						0.00				0.00		0.00			0.00
S	mol %						0.00				0.00		0.00			0.00
HCN	mol %						0.00				0.00		0.00			0.00
NH3	mol %						0.00				0.00		0.00			0.40
CH3OH	mol %						0.00				0.00		0.00			0.04
HCl	mol %						0.00				0.00		0.00			0.14
Σ	mass %	100.00	100.00	100.00	100.00	100.00	100.00	100.00	0.00	100.00	100.00	100.00	100.00	100.00	100.00	100.00
H2	mass %			0.00	0.00	0.00	35.78				0.00		2.80			0.00
CO	mass %			0.00	0.00	0.00	21.49				0.00		75.61			0.03
CO2	mass %		0.05	0.00	0.00	0.00	4.39				0.31		4.24			0.00
N2	mass %		75.06	1.69	99.89	99.89	30.90				84.18		5.64			0.00
Ar	mass %		1.26	3.80	0.04	0.04	7.31				0.40		1.58			0.00
CH4	mass %			0.00	0.00	0.00	0.09				0.00		0.02			0.00
O2	mass %		23.00	94.51	0.07	0.07	0.00				3.51		0.00			0.00
H2O	mass %	5.50	0.63	0.00	0.00	0.00	0.00	100.00		100.00	11.60		8.62	100.00	100.00	98.84
H2S	mass %			0.00	0.00	0.00	0.00				0.00		1.28			0.02
COS	mass %			0.00	0.00	0.00	0.00				0.00		0.20			0.18
SO2	mass %			0.00	0.00	0.00	0.00				0.00		0.00			0.00
S	mass %			0.00	0.00	0.00	0.00				0.00		0.00			0.01
HCN	mass %			0.00	0.00	0.00	0.00				0.00		0.00			0.60
NH3	mass %			0.00	0.00	0.00	0.00				0.00		0.00			0.04
CH3OH	mass %			0.00	0.00	0.00	0.03				0.00		0.00			0.00
HCl	mass %			0.00	0.00	0.00	0.00				0.00		0.00			0.28
coal	mass %	87.13		0.00	0.00	0.00	0.00				0.00		0.00			0.00
ash	mass %	7.37		0.00	0.00	0.00	0.00				0.00	97.58	0.00			0.00
C	mass %			0.00	0.00	0.00	0.00				0.00	2.42	0.00			0.00
solids	mass %	94.50	0.00	0.00	0.00	0.00	0.00	0.00	0.00	0.00	0.00	100.00	0.00	0.00	0.00	0.00

Appendix B4 – CHEMCAD-flow sheet for the model of the Siemens gasifier

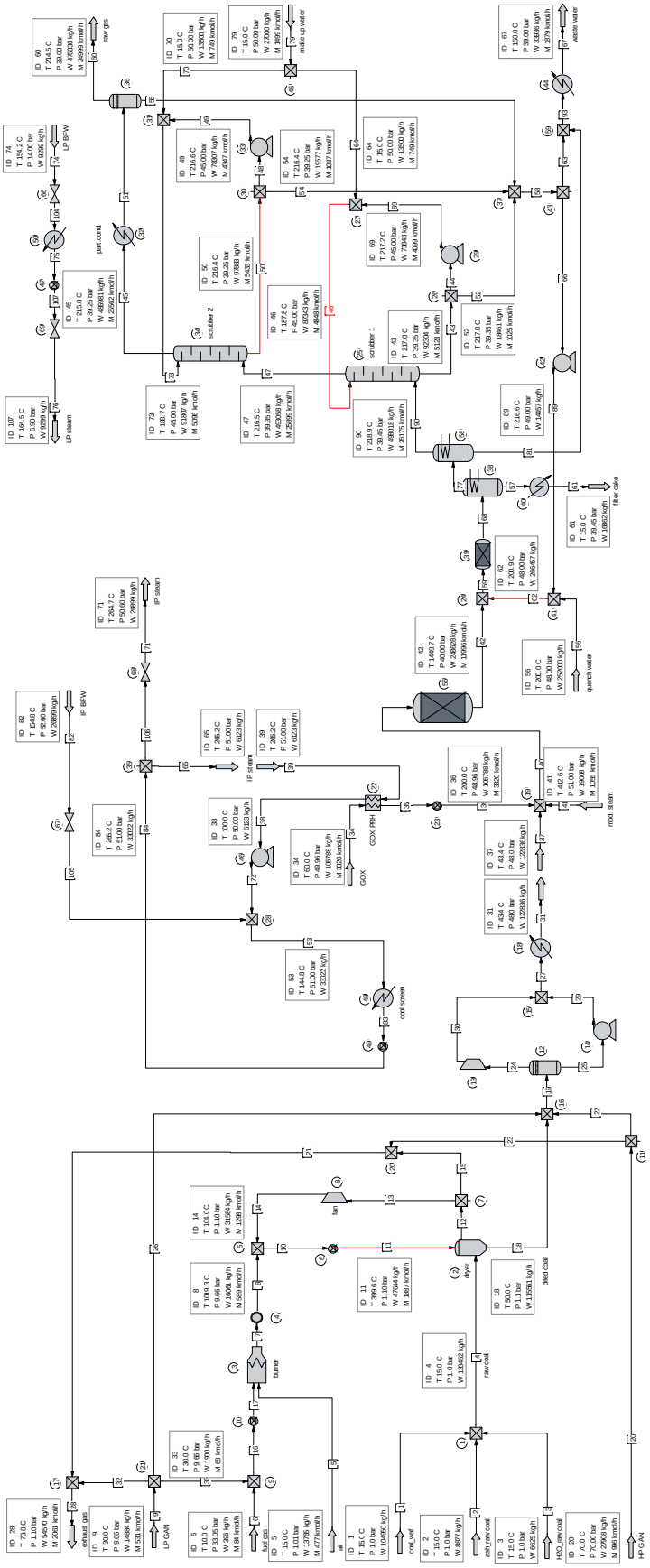

Appendix B5 – Heat and material balance for the model of the Siemens gasifier

stream ID		0-2-coal-1	0-2-air-1	1-2-GOX-1	1-2-GAN-1	1-2-GAN-2	3-2-wa-2	4-2-gas-2	8-2-st-1	8-2-BFW-1	8-2-BFW-2	10-2-mu-1	2-0-eg-1	2-0-slag-1	2-3-gas-1	2-8-st-5	2-8-st-6	2-10-ww-1
name		raw coal	air	GOX	HP GAN	LP GAN	quench water	fuel gas	IP steam	IP BFW	LP BFW	make up water	exhaust gas	filter cake	raw gas	IP steam	LP steam	waste water
t	°C	15.0	15.0	60.0	70.0	30.0	200.0	10.0	412.6	154.8	154.2	15.0	73.8		214.5	264.7	163.4	150.0
p	bar		1.01	50.0	70.0	9.7	48.0	33.0	51.0	52.6	14.0	50.0	1.1		39.0	50.6	6.6	39.0
m	kg/s	34.722	3.968	30.783	8.045	4.291	72.643	0.114	5.479	7.599	2.681	7.783	15.731	4.861	137.454	7.599	2.681	9.782
n	kmol/s		0.138	0.957	0.287	0.153	4.032	0.0242	0.304	0.422	0.149	0.432	0.594		7.206	0.422	0.149	0.542
V	Nm³/h		11,097	77,223	23,166	12,355		1,954					47,929		581,466			
LHV	kJ/kg	29,887						48,741							6,049			
HHV	kJ/kg	31,116						57,267							6,418			
h	kJ/kg		-99	22	38	3	-15,124	-1,415	-12,757	-15,328	-15,330	-15,919	-1,535		-8,492	-13,190	-13,221	-15,243
s	J/kgK		124	-873	-1,141	-656	-7,080	-5,021	-2,729	-7,522	-7,528	-9,184	4		-472	-3,447	-2,681	-7,529
M	kg/kmol		28.85	32.16	28.02	28.02	18.02	4.71	18.01	18.01	18.01	18.01	26.48		19.07	18.01	18.01	18.06
Σ	mol %		100.00	100.00	100.00	100.00	100.00	100.00	100.00	100.00	100.00	100.00	100.00		100.00	100.00	100.00	100.00
H2	mol %		0.00	0.00	0.00	0.00	0.00	90.35	0.00	0.00	0.00	0.00	0.00		15.40	0.00	0.00	0.00
CO	mol %		0.00	0.00	0.00	0.00	0.00	3.83	0.00	0.00	0.00	0.00	0.00		26.78	0.00	0.00	0.00
CO2	mol %		0.03	0.00	0.00	0.00	0.01	0.50	0.00	0.00	0.00	0.00	0.19		2.03	0.00	0.00	0.00
N2	mol %		77.31	1.94	99.91	99.91	0.00	4.35	0.00	0.00	0.00	0.00	79.53		1.52	0.00	0.00	0.00
Ar	mol %		0.91	3.06	0.03	0.03	0.00	0.93	0.00	0.00	0.00	0.00	0.27		0.41	0.00	0.00	0.00
CH4	mol %		0.00	0.00	0.00	0.00	0.00	0.03	0.00	0.00	0.00	0.00	0.00		0.02	0.00	0.00	0.00
O2	mol %		20.74	95.00	0.06	0.06	0.00	0.00	0.00	0.00	0.00	0.00	2.92		0.00	0.00	0.00	0.00
H2O	mol %		1.01	0.00	0.00	0.00	99.99	0.00	100.00	100.00	100.00	100.00	17.10		53.43	100.00	100.00	99.62
H2S	mol %		0.00	0.00	0.00	0.00	0.00	0.00	0.00	0.00	0.00	0.00	0.00		0.39	0.00	0.00	0.00
COS	mol %		0.00	0.00	0.00	0.00	0.00	0.00	0.00	0.00	0.00	0.00	0.00		0.04	0.00	0.00	0.00
SO2	mol %		0.00	0.00	0.00	0.00	0.00	0.00	0.00	0.00	0.00	0.00	0.00		0.00	0.00	0.00	0.00
S	mol %		0.00	0.00	0.00	0.00	0.00	0.00	0.00	0.00	0.00	0.00	0.00		0.00	0.00	0.00	0.00
HCN	mol %		0.00	0.00	0.00	0.00	0.00	0.00	0.00	0.00	0.00	0.00	0.00		0.00	0.00	0.00	0.00
NH3	mol %		0.00	0.00	0.00	0.00	0.00	0.00	0.00	0.00	0.00	0.00	0.00		0.00	0.00	0.00	0.26
CH3OH	mol %		0.00	0.00	0.00	0.00	0.00	0.00	0.00	0.00	0.00	0.00	0.00		0.00	0.00	0.00	0.03
HCl	mol %		0.00	0.00	0.00	0.00	0.00	0.00	0.00	0.00	0.00	0.00	0.00		0.00	0.00	0.00	0.09
Σ	mass %	100.00	100.00	100.00	100.00	100.00	100.00	100.00	100.00	100.00	100.00	100.00	100.00	100.00	100.00	100.00	100.00	100.00
H2	mass %		0.00	0.00	0.00	0.00	0.00	38.66	0.00	0.00	0.00	0.00	0.00		1.63	0.00	0.00	0.00
CO	mass %		0.00	0.00	0.00	0.00	0.00	22.77	0.00	0.00	0.00	0.00	0.00		39.32	0.00	0.00	0.00
CO2	mass %		0.05	0.00	0.00	0.00	0.01	4.67	0.00	0.00	0.00	0.00	0.31		4.67	0.00	0.00	0.00
N2	mass %		75.06	1.69	99.89	99.89	0.00	25.88	0.00	0.00	0.00	0.00	84.13		2.23	0.00	0.00	0.00
Ar	mass %		1.26	3.80	0.05	0.05	0.00	7.88	0.00	0.00	0.00	0.00	0.40		0.85	0.00	0.00	0.00
CH4	mass %		0.00	0.00	0.00	0.00	0.00	0.12	0.00	0.00	0.00	0.00	0.00		0.01	0.00	0.00	0.00
O2	mass %		23.00	94.51	0.07	0.07	0.00	0.00	0.00	0.00	0.00	0.00	3.52		0.00	0.00	0.00	0.00
H2O	mass %	5.50	0.63	0.00	0.00	0.00	99.98	0.00	100.00	100.00	100.00	100.00	11.63	44.72	50.46	100.00	100.00	99.39
H2S	mass %		0.00	0.00	0.00	0.00	0.01	0.00	0.00	0.00	0.00	0.00	0.00		0.70	0.00	0.00	0.00
COS	mass %		0.00	0.00	0.00	0.00	0.00	0.00	0.00	0.00	0.00	0.00	0.00		0.12	0.00	0.00	0.01
SO2	mass %		0.00	0.00	0.00	0.00	0.00	0.00	0.00	0.00	0.00	0.00	0.00		0.00	0.00	0.00	0.00
S	mass %		0.00	0.00	0.00	0.00	0.00	0.00	0.00	0.00	0.00	0.00	0.00		0.00	0.00	0.00	0.01
HCN	mass %		0.00	0.00	0.00	0.00	0.00	0.00	0.00	0.00	0.00	0.00	0.00		0.00	0.00	0.00	0.39
NH3	mass %		0.00	0.00	0.00	0.00	0.00	0.00	0.00	0.00	0.00	0.00	0.00		0.00	0.00	0.00	0.03
CH3OH	mass %		0.00	0.00	0.00	0.00	0.00	0.03	0.00	0.00	0.00	0.00	0.00		0.00	0.00	0.00	0.00
HCl	mass %		0.00	0.00	0.00	0.00	0.00	0.00	0.00	0.00	0.00	0.00	0.00		0.00	0.00	0.00	0.18
coal	mass %	87.13	0.00	0.00	0.00	0.00	0.00	0.00	0.00	0.00	0.00	0.00	0.00		0.00	0.00	0.00	0.00
ash	mass %	7.37	0.00	0.00	0.00	0.00	0.00	0.00	0.00	0.00	0.00	0.00	0.00	52.65	0.00	0.00	0.00	0.00
C	mass %		0.00	0.00	0.00	0.00	0.00	0.00	0.00	0.00	0.00	0.00	0.00	2.63	0.00	0.00	0.00	0.00
solids	mass %	94.50	0.00	0.00	0.00	0.00	0.00	0.00	0.00	0.00	0.00	0.00	0.00	55.28	0.00	0.00	0.00	0.00

Appendix B6 – CHEMCAD-flow sheet for the model of the CoP gasifier

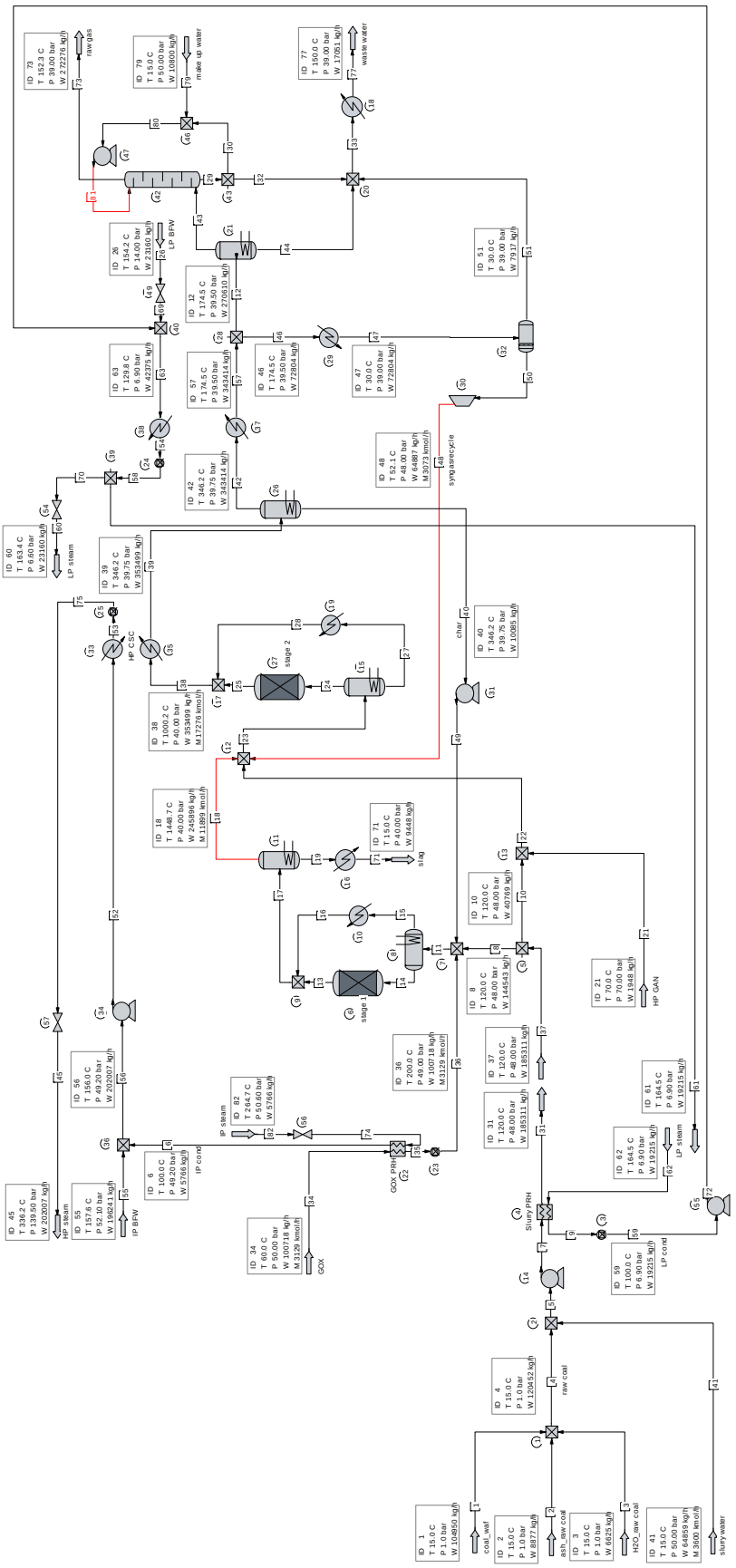

Appendix B7 – Heat and material balance for the model of the CoP gasifier

stream ID		0-2-coal-1	10-2-wa-1	1-2-GOX-1	1-2-GAN-1	8-2-st-3	8-2-BFW-1	8-2-BFW-2	10-2-mu-1	2-0-slag-1	2-3-gas-1	2-8-st-4	2-8-st-6	2-10-ww-1
name		raw coal	slurry water	GOX	HP GAN	IP steam	IP BFW	LP BFW	make up water	slag	raw gas	HP steam	LP steam	waste water
t	°C	15.0	15.0	60.0	70.0	264.7	157.6	154.2	15.0		152.3	336.2	163.4	150.0
p	bar		50.0	50.0	70.0	50.6	52.1	14.0	50.0		39.0	139.5	6.6	39.0
m	kg/s	35.101	18.901	29.351	0.568	1.680	57.187	6.749	3.147	2.753	79.345	58.867	6.749	4.969
n	kmol/s		1.049	0.912	0.020	0.093	3.174	0.375	0.175		3.832	3.268	0.375	0.275
V	Nm³/h			73,575	1,635						309,164			
LHV	kJ/kg	29,887									10,402			
HHV	kJ/kg	31,116									11,193			
h	kJ/kg		-15,919	22	38	-13,190	-15,315	-15,330	-15,919		-5,803	-13,324	-13,221	-15,276
s	J/kgK		-9,184	-873	-1,143	-3,446	-7,493	-7,528	-9,184		932	-4,056	-2,681	-7,548
M	kg/kmol		18.01	32.19	28.02	18.01	18.01	18.01	18.01		20.71	18.01	18.01	18.05
Σ	mol %		100.00	100.00	100.00	100.00	100.00	100.00	100.00		100.00	100.00	100.00	100.00
H2	mol %		0.00								28.98			0.00
CO	mol %		0.00								39.77			0.00
CO2	mol %		0.00								11.44			0.00
N2	mol %		0.00	1.74	99.98						1.38			0.00
Ar	mol %		0.00	3.26	0.01						0.78			0.00
CH4	mol %		0.00								3.56			0.00
O2	mol %		0.00	95.00	0.01						0.00			0.00
H2O	mol %		100.00			100.00	100.00	100.00	100.00		13.28	100.00	100.00	99.63
H2S	mol %		0.00								0.76			0.00
COS	mol %		0.00								0.05			0.00
SO2	mol %		0.00								0.00			0.00
S	mol %		0.00								0.00			0.00
HCN	mol %		0.00								0.00			0.00
NH3	mol %		0.00								0.00			0.01
CH3OH	mol %		0.00								0.00			0.18
HCl	mol %		0.00								0.00			0.18
Σ	mass %	100.00	100.00	100.00	100.00	0.00	0.00	0.00	0.00	100.00	100.00	100.00	100.00	100.00
H2	mass %		0.00								2.82			0.00
CO	mass %		0.00								53.80			0.00
CO2	mass %		0.00								24.31			0.00
N2	mass %		0.00	1.52	99.97	0.00	0.00	0.00	0.00		1.87			0.00
Ar	mass %		0.00	4.04	0.01	0.00	0.00	0.00	0.00		1.50			0.00
CH4	mass %		0.00								2.76			0.00
O2	mass %		0.00	94.44	0.01	0.00	0.00	0.00	0.00		0.00			0.00
H2O	mass %	5.50	100.00								11.55	100.00	100.00	99.45
H2S	mass %		0.00								1.26			0.00
COS	mass %		0.00								0.14			0.00
SO2	mass %		0.00								0.00			0.00
S	mass %		0.00								0.00			0.00
HCN	mass %		0.00								0.00			0.01
NH3	mass %		0.00								0.00			0.17
CH3OH	mass %		0.00								0.00			0.00
HCl	mass %		0.00								0.00			0.36
coal	mass %	87.13	0.00								0.00			0.00
ash	mass %	7.37	0.00							93.96	0.00			0.00
C	mass %		0.00							6.04	0.00			0.00
solids	mass %	94.50	0.00	0.00	0.00	0.00	0.00	0.00	0.00	100.00	0.00			0.00

Appendix B8 – CHEMCAD-flow sheet for the model of the GE-R

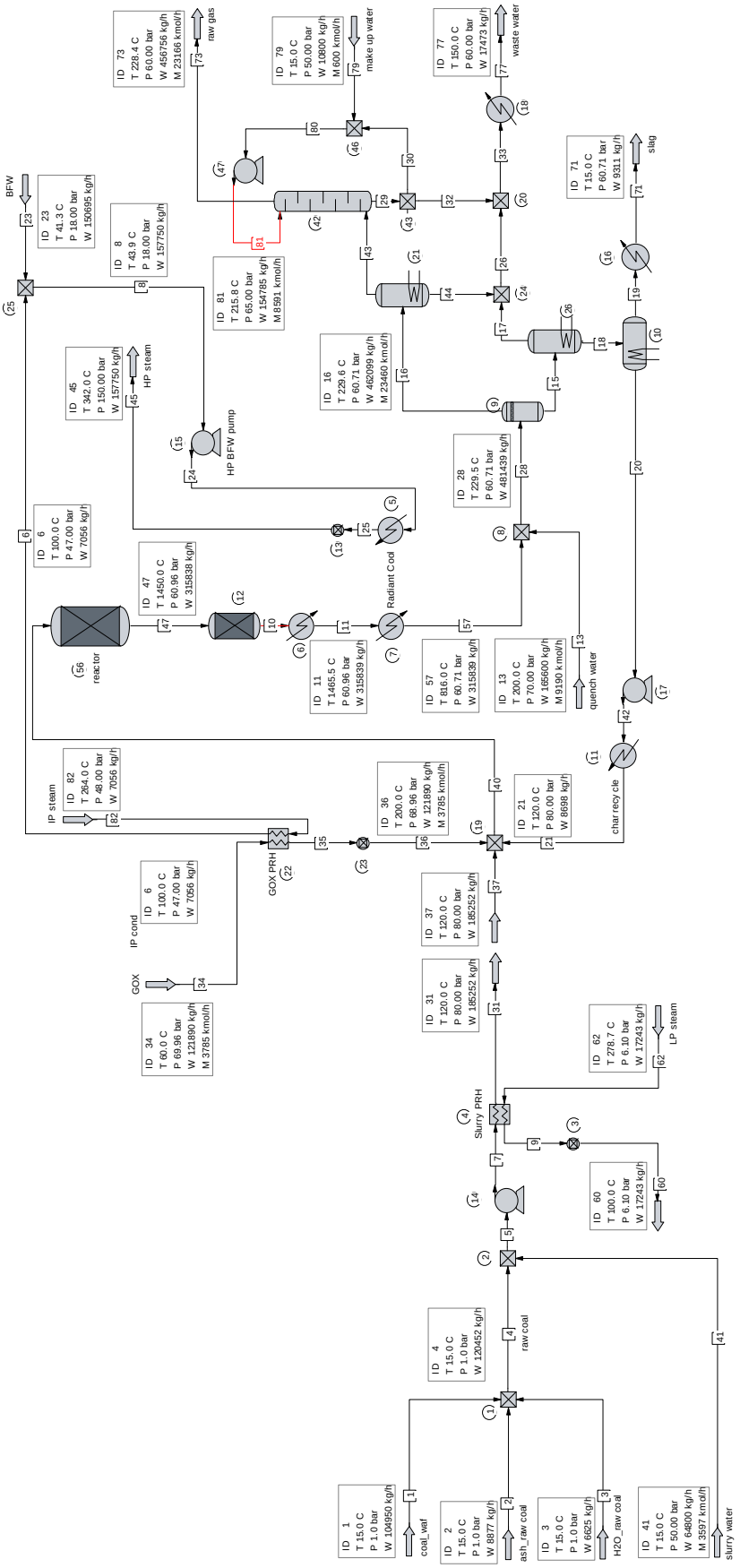

Appendix B9 – Heat and material balance for the model of the GE-R

stream ID		0-2-coal-1	10-2-wa-1	1-2-GOX-1	8-2-st-3	8-2-st-2	8-2-BFW-5	3-2-wa-2	10-2-mu-1	2-3-gas-1	2-0-slag-1	2-8-st-4	2-8-cond-1	2-10-ww-1
name		raw coal	slurry water	GOX	IP steam	LP steam	BFW	quench water	make up water	raw gas	slag	HP steam	LP cond	waste water
t	°C	15.0	15.0	60.0	264.0	278.7	41.3	200.0	15.0	228.4		342.0	100.0	150.0
p	bar		50.0	70.0	48.0	6.1	18.0	70.0	50.0	60.0		150.0	6.1	60.0
m	kg/s	37.776	20.322	38.227	2.213	5.408	47.261	51.935	3.387	143.247	2.920	49.473	5.408	5.480
n	kmol/s		1.128	1.187	0.123	0.300	2.623	2.882	0.188	7.265		2.746	0.300	0.303
V	Nm³/h			95,789						586,234				
LHV	kJ/kg	29,887		0						5,731				
HHV	kJ/kg	31,116		0						6,146				
h	kJ/kg		-15,919	19	-13,177	-12,965	-15,809	-15,122	-15,919	-8,638		-13,336	-15,562	-15,209
s	J/kgK		-9,184	-970	-3,403	-2,125	-8,822	-7,078	-9,184	-608		-4,110	-8,105	-7,513
M	kg/kmol		18.01	32.20	18.01	18.01	18.01	0.00	18.01	19.72		18.01	18.01	18.08
Σ	mol %		100.00	100.00	100.00	100.00	100.00	100.00	100.00	100.00		100.00	100.00	100.00
H2	mol %		0.00	0.00	0.00	0.00	0.00	0.00	0.00	17.73		0.00	0.00	0.00
CO	mol %		0.00	0.00	0.00	0.00	0.00	0.00	0.00	23.58		0.00	0.00	0.00
CO2	mol %		0.00	0.00	0.00	0.00	0.00	0.01	0.00	7.42		0.00	0.00	0.00
N2	mol %		0.00	1.64	0.00	0.00	0.00	0.00	0.00	0.51		0.00	0.00	0.00
Ar	mol %		0.00	3.36	0.00	0.00	0.00	0.00	0.00	0.55		0.00	0.00	0.00
CH4	mol %		0.00	0.00	0.00	0.00	0.00	0.00	0.00	0.12		0.00	0.00	0.00
O2	mol %		0.00	95.00	0.00	0.00	0.00	0.00	0.00	0.00		0.00	0.00	0.00
H2O	mol %		100.00	0.00	100.00	100.00	100.00	99.98	100.00	49.62		100.00	100.00	99.48
H2S	mol %		0.00	0.00	0.00	0.00	0.00	0.01	0.00	0.43		0.00	0.00	0.00
COS	mol %		0.00	0.00	0.00	0.00	0.00	0.00	0.00	0.03		0.00	0.00	0.00
SO2	mol %		0.00	0.00	0.00	0.00	0.00	0.00	0.00	0.00		0.00	0.00	0.00
S	mol %		0.00	0.00	0.00	0.00	0.00	0.00	0.00	0.00		0.00	0.00	0.00
HCN	mol %		0.00	0.00	0.00	0.00	0.00	0.00	0.00	0.00		0.00	0.00	0.00
NH3	mol %		0.00	0.00	0.00	0.00	0.00	0.00	0.00	0.00		0.00	0.00	0.29
CH3OH	mol %		0.00	0.00	0.00	0.00	0.00	0.00	0.00	0.00		0.00	0.00	0.04
HCl	mol %		0.00	0.00	0.00	0.00	0.00	0.00	0.00	0.00		0.00	0.00	0.18
Σ	mass %	100.00	100.00	100.00	100.00	100.00	100.00	100.00	100.00	100.00	100.00	100.00	100.00	100.00
H2	mass %		0.00	0.00	0.00	0.00	0.00	0.00	0.00	1.81		0.00	0.00	0.00
CO	mass %		0.00	0.00	0.00	0.00	0.00	0.00	0.00	33.50		0.00	0.00	0.00
CO2	mass %		0.00	0.00	0.00	0.00	0.00	0.02	0.00	16.56		0.00	0.00	0.00
N2	mass %		0.00	1.43	0.00	0.00	0.00	0.00	0.00	0.73		0.00	0.00	0.00
Ar	mass %		0.00	4.17	0.00	0.00	0.00	0.00	0.00	1.11		0.00	0.00	0.00
CH4	mass %		0.00	0.00	0.00	0.00	0.00	0.00	0.00	0.10		0.00	0.00	0.00
O2	mass %		0.00	94.40	0.00	0.00	0.00	0.00	0.00	0.00		0.00	0.00	0.00
H2O	mass %	5.50	100.00	0.00	100.00	100.00	100.00	99.96	100.00	45.34		100.00	100.00	99.15
H2S	mass %		0.00	0.00	0.00	0.00	0.00	0.02	0.00	0.75		0.00	0.00	0.00
COS	mass %		0.00	0.00	0.00	0.00	0.00	0.00	0.00	0.10		0.00	0.00	0.01
SO2	mass %		0.00	0.00	0.00	0.00	0.00	0.00	0.00	0.00		0.00	0.00	0.00
S	mass %		0.00	0.00	0.00	0.00	0.00	0.00	0.00	0.00		0.00	0.00	0.01
HCN	mass %		0.00	0.00	0.00	0.00	0.00	0.00	0.00	0.00		0.00	0.00	0.43
NH3	mass %		0.00	0.00	0.00	0.00	0.00	0.00	0.00	0.00		0.00	0.00	0.04
CH3OH	mass %		0.00	0.00	0.00	0.00	0.00	0.00	0.00	0.00		0.00	0.00	0.00
HCl	mass %		0.00	0.00	0.00	0.00	0.00	0.00	0.00	0.00		0.00	0.00	0.36
coal	mass %	87.13	0.00	0.00	0.00	0.00	0.00	0.00	0.00	0.00		0.00	0.00	0.00
ash	mass %	7.37	0.00	0.00	0.00	0.00	0.00	0.00	0.00	0.00	95.35	0.00	0.00	0.00
C	mass %		0.00	0.00	0.00	0.00	0.00	0.00	0.00	0.00	4.65	0.00	0.00	0.00
solids	mass %	94.50	0.00	0.00	0.00	0.00	0.00	0.00	0.00	0.00	100.00	0.00	0.00	0.00

Appendix C1 – Process flow diagram for the CO-shift cycle (CC-IGCC / GE-R)

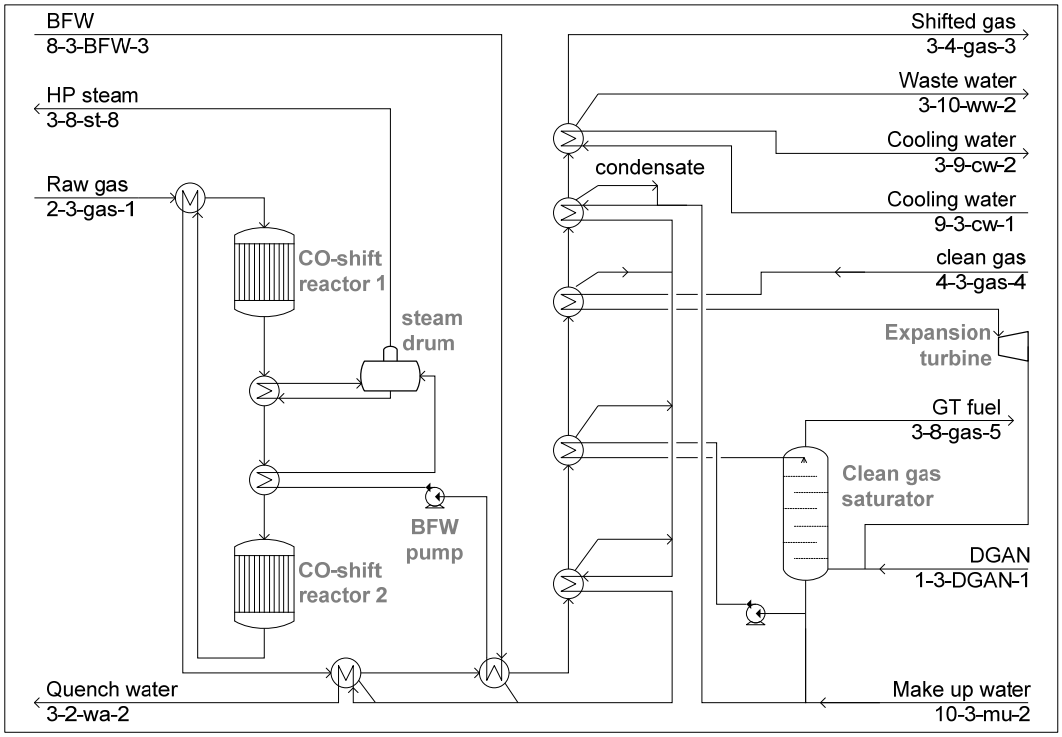

Appendix C2 – Process flow diagram for the CO-shift cycle (CC-IGCC / CoP gasifier)

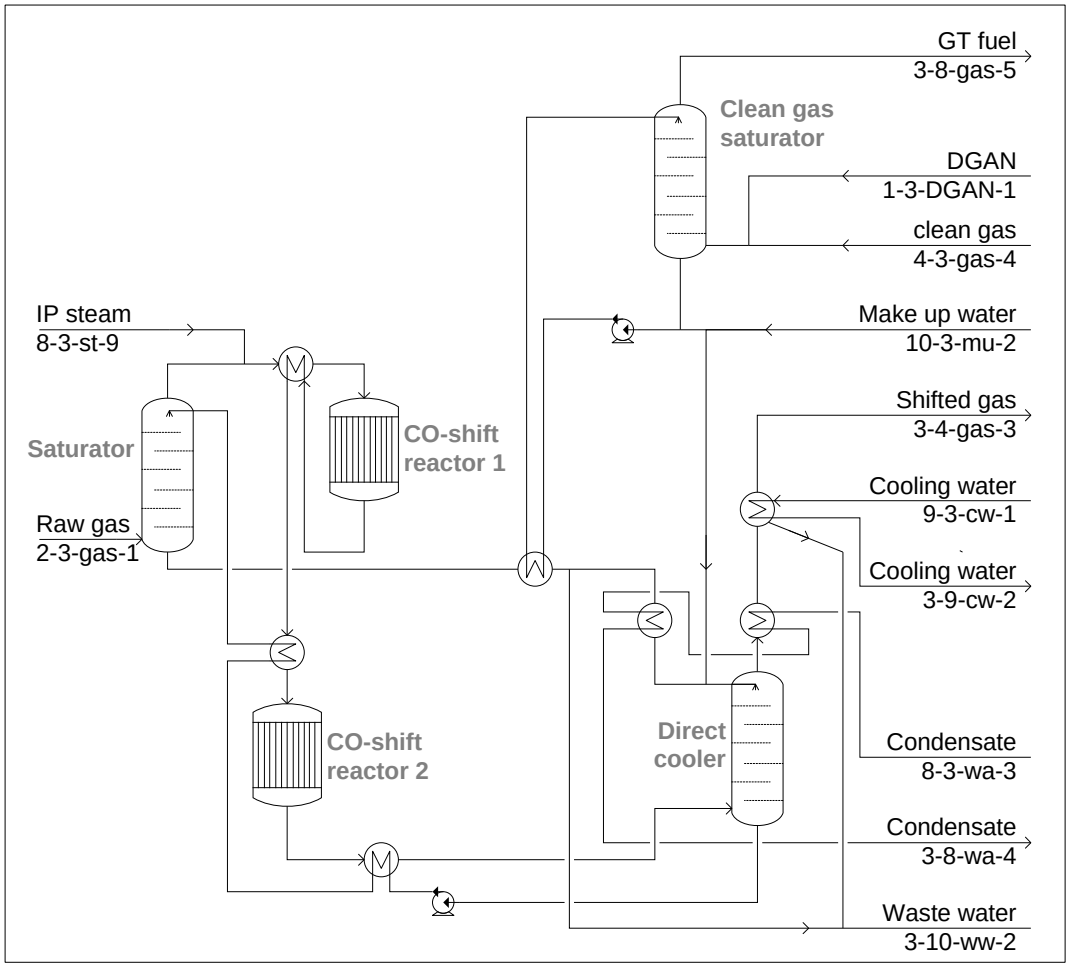

Appendix C3 – CHEMCAD CO-shift model for the CC-IGCC / SCGP

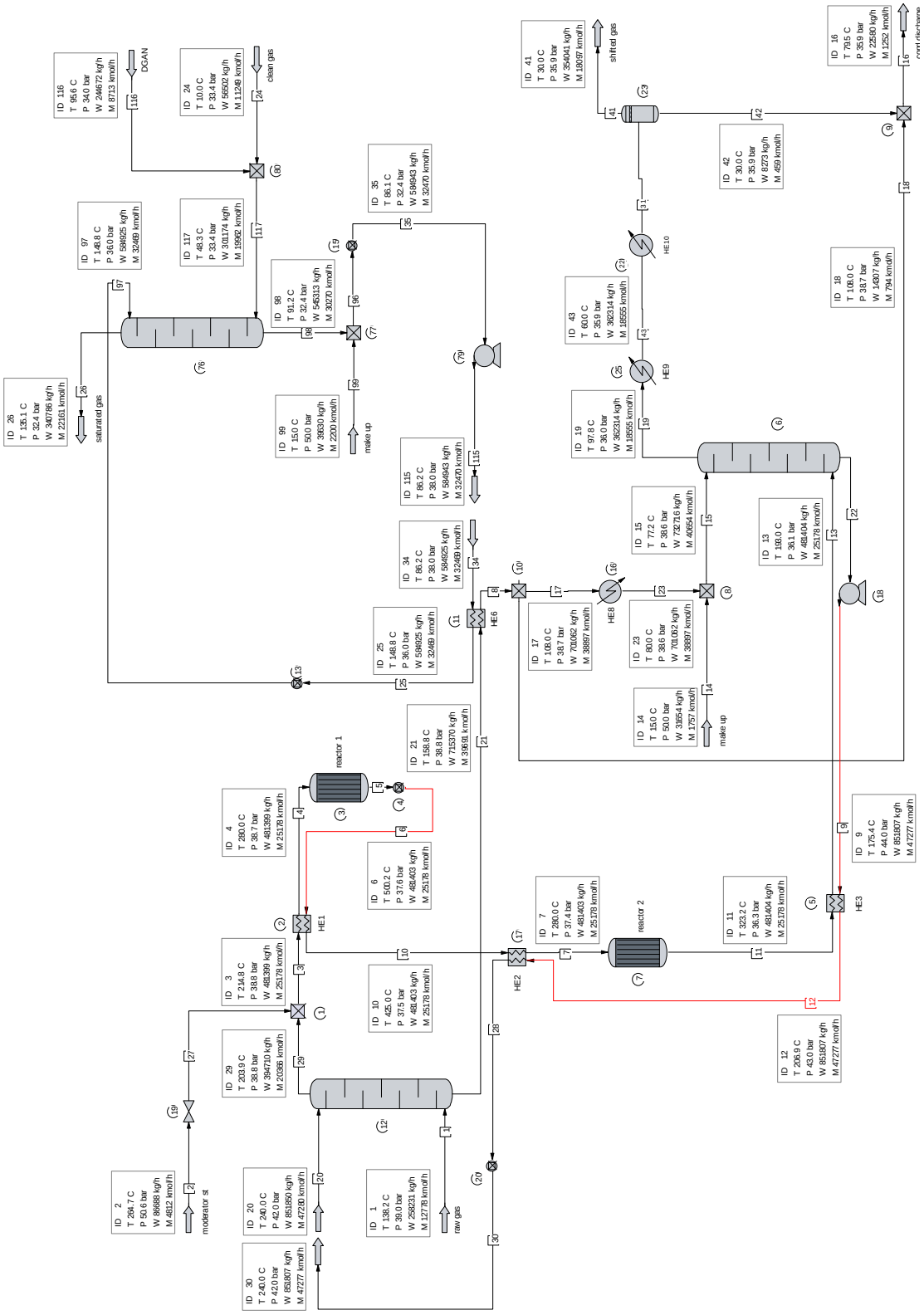

Appendix C4 – Heat and material balance for the CO-shift model (CC-IGCC / SCGP)

stream ID		1-3-DGAN-1	2-3-gas-1	2-3-st-7	4-3-gas-4	9-3-cw-1	10-3-mu-2	3-4-gas-3	3-8-gas-5	3-9-cw-2	3-10-ww-2
name		DGAN	raw gas	IP steam	clean gas	cooling water	make up water	shifted gas	GT fuel	cooling water	waste water
t	°C	95.6	138.2	264.7	10.0	20.0	15.0	30.0	136.8	30.0	80.3
p	bar	34.0	39.0	50.6	33.4	6.0	50.0	35.9	32.4	4.0	35.9
m	kg/s	70.351	74.249	24.926	16.246	155	20.997	101.821	98.611	155	6.337
n	kmol/s	2.505	3.674	1.384	3.235	8.627	1.166	5.205	6.407	8.627	0.352
V	Nm³/h	202,147	296,453		260,995			419,963	516,955		
LHV	kJ/kg		11,226		45,147			7,426			
HHV	kJ/kg		12,073		53,037			8,712			
h	kJ/kg	70	-4,386	-13,190	-1,329	-15,898	-15,919	-7,708	-1,633	-15,856	-15,629
s	J/kgK	-814	1,604	-3,446	-4,654	-9,113	-9,184	-946	-925	-8,974	-8,321
M	kg/kmol	28.07	20.20	18.00	5.01	18.00	18.00	19.59	15.38	18.00	18.01
Σ	mol %	100.00	100.00	100.00	100.00	100.00	100.00	100.00	100.00	100.00	100.00
H2	mol %	0.00	28.11	0.00	89.15	0.00	0.00	55.92	45.01	0.00	0.01
CO	mol %	0.00	54.55	0.00	3.85	0.00	0.00	2.42	1.95	0.00	0.01
CO2	mol %	0.00	1.95	0.00	0.50	0.00	0.00	37.48	0.25	0.00	0.02
N2	mol %	98.93	4.07	0.00	5.54	0.00	0.00	2.87	41.48	0.00	0.00
Ar	mol %	0.31	0.80	0.00	0.92	0.00	0.00	0.56	0.59	0.00	0.00
CH4	mol %	0.00	0.03	0.00	0.03	0.00	0.00	0.02	0.01	0.00	0.00
O2	mol %	0.76	0.00	0.00	0.00	0.00	0.00	0.00	0.30	0.00	0.00
H2O	mol %	0.00	9.67	100.00	0.00	100.00	100.00	0.14	10.41	100.00	99.93
H2S	mol %	0.00	0.76	0.00	0.00	0.00	0.00	0.56	0.00	0.00	0.02
COS	mol %	0.00	0.07	0.00	0.00	0.00	0.00	0.03	0.00	0.00	0.01
CS2	mol %	0.00	0.00	0.00	0.00	0.00	0.00	0.00	0.00	0.00	0.00
SO2	mol %	0.00	0.00	0.00	0.00	0.00	0.00	0.00	0.00	0.00	0.00
S	mol %	0.00	0.00	0.00	0.00	0.00	0.00	0.00	0.00	0.00	0.00
HCN	mol %	0.00	0.00	0.00	0.00	0.00	0.00	0.00	0.00	0.00	0.00
NH3	mol %	0.00	0.00	0.00	0.00	0.00	0.00	0.00	0.00	0.00	0.00
CH3OH	mol %	0.00	0.00	0.00	0.00	0.00	0.00	0.00	0.00	0.00	0.00
Σ	mass %	100.00	100.00	100.00	100.00	100.00	100.00	100.00	100.00	100.00	100.00
H2	mass %	0.00	2.80	0.00	35.78	0.00	0.00	5.76	5.89	0.00	0.00
CO	mass %	0.00	75.61	0.00	21.50	0.00	0.00	3.47	3.54	0.00	0.02
CO2	mass %	0.00	4.24	0.00	4.38	0.00	0.00	84.32	0.72	0.00	0.06
N2	mass %	98.69	5.64	0.00	30.91	0.00	0.00	4.11	75.50	0.00	0.00
Ar	mass %	0.44	1.58	0.00	7.31	0.00	0.00	1.15	1.52	0.00	0.00
CH4	mass %	0.00	0.02	0.00	0.09	0.00	0.00	0.02	0.02	0.00	0.00
O2	mass %	0.87	0.00	0.00	0.00	0.00	0.00	0.00	0.62	0.00	0.00
H2O	mass %	0.00	8.62	100.00	0.00	100.00	100.00	0.12	12.18	100.00	99.85
H2S	mass %	0.00	1.28	0.00	0.00	0.00	0.00	0.97	0.00	0.00	0.04
COS	mass %	0.00	0.20	0.00	0.00	0.00	0.00	0.08	0.00	0.00	0.03
CS2	mass %	0.00	0.00	0.00	0.00	0.00	0.00	0.00	0.00	0.00	0.00
SO2	mass %	0.00	0.00	0.00	0.00	0.00	0.00	0.00	0.00	0.00	0.00
S	mass %	0.00	0.00	0.00	0.00	0.00	0.00	0.00	0.00	0.00	0.00
HCN	mass %	0.00	0.00	0.00	0.00	0.00	0.00	0.00	0.00	0.00	0.00
NH3	mass %	0.00	0.00	0.00	0.00	0.00	0.00	0.00	0.00	0.00	0.00
CH3OH	mass %	0.00	0.00	0.00	0.03	0.00	0.00	0.00	0.00	0.00	0.00

Appendix C5 – CHEMCAD CO-shift model for the CC-IGCC / Siemens gasifier

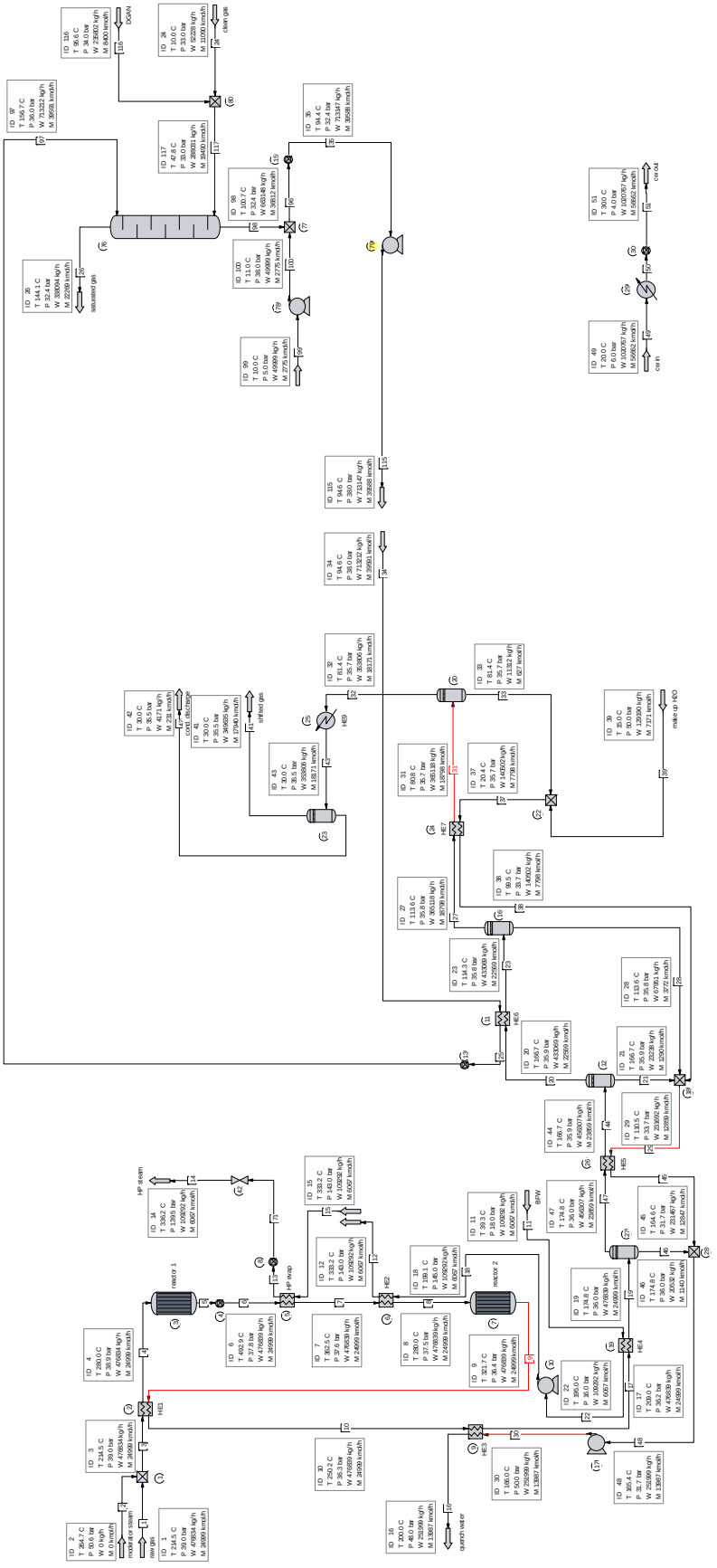

Appendix C6 – Heat and material balance for the CO-shift model (CC-IGCC / Siemens gasifier)

stream ID		1-3-DGAN-1	2-3-gas-1	4-3-gas-4	8-3-BFW-3	9-3-cw-1	10-3-mu-2	3-2-wa-2	3-4-gas-3	3-8-gas-5	3-8-st-8	3-9-cw-2	3-10-ww-2
name		DGAN	raw gas	clean gas	BFW	cooling water	make up water	quench water	shifted gas	GT fuel	HP steam	cooling water	waste water
t	°C	95.6	214.5	10.0	39.3	20.0	15.0	200.0	30.0	144.1	336.2	30.0	30.0
p	bar	34.0	39.0	33.0	18.0	6.0	50.0	48.0	35.5	32.4	139.5	4.0	35.5
m	kg/s	67.974	137.455	15.056	31.505	294.252	51.654	72.643	100.788	97.461	31.505	294.252	1.202
n	kmol/s	2.421	7.206	3.197	1.749	16.334	2.867	4.032	5.171	6.419	1.749	16.334	0.067
V	Nm³/h	195,383	581,470	257,958					417,276	517,979			
LHV	kJ/kg		6,049	48,759					7,510	7,532			
HHV	kJ/kg		7,656	57,288					8,813	9,213			
h	kJ/kg	70	-8,493	-1,413	-15,817	-15,898	-15,919	-15,124	-7,797	-1,968	-13,324	-15,856	-15,835
s	J/kgK	-817	-473	-5,012	-8,849	-9,113	-9,184	-7,080	-957	-964	-4,056	-8,974	-8,956
M	kg/kmol	28.06	19.06	4.69	18.00	18.00	18.00	18.00	19.51	15.17	18.00	18.00	18.02
Σ	mol %	100.00	100.00	100.00	100.00	100.00	100.00	100.00	100.00	100.00	100.00	100.00	100.00
H2	mol %	0.00	15.40	90.35	0.00	0.00	0.00	0.00	56.38	45.00	0.00	0.00	0.00
CO	mol %	0.00	26.78	3.83	0.00	0.00	0.00	0.00	2.39	1.91	0.00	0.00	0.00
CO2	mol %	0.00	2.03	0.50	0.00	0.00	0.00	0.01	37.79	0.25	0.00	0.00	0.07
N2	mol %	99.12	1.52	4.37	0.00	0.00	0.00	0.00	2.12	39.56	0.00	0.00	0.00
Ar	mol %	0.28	0.41	0.91	0.00	0.00	0.00	0.00	0.57	0.56	0.00	0.00	0.00
CH4	mol %	0.00	0.02	0.03	0.00	0.00	0.00	0.00	0.02	0.02	0.00	0.00	0.00
O2	mol %	0.59	0.00	0.00	0.00	0.00	0.00	0.00	0.00	0.22	0.00	0.00	0.00
H2O	mol %	0.00	53.43	0.00	100.00	100.00	100.00	99.99	0.14	12.48	100.00	100.00	99.90
H2S	mol %	0.00	0.39	0.00	0.00	0.00	0.00	0.00	0.59	0.00	0.00	0.00	0.03
COS	mol %	0.00	0.04	0.00	0.00	0.00	0.00	0.00	0.00	0.00	0.00	0.00	0.00
CS2	mol %	0.00	0.00	0.00	0.00	0.00	0.00	0.00	0.00	0.00	0.00	0.00	0.00
SO2	mol %	0.00	0.00	0.00	0.00	0.00	0.00	0.00	0.00	0.00	0.00	0.00	0.00
S	mol %	0.00	0.00	0.00	0.00	0.00	0.00	0.00	0.00	0.00	0.00	0.00	0.00
HCN	mol %	0.00	0.00	0.00	0.00	0.00	0.00	0.00	0.00	0.00	0.00	0.00	0.00
NH3	mol %	0.00	0.00	0.00	0.00	0.00	0.00	0.00	0.00	0.00	0.00	0.00	0.00
CH3OH	mol %	0.00	0.00	0.00	0.00	0.00	0.00	0.00	0.00	0.00	0.00	0.00	0.00
Σ	mass %	100.00	100.00	100.00	100.00	100.00	100.00	100.00	100.00	100.00	100.00	100.00	100.00
H2	mass %	0.00	1.63	38.67	0.00	0.00	0.00	0.00	5.83	5.97	0.00	0.00	0.00
CO	mass %	0.00	39.32	22.78	0.00	0.00	0.00	0.00	3.44	3.52	0.00	0.00	0.00
CO2	mass %	0.00	4.67	4.68	0.00	0.00	0.00	0.01	85.34	0.72	0.00	0.00	0.17
N2	mass %	98.92	2.23	25.99	0.00	0.00	0.00	0.00	3.04	73.01	0.00	0.00	0.00
Ar	mass %	0.41	0.85	7.73	0.00	0.00	0.00	0.00	1.16	1.48	0.00	0.00	0.00
CH4	mass %	0.00	0.01	0.12	0.00	0.00	0.00	0.00	0.02	0.02	0.00	0.00	0.00
O2	mass %	0.68	0.00	0.00	0.00	0.00	0.00	0.00	0.00	0.47	0.00	0.00	0.00
H2O	mass %	0.00	50.46	0.00	100.00	100.00	100.00	99.98	0.13	14.81	100.00	100.00	99.76
H2S	mass %	0.00	0.70	0.00	0.00	0.00	0.00	0.01	1.03	0.00	0.00	0.00	0.06
COS	mass %	0.00	0.12	0.00	0.00	0.00	0.00	0.00	0.01	0.00	0.00	0.00	0.00
CS2	mass %	0.00	0.00	0.00	0.00	0.00	0.00	0.00	0.00	0.00	0.00	0.00	0.00
SO2	mass %	0.00	0.00	0.00	0.00	0.00	0.00	0.00	0.00	0.00	0.00	0.00	0.00
S	mass %	0.00	0.00	0.00	0.00	0.00	0.00	0.00	0.00	0.00	0.00	0.00	0.00
HCN	mass %	0.00	0.00	0.00	0.00	0.00	0.00	0.00	0.00	0.00	0.00	0.00	0.00
NH3	mass %	0.00	0.00	0.00	0.00	0.00	0.00	0.00	0.00	0.00	0.00	0.00	0.00
CH3OH	mass %	0.00	0.00	0.03	0.00	0.00	0.00	0.00	0.00	0.00	0.00	0.00	0.00

Appendix C7 – CHEMCAD CO-shift model for the CC-IGCC / CoP gasifier

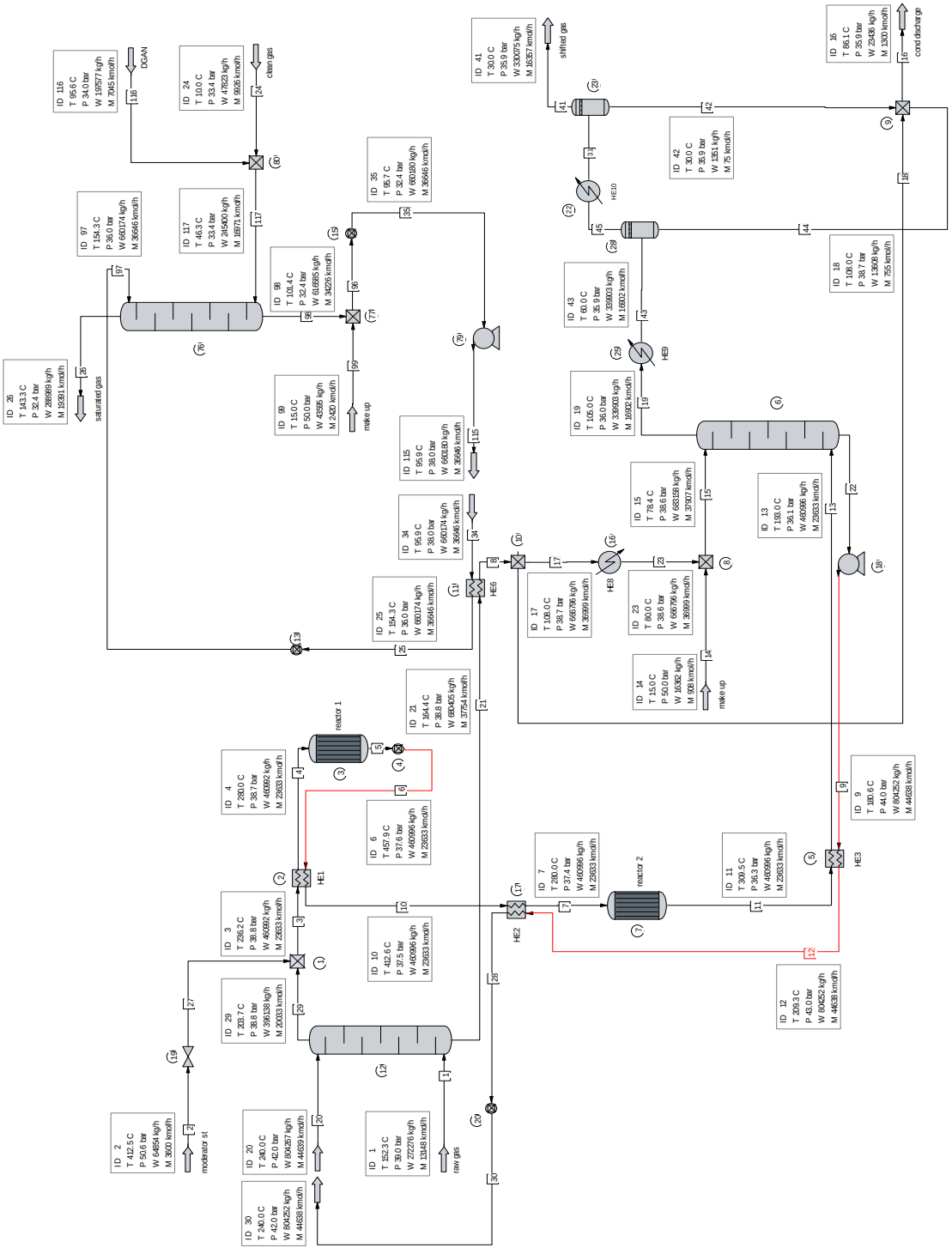

Appendix C8 – Heat and material balance for the CO-shift model (CC-IGCC / CoP gasifier

stream ID		1-3-DGAN-1	2-3-gas-1	4-3-gas-4	8-3-st-9	9-3-cw-1	10-3-mu-2	3-4-gas-3	3-8-gas-5	3-9-cw-2	3-10-ww-2
name		DGAN	raw gas	clean gas	IP steam	cooling water	make up water	shifted gas	GT fuel	cooling water	waste water
t	°C	95.6	152.3	10.0	412.5	20.0	15.0	30.0	143.3	30.0	75.4
p	bar	34.0	39.0	33.4	50.6	6.0	50.0	35.9	32.4	4.0	35.9
m	kg/s	57.576	79.345	13.936	18.899	147	17.489	96.183	84.215	147	6.833
n	kmol/s	2.053	3.832	2.893	1.049	8.157	0.971	4.766	5.651	8.157	0.379
V	Nm³/h	165,655	309,164	233,398				384,603	455,946		
LHV	kJ/kg		10,402	53,498				7,965	8,853		
HHV	kJ/kg		11,476	62,444				9,284	10,704		
h	kJ/kg	70	-5,804	-1,900	-12,756	-15,898	-15,919	-7,913	-2,096	-15,856	-15,649
s	J/kgK	-825	930	-5,639	-2,725	-9,113	-9,184	-1,038	-1,090	-8,974	-8,379
M	kg/kmol	28.03	20.71	4.80	18.00	18.00	18.00	20.20	14.89	18.00	18.01
Σ	mol %	100.00	100.00	100.00	100.00	100.00	100.00	100.00	100.00	100.00	100.00
H2	mol %	0.00	28.98	87.91	0.00	0.00	0.00	53.44	45.00	0.00	0.01
CO	mol %	0.00	39.77	3.01	0.00	0.00	0.00	1.83	1.54	0.00	0.01
CO2	mol %	0.00	11.44	0.50	0.00	0.00	0.00	39.35	0.26	0.00	0.03
N2	mol %	99.59	1.38	2.96	0.00	0.00	0.00	1.11	37.70	0.00	0.00
Ar	mol %	0.18	0.78	1.05	0.00	0.00	0.00	0.62	0.61	0.00	0.00
CH4	mol %	0.00	3.56	4.56	0.00	0.00	0.00	2.86	2.34	0.00	0.00
O2	mol %	0.22	0.00	0.00	0.00	0.00	0.00	0.00	0.08	0.00	0.00
H2O	mol %	0.00	13.28	0.00	100.00	100.00	100.00	0.14	12.48	100.00	99.92
H2S	mol %	0.00	0.76	0.00	0.00	0.00	0.00	0.63	0.00	0.00	0.02
COS	mol %	0.00	0.05	0.00	0.00	0.00	0.00	0.02	0.00	0.00	0.01
CS2	mol %	0.00	0.00	0.00	0.00	0.00	0.00	0.00	0.00	0.00	0.00
SO2	mol %	0.00	0.00	0.00	0.00	0.00	0.00	0.00	0.00	0.00	0.00
S	mol %	0.00	0.00	0.00	0.00	0.00	0.00	0.00	0.00	0.00	0.00
HCN	mol %	0.00	0.00	0.00	0.00	0.00	0.00	0.00	0.00	0.00	0.00
NH3	mol %	0.00	0.00	0.00	0.00	0.00	0.00	0.00	0.00	0.00	0.00
CH3OH	mol %	0.00	0.00	0.00	0.00	0.00	0.00	0.00	0.00	0.00	0.00
Σ	mass %	100.00	100.00	100.00	100.00	100.00	100.00	100.00	100.00	100.00	100.00
H2	mass %	0.00	2.82	36.78	0.00	0.00	0.00	5.34	6.09	0.00	0.00
CO	mass %	0.00	53.80	17.52	0.00	0.00	0.00	2.54	2.90	0.00	0.01
CO2	mass %	0.00	24.31	4.56	0.00	0.00	0.00	85.83	0.76	0.00	0.08
N2	mass %	99.48	1.87	17.20	0.00	0.00	0.00	1.54	70.86	0.00	0.00
Ar	mass %	0.26	1.50	8.72	0.00	0.00	0.00	1.23	1.62	0.00	0.00
CH4	mass %	0.00	2.76	15.20	0.00	0.00	0.00	2.27	2.51	0.00	0.00
O2	mass %	0.25	0.00	0.00	0.00	0.00	0.00	0.00	0.17	0.00	0.00
H2O	mass %	0.00	11.55	0.00	100.00	100.00	100.00	0.12	15.08	100.00	99.84
H2S	mass %	0.00	1.26	0.00	0.00	0.00	0.00	1.06	0.00	0.00	0.04
COS	mass %	0.00	0.14	0.00	0.00	0.00	0.00	0.06	0.00	0.00	0.02
CS2	mass %	0.00	0.00	0.00	0.00	0.00	0.00	0.00	0.00	0.00	0.00
SO2	mass %	0.00	0.00	0.00	0.00	0.00	0.00	0.00	0.00	0.00	0.00
S	mass %	0.00	0.00	0.00	0.00	0.00	0.00	0.00	0.00	0.00	0.00
HCN	mass %	0.00	0.00	0.00	0.00	0.00	0.00	0.00	0.00	0.00	0.00
NH3	mass %	0.00	0.00	0.00	0.00	0.00	0.00	0.00	0.00	0.00	0.00
CH3OH	mass %	0.00	0.00	0.03	0.00	0.00	0.00	0.00	0.00	0.00	0.00

Appendix C9 – CHEMCAD CO-shift model for the CC-IGCC / GE-R gasifier

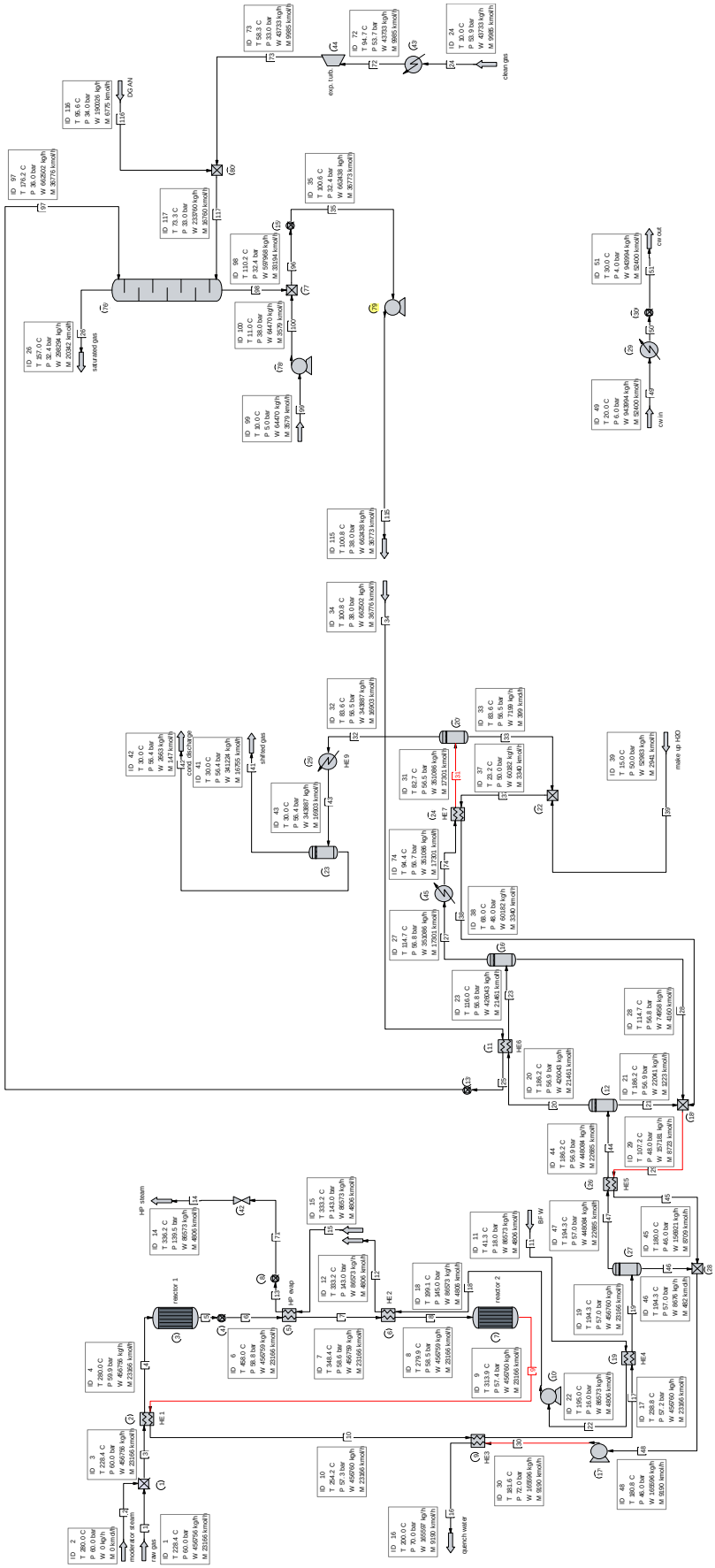

Appendix C10 – Heat and material balance for the CO-shift model (CC-IGCC / GE-R

stream ID		1-3-DGAN-1	2-3-gas-1	4-3-gas-4	8-3-BFW-3	9-3-cw-1	10-3-mu-2	3-2-wa-2	3-4-gas-3	3-8-gas-5	3-8-st-8	3-9-cw-2	3-10-ww-2
name		DGAN	raw gas	clean gas	BFW	cooling water	make up water	quench water	shifted gas	GT fuel	HP steam	cooling water	waste water
t	°C	95.6	228.4	10.0	41.3	20.0	15.0	200.0	30.0	157.0	336.2	30.0	30.0
p	bar	34.0	60.0	53.9	18.0	6.0	50.0	70.0	56.4	32.4	139.5	4.0	56.4
m	kg/s	59.596	143.247	13.716	27.151	296.054	36.836	51.934	107.014	93.550	27.151	296.054	0.835
n	kmol/s	2.125	7.265	3.131	1.507	16.434	2.045	2.882	5.255	6.380	1.507	16.434	0.046
V	Nm³/h	171,445	586,234	252,669					424,002	514,763			
LHV	kJ/kg		5,731	53,716					7,059	7,875			
HHV	kJ/kg		7,259	63,071					8,276	9,778			
h	kJ/kg	70	-8,638	-1,604	-15,809	-15,898	-15,919	-15,122	-7,999	-2,869	-13,324	-15,856	-15,814
s	J/kgK	-825	-610	-6,408	-8,822	-9,113	-9,184	-7,079	-1,143	-1,088	-4,056	-8,974	-8,935
M	kg/kmol	28.03	19.71	4.37	18.00	18.00	18.00	18.00	20.39	14.65	18.00	18.00	18.05
Σ	mol %	100.00	100.00	100.00	100.00	100.00	100.00	100.00	100.00	100.00	100.00	100.00	100.00
H2	mol %	0.00	17.73	91.68	0.00	0.00	0.00	0.00	54.73	45.00	0.00	0.00	0.00
CO	mol %	0.00	23.58	4.00	0.00	0.00	0.00	0.00	2.39	1.96	0.00	0.00	0.00
CO2	mol %	0.00	7.42	0.50	0.00	0.00	0.00	0.01	40.51	0.25	0.00	0.00	0.16
N2	mol %	99.58	0.51	2.24	0.00	0.00	0.00	0.00	0.71	34.27	0.00	0.00	0.00
Ar	mol %	0.22	0.55	1.29	0.00	0.00	0.00	0.00	0.76	0.71	0.00	0.00	0.00
CH4	mol %	0.00	0.12	0.27	0.00	0.00	0.00	0.00	0.17	0.13	0.00	0.00	0.00
O2	mol %	0.20	0.00	0.00	0.00	0.00	0.00	0.00	0.00	0.07	0.00	0.00	0.00
H2O	mol %	0.00	49.62	0.00	100.00	100.00	100.00	99.98	0.10	17.61	100.00	100.00	99.79
H2S	mol %	0.00	0.43	0.00	0.00	0.00	0.00	0.01	0.63	0.00	0.00	0.00	0.06
COS	mol %	0.00	0.03	0.00	0.00	0.00	0.00	0.00	0.00	0.00	0.00	0.00	0.00
CS2	mol %	0.00	0.00	0.00	0.00	0.00	0.00	0.00	0.00	0.00	0.00	0.00	0.00
SO2	mol %	0.00	0.00	0.00	0.00	0.00	0.00	0.00	0.00	0.00	0.00	0.00	0.00
S	mol %	0.00	0.00	0.00	0.00	0.00	0.00	0.00	0.00	0.00	0.00	0.00	0.00
HCN	mol %	0.00	0.00	0.00	0.00	0.00	0.00	0.00	0.00	0.00	0.00	0.00	0.00
NH3	mol %	0.00	0.00	0.00	0.00	0.00	0.00	0.00	0.00	0.00	0.00	0.00	0.00
CH3OH	mol %	0.00	0.00	0.01	0.00	0.00	0.00	0.00	0.00	0.00	0.00	0.00	0.00
Σ	mass %	100.00	100.00	100.00	100.00	100.00	100.00	100.00	100.00	100.00	100.00	100.00	100.00
H2	mass %	0.00	1.81	42.19	0.00	0.00	0.00	0.00	5.42	6.19	0.00	0.00	0.00
CO	mass %	0.00	33.50	25.58	0.00	0.00	0.00	0.00	3.28	3.75	0.00	0.00	0.00
CO2	mass %	0.00	16.56	5.02	0.00	0.00	0.00	0.02	87.55	0.74	0.00	0.00	0.38
N2	mass %	99.46	0.73	14.33	0.00	0.00	0.00	0.00	0.98	65.46	0.00	0.00	0.00
Ar	mass %	0.31	1.11	11.81	0.00	0.00	0.00	0.00	1.49	1.93	0.00	0.00	0.00
CH4	mass %	0.00	0.10	1.01	0.00	0.00	0.00	0.00	0.13	0.15	0.00	0.00	0.00
O2	mass %	0.23	0.00	0.00	0.00	0.00	0.00	0.00	0.00	0.14	0.00	0.00	0.00
H2O	mass %	0.00	45.34	0.00	100.00	100.00	100.00	99.96	0.09	21.63	100.00	100.00	99.51
H2S	mass %	0.00	0.75	0.00	0.00	0.00	0.00	0.02	1.06	0.00	0.00	0.00	0.11
COS	mass %	0.00	0.10	0.00	0.00	0.00	0.00	0.00	0.01	0.00	0.00	0.00	0.00
CS2	mass %	0.00	0.00	0.00	0.00	0.00	0.00	0.00	0.00	0.00	0.00	0.00	0.00
SO2	mass %	0.00	0.00	0.00	0.00	0.00	0.00	0.00	0.00	0.00	0.00	0.00	0.00
S	mass %	0.00	0.00	0.00	0.00	0.00	0.00	0.00	0.00	0.00	0.00	0.00	0.00
HCN	mass %	0.00	0.00	0.00	0.00	0.00	0.00	0.00	0.00	0.00	0.00	0.00	0.00
NH3	mass %	0.00	0.00	0.00	0.00	0.00	0.00	0.00	0.00	0.00	0.00	0.00	0.00
CH3OH	mass %	0.00	0.00	0.06	0.00	0.00	0.00	0.00	0.00	0.01	0.00	0.00	0.00

Appendix D1 – CHEMCAD model of the AGR unit for the CC-IGCC

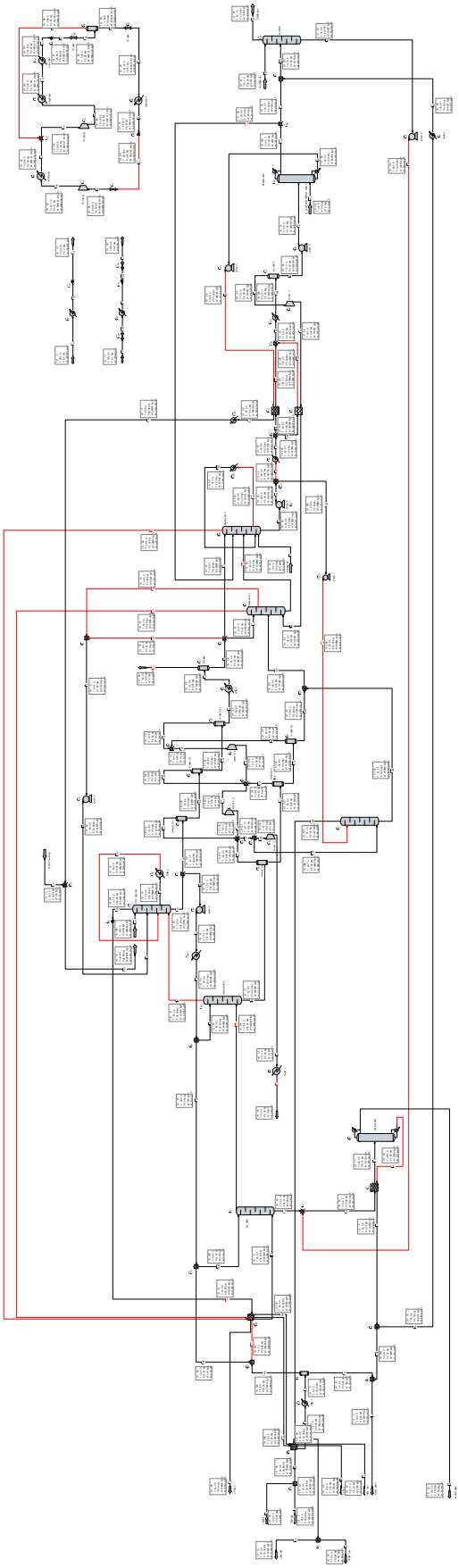

Appendix D2 – CHEMCAD model of the TGT process for the CC-IGCC

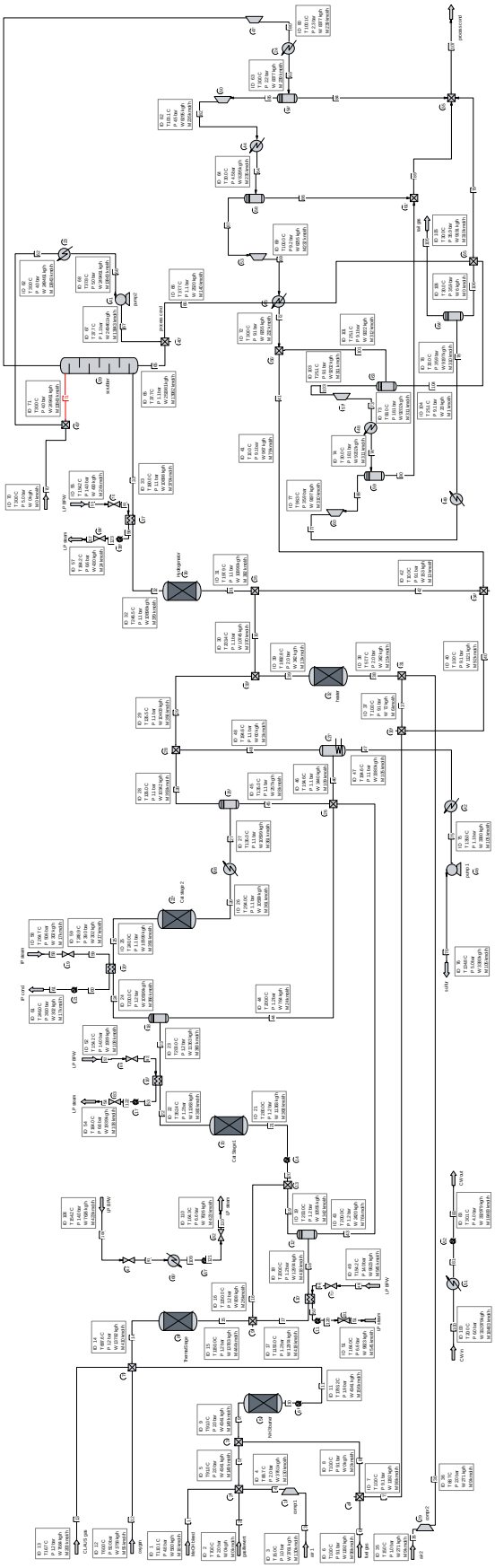

Appendix D3 – CHEMCAD model of the CO_2-compressor for the CC-IGCC

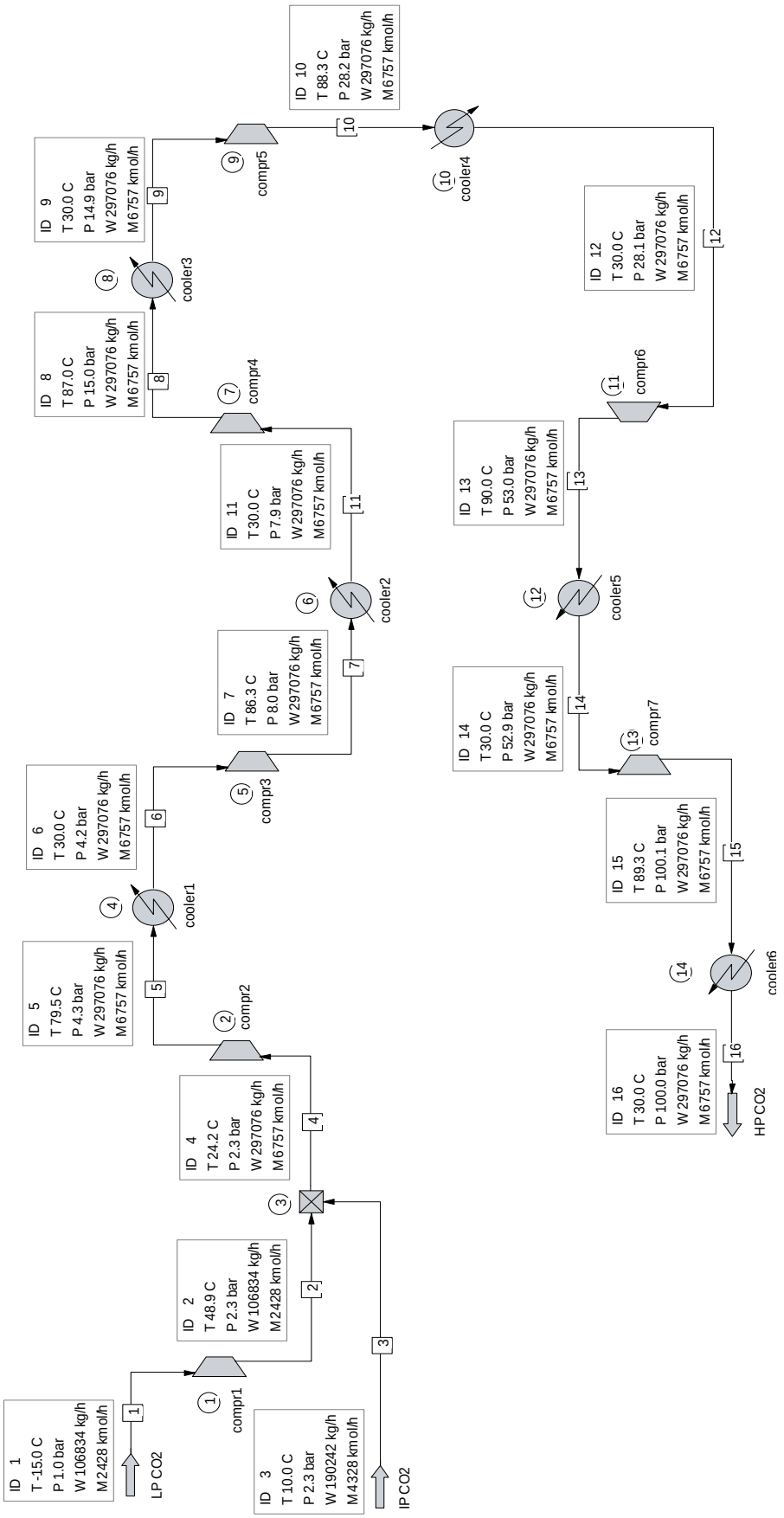

Appendix D4 – Heat and material balance for the AGR unit (CC-IGCC / SCGP)

stream ID		0-4-met-1	3-4-gas-3	5-4-gas-6	8-4-st-10	9-4-cw-3	10-4-mu-3	4-2-gas-2	4-3-gas-4	4-5-gas-7	4-5-gas-8	4-5-met-2	4-6-CO2-1	4-6-CO2-2	4-8-cond-2	4-9-cw-4	4-10-ww-3
name		fresh MeOH	feed gas	tail gas	LP steam	CW in	demin water	fuel gas	clean gas	TGT fuel	CLAUS gas	MeOH bleed	LP CO2	IP CO2	LP cond	CW out	waste water
t	°C	15.0	30.0	30.0	275.8	20.0	15.0	10.0	10.0	10.0	16.7	110.1	-15.0	10.0	150.8	30.0	42.9
p	bar	36.88	35.88	35.89	6.10	6.00	50.00	33.38	33.38	9.10	1.20	4.80	1.05	2.30	4.80	4.00	4.55
m	kg/s	0.212	101.821	2.643	9.476	877	1.658	0.123	16.246	0.343	2.209	0.167	30.718	54.703	9.476	877	1.826
n	kmol/s	0.007	5.205	0.089	0.526	48.667	0.092	0.024	3.235	0.028	0.057	0.005	0.698	1.245	0.526	48.667	0.100
V	Nm³/h	535	419,963	7,194				1,974	260,995	2,273	4,637	421	56,342	100,423			
LHV	kJ/kg	19,899	7,426	2,395				45,147	45,147	16,262	7,839	16,376					
HHV	kJ/kg	22,671	8,712	2,728				53,037	53,037	18,883	8,500	18,756					
h	kJ/kg	-7,581	-7,708	-5,036	-12,971	-15,898	-15,919	-1,332	-1,332	-5,016	-4,628	-6,689	-8,974	-8,952	-15,316	-15,856	-15,517
s	J/kgK	-8,002.5	-947	-484.9	-2,136.2	-9,113.2	-9,184.4	-4,663.9	-4,663.9	-339.9	804.4	-3,240.6	-64.1	-134.2	-7,498.3	-8,974.4	-8,752.0
M	kg/kmol	32.00	19.59	29.66	18.00	18.00	18.00	5.01	5.01	12.17	38.44	31.91	44.08	44.04	18.00	18.00	18.28
Σ	mol %	100.00	100.00	100.00	100.00	100.00	100.00	100.00	100.00	100.00	100.00	100.00	100.00	100.00	100.00	100.00	100.00
H2	mol %	0.00	55.92	18.06	0.00	0.00	0.00	89.15	89.15	70.44	0.00	0.01	0.03	0.10	0.00	0.00	0.00
CO	mol %	0.00	2.42	2.35	0.00	0.00	0.00	3.85	3.85	7.20	0.00	0.00	0.01	0.04	0.00	0.00	0.00
CO2	mol %	0.00	37.48	36.88	0.00	0.00	0.00	0.50	0.50	13.28	40.40	8.84	99.93	99.80	0.00	0.00	0.06
N2	mol %	0.00	2.87	36.92	0.00	0.00	0.00	5.54	5.54	5.51	0.00	0.00	0.00	0.01	0.00	0.00	0.00
Ar	mol %	0.00	0.56	1.65	0.00	0.00	0.00	0.92	0.92	2.21	0.00	0.00	0.00	0.02	0.00	0.00	0.00
CH4	mol %	0.00	0.02	0.02	0.00	0.00	0.00	0.03	0.03	0.05	0.00	0.00	0.00	0.00	0.00	0.00	0.00
O2	mol %	0.00	0.00	0.00	0.00	0.00	0.00	0.00	0.00	0.00	0.00	0.00	0.00	0.00	0.00	0.00	0.00
H2O	mol %	0.00	0.14	0.16	100.00	100.00	100.00	0.00	0.00	0.00	1.55	8.65	0.00	0.00	100.00	100.00	98.05
H2S	mol %	0.00	0.56	3.94	0.00	0.00	0.00	0.00	0.00	1.26	55.68	2.51	0.00	0.00	0.00	0.00	0.00
COS	mol %	0.00	0.03	0.01	0.00	0.00	0.00	0.00	0.00	0.04	2.34	0.01	0.00	0.00	0.00	0.00	0.00
CS2	mol %	0.00	0.00	0.00	0.00	0.00	0.00	0.00	0.00	0.00	0.00	0.00	0.00	0.00	0.00	0.00	0.00
SO2	mol %	0.00	0.00	0.00	0.00	0.00	0.00	0.00	0.00	0.00	0.00	0.00	0.00	0.00	0.00	0.00	0.00
S	mol %	0.00	0.00	0.00	0.00	0.00	0.00	0.00	0.00	0.00	0.00	0.00	0.00	0.00	0.00	0.00	0.00
HCN	mol %	0.00	0.00	0.00	0.00	0.00	0.00	0.00	0.00	0.00	0.00	0.00	0.00	0.00	0.00	0.00	0.00
NH3	mol %	0.00	0.00	0.01	0.00	0.00	0.00	0.00	0.00	0.00	0.02	0.01	0.00	0.00	0.00	0.00	0.00
CH3OH	mol %	100.00	0.00	0.00	0.00	0.00	0.00	0.00	0.00	0.01	0.00	79.98	0.02	0.02	0.00	0.00	1.89
Σ	mass %	100.00	100.00	100.00	100.00	100.00	100.00	100.00	100.00	100.00	100.00	100.00	100.00	100.00	100.00	100.00	100.00
H2	mass %	0.00	5.76	1.23	0.00	0.00	0.00	35.78	35.78	11.67	0.00	0.00	0.00	0.00	0.00	0.00	0.00
CO	mass %	0.00	3.47	2.22	0.00	0.00	0.00	21.50	21.50	16.57	0.00	0.00	0.01	0.02	0.00	0.00	0.00
CO2	mass %	0.00	84.32	54.76	0.00	0.00	0.00	4.38	4.38	48.01	46.25	12.18	99.97	99.93	0.00	0.00	0.15
N2	mass %	0.00	4.11	34.90	0.00	0.00	0.00	30.91	30.91	12.69	0.00	0.00	0.00	0.01	0.00	0.00	0.00
Ar	mass %	0.00	1.15	2.22	0.00	0.00	0.00	7.31	7.31	7.24	0.00	0.00	0.00	0.01	0.00	0.00	0.00
CH4	mass %	0.00	0.02	0.01	0.00	0.00	0.00	0.09	0.09	0.07	0.00	0.00	0.00	0.00	0.00	0.00	0.00
O2	mass %	0.00	0.00	0.00	0.00	0.00	0.00	0.00	0.00	0.00	0.00	0.00	0.00	0.00	0.00	0.00	0.00
H2O	mass %	0.00	0.12	0.10	100.00	100.00	100.00	0.00	0.00	0.00	0.73	4.88	0.00	0.00	100.00	100.00	96.54
H2S	mass %	0.00	0.97	4.53	0.00	0.00	0.00	0.00	0.00	3.53	49.35	2.67	0.00	0.00	0.00	0.00	0.00
COS	mass %	0.00	0.08	0.03	0.00	0.00	0.00	0.00	0.00	0.19	3.66	0.02	0.00	0.00	0.00	0.00	0.00
CS2	mass %	0.00	0.00	0.00	0.00	0.00	0.00	0.00	0.00	0.00	0.00	0.00	0.00	0.00	0.00	0.00	0.00
SO2	mass %	0.00	0.00	0.00	0.00	0.00	0.00	0.00	0.00	0.00	0.00	0.00	0.00	0.00	0.00	0.00	0.00
S	mass %	0.00	0.00	0.00	0.00	0.00	0.00	0.00	0.00	0.00	0.00	0.00	0.00	0.00	0.00	0.00	0.00
HCN	mass %	0.00	0.00	0.00	0.00	0.00	0.00	0.00	0.00	0.00	0.00	0.00	0.00	0.00	0.00	0.00	0.00
NH3	mass %	0.00	0.00	0.01	0.00	0.00	0.00	0.00	0.00	0.00	0.01	0.00	0.00	0.00	0.00	0.00	0.00
CH3OH	mass %	100.00	0.00	0.00	0.00	0.00	0.00	0.03	0.03	0.02	0.00	80.24	0.01	0.02	0.00	0.00	3.31

Appendix D5 – Heat and material balance for the AGR unit (CC-IGCC / Siemens gasifier)

stream ID		0-4-met-1	3-4-gas-3	5-4-gas-6	8-4-st-10	9-4-cw-3	10-4-mu-3	4-2-gas-2	4-3-gas-4	4-5-gas-7	4-5-gas-8	4-5-met-2	4-6-CO2-1	4-6-CO2-2	4-8-cond-2	4-9-cw-4	4-10-ww-3
name		fresh MeOH	feed gas	tail gas	LP steam	CW in	demin water	fuel gas	clean gas	TGT fuel	CLAUS gas	MeOH bleed	LP CO2	IP CO2	LP cond	CW out	waste water
t	°C	15.0	30.0	30.0	277.0	20.0	15.0	10.0	10.0	10.0	16.3	110.1	-15.0	10.0	150.8	30.0	42.9
p	bar	36.55	35.55	35.89	6.10	6.00	50.00	33.05	33.05	9.10	1.20	4.80	1.05	2.30	4.80	4.00	4.55
m	kg/s	0.212	100.788	2.519	8.903	845	1.662	0.114	15.062	0.327	2.151	0.165	30.814	54.716	8.903	845	1.831
n	kmol/s	0.007	5.171	0.086	0.494	46.896	0.092	0.024	3.197	0.028	0.057	0.005	0.700	1.245	0.494	46.896	0.100
V	Nm³/h	535	417.276	6,921				1,954	257,963	2,228	4,570	417	56,518	100,446			
LHV	kJ/kg	19,899	7,510	2,230				48,741	48,741	16,910	7,799	16,307					
HHV	kJ/kg	22,671	8,813	2,556				57,267	57,267	19,645	8,484	18,680					
h	kJ/kg	-7,581	-7,798	-5,079	-12,969	-15,898	-15,919	-1,415	-1,415	-5,149	-4,703	-6,700	-8,974	-8,952	-15,316	-15,856	-15,517
s	J/kgK	-8,002.4	-957	-515.3	-2,131.6	-9,113.2	-9,184.4	-5,020.2	-5,020.2	-377.6	758.6	-3,224.6	-64.1	-134.3	-7,498.3	-8,974.4	-8,751.9
M	kg/kmol	32.00	19.51	29.39	18.00	18.00	18.00	4.70	4.70	11.86	37.97	31.89	44.08	44.04	18.00	18.00	18.28
Σ	mol %	100.00	100.00	100.00	100.00	100.00	100.00	100.00	100.00	100.00	100.00	100.00	100.00	100.00	100.00	100.00	100.00
H2	mol %	0.00	56.38	18.80	0.00	0.00	0.00	90.35	90.35	71.62	0.00	0.01	0.03	0.11	0.00	0.00	0.00
CO	mol %	0.00	2.39	2.38	0.00	0.00	0.00	3.83	3.83	7.17	0.00	0.00	0.01	0.04	0.00	0.00	0.00
CO2	mol %	0.00	37.79	36.93	0.00	0.00	0.00	0.50	0.50	13.30	41.30	8.97	99.93	99.80	0.00	0.00	0.06
N2	mol %	0.00	2.12	37.46	0.00	0.00	0.00	4.35	4.35	4.34	0.00	0.00	0.00	0.01	0.00	0.00	0.00
Ar	mol %	0.00	0.57	1.70	0.00	0.00	0.00	0.93	0.93	2.23	0.00	0.00	0.00	0.02	0.00	0.00	0.00
CH4	mol %	0.00	0.02	0.02	0.00	0.00	0.00	0.03	0.03	0.06	0.00	0.00	0.00	0.00	0.00	0.00	0.00
O2	mol %	0.00	0.00	0.00	0.00	0.00	0.00	0.00	0.00	0.00	0.00	0.00	0.00	0.00	0.00	0.00	0.00
H2O	mol %	0.00	0.14	0.16	100.00	100.00	100.00	0.00	0.00	0.00	1.52	8.90	0.00	0.00	100.00	100.00	98.05
H2S	mol %	0.00	0.59	2.53	0.00	0.00	0.00	0.00	0.00	1.26	56.99	2.59	0.00	0.00	0.00	0.00	0.00
COS	mol %	0.00	0.00	0.00	0.00	0.00	0.00	0.00	0.00	0.00	0.17	0.00	0.00	0.00	0.00	0.00	0.00
CS2	mol %	0.00	0.00	0.00	0.00	0.00	0.00	0.00	0.00	0.00	0.00	0.00	0.00	0.00	0.00	0.00	0.00
SO2	mol %	0.00	0.00	0.00	0.00	0.00	0.00	0.00	0.00	0.00	0.00	0.00	0.00	0.00	0.00	0.00	0.00
S	mol %	0.00	0.00	0.00	0.00	0.00	0.00	0.00	0.00	0.00	0.00	0.00	0.00	0.00	0.00	0.00	0.00
HCN	mol %	0.00	0.00	0.00	0.00	0.00	0.00	0.00	0.00	0.00	0.00	0.00	0.00	0.00	0.00	0.00	0.00
NH3	mol %	0.00	0.00	0.01	0.00	0.00	0.00	0.00	0.00	0.00	0.01	0.01	0.00	0.00	0.00	0.00	0.00
CH3OH	mol %	100.00	0.00	0.00	0.00	0.00	0.00	0.00	0.00	0.01	0.00	79.52	0.02	0.02	0.00	0.00	1.89
Σ	mass %	100.00	100.00	100.00	100.00	100.00	100.00	100.00	100.00	100.00	100.00	100.00	100.00	100.00	100.00	100.00	100.00
H2	mass %	0.00	5.83	1.29	0.00	0.00	0.00	38.66	38.66	12.17	0.00	0.00	0.00	0.00	0.00	0.00	0.00
CO	mass %	0.00	3.44	2.27	0.00	0.00	0.00	22.77	22.77	16.93	0.00	0.00	0.01	0.02	0.00	0.00	0.00
CO2	mass %	0.00	85.34	55.33	0.00	0.00	0.00	4.67	4.67	49.37	47.86	12.37	99.97	99.93	0.00	0.00	0.15
N2	mass %	0.00	3.04	35.73	0.00	0.00	0.00	25.88	25.88	10.26	0.00	0.00	0.00	0.01	0.00	0.00	0.00
Ar	mass %	0.00	1.16	2.32	0.00	0.00	0.00	7.88	7.88	7.52	0.00	0.00	0.00	0.01	0.00	0.00	0.00
CH4	mass %	0.00	0.02	0.01	0.00	0.00	0.00	0.12	0.12	0.08	0.00	0.00	0.00	0.00	0.00	0.00	0.00
O2	mass %	0.00	0.00	0.00	0.00	0.00	0.00	0.00	0.00	0.00	0.00	0.00	0.00	0.00	0.00	0.00	0.00
H2O	mass %	0.00	0.13	0.10	100.00	100.00	100.00	0.00	0.00	0.00	0.72	5.02	0.00	0.00	100.00	100.00	96.54
H2S	mass %	0.00	1.03	2.94	0.00	0.00	0.00	0.00	0.00	3.63	51.13	2.76	0.00	0.00	0.00	0.00	0.00
COS	mass %	0.00	0.01	0.00	0.00	0.00	0.00	0.00	0.00	0.01	0.28	0.00	0.00	0.00	0.00	0.00	0.00
CS2	mass %	0.00	0.00	0.00	0.00	0.00	0.00	0.00	0.00	0.00	0.00	0.00	0.00	0.00	0.00	0.00	0.00
SO2	mass %	0.00	0.00	0.00	0.00	0.00	0.00	0.00	0.00	0.00	0.00	0.00	0.00	0.00	0.00	0.00	0.00
S	mass %	0.00	0.00	0.00	0.00	0.00	0.00	0.00	0.00	0.00	0.00	0.00	0.00	0.00	0.00	0.00	0.00
HCN	mass %	0.00	0.00	0.00	0.00	0.00	0.00	0.00	0.00	0.00	0.00	0.00	0.00	0.00	0.00	0.00	0.00
NH3	mass %	0.00	0.00	0.01	0.00	0.00	0.00	0.00	0.00	0.00	0.01	0.00	0.00	0.00	0.00	0.00	0.00
CH3OH	mass %	100.00	0.00	0.00	0.00	0.00	0.00	0.03	0.03	0.02	0.00	79.83	0.01	0.02	0.00	0.00	3.31

Appendix D6 – Heat and material balance for the AGR unit (CC-IGCC / CoP gasifier)

stream ID		0-4-met-1	3-4-gas-3	5-4-gas-6	8-4-st-10	9-4-cw-3	10-4-mu-3	4-2-gas-2	4-3-gas-4	4-5-gas-7	4-5-gas-8	4-5-met-2	4-6-CO2-1	4-6-CO2-2	4-8-cond-2	4-9-cw-4	4-10-ww-3
name		fresh MeOH	feed gas	tail gas	LP steam	CW in	demin water	fuel gas	clean gas	TGT fuel	CLAUS gas	MeOH bleed	LP CO2	IP CO2	LP cond	CW out	waste water
t	°C	15.0	30.0	30.0	274.8	20.0	10.0	10.0	10.0	10.0	12.9	109.5	-15.0	10.0	150.8	30.0	42.9
p	bar	36.88	35.88	35.94	6.10	6.00	5.00	33.38	33.38	9.30	1.20	4.80	1.05	2.30	4.80	4.00	4.55
m	kg/s	0.220	96.183	2.766	8.593	796	1.522	0.000	13.936	0.391	2.261	0.170	28.337	53.908	8.593	796	1.680
n	kmol/s	0.007	4.766	0.094	0.477	44.202	0.085	0.000	2.893	0.030	0.059	0.005	0.644	1.228	0.477	44.202	0.092
V	Nm³/h	553	384.603	7.559				0	233.398	2.434	4.744	427	51.993	99.107			
LHV	kJ/kg	19,899	7,965	3,340				53.497	53.497	22.237	7.708	16.646					
HHV	kJ/kg	22.671	9.284	3.774				62.444	62.444	25.384	8.363	19.042					
h	kJ/kg	-7,581	-7,913	-5,107	-12,974	-15,898	-15,940	-1,902	-1,902	-5,362	-4,713	-6,623	-8,974	-8,949	-15,316	-15,856	-15,516
s	J/kgK	-8,002.5	-1,039	-613.0	-2,140.1	-9,113.2	-9,257.3	-5,648.7	-5,648.7	-1,268.9	772.1	-3,289.4	-64.6	-137.6	-7,498.3	-8,974.4	-8,751.4
M	kg/kmol	32.00	20.20	29.55	18.00	18.00	18.00	4.80	4.80	12.95	38.44	32.09	44.06	43.98	18.00	18.00	18.28
Σ	mol %	100.0000	100.0000	100.0000	100.0000	100.0000	100.0000	100.0000	100.0000	100.0000	100.0000	100.0000	100.0000	100.0000	100.0000	100.0000	100.0000
H2	mol %	0.00	53.44	16.03	0.00	0.00	0.00	87.91	87.91	60.44	0.00	0.00	0.02	0.07	0.00	0.00	0.00
CO	mol %	0.00	1.83	1.82	0.00	0.00	0.00	3.01	3.01	5.14	0.00	0.00	0.01	0.02	0.00	0.00	0.00
CO2	mol %	0.00	39.35	36.56	0.00	0.00	0.00	0.50	0.50	13.14	41.66	8.57	99.87	99.57	0.00	0.00	0.06
N2	mol %	0.00	1.11	35.69	0.00	0.00	0.00	2.96	2.96	2.58	0.00	0.00	0.00	0.00	0.00	0.00	0.00
Ar	mol %	0.00	0.62	1.72	0.00	0.00	0.00	1.05	1.05	2.37	0.00	0.00	0.01	0.01	0.00	0.00	0.00
CH4	mol %	0.00	2.86	4.66	0.00	0.00	0.00	4.56	4.56	15.10	0.00	0.00	0.07	0.30	0.00	0.00	0.00
O2	mol %	0.00	0.00	0.00	0.00	0.00	0.00	0.00	0.00	0.00	0.00	0.00	0.00	0.00	0.00	0.00	0.00
H2O	mol %	0.00	0.14	0.16	100.00	100.00	100.00	0.00	0.00	0.00	1.22	7.13	0.00	0.00	100.00	100.00	98.04
H2S	mol %	0.00	0.63	3.31	0.00	0.00	0.00	0.00	0.00	1.20	55.44	2.40	0.00	0.00	0.00	0.00	0.00
COS	mol %	0.00	0.02	0.01	0.00	0.00	0.00	0.00	0.00	0.03	1.67	0.01	0.00	0.00	0.00	0.00	0.00
CS2	mol %	0.00	0.00	0.00	0.00	0.00	0.00	0.00	0.00	0.00	0.00	0.00	0.00	0.00	0.00	0.00	0.00
SO2	mol %	0.00	0.00	0.00	0.00	0.00	0.00	0.00	0.00	0.00	0.00	0.00	0.00	0.00	0.00	0.00	0.00
S	mol %	0.00	0.00	0.00	0.00	0.00	0.00	0.00	0.00	0.00	0.00	0.00	0.00	0.00	0.00	0.00	0.00
HCN	mol %	0.00	0.00	0.00	0.00	0.00	0.00	0.00	0.00	0.00	0.00	0.00	0.00	0.00	0.00	0.00	0.00
NH3	mol %	0.00	0.00	0.01	0.00	0.00	0.00	0.00	0.00	0.00	0.02	0.01	0.00	0.00	0.00	0.00	0.00
CH3OH	mol %	100.00	0.00	0.00	0.00	0.00	0.00	0.00	0.00	0.01	0.00	81.88	0.02	0.02	0.00	0.00	1.89
Σ	mass %	100.0000	100.0000	100.0000	100.0000	100.0000	100.0000	100.0000	100.0000	100.0000	100.0000	100.0000	100.0000	100.0000	100.0000	100.0000	100.0000
H2	mass %	0.00	5.34	1.09	0.00	0.00	0.00	36.78	36.78	9.40	0.00	0.00	0.00	0.00	0.00	0.00	0.00
CO	mass %	0.00	2.54	1.73	0.00	0.00	0.00	17.52	17.52	11.12	0.00	0.00	0.00	0.01	0.00	0.00	0.00
CO2	mass %	0.00	85.83	54.49	0.00	0.00	0.00	4.56	4.56	44.62	47.69	11.74	99.95	99.84	0.00	0.00	0.15
N2	mass %	0.00	1.54	33.86	0.00	0.00	0.00	17.20	17.20	5.58	0.00	0.00	0.00	0.00	0.00	0.00	0.00
Ar	mass %	0.00	1.23	2.33	0.00	0.00	0.00	8.72	8.72	7.31	0.00	0.00	0.00	0.01	0.00	0.00	0.00
CH4	mass %	0.00	2.27	2.53	0.00	0.00	0.00	15.20	15.20	18.69	0.00	0.00	0.03	0.11	0.00	0.00	0.00
O2	mass %	0.00	0.00	0.00	0.00	0.00	0.00	0.00	0.00	0.00	0.00	0.00	0.00	0.00	0.00	0.00	0.00
H2O	mass %	0.00	0.12	0.10	100.00	100.00	100.00	0.00	0.00	0.00	0.57	4.00	0.00	0.00	100.00	100.00	96.53
H2S	mass %	0.00	1.06	3.82	0.00	0.00	0.00	0.00	0.00	3.14	49.13	2.55	0.00	0.00	0.00	0.00	0.00
COS	mass %	0.00	0.06	0.02	0.00	0.00	0.00	0.00	0.00	0.13	2.60	0.01	0.00	0.00	0.00	0.00	0.00
CS2	mass %	0.00	0.00	0.00	0.00	0.00	0.00	0.00	0.00	0.00	0.00	0.00	0.00	0.00	0.00	0.00	0.00
SO2	mass %	0.00	0.00	0.00	0.00	0.00	0.00	0.00	0.00	0.00	0.00	0.00	0.00	0.00	0.00	0.00	0.00
S	mass %	0.00	0.00	0.00	0.00	0.00	0.00	0.00	0.00	0.00	0.00	0.00	0.00	0.00	0.00	0.00	0.00
HCN	mass %	0.00	0.00	0.00	0.00	0.00	0.00	0.00	0.00	0.00	0.00	0.00	0.00	0.00	0.00	0.00	0.00
NH3	mass %	0.00	0.00	0.01	0.00	0.00	0.00	0.00	0.00	0.00	0.01	0.00	0.00	0.00	0.00	0.00	0.00
CH3OH	mass %	100.00	0.00	0.00	0.00	0.00	0.00	0.03	0.03	0.02	0.00	81.69	0.01	0.02	0.00	0.00	3.32

Appendix D7 – Heat and material balance for the AGR unit (CC-IGCC / GE-R)

stream ID		0-4-met-1	3-4-gas-3	5-4-gas-6	8-4-st-10	9-4-cw-3	10-4-mu-3	4-2-gas-2	4-3-gas-4	4-5-gas-7	4-5-gas-8	4-5-met-2	4-6-CO2-1	4-6-CO2-2	4-8-cond-2	4-9-cw-4	4-10-ww-3
name		fresh MeOH	feed gas	tail gas	LP steam	CW in	demin water	fuel gas	clean gas	TGT fuel	CLAUS gas	MeOH bleed	LP CO2	IP CO2	LP cond	CW out	waste water
t	°C	15.0	30.0	30.0	278.7	20.0	15.0	10.0	10.0	10.0	17.5	115.2	-15.0	10.0	150.8	30.0	43.9
p	bar	57.42	56.42	56.80	6.10	6.00	50.00	53.92	53.92	14.60	1.20	4.80	1.80	3.30	4.80	4.00	4.55
m	kg/s	0.264	107.014	3.716	8.810	754	2.260	0.000	13.716	0.582	3.138	0.170	30.290	62.949	8.810	754	2.400
n	kmol/s	0.008	5.255	0.117	0.489	41.856	0.125	0.000	3.131	0.037	0.080	0.006	0.688	1.432	0.489	41.856	0.131
V	Nm³/h	664	424.002	9.404				0.000	252.669	2.953	6.453	454	55.553	115.507			
LHV	kJ/kg	19.899	7.059	1.834				53.716	53.716	11.596	5.824	16.583					
HHV	kJ/kg	22.671	8.276	2.100				63.071	63.071	13.446	6.341	19.117					
h	kJ/kg	-7.579	-8.000	-6.145	-12.965	-15.898	-15.919	-1.606	-1.606	-6.532	-5.787	-6.893	-8.975	-8.954	-15.316	-15.856	-15.508
s	J/kgK	-8.006.1	-1.144	-657.2	-2.125.3	-9.113.2	-9.184.4	-6.419.4	-6.419.4	-565.5	604.6	-3.415.7	-168.7	-206.7	-7.498.3	-8.974.4	-8.740.6
M	kg/kmol	32.00	20.39	31.92	18.00	18.00	18.00	4.37	4.37	15.90	39.25	30.22	44.08	44.06	18.00	18.00	18.28
Σ	mol %	100.00	100.00	100.00	100.00	100.00	100.00	100.00	100.00	100.00	100.00	100.00	100.00	100.00	100.00	100.00	100.00
H2	mol %	0.00	54.73	16.22	0.00	0.00	0.00	91.68	91.68	62.82	0.00	0.00	0.02	0.05	0.00	0.00	0.00
CO	mol %	0.00	2.39	1.98	0.00	0.00	0.00	4.00	4.00	6.00	0.00	0.00	0.01	0.02	0.00	0.00	0.00
CO2	mol %	0.00	40.51	48.78	0.00	0.00	0.00	0.50	0.50	24.29	54.25	4.24	99.93	99.85	0.00	0.00	0.05
N2	mol %	0.00	0.71	28.76	0.00	0.00	0.00	2.24	2.24	1.70	0.00	0.00	0.00	0.00	0.00	0.00	0.00
Ar	mol %	0.00	0.76	1.62	0.00	0.00	0.00	1.29	1.29	2.69	0.00	0.00	0.01	0.02	0.00	0.00	0.00
CH4	mol %	0.00	0.17	0.24	0.00	0.00	0.00	0.27	0.27	0.83	0.00	0.00	0.01	0.01	0.00	0.00	0.00
O2	mol %	0.00	0.00	0.00	0.00	0.00	0.00	0.00	0.00	0.00	0.00	0.00	0.00	0.00	0.00	0.00	0.00
H2O	mol %	0.00	0.10	0.14	100.00	100.00	100.00	0.00	0.00	0.00	1.64	16.67	0.00	0.00	100.00	100.00	98.01
H2S	mol %	0.00	0.63	2.23	0.00	0.00	0.00	0.00	0.00	1.64	43.95	2.15	0.00	0.00	0.00	0.00	0.00
COS	mol %	0.00	0.00	0.00	0.00	0.00	0.00	0.00	0.00	0.00	0.14	0.00	0.00	0.00	0.00	0.00	0.00
CS2	mol %	0.00	0.00	0.00	0.00	0.00	0.00	0.00	0.00	0.00	0.00	0.00	0.00	0.00	0.00	0.00	0.00
SO2	mol %	0.00	0.00	0.00	0.00	0.00	0.00	0.00	0.00	0.00	0.00	0.00	0.00	0.00	0.00	0.00	0.00
S	mol %	0.00	0.00	0.00	0.00	0.00	0.00	0.00	0.00	0.00	0.00	0.00	0.00	0.00	0.00	0.00	0.00
HCN	mol %	0.00	0.00	0.00	0.00	0.00	0.00	0.00	0.00	0.00	0.00	0.00	0.00	0.00	0.00	0.00	0.00
NH3	mol %	0.00	0.00	0.01	0.00	0.00	0.00	0.00	0.00	0.00	0.01	0.00	0.00	0.00	0.00	0.00	0.00
CH3OH	mol %	100.00	0.00	0.01	0.00	0.00	0.00	0.01	0.01	0.04	0.00	76.93	0.03	0.04	0.00	0.00	1.94
Σ	mass %	100.00	100.00	100.00	100.00	100.00	100.00	100.00	100.00	100.00	100.00	100.00	100.00	100.00	100.00	100.00	100.00
H2	mass %	0.00	5.42	1.03	0.00	0.00	0.00	42.19	42.19	7.97	0.00	0.00	0.00	0.00	0.00	0.00	0.00
CO	mass %	0.00	3.28	1.74	0.00	0.00	0.00	25.58	25.58	10.58	0.00	0.00	0.01	0.01	0.00	0.00	0.00
CO2	mass %	0.00	87.55	67.33	0.00	0.00	0.00	5.02	5.02	67.26	60.85	6.16	99.96	99.93	0.00	0.00	0.11
N2	mass %	0.00	0.98	25.27	0.00	0.00	0.00	14.33	14.33	2.99	0.00	0.00	0.00	0.00	0.00	0.00	0.00
Ar	mass %	0.00	1.49	2.03	0.00	0.00	0.00	11.81	11.81	6.76	0.00	0.00	0.01	0.01	0.00	0.00	0.00
CH4	mass %	0.00	0.13	0.12	0.00	0.00	0.00	1.01	1.01	0.83	0.00	0.00	0.00	0.01	0.00	0.00	0.00
O2	mass %	0.00	0.00	0.00	0.00	0.00	0.00	0.00	0.00	0.00	0.00	0.00	0.00	0.00	0.00	0.00	0.00
H2O	mass %	0.00	0.09	0.08	100.00	100.00	100.00	0.00	0.00	0.00	0.75	9.93	0.00	0.00	100.00	100.00	96.48
H2S	mass %	0.00	1.06	2.39	0.00	0.00	0.00	0.00	0.00	3.52	38.17	2.42	0.00	0.00	0.00	0.00	0.00
COS	mass %	0.00	0.01	0.00	0.00	0.00	0.00	0.00	0.00	0.01	0.22	0.00	0.00	0.00	0.00	0.00	0.00
CS2	mass %	0.00	0.00	0.00	0.00	0.00	0.00	0.00	0.00	0.00	0.00	0.00	0.00	0.00	0.00	0.00	0.00
SO2	mass %	0.00	0.00	0.00	0.00	0.00	0.00	0.00	0.00	0.00	0.00	0.00	0.00	0.00	0.00	0.00	0.00
S	mass %	0.00	0.00	0.00	0.00	0.00	0.00	0.00	0.00	0.00	0.00	0.00	0.00	0.00	0.00	0.00	0.00
HCN	mass %	0.00	0.00	0.00	0.00	0.00	0.00	0.00	0.00	0.00	0.00	0.00	0.00	0.00	0.00	0.00	0.00
NH3	mass %	0.00	0.00	0.00	0.00	0.00	0.00	0.00	0.00	0.00	0.00	0.00	0.00	0.00	0.00	0.00	0.00
CH3OH	mass %	100.00	0.00	0.01	0.00	0.00	0.00	0.06	0.06	0.09	0.00	81.48	0.02	0.03	0.00	0.00	3.40

Appendix D8 – Heat and material balance for the TGT process (CC-IGCC / SCGP)

stream ID		0-5-air-2	1-5-GOX-2	4-5-gas-7	4-5-gas-8	4-5-met-2	8-5-st-12	8-5-BFW-4	9-5-cw-7	5-0-S-1	5-4-gas-6	5-8-st-11	5-8-cond-3	5-9-cw-8	5-10-ww-4
name		air	GOX	TGT fuel	CLAUS gas	MeOH bleed	IP steam	LP BFW	CW in	sulfur	tail gas	LP steam	IP condensate	CW out	waste water
t	°C	15.0	60.0	10.0	16.7	110.1	264.7	154.2	20.0	134.8	30.0	164.0	246.0	30.1	37.2
p	bar	1.01	50.00	9.10	1.20	4.80	50.60	14.00	6.00	5.00	35.89	6.60	38.00	4.00	1.10
m	kg/s	1.159	0.505	0.343	2.209	0.167	0.087	5.698	95.742	0.972	2.643	5.698	0.087	95.742	0.769
n	kmol/s	0.040	0.016	0.028	0.057	0.005	0.005	0.316	5.315	0.030	0.089	0.316	0.005	5.315	0.043
V	Nm³/h	3,242	1,268	2,273	4,637	421					7,194				
LHV	kJ/kg			16,263	7,839	16,376				8,916	2,395				
HHV	kJ/kg			18,884	8,500	18,755				8,916	2,728				
h	kJ/kg	-99	26	-5,017	-4,628	-6,689	-13,190	-15,330	-15,898	-3,000	-5,036	-13,219	-14,909	-15,855	-15,820
s	J/kgK	125	-867	-340	804	-3,241	-3,446	-7,528	-9,113	-4,212	-485	-2,678	-6,655	-8,973	-8,871
M	kg/kmol	28.84	32.17	12.17	38.44	31.91	18.00	18.00	18.00	32.00	29.66	18.00	18.00	18.00	18.01
Σ	mol %	100.00	100.00	100.00	100.00	100.00	100.00	100.00	100.00	100.00	100.00	100.00	100.00	100.00	100.00
H2	mol %	0.00	0.00	70.44	0.00	0.01	0.00	0.00	0.00	0.00	18.06	0.00	0.00	0.00	0.00
CO	mol %	0.00	0.00	7.20	0.00	0.00	0.00	0.00	0.00	0.00	2.35	0.00	0.00	0.00	0.00
CO2	mol %	0.03	0.00	13.28	40.40	8.84	0.00	0.00	0.00	0.00	36.88	0.00	0.00	0.00	0.03
N2	mol %	77.32	1.94	5.51	0.00	0.00	0.00	0.00	0.00	0.00	36.92	0.00	0.00	0.00	0.00
Ar	mol %	0.91	3.06	2.21	0.00	0.00	0.00	0.00	0.00	0.00	1.65	0.00	0.00	0.00	0.00
CH4	mol %	0.00	0.00	0.05	0.00	0.00	0.00	0.00	0.00	0.00	0.02	0.00	0.00	0.00	0.00
O2	mol %	20.74	95.00	0.00	0.00	0.00	0.00	0.00	0.00	0.00	0.00	0.00	0.00	0.00	0.00
H2O	mol %	1.01	0.00	0.00	1.55	8.65	100.00	100.00	100.00	0.00	0.16	100.00	100.00	100.00	99.97
H2S	mol %	0.00	0.00	1.26	55.68	2.51	0.00	0.00	0.00	0.00	3.94	0.00	0.00	0.00	0.01
COS	mol %	0.00	0.00	0.04	2.34	0.01	0.00	0.00	0.00	0.00	0.01	0.00	0.00	0.00	0.00
CS2	mol %	0.00	0.00	0.00	0.00	0.00	0.00	0.00	0.00	0.00	0.00	0.00	0.00	0.00	0.00
SO2	mol %	0.00	0.00	0.00	0.00	0.00	0.00	0.00	0.00	0.00	0.00	0.00	0.00	0.00	0.00
S	mol %	0.00	0.00	0.00	0.00	0.00	0.00	0.00	0.00	100.00	0.00	0.00	0.00	0.00	0.00
HCN	mol %	0.00	0.00	0.00	0.00	0.00	0.00	0.00	0.00	0.00	0.00	0.00	0.00	0.00	0.00
NH3	mol %	0.00	0.00	0.00	0.02	0.01	0.00	0.00	0.00	0.00	0.01	0.00	0.00	0.00	0.00
CH3OH	mol %	0.00	0.00	0.01	0.00	79.98	0.00	0.00	0.00	0.00	0.00	0.00	0.00	0.00	0.00
Σ	mass %	100.00	100.00	100.00	100.00	100.00	100.00	100.00	100.00	100.00	100.00	100.00	100.00	100.00	100.00
H2	mass %	0.00	0.00	11.67	0.00	0.00	0.00	0.00	0.00	0.00	1.23	0.00	0.00	0.00	0.00
CO	mass %	0.00	0.00	16.58	0.00	0.00	0.00	0.00	0.00	0.00	2.22	0.00	0.00	0.00	0.00
CO2	mass %	0.05	0.00	48.01	46.25	12.18	0.00	0.00	0.00	0.00	54.76	0.00	0.00	0.00	0.06
N2	mass %	75.07	1.69	12.69	0.00	0.00	0.00	0.00	0.00	0.00	34.90	0.00	0.00	0.00	0.00
Ar	mass %	1.26	3.80	7.24	0.00	0.00	0.00	0.00	0.00	0.00	2.22	0.00	0.00	0.00	0.00
CH4	mass %	0.00	0.00	0.07	0.00	0.00	0.00	0.00	0.00	0.00	0.01	0.00	0.00	0.00	0.00
O2	mass %	23.00	94.51	0.00	0.00	0.00	0.00	0.00	0.00	0.00	0.00	0.00	0.00	0.00	0.00
H2O	mass %	0.63	0.00	0.00	0.73	4.88	100.00	100.00	100.00	0.00	0.10	100.00	100.00	100.00	99.92
H2S	mass %	0.00	0.00	3.53	49.35	2.67	0.00	0.00	0.00	0.00	4.53	0.00	0.00	0.00	0.01
COS	mass %	0.00	0.00	0.19	3.66	0.02	0.00	0.00	0.00	0.00	0.03	0.00	0.00	0.00	0.00
CS2	mass %	0.00	0.00	0.00	0.00	0.00	0.00	0.00	0.00	0.00	0.00	0.00	0.00	0.00	0.00
SO2	mass %	0.00	0.00	0.00	0.00	0.00	0.00	0.00	0.00	0.00	0.00	0.00	0.00	0.00	0.00
S	mass %	0.00	0.00	0.00	0.00	0.00	0.00	0.00	0.00	100.00	0.00	0.00	0.00	0.00	0.00
HCN	mass %	0.00	0.00	0.00	0.00	0.00	0.00	0.00	0.00	0.00	0.00	0.00	0.00	0.00	0.00
NH3	mass %	0.00	0.00	0.00	0.01	0.00	0.00	0.00	0.00	0.00	0.01	0.00	0.00	0.00	0.00
CH3OH	mass %	0.00	0.00	0.02	0.00	80.24	0.00	0.00	0.00	0.00	0.00	0.00	0.00	0.00	0.00

Appendix D9 – Heat and material balance for the TGT process (CC-IGCC / Siemens gasifier)

stream ID		0-5-air-2	1-5-GOX-2	4-5-gas-7	4-5-gas-8	4-5-met-2	8-5-st-12	8-5-BFW-4	9-5-cw-7	5-0-S-1	5-4-gas-6	5-8-st-11	5-8-cond-3	5-9-cw-8	5-10-ww-4
name		air	GOX	TGT fuel	CLAUS gas	MeOH bleed	IP steam	LP BFW	CW in	sulfur	tail gas	LP steam	IP condensate	CW out	waste water
t	°C	15.0	60.0	10.0	16.3	110.1	264.7	154.2	20.0	134.8	30.0	164.0	246.0	29.8	37.1
p	bar	1.01	50.00	9.10	1.20	4.80	50.60	14.00	6.00	5.00	35.89	6.60	38.00	4.00	1.10
m	kg/s	1.143	0.511	0.327	2.151	0.165	0.085	5.853	99.105	0.984	2.519	5.853	0.085	99.105	0.795
n	kmol/s	0.040	0.016	0.028	0.057	0.005	0.005	0.325	5.501	0.031	0.086	0.325	0.005	5.501	0.044
V	Nm³/h	3,196	1,282	2,228	4,570	417					6,921				
LHV	kJ/kg	0	0	16,910	7,799	16,307				8,916	2,230				
HHV	kJ/kg	0	0	19,645	8,484	18,680				8,916	2,556				
h	kJ/kg	-99	26	-5,149	-4,703	-6,700	-13,190	-15,330	-15,898	-3,000	-5,079	-13,219	-14,909	-15,857	-15,821
s	J/kgK	125	-867	-378	759	-3,225	-3,446	-7,528	-9,113	-4,212	-515	-2,678	-6,655	-8,977	-8,873
M	kg/kmol	28.84	32.17	11.86	37.97	31.89	18.00	18.00	18.00	32.00	29.39	18.00	18.00	18.00	18.01
Σ	mol %	100.00	100.00	100.00	100.00	100.00	100.00	100.00	100.00	100.00	100.00	100.00	100.00	100.00	100.00
H2	mol %	0.00	0.00	71.62	0.00	0.01	0.00	0.00	0.00	0.00	18.80	0.00	0.00	0.00	0.00
CO	mol %	0.00	0.00	7.17	0.00	0.00	0.00	0.00	0.00	0.00	2.38	0.00	0.00	0.00	0.00
CO2	mol %	0.03	0.00	13.30	41.30	8.97	0.00	0.00	0.00	0.00	36.93	0.00	0.00	0.00	0.03
N2	mol %	77.32	1.90	4.34	0.00	0.00	0.00	0.00	0.00	0.00	37.46	0.00	0.00	0.00	0.00
Ar	mol %	0.91	3.10	2.23	0.00	0.00	0.00	0.00	0.00	0.00	1.70	0.00	0.00	0.00	0.00
CH4	mol %	0.00	0.00	0.06	0.00	0.00	0.00	0.00	0.00	0.00	0.02	0.00	0.00	0.00	0.00
O2	mol %	20.74	95.00	0.00	0.00	0.00	0.00	0.00	0.00	0.00	0.00	0.00	0.00	0.00	0.00
H2O	mol %	1.01	0.00	0.00	1.52	8.90	100.00	100.00	100.00	0.00	0.16	100.00	100.00	100.00	99.97
H2S	mol %	0.00	0.00	1.26	56.99	2.59	0.00	0.00	0.00	0.00	2.53	0.00	0.00	0.00	0.00
COS	mol %	0.00	0.00	0.00	0.17	0.00	0.00	0.00	0.00	0.00	0.00	0.00	0.00	0.00	0.00
CS2	mol %	0.00	0.00	0.00	0.00	0.00	0.00	0.00	0.00	0.00	0.00	0.00	0.00	0.00	0.00
SO2	mol %	0.00	0.00	0.00	0.00	0.00	0.00	0.00	0.00	0.00	0.00	0.00	0.00	0.00	0.00
S	mol %	0.00	0.00	0.00	0.00	0.00	0.00	0.00	0.00	100.00	0.00	0.00	0.00	0.00	0.00
HCN	mol %	0.00	0.00	0.00	0.00	0.00	0.00	0.00	0.00	0.00	0.00	0.00	0.00	0.00	0.00
NH3	mol %	0.00	0.00	0.00	0.01	0.01	0.00	0.00	0.00	0.00	0.01	0.00	0.00	0.00	0.00
CH3OH	mol %	0.00	0.00	0.01	0.00	79.52	0.00	0.00	0.00	0.00	0.00	0.00	0.00	0.00	0.00
Σ	mass %	100.00	100.00	100.00	100.00	100.00	100.00	100.00	100.00	100.00	100.00	100.00	100.00	100.00	100.00
H2	mass %	0.00	0.00	12.17	0.00	0.00	0.00	0.00	0.00	0.00	1.29	0.00	0.00	0.00	0.00
CO	mass %	0.00	0.00	16.93	0.00	0.00	0.00	0.00	0.00	0.00	2.27	0.00	0.00	0.00	0.00
CO2	mass %	0.05	0.00	49.37	47.86	12.37	0.00	0.00	0.00	0.00	55.33	0.00	0.00	0.00	0.06
N2	mass %	75.07	1.66	10.26	0.00	0.00	0.00	0.00	0.00	0.00	35.73	0.00	0.00	0.00	0.00
Ar	mass %	1.26	3.84	7.52	0.00	0.00	0.00	0.00	0.00	0.00	2.32	0.00	0.00	0.00	0.00
CH4	mass %	0.00	0.00	0.08	0.00	0.00	0.00	0.00	0.00	0.00	0.01	0.00	0.00	0.00	0.00
O2	mass %	23.00	94.50	0.00	0.00	0.00	0.00	0.00	0.00	0.00	0.00	0.00	0.00	0.00	0.00
H2O	mass %	0.63	0.00	0.00	0.72	5.02	100.00	100.00	100.00	0.00	0.10	100.00	100.00	100.00	99.93
H2S	mass %	0.00	0.00	3.63	51.13	2.76	0.00	0.00	0.00	0.00	2.94	0.00	0.00	0.00	0.01
COS	mass %	0.00	0.00	0.01	0.28	0.00	0.00	0.00	0.00	0.00	0.00	0.00	0.00	0.00	0.00
CS2	mass %	0.00	0.00	0.00	0.00	0.00	0.00	0.00	0.00	0.00	0.00	0.00	0.00	0.00	0.00
SO2	mass %	0.00	0.00	0.00	0.00	0.00	0.00	0.00	0.00	0.00	0.00	0.00	0.00	0.00	0.00
S	mass %	0.00	0.00	0.00	0.00	0.00	0.00	0.00	0.00	100.00	0.00	0.00	0.00	0.00	0.00
HCN	mass %	0.00	0.00	0.00	0.00	0.00	0.00	0.00	0.00	0.00	0.00	0.00	0.00	0.00	0.00
NH3	mass %	0.00	0.00	0.00	0.01	0.00	0.00	0.00	0.00	0.00	0.01	0.00	0.00	0.00	0.00
CH3OH	mass %	0.00	0.00	0.02	0.00	79.83	0.00	0.00	0.00	0.00	0.00	0.00	0.00	0.00	0.00

Appendix D10 – Heat and material balance for the TGT process (CC-IGCC / CoP gasifier)

stream ID		0-5-air-2	1-5-GOX-2	4-5-gas-7	4-5-gas-8	4-5-met-2	8-5-st-12	8-5-BFW-4	9-5-cw-7	5-0-S-1	5-4-gas-6	5-8-st-11	5-8-cond-3	5-9-cw-8	5-10-ww-4
name		air	GOX	TGT fuel	CLAUS gas	MeOH bleed	IP steam	LP BFW	CW in	sulfur	tail gas	LP steam	IP condensate	CW out	waste water
t	°C	15.0	60.0	10.0	12.9	109.5	264.7	154.2	20.0	134.8	30.0	164.0	246.0	30.0	37.2
p	bar	1.01	49.96	9.30	1.20	4.80	50.60	14.00	6.00	5.00	35.94	6.60	38.00	4.00	1.10
m	kg/s	1.208	0.514	0.391	2.260	0.170	0.089	5.813	100.187	0.992	2.766	5.813	0.089	100.187	0.785
n	kmol/s	0.042	0.016	0.030	0.059	0.005	0.005	0.323	5.561	0.031	0.094	0.323	0.005	5.561	0.044
V	Nm³/h	3,379	1,290	2,434	4,744	427					7,559				
LHV	kJ/kg			22,236	7,708	16,646				8,916	3,340				
HHV	kJ/kg			25,384	8,363	19,043				8,916	3,774				
h	kJ/kg	-99	26	-5,362	-4,712	-6,622	-13,190	-15,330	-15,898	-3,000	-5,107	-13,219	-14,909	-15,856	-15,820
s	J/kgK	125	-866	-1,269	772	-3,289	-3,446	-7,528	-9,113	-4,212	-613	-2,678	-6,655	-8,975	-8,871
M	kg/kmol	28.84	32.19	12.95	38.44	32.09	18.00	18.00	18.00	32.00	29.55	18.00	18.00	18.00	18.01
Σ	mol %	100.00	100.00	100.00	100.00	100.00	100.00	100.00	100.00	100.00	100.00	100.00	100.00	100.00	100.00
H2	mol %	0.00	0.00	60.44	0.00	0.00	0.00	0.00	0.00	0.00	16.03	0.00	0.00	0.00	0.00
CO	mol %	0.00	0.00	5.14	0.00	0.00	0.00	0.00	0.00	0.00	1.82	0.00	0.00	0.00	0.00
CO2	mol %	0.03	0.00	13.14	41.66	8.57	0.00	0.00	0.00	0.00	36.56	0.00	0.00	0.00	0.03
N2	mol %	77.32	1.74	2.58	0.00	0.00	0.00	0.00	0.00	0.00	35.69	0.00	0.00	0.00	0.00
Ar	mol %	0.91	3.26	2.37	0.00	0.00	0.00	0.00	0.00	0.00	1.72	0.00	0.00	0.00	0.00
CH4	mol %	0.00	0.00	15.09	0.00	0.00	0.00	0.00	0.00	0.00	4.66	0.00	0.00	0.00	0.00
O2	mol %	20.74	95.00	0.00	0.00	0.00	0.00	0.00	0.00	0.00	0.00	0.00	0.00	0.00	0.00
H2O	mol %	1.01	0.00	0.00	1.22	7.13	100.00	100.00	100.00	0.00	0.16	100.00	100.00	100.00	99.97
H2S	mol %	0.00	0.00	1.20	55.44	2.40	0.00	0.00	0.00	0.00	3.31	0.00	0.00	0.00	0.00
COS	mol %	0.00	0.00	0.03	1.67	0.01	0.00	0.00	0.00	0.00	0.01	0.00	0.00	0.00	0.00
CS2	mol %	0.00	0.00	0.00	0.00	0.00	0.00	0.00	0.00	0.00	0.00	0.00	0.00	0.00	0.00
SO2	mol %	0.00	0.00	0.00	0.00	0.00	0.00	0.00	0.00	0.00	0.00	0.00	0.00	0.00	0.00
S	mol %	0.00	0.00	0.00	0.00	0.00	0.00	0.00	0.00	100.00	0.00	0.00	0.00	0.00	0.00
HCN	mol %	0.00	0.00	0.00	0.00	0.00	0.00	0.00	0.00	0.00	0.00	0.00	0.00	0.00	0.00
NH3	mol %	0.00	0.00	0.00	0.02	0.01	0.00	0.00	0.00	0.00	0.01	0.00	0.00	0.00	0.00
CH3OH	mol %	0.00	0.00	0.01	0.00	81.88	0.00	0.00	0.00	0.00	0.00	0.00	0.00	0.00	0.00
Σ	mass %	100.00	100.00	100.00	100.00	100.00	100.00	100.00	100.00	100.00	100.00	100.00	100.00	100.00	100.00
H2	mass %	0.00	0.00	9.40	0.00	0.00	0.00	0.00	0.00	0.00	1.09	0.00	0.00	0.00	0.00
CO	mass %	0.00	0.00	11.12	0.00	0.00	0.00	0.00	0.00	0.00	1.73	0.00	0.00	0.00	0.00
CO2	mass %	0.05	0.00	44.62	47.69	11.74	0.00	0.00	0.00	0.00	54.49	0.00	0.00	0.00	0.06
N2	mass %	75.07	1.51	5.58	0.00	0.00	0.00	0.00	0.00	0.00	33.86	0.00	0.00	0.00	0.00
Ar	mass %	1.26	4.05	7.31	0.00	0.00	0.00	0.00	0.00	0.00	2.33	0.00	0.00	0.00	0.00
CH4	mass %	0.00	0.00	18.68	0.00	0.00	0.00	0.00	0.00	0.00	2.53	0.00	0.00	0.00	0.00
O2	mass %	23.00	94.44	0.00	0.00	0.00	0.00	0.00	0.00	0.00	0.00	0.00	0.00	0.00	0.00
H2O	mass %	0.63	0.00	0.00	0.57	4.00	100.00	100.00	100.00	0.00	0.10	100.00	100.00	100.00	99.92
H2S	mass %	0.00	0.00	3.14	49.13	2.55	0.00	0.00	0.00	0.00	3.82	0.00	0.00	0.00	0.01
COS	mass %	0.00	0.00	0.13	2.60	0.01	0.00	0.00	0.00	0.00	0.02	0.00	0.00	0.00	0.00
CS2	mass %	0.00	0.00	0.00	0.00	0.00	0.00	0.00	0.00	0.00	0.00	0.00	0.00	0.00	0.00
SO2	mass %	0.00	0.00	0.00	0.00	0.00	0.00	0.00	0.00	0.00	0.00	0.00	0.00	0.00	0.00
S	mass %	0.00	0.00	0.00	0.00	0.00	0.00	0.00	0.00	100.00	0.00	0.00	0.00	0.00	0.00
HCN	mass %	0.00	0.00	0.00	0.00	0.00	0.00	0.00	0.00	0.00	0.00	0.00	0.00	0.00	0.00
NH3	mass %	0.00	0.00	0.00	0.01	0.00	0.00	0.00	0.00	0.00	0.01	0.00	0.00	0.00	0.00
CH3OH	mass %	0.00	0.00	0.02	0.00	81.69	0.00	0.00	0.00	0.00	0.00	0.00	0.00	0.00	0.00

Appendix D11 – Heat and material balance for the TGT process (CC-IGCC / GE-R)

stream ID		0-5-air-2	1-5-GOX-2	4-5-gas-7	4-5-gas-8	4-5-met-2	8-5-st-12	8-5-BFW-4	9-5-cw-7	5-0-S-1	5-4-gas-6	5-8-st-11	5-8-cond-3	5-9-cw-8	5-10-ww-4
name		air	GOX	TGT fuel	CLAUS gas	MeOH bleed	IP steam	LP BFW	CW in	sulfur	tail gas	LP steam	IP condensate	CW out	waste water
t	°C	15.0	60.0	10.0	17.5	115.2	264.7	154.2	20.0	134.8	30.0	164.0	246.0	29.9	37.3
p	bar	1.01	70.00	14.60	1.20	4.80	50.60	14.00	6.00	5.00	56.80	6.60	38.00	4.00	1.10
m	kg/s	1.215	0.558	0.582	3.138	0.170	0.111	6.118	122.602	1.070	3.716	6.118	0.111	122.602	0.876
n	kmol/s	0.042	0.017	0.037	0.080	0.006	0.006	0.340	6.806	0.033	0.117	0.340	0.006	6.806	0.049
V	Nm³/h	3,398	1,400	2,953	6,453	454					9,405				
LHV	kJ/kg			11,596	5,824	16,583				8,916	1,834				
HHV	kJ/kg			13,446	6,341	19,117				8,916	2,100				
h	kJ/kg	-99	23	-6,532	-5,787	-6,893	-13,190	-15,330	-15,898	-3,000	-6,145	-13,219	-14,909	-15,856	-15,817
s	J/kgK	125	-961	-565	605	-3,416	-3,446	-7,528	-9,113	-4,212	-657	-2,678	-6,655	-8,976	-8,868
M	kg/kmol	28.84	32.16	15.90	39.25	30.22	18.00	18.00	18.00	32.00	31.92	18.00	18.00	18.00	18.01
Σ	mol %	100.00	100.00	100.00	100.00	100.00	100.00	100.00	100.00	100.00	100.00	100.00	100.00	100.00	100.00
H2	mol %	0.00	0.00	62.82	0.00	0.00	0.00	0.00	0.00	0.00	16.22	0.00	0.00	0.00	0.00
CO	mol %	0.00	0.00	6.00	0.00	0.00	0.00	0.00	0.00	0.00	1.98	0.00	0.00	0.00	0.00
CO2	mol %	0.03	0.00	24.29	54.25	4.24	0.00	0.00	0.00	0.00	48.78	0.00	0.00	0.00	0.04
N2	mol %	77.32	1.99	1.70	0.00	0.00	0.00	0.00	0.00	0.00	28.76	0.00	0.00	0.00	0.00
Ar	mol %	0.91	3.01	2.69	0.00	0.00	0.00	0.00	0.00	0.00	1.62	0.00	0.00	0.00	0.00
CH4	mol %	0.00	0.00	0.83	0.00	0.00	0.00	0.00	0.00	0.00	0.24	0.00	0.00	0.00	0.00
O2	mol %	20.74	95.00	0.00	0.00	0.00	0.00	0.00	0.00	0.00	0.00	0.00	0.00	0.00	0.00
H2O	mol %	1.01	0.00	0.00	1.64	16.67	100.00	100.00	100.00	0.00	0.14	100.00	100.00	100.00	99.95
H2S	mol %	0.00	0.00	1.64	43.95	2.15	0.00	0.00	0.00	0.00	2.23	0.00	0.00	0.00	0.00
COS	mol %	0.00	0.00	0.00	0.14	0.00	0.00	0.00	0.00	0.00	0.00	0.00	0.00	0.00	0.00
CS2	mol %	0.00	0.00	0.00	0.00	0.00	0.00	0.00	0.00	0.00	0.00	0.00	0.00	0.00	0.00
SO2	mol %	0.00	0.00	0.00	0.00	0.00	0.00	0.00	0.00	0.00	0.00	0.00	0.00	0.00	0.00
S	mol %	0.00	0.00	0.00	0.00	0.00	0.00	0.00	0.00	100.00	0.00	0.00	0.00	0.00	0.00
HCN	mol %	0.00	0.00	0.00	0.00	0.00	0.00	0.00	0.00	0.00	0.00	0.00	0.00	0.00	0.00
NH3	mol %	0.00	0.00	0.00	0.01	0.00	0.00	0.00	0.00	0.00	0.01	0.00	0.00	0.00	0.00
CH3OH	mol %	0.00	0.00	0.04	0.00	76.93	0.00	0.00	0.00	0.00	0.01	0.00	0.00	0.00	0.01
Σ	mass %	100.00	100.00	100.00	100.00	100.00	100.00	100.00	100.00	100.00	100.00	100.00	100.00	100.00	100.00
H2	mass %	0.00	0.00	7.97	0.00	0.00	0.00	0.00	0.00	0.00	1.03	0.00	0.00	0.00	0.00
CO	mass %	0.00	0.00	10.58	0.00	0.00	0.00	0.00	0.00	0.00	1.74	0.00	0.00	0.00	0.00
CO2	mass %	0.05	0.00	67.26	60.85	6.16	0.00	0.00	0.00	0.00	67.33	0.00	0.00	0.00	0.09
N2	mass %	75.07	1.73	2.99	0.00	0.00	0.00	0.00	0.00	0.00	25.27	0.00	0.00	0.00	0.00
Ar	mass %	1.26	3.74	6.76	0.00	0.00	0.00	0.00	0.00	0.00	2.03	0.00	0.00	0.00	0.00
CH4	mass %	0.00	0.00	0.83	0.00	0.00	0.00	0.00	0.00	0.00	0.12	0.00	0.00	0.00	0.00
O2	mass %	23.00	94.53	0.00	0.00	0.00	0.00	0.00	0.00	0.00	0.00	0.00	0.00	0.00	0.00
H2O	mass %	0.63	0.00	0.00	0.75	9.93	100.00	100.00	100.00	0.00	0.08	100.00	100.00	100.00	99.89
H2S	mass %	0.00	0.00	3.52	38.17	2.42	0.00	0.00	0.00	0.00	2.38	0.00	0.00	0.00	0.01
COS	mass %	0.00	0.00	0.01	0.22	0.00	0.00	0.00	0.00	0.00	0.00	0.00	0.00	0.00	0.00
CS2	mass %	0.00	0.00	0.00	0.00	0.00	0.00	0.00	0.00	0.00	0.00	0.00	0.00	0.00	0.00
SO2	mass %	0.00	0.00	0.00	0.00	0.00	0.00	0.00	0.00	0.00	0.00	0.00	0.00	0.00	0.00
S	mass %	0.00	0.00	0.00	0.00	0.00	0.00	0.00	0.00	100.00	0.00	0.00	0.00	0.00	0.00
HCN	mass %	0.00	0.00	0.00	0.00	0.00	0.00	0.00	0.00	0.00	0.00	0.00	0.00	0.00	0.00
NH3	mass %	0.00	0.00	0.00	0.00	0.00	0.00	0.00	0.00	0.00	0.00	0.00	0.00	0.00	0.00
CH3OH	mass %	0.00	0.00	0.09	0.00	81.48	0.00	0.00	0.00	0.00	0.01	0.00	0.00	0.00	0.01

Appendix D12 – Heat and material balance for the CO_2-compressor (CC-IGCC / SCGP)

stream ID		4-6-CO2-1	4-6-CO2-2	9-6-cw-5	6-0-CO2-3	6-9-cw-6
name		LP CO2	IP CO2	CW in	HP CO2	CW out
t	°C	-15.0	10.0	20.0	30.0	30.0
p	bar	1.05	2.30	6.00	100.00	4.00
m	kg/s	30.718	54.701	1,014.013	85.419	1,014.013
n	kmol/s	0.698	1.245	56.287	1.943	56.287
V	Nm³/h	56,341	100,419		156,760	
LHV	kJ/kg					
h	kJ/kg	-8,974	-8,952	-15,898	-9,165	-15,856
s	J/kgK	-64	-134	-9,113	-1,425	-8,974
M	kg/kmol	44.08	44.04	18.00	44.06	18.00
Σ	mol %	100.0000	100.0000	100.0000	100.0000	100.0000
H2	mol %	0.03	0.10	0.00	0.08	0.00
CO	mol %	0.01	0.04	0.00	0.03	0.00
CO2	mol %	99.93	99.80	0.00	99.85	0.00
N2	mol %	0.00	0.01	0.00	0.01	0.00
Ar	mol %	0.00	0.02	0.00	0.01	0.00
CH4	mol %	0.00	0.00	0.00	0.00	0.00
O2	mol %	0.00	0.00	0.00	0.00	0.00
H2O	mol %	0.00	0.00	100.00	0.00	100.00
H2S	mol %	0.00	0.00	0.00	0.00	0.00
COS	mol %	0.00	0.00	0.00	0.00	0.00
CS2	mol %	0.00	0.00	0.00	0.00	0.00
SO2	mol %	0.00	0.00	0.00	0.00	0.00
S	mol %	0.00	0.00	0.00	0.00	0.00
HCN	mol %	0.00	0.00	0.00	0.00	0.00
NH3	mol %	0.00	0.00	0.00	0.00	0.00
CH3OH	mol %	0.02	0.02	0.00	0.02	0.00
Σ	mass %	100.0000	100.0000	100.0000	100.0000	100.0000
H2	mass %	0.00	0.00	0.00	0.00	0.00
CO	mass %	0.01	0.02	0.00	0.02	0.00
CO2	mass %	99.97	99.93	0.00	99.95	0.00
N2	mass %	0.00	0.01	0.00	0.01	0.00
Ar	mass %	0.00	0.01	0.00	0.01	0.00
CH4	mass %	0.00	0.00	0.00	0.00	0.00
O2	mass %	0.00	0.00	0.00	0.00	0.00
H2O	mass %	0.00	0.00	100.00	0.00	100.00
H2S	mass %	0.00	0.00	0.00	0.00	0.00
COS	mass %	0.00	0.00	0.00	0.00	0.00
CS2	mass %	0.00	0.00	0.00	0.00	0.00
SO2	mass %	0.00	0.00	0.00	0.00	0.00
S	mass %	0.00	0.00	0.00	0.00	0.00
HCN	mass %	0.00	0.00	0.00	0.00	0.00
NH3	mass %	0.00	0.00	0.00	0.00	0.00
CH3OH	mass %	0.01	0.02	0.00	0.02	0.00

Appendix D13 – Heat and material balance for the CO_2-compressor (CC-IGCC / Siemens gasifier)

name		LP CO2	IP CO2	CW in	HP CO2	CW out
t	°C	-15.0	10.0	20.0	30.0	30.0
p	bar	1.05	2.30	6.00	100.00	4.00
m	kg/s	30.813	54.713	1,015.484	85.527	1,015.484
n	kmol/s	0.700	1.245	56.369	1.945	56.369
V	Nm³/h	56,517	100,442		156,958	
LHV	kJ/kg					
h	kJ/kg	-8,974	-8,952	-15,898	-9,166	-15,856
s	J/kgK	-64	-134	-9,113	-1,425	-8,974
M	kg/kmol	44.08	44.04	18.00	44.06	18.00
Σ	mol %	100.0000	100.0000	100.0000	100.0000	100.0000
H2	mol %	0.03	0.11	0.00	0.08	0.00
CO	mol %	0.01	0.04	0.00	0.03	0.00
CO2	mol %	99.93	99.80	0.00	99.85	0.00
N2	mol %	0.00	0.01	0.00	0.01	0.00
Ar	mol %	0.00	0.02	0.00	0.01	0.00
CH4	mol %	0.00	0.00	0.00	0.00	0.00
O2	mol %	0.00	0.00	0.00	0.00	0.00
H2O	mol %	0.00	0.00	100.00	0.00	100.00
H2S	mol %	0.00	0.00	0.00	0.00	0.00
COS	mol %	0.00	0.00	0.00	0.00	0.00
CS2	mol %	0.00	0.00	0.00	0.00	0.00
SO2	mol %	0.00	0.00	0.00	0.00	0.00
S	mol %	0.00	0.00	0.00	0.00	0.00
HCN	mol %	0.00	0.00	0.00	0.00	0.00
NH3	mol %	0.00	0.00	0.00	0.00	0.00
CH3OH	mol %	0.02	0.02	0.00	0.02	0.00
Σ	mass %	100.0000	100.0000	100.0000	100.0000	100.0000
H2	mass %	0.00	0.00	0.00	0.00	0.00
CO	mass %	0.01	0.02	0.00	0.02	0.00
CO2	mass %	99.97	99.93	0.00	99.95	0.00
N2	mass %	0.00	0.01	0.00	0.00	0.00
Ar	mass %	0.00	0.01	0.00	0.01	0.00
CH4	mass %	0.00	0.00	0.00	0.00	0.00
O2	mass %	0.00	0.00	0.00	0.00	0.00
H2O	mass %	0.00	0.00	100.00	0.00	100.00
H2S	mass %	0.00	0.00	0.00	0.00	0.00
COS	mass %	0.00	0.00	0.00	0.00	0.00
CS2	mass %	0.00	0.00	0.00	0.00	0.00
SO2	mass %	0.00	0.00	0.00	0.00	0.00
S	mass %	0.00	0.00	0.00	0.00	0.00
HCN	mass %	0.00	0.00	0.00	0.00	0.00
NH3	mass %	0.00	0.00	0.00	0.00	0.00
CH3OH	mass %	0.01	0.02	0.00	0.02	0.00

Appendix D14 – Heat and material balance for the CO_2-compressor (CC-IGCC / CoP gasifier)

stream ID		4-6-CO2-1	4-6-CO2-2	9-6-cw-5	6-0-CO2-3	6-9-cw-6
name		LP CO2	IP CO2	CW in	HP CO2	CW out
t	°C	-15.0	10.0	20.0	30.0	30.0
p	bar	1.05	2.30	6.00	100.00	4.00
m	kg/s	28.337	53.906	975.069	82.243	975.069
n	kmol/s	0.644	1.228	54.125	1.873	54.125
V	Nm³/h	51,993	99,104		151,098	
LHV	kJ/kg					
h	kJ/kg	-8,974	-8,949	-15,898	-9,163	-15,856
s	J/kgK	-65	-138	-9,113	-1,427	-8,974
M	kg/kmol	44.06	43.98	18.00	44.01	18.00
Σ	mol %	100.00	100.00	100.00	100.00	100.00
H2	mol %	0.02	0.07	0.00	0.05	0.00
CO	mol %	0.01	0.02	0.00	0.01	0.00
CO2	mol %	99.87	99.57	0.00	99.67	0.00
N2	mol %	0.00	0.00	0.00	0.00	0.00
Ar	mol %	0.00	0.01	0.00	0.01	0.00
CH4	mol %	0.07	0.30	0.00	0.22	0.00
O2	mol %	0.00	0.00	0.00	0.00	0.00
H2O	mol %	0.00	0.00	100.00	0.00	100.00
H2S	mol %	0.00	0.00	0.00	0.00	0.00
COS	mol %	0.00	0.00	0.00	0.00	0.00
CS2	mol %	0.00	0.00	0.00	0.00	0.00
SO2	mol %	0.00	0.00	0.00	0.00	0.00
S	mol %	0.00	0.00	0.00	0.00	0.00
HCN	mol %	0.00	0.00	0.00	0.00	0.00
NH3	mol %	0.00	0.00	0.00	0.00	0.00
CH3OH	mol %	0.02	0.02	0.00	0.02	0.00
Σ	mass %	100.00	100.00	100.00	100.00	100.00
H2	mass %	0.00	0.00	0.00	0.00	0.00
CO	mass %	0.00	0.01	0.00	0.01	0.00
CO2	mass %	99.95	99.84	0.00	99.88	0.00
N2	mass %	0.00	0.00	0.00	0.00	0.00
Ar	mass %	0.00	0.01	0.00	0.01	0.00
CH4	mass %	0.03	0.11	0.00	0.08	0.00
O2	mass %	0.00	0.00	0.00	0.00	0.00
H2O	mass %	0.00	0.00	100.00	0.00	100.00
H2S	mass %	0.00	0.00	0.00	0.00	0.00
COS	mass %	0.00	0.00	0.00	0.00	0.00
CS2	mass %	0.00	0.00	0.00	0.00	0.00
SO2	mass %	0.00	0.00	0.00	0.00	0.00
S	mass %	0.00	0.00	0.00	0.00	0.00
HCN	mass %	0.00	0.00	0.00	0.00	0.00
NH3	mass %	0.00	0.00	0.00	0.00	0.00
CH3OH	mass %	0.01	0.02	0.00	0.02	0.00

Appendix D15 – Heat and material balance for the CO_2-compressor (CC-IGCC / GE-R)

stream ID		4-6-CO2-1	4-6-CO2-2	9-6-cw-5	6-0-CO2-3	6-9-cw-6
name		LP CO2	IP CO2	CW in	HP CO2	CW out
t	°C	-15.0	10.0	20.0	30.0	30.0
p	bar	1.80	3.30	6.00	100.00	4.00
m	kg/s	30.290	62.949	1,019.194	93.239	1,019.194
n	kmol/s	0.688	1.432	56.575	2.120	56.575
V	Nm³/h	55,553	115,507		171,059	
LHV	kJ/kg					
h	kJ/kg	-8,975	-8,954	-15,898	-9,166	-15,856
s	J/kgK	-169	-207	-9,113	-1,427	-8,974
M	kg/kmol	44.08	44.06	18.00	44.07	18.00
Σ	mol %	100.00	100.00	100.00	100.00	100.00
H2	mol %	0.02	0.05	0.00	0.04	0.00
CO	mol %	0.01	0.02	0.00	0.02	0.00
CO2	mol %	99.93	99.85	0.00	99.88	0.00
N2	mol %	0.00	0.00	0.00	0.00	0.00
Ar	mol %	0.01	0.02	0.00	0.01	0.00
CH4	mol %	0.01	0.01	0.00	0.01	0.00
O2	mol %	0.00	0.00	0.00	0.00	0.00
H2O	mol %	0.00	0.00	100.00	0.00	100.00
H2S	mol %	0.00	0.00	0.00	0.00	0.00
COS	mol %	0.00	0.00	0.00	0.00	0.00
CS2	mol %	0.00	0.00	0.00	0.00	0.00
SO2	mol %	0.00	0.00	0.00	0.00	0.00
S	mol %	0.00	0.00	0.00	0.00	0.00
HCN	mol %	0.00	0.00	0.00	0.00	0.00
NH3	mol %	0.00	0.00	0.00	0.00	0.00
CH3OH	mol %	0.03	0.04	0.00	0.04	0.00
Σ	mass %	100.00	100.00	100.00	100.00	100.00
H2	mass %	0.00	0.00	0.00	0.00	0.00
CO	mass %	0.01	0.01	0.00	0.01	0.00
CO2	mass %	99.96	99.93	0.00	99.94	0.00
N2	mass %	0.00	0.00	0.00	0.00	0.00
Ar	mass %	0.01	0.01	0.00	0.01	0.00
CH4	mass %	0.00	0.01	0.00	0.00	0.00
O2	mass %	0.00	0.00	0.00	0.00	0.00
H2O	mass %	0.00	0.00	100.00	0.00	100.00
H2S	mass %	0.00	0.00	0.00	0.00	0.00
COS	mass %	0.00	0.00	0.00	0.00	0.00
CS2	mass %	0.00	0.00	0.00	0.00	0.00
SO2	mass %	0.00	0.00	0.00	0.00	0.00
S	mass %	0.00	0.00	0.00	0.00	0.00
HCN	mass %	0.00	0.00	0.00	0.00	0.00
NH3	mass %	0.00	0.00	0.00	0.00	0.00
CH3OH	mass %	0.02	0.03	0.00	0.03	0.00

Appendix E1 – Parameters for reference point calculation with the generic GT model

Fixed parameters	Unit	Value
$\Delta p_{inlet} = \Delta p_{outlet}$	mbar	10
Δp_{comb}	%	3
η_{comb}	%	100
η_{mech}	%	99.6
η_{G}	%	98.5
Target parameters	**Unit**	**Value**
Gross power output	MW	292
Gross efficiency (Fuel mass flow	% kg CH_4/s	39.8 14.669)
Compressor pressure ratio	-	18.2
Exhaust gas temperature	°C	577
Hot gas temperature (T_7)	°C	1450
Turbine inlet temperature (T_9)	°C	1245
Blade temperature (T_{blade})	°C	900
Adjusted parameters	**Unit**	**Value**
$\eta_{p,compr}$	%	94
Cool frac	%	22.4
$\eta_{p,uc\ turb}$	%	93.2
$\eta_{p,c\ turb}$	%	91.16
Compressor mass flow	kg/s	684

Appendix E2 – Reference parameters for off-design calculations

Parameter	Unit	Value
m_1_ref	kg/s	684
m_8_ref	kg/s	153.011
m_9_ref	kg/s	698.669
t_7_ref	°C	1450
t_9_ref	°C	1245
t_blade_ref	°C	900
p_9_ref	bar	17.71
Δp_comb_ref	bar	0.55
Π_compr,ref	-	18.2
Π_turb,ref	-	17.3

Appendix E3 – CHEMCAD model of the GT process for the CC-IGCC

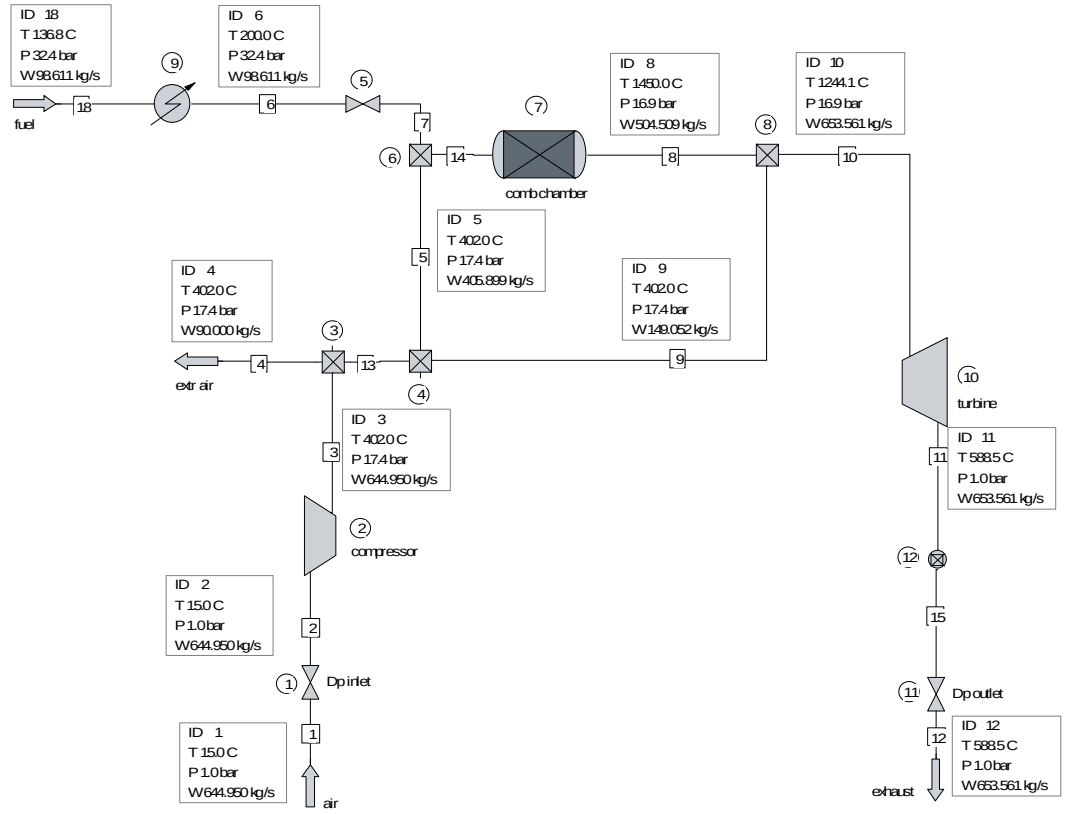

Appendix E4 – Heat and material balance for the gas turbine(CC-IGCC /SCGP)

stream ID		0-7-air-3	8-7-gas-9	7-8-air-4	7-8-eg-2
name		ambient air	GT fuel	extraction air	exhaust gas
t	°C	15.0	200.0	402.0	588.5
p	bar	1.0	32.4	17.4	1.0
m	kg/s	644.950	98.611	90.000	653.561
n	kmol/s	22.353	6.407	3.119	24.136
V	Nm³/h	1,803,646	516,956	251,691	1,947,551
LHV	kJ/kg		7,139		
HHV	kJ/kg		8,738		
h	kJ/kg	-99.5	-1,505.5	302.2	-825.6
s	J/kgK	124.3	-635.4	182.5	1,162.2
M	kg/kmol	28.84	15.38	28.84	27.07
Σ	mol %	100.00	100.00	100.00	100.00
H2	mol %	0.00	45.01	0.00	0.00
CO	mol %	0.00	1.95	0.00	0.00
CO2	mol %	0.03	0.25	0.03	0.61
N2	mol %	77.32	41.48	77.32	72.62
Ar	mol %	0.91	0.59	0.91	0.88
CH4	mol %	0.00	0.01	0.00	0.00
O2	mol %	20.74	0.30	20.74	10.36
H2O	mol %	1.01	10.41	1.01	15.52
Σ	mass %	100.00	100.00	100.00	100.00
H2	mass %	0.00	5.89	0.00	0.00
CO	mass %	0.00	3.54	0.00	0.00
CO2	mass %	0.05	0.72	0.05	1.00
N2	mass %	75.07	75.50	75.07	75.13
Ar	mass %	1.26	1.52	1.26	1.30
CH4	mass %	0.00	0.02	0.00	0.00
O2	mass %	23.00	0.62	23.00	12.25
H2O	mass %	0.63	12.18	0.63	10.33

Appendix E5 – Heat and material balance for the gas turbine (CC-IGCC / Siemens gasifier)

stream ID		0-7-air-3	8-7-gas-9	7-8-air-4	7-8-eg-2
name		ambient air	GT fuel	extraction air	exhaust gas
t	°C	15.0	200.0	401.6	589.6
p	bar	1.0	32.4	17.4	1.0
m	kg/s	643.600	97.461	90.000	651.060
n	kmol/s	22.306	6.419	3.119	24.101
V	Nm³/h	1,799,870	517,979	251,691	1,944,697
LHV	kJ/kg		7,169		
HHV	kJ/kg		8,850		
h	kJ/kg	-99.5	-1,852.4	301.8	-877.7
s	J/kgK	124.3	-703.8	182.4	1,158.9
M	kg/kmol	28.84	15.17	28.84	27.00
Σ	mol %	100.00	100.00	100.00	100.00
H2	mol %	0.00	45.00	0.00	0.00
CO	mol %	0.00	1.91	0.00	0.00
CO2	mol %	0.03	0.25	0.03	0.61
N2	mol %	77.32	39.56	77.32	72.09
Ar	mol %	0.91	0.56	0.91	0.87
CH4	mol %	0.00	0.02	0.00	0.00
O2	mol %	20.74	0.22	20.74	10.31
H2O	mol %	1.01	12.48	1.01	16.12
Σ	mass %	100.00	100.00	100.00	100.00
H2	mass %	0.00	5.97	0.00	0.00
CO	mass %	0.00	3.52	0.00	0.00
CO2	mass %	0.05	0.72	0.05	0.99
N2	mass %	75.07	73.01	75.07	74.76
Ar	mass %	1.26	1.48	1.26	1.29
CH4	mass %	0.00	0.02	0.00	0.00
O2	mass %	23.00	0.47	23.00	12.21
H2O	mass %	0.63	14.81	0.63	10.75

Appendix E6 – Heat and material balance for the gas turbine (CC-IGCC / CoP gasifier)

stream ID		0-7-air-3	7-8-air-4		8-7-gas-9	7-8-eg-2
name		ambient air	extraction air	fuel	GT fuel	exhaust gas
t	°C	15.0	404.3	143.3	200.0	587.1
p	bar	1.0	17.6	32.4	32.4	1.0
m	kg/s	675.2	90.0	84.2	84.2	669.4
n	kmol/s	23.4	3.1	5.7	5.7	24.6
V	Nm³/h	1,888,102	251,691	455,946	455,946	1,986,259
LHV	kJ/kg			8,483	8,483	
HHV	kJ/kg			10,334	10,334	
h	kJ/kg	-99.5	304.7	-2,093.7	-1,975.2	-837.7
s	J/kgK	124.3	182.7	-1,084.5	-817.8	1,170.0
M	kg/kmol	28.84	28.84	14.89	14.89	27.18
Σ	mol %	100.00	100.00	100.00	100.00	100.00
H2	mol %	0.00	0.00	45.00	45.00	0.00
CO	mol %	0.00	0.00	1.54	1.54	0.00
CO2	mol %	0.03	0.03	0.26	0.26	0.98
N2	mol %	77.32	77.32	37.70	37.70	72.35
Ar	mol %	0.91	0.91	0.61	0.61	0.89
CH4	mol %	0.00	0.00	2.34	2.34	0.00
O2	mol %	20.74	20.74	0.08	0.08	10.69
H2O	mol %	1.01	1.01	12.48	12.48	15.10
Σ	mass %	100.00	100.00	100.00	100.00	100.00
H2	mass %	0.00	0.00	6.09	6.09	0.00
CO	mass %	0.00	0.00	2.90	2.90	0.00
CO2	mass %	0.05	0.05	0.76	0.76	1.58
N2	mass %	75.07	75.07	70.86	70.86	74.54
Ar	mass %	1.26	1.26	1.62	1.62	1.30
CH4	mass %	0.00	0.00	2.51	2.51	0.00
O2	mass %	23.00	23.00	0.17	0.17	12.58
H2O	mass %	0.63	0.63	15.08	15.08	10.00

Appendix E7 – Heat and material balance for the gas turbine (CC-IGCC / GE-R)

stream ID		0-7-air-3	8-7-gas-9	7-8-air-4	7-8-eg-2
name		ambient air	GT fuel	extraction air	exhaust gas
t	°C	15.0	200.0	401.1	592.3
p	bar	1.0	32.4	17.3	1.0
m	kg/s	643.300	93.550	90.000	646.849
n	kmol/s	22.296	6.380	3.119	24.058
V	Nm³/h	1,799,032	514,763	251,691	1,941,239
LHV	kJ/kg		7,345		
HHV	kJ/kg		9,247		
h	kJ/kg	-99.5	-2,774.1	301.2	-1,005.4
s	J/kgK	124.3	-877.6	182.4	1,152.5
M	kg/kmol	28.84	14.65	28.84	26.87
Σ	mol %	100.00	100.00	100.00	100.00
H2	mol %	0.00	45.00	0.00	0.00
CO	mol %	0.00	1.96	0.00	0.00
CO2	mol %	0.03	0.25	0.03	0.65
N2	mol %	77.32	34.27	77.32	70.71
Ar	mol %	0.91	0.71	0.91	0.91
CH4	mol %	0.00	0.13	0.00	0.00
O2	mol %	20.74	0.07	20.74	10.25
H2O	mol %	1.01	17.61	1.01	17.48
Σ	mass %	100.00	100.00	100.00	100.00
H2	mass %	0.00	6.19	0.00	0.00
CO	mass %	0.00	3.75	0.00	0.00
CO2	mass %	0.05	0.74	0.05	1.06
N2	mass %	75.07	65.46	75.07	73.68
Ar	mass %	1.26	1.93	1.26	1.35
CH4	mass %	0.00	0.15	0.00	0.00
O2	mass %	23.00	0.14	23.00	12.19
H2O	mass %	0.63	21.63	0.63	11.71

Appendix F1 – Relevant boundary conditions for water-/steam cycle simulations

HRSG	Unit	Value
ΔT Pinch point HP-evaporator	K	10 – 60
ΔT Pinch point IP-evaporator	K	10
ΔT Pinch point LP-evaporator	K	10
ΔT Approach point HP-superheater	K	25
HRSG-inlet temperature (condensate)	°C	90
Fuel preheater outlet temperature	°C	200
Steam turbine and condenser	**Unit**	**Value**
Live steam parameters	bar/°C	129/565
Reheat steam parameters	bar/°C	46/565
LP-steam parameters	bar/°C	6/260
Isentropic efficiency (HP-turbine)	%	89
Isentropic efficiency (IP-turbine)	%	93
Isentropic efficiency (LP-turbine)	%	87
Condenser vacuum	mbar	49

Appendix F2 – CHEMCAD model of the water-/steam cycle for the CC-IGCC / SCGP

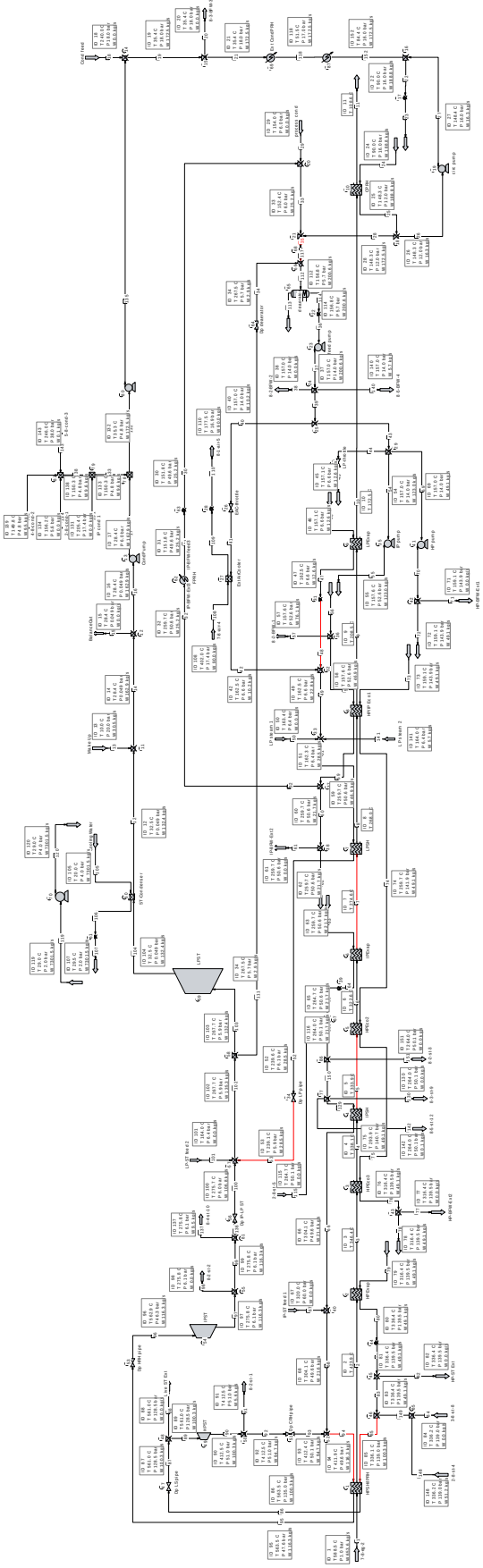

Appendix F3 – Heat and material balance for the water-/steam cycle (CC-IGCC / SCGP)

stream ID		3-8-gas-5	7-8-air-4	7-8-eg-2	2-8-st-4	4-8-cond-2	5-8-st-11	5-8-cond-3	IP-BFW-feed3	9-8-cw-10	10-8-mu-4	8-0-eg-3	8-1-air-5	8-7-gas-9	8-2-st-1	8-2-BFW-1	8-4-st-10	8-5-BFW-4	8-5-st-12	IP-BFW-Ext3	8-2-st-3	8-9-cw-9
name		GT fuel	extraction air	exhaust gas	HP steam	condensate	LP steam	condensate	IP-BFW-feed3	cooling water	make up water	exhaust gas to stack	GT extraction air	GT fuel	IP steam	IP BFW	LP steam	LP BFW	IP steam	IP-BFW-Ext3	IP steam	cooling water
t	°C	6.407	402.0	588.5	336.2	149.8	164.0	246.0	151.8	20.0	10.0	106.0	177.5	200.0	412.5	157.6	275.8	157.0	264.0	259.7	264.0	29.5
p	bar	516.956	17.40	1.05	139.00	4.80	6.40	38.00	49.60	4.00	20.00	1.05	16.90	32.4	51.00	52.60	6.10	14.00	50.10	50.60	50.10	2.00
m	kg/s	32.4	90.000	653.560	51.167	9.476	5.698	0.087	25.212	7,302	30.514	653.560	90.000	98.611	5.590	76.091	9.476	5.698	0.087	25.212	0.000	7,302
n	kmol/s	1.136	3.119	24.136	2.840	0.526	0.316	0.005	1.399	405.302	1.694	24.136	3.119	6.407	0.310	4.224	0.526	0.316	0.005	1.399	0.000	405.302
V	Nm³/h	98.611	251.691	1,947.543								1,947.543	251.691	516.956								
LHV	kJ/kg	7.139												7.139								
HHV	kJ/kg	8.738												8.738								
h	kJ/kg	-1,630.9	302	-826	-13.336	-15.350	-13.217	-14.915	-15.339	-15.897	-15.938	-1.387	65	-1,505.5	-12.718	-15.314	-12.970	-15.319	-13.188	-14.848	-13.188	-15.858
s	J/kgK	-919.9	0	1	-4	-8	-3	-7	-8	-9	-9	0	0	-635.4	-3	-7	-2	-8	-3	-7	-3	-9
M	kg/kmol	15.38	28.84	27.07	18.00	18.00	18.00	18.00	18.00	18.00	18.00	27.07	28.84	15.38	18.00	18.00	18.00	18.00	18.00	18.00	18.00	18.00
Σ	mol %	100.00	100.00	100.00	100.00	100.00	100.00	100.00	100.00	100.00	100.00	100.00	100.00	100.00	100.00	100.00	100.00	100.00	100.00	100.00	100.00	100.00
H2	mol %	45.01	0.00	0.00	0.00	0.00	0.00	0.00	0.00	0.00	0.00	0.00	0.00	45.01	0.00	0.00	0.00	0.00	0.00	0.00	0.00	0.00
CO	mol %	1.95	0.00	0.00	0.00	0.00	0.00	0.00	0.00	0.00	0.00	0.00	0.00	1.95	0.00	0.00	0.00	0.00	0.00	0.00	0.00	0.00
CO2	mol %	0.25	0.03	0.61	0.00	0.00	0.00	0.00	0.00	0.00	0.00	0.61	0.03	0.25	0.00	0.00	0.00	0.00	0.00	0.00	0.00	0.00
N2	mol %	41.48	77.32	72.62	0.00	0.00	0.00	0.00	0.00	0.00	0.00	72.62	77.32	41.48	0.00	0.00	0.00	0.00	0.00	0.00	0.00	0.00
Ar	mol %	0.59	0.91	0.88	0.00	0.00	0.00	0.00	0.00	0.00	0.00	0.88	0.91	0.59	0.00	0.00	0.00	0.00	0.00	0.00	0.00	0.00
CH4	mol %	0.01	0.00	0.00	0.00	0.00	0.00	0.00	0.00	0.00	0.00	0.00	0.00	0.01	0.00	0.00	0.00	0.00	0.00	0.00	0.00	0.00
O2	mol %	0.30	20.74	10.36	0.00	0.00	0.00	0.00	0.00	0.00	0.00	10.36	20.74	0.30	0.00	0.00	0.00	0.00	0.00	0.00	0.00	0.00
H2O	mol %	10.41	1.01	15.52	100.00	100.00	100.00	100.00	100.00	100.00	100.00	15.52	1.01	10.41	100.00	100.00	100.00	100.00	100.00	100.00	100.00	100.00
H2S	mol %	0.00	0.00	0.00	0.00	0.00	0.00	0.00	0.00	0.00	0.00	0.00	0.00	0.00	0.00	0.00	0.00	0.00	0.00	0.00	0.00	0.00
COS	mol %	0.00	0.00	0.00	0.00	0.00	0.00	0.00	0.00	0.00	0.00	0.00	0.00	0.00	0.00	0.00	0.00	0.00	0.00	0.00	0.00	0.00
CS2	mol %	0.00	0.00	0.00	0.00	0.00	0.00	0.00	0.00	0.00	0.00	0.00	0.00	0.00	0.00	0.00	0.00	0.00	0.00	0.00	0.00	0.00
SO2	mol %	0.00	0.00	0.00	0.00	0.00	0.00	0.00	0.00	0.00	0.00	0.00	0.00	0.00	0.00	0.00	0.00	0.00	0.00	0.00	0.00	0.00
S	mol %	0.00	0.00	0.00	0.00	0.00	0.00	0.00	0.00	0.00	0.00	0.00	0.00	0.00	0.00	0.00	0.00	0.00	0.00	0.00	0.00	0.00
HCN	mol %	0.00	0.00	0.00	0.00	0.00	0.00	0.00	0.00	0.00	0.00	0.00	0.00	0.00	0.00	0.00	0.00	0.00	0.00	0.00	0.00	0.00
NH3	mol %	0.00	0.00	0.00	0.00	0.00	0.00	0.00	0.00	0.00	0.00	0.00	0.00	0.00	0.00	0.00	0.00	0.00	0.00	0.00	0.00	0.00
CH3OH	mol %	0.00	0.00	0.00	0.00	0.00	0.00	0.00	0.00	0.00	0.00	0.00	0.00	0.00	0.00	0.00	0.00	0.00	0.00	0.00	0.00	0.00
Σ	mass %	100.00	100.00	100.00	100.00	100.00	100.00	100.00	100.00	100.00	100.00	100.00	100.00	100.00	100.00	100.00	100.00	100.00	100.00	100.00	100.00	100.00
H2	mass %	5.89	0.00	0.00	0.00	0.00	0.00	0.00	0.00	0.00	0.00	0.00	0.00	5.89	0.00	0.00	0.00	0.00	0.00	0.00	0.00	0.00
CO	mass %	3.54	0.00	0.00	0.00	0.00	0.00	0.00	0.00	0.00	0.00	0.00	0.00	3.54	0.00	0.00	0.00	0.00	0.00	0.00	0.00	0.00
CO2	mass %	0.72	0.05	1.00	0.00	0.00	0.00	0.00	0.00	0.00	0.00	1.00	0.05	0.72	0.00	0.00	0.00	0.00	0.00	0.00	0.00	0.00
N2	mass %	75.50	75.07	75.13	0.00	0.00	0.00	0.00	0.00	0.00	0.00	75.13	75.07	75.50	0.00	0.00	0.00	0.00	0.00	0.00	0.00	0.00
Ar	mass %	1.52	1.26	1.30	0.00	0.00	0.00	0.00	0.00	0.00	0.00	1.30	1.26	1.52	0.00	0.00	0.00	0.00	0.00	0.00	0.00	0.00
CH4	mass %	0.02	0.00	0.00	0.00	0.00	0.00	0.00	0.00	0.00	0.00	0.00	0.00	0.02	0.00	0.00	0.00	0.00	0.00	0.00	0.00	0.00
O2	mass %	0.62	23.00	12.25	0.00	0.00	0.00	0.00	0.00	0.00	0.00	12.25	23.00	0.62	0.00	0.00	0.00	0.00	0.00	0.00	0.00	0.00
H2O	mass %	12.18	0.63	10.33	100.00	100.00	100.00	100.00	100.00	100.00	100.00	10.33	0.63	12.18	100.00	100.00	100.00	100.00	100.00	100.00	100.00	100.00
H2S	mass %	0.00	0.00	0.00	0.00	0.00	0.00	0.00	0.00	0.00	0.00	0.00	0.00	0.00	0.00	0.00	0.00	0.00	0.00	0.00	0.00	0.00
COS	mass %	0.00	0.00	0.00	0.00	0.00	0.00	0.00	0.00	0.00	0.00	0.00	0.00	0.00	0.00	0.00	0.00	0.00	0.00	0.00	0.00	0.00
CS2	mass %	0.00	0.00	0.00	0.00	0.00	0.00	0.00	0.00	0.00	0.00	0.00	0.00	0.00	0.00	0.00	0.00	0.00	0.00	0.00	0.00	0.00
SO2	mass %	0.00	0.00	0.00	0.00	0.00	0.00	0.00	0.00	0.00	0.00	0.00	0.00	0.00	0.00	0.00	0.00	0.00	0.00	0.00	0.00	0.00
S	mass %	0.00	0.00	0.00	0.00	0.00	0.00	0.00	0.00	0.00	0.00	0.00	0.00	0.00	0.00	0.00	0.00	0.00	0.00	0.00	0.00	0.00
HCN	mass %	0.00	0.00	0.00	0.00	0.00	0.00	0.00	0.00	0.00	0.00	0.00	0.00	0.00	0.00	0.00	0.00	0.00	0.00	0.00	0.00	0.00
NH3	mass %	0.00	0.00	0.00	0.00	0.00	0.00	0.00	0.00	0.00	0.00	0.00	0.00	0.00	0.00	0.00	0.00	0.00	0.00	0.00	0.00	0.00
CH3OH	mass %	0.00	0.00	0.00	0.00	0.00	0.00	0.00	0.00	0.00	0.00	0.00	0.00	0.00	0.00	0.00	0.00	0.00	0.00	0.00	0.00	0.00

Appendix F4 – CHEMCAD model of the water-/steam cycle for the CC-IGCC / Siemens gasifier

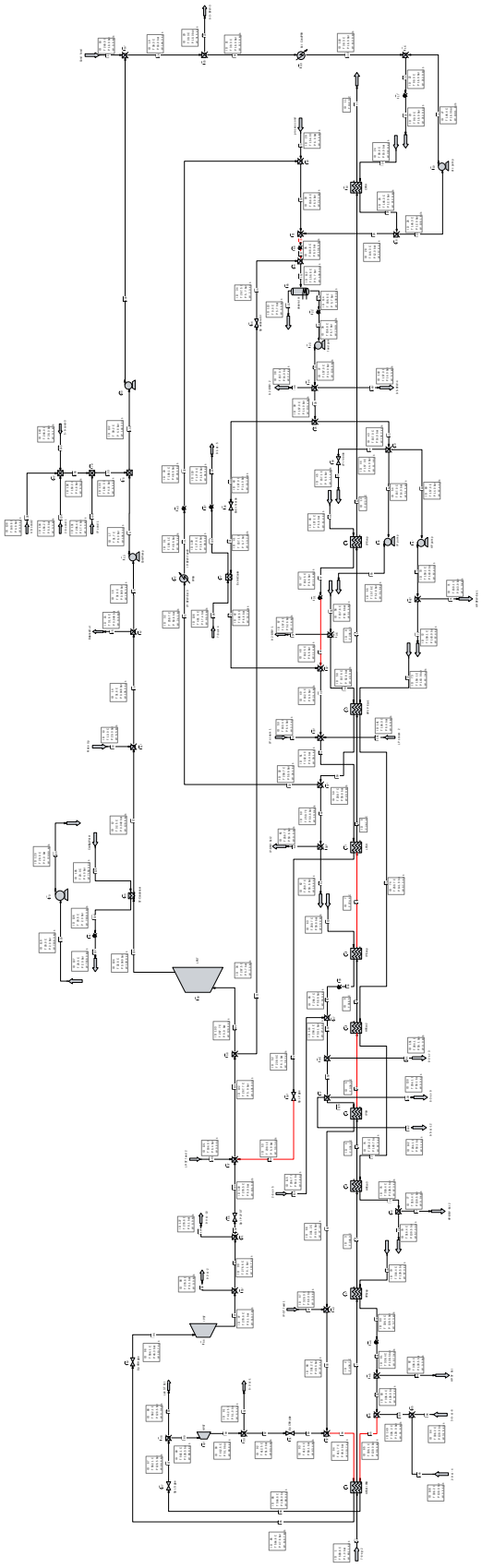

Appendix F5 – Heat and material balance for the water-/steam cycle (CC-IGCC / Siemens gasifier)

stream ID		3-8-gas-5	7-8-air-4	7-8-eg-2	2-8-st-5	2-8-st-6	3-8-st-8	4-8-cond-2	5-8-st-11	5-8-cond-3	9-8-cw-10	10-8-mu-4	8-0-eg-3	8-1-air-5	8-7-gas-9	8-2-st-1	8-2-BFW-1	8-2-BFW-2	8-3-BFW-3	8-4-st-10	8-5-BFW-4	8-5-st-12	8-9-cw-9
name		GT fuel	extraction air	exhaust gas	IP steam	LP steam	HP steam	condensate	LP steam	condensate	cooling water	make up water	exhaust gas to stack	GT extraction air	GT fuel	IP steam	IP BFW	LP BFW	BFW	LP steam	LP BFW	IP steam	cooling water
t	°C	144.1	401.6	589.6	264.7	163.4	336.2	149.8	164.0	246.0	20.0	10.0	102.9	177.5	200.0	412.5	157.6	157.0	39.3	276.6	157.0	264.1	29.5
p	bar	32.4	17.37	1.05	50.10	6.40	139.00	4.80	6.40	38.00	4.00	20.00	1.05	16.87	32.4	51.00	52.60	14.00	18.00	6.10	14.00	50.10	2.00
m	kg/s	97.461	90.000	651.059	7.599	2.681	31.505	8.903	5.853	0.085	7,159	5.480	651.059	90.000	97.461	5.479	7.599	2.681	31.505	8.903	5.853	0.085	7,159
n	kmol/s	6.419	3.119	24.101	0.422	0.149	1.749	0.494	0.325	0.005	397.393	0.304	24.101	3.119	6.419	0.304	0.422	0.149	1.749	0.494	0.325	0.005	397.393
V	Nm³/h	517.979	251.691	1,944.689									1,944.689	251.691	517.979								
LHV	kJ/kg	7.169													7.169								
HHV	kJ/kg	8.850													8.850								
h	kJ/kg	-1.965.8	302	-878	-13,185	-13,218	-13,336	-15,350	-13,217	-14,915	-15,897	-15,938	-1,447	65	-1,852.4	-12,715	-15,314	-15,319	-15,815	-12,968	-15,319	-13,187	-15,858
s	J/kgK	-958.8	0.18	1.16	-3.43	-2.66	-4.02	-7.57	-2.66	-6.65	-9.12	-9.26	0.20	-0.23	-703.8	-2.71	-7.50	-7.50	-8.85	-2.13	-7.50	-3.44	-8.98
M	kg/kmol	15.17	28.84	27.00	18.00	18.00	18.00	18.00	18.00	18.00	18.00	18.00	27.00	28.84	15.17	18.00	18.00	18.00	18.00	18.00	18.00	18.00	18.00
Σ	mol %	100.00	100.00	100.00	100.00	100.00	100.00	100.00	100.00	100.00	100.00	100.00	100.00	100.00	100.00	100.00	100.00	100.00	100.00	100.00	100.00	100.00	100.00
H2	mol %	45.00	0.00	0.00	0.00	0.00	0.00	0.00	0.00	0.00	0.00	0.00	0.00	0.00	45.00	0.00	0.00	0.00	0.00	0.00	0.00	0.00	0.00
CO	mol %	1.91	0.00	0.00	0.00	0.00	0.00	0.00	0.00	0.00	0.00	0.00	0.00	0.00	1.91	0.00	0.00	0.00	0.00	0.00	0.00	0.00	0.00
CO2	mol %	0.25	0.03	0.61	0.00	0.00	0.00	0.00	0.00	0.00	0.00	0.00	0.61	0.03	0.25	0.00	0.00	0.00	0.00	0.00	0.00	0.00	0.00
N2	mol %	39.56	77.32	72.09	0.00	0.00	0.00	0.00	0.00	0.00	0.00	0.00	72.09	77.32	39.56	0.00	0.00	0.00	0.00	0.00	0.00	0.00	0.00
Ar	mol %	0.56	0.91	0.87	0.00	0.00	0.00	0.00	0.00	0.00	0.00	0.00	0.87	0.91	0.56	0.00	0.00	0.00	0.00	0.00	0.00	0.00	0.00
CH4	mol %	0.02	0.00	0.00	0.00	0.00	0.00	0.00	0.00	0.00	0.00	0.00	0.00	0.00	0.02	0.00	0.00	0.00	0.00	0.00	0.00	0.00	0.00
O2	mol %	0.22	20.74	10.31	0.00	0.00	0.00	0.00	0.00	0.00	0.00	0.00	10.31	20.74	0.22	0.00	0.00	0.00	0.00	0.00	0.00	0.00	0.00
H2O	mol %	12.48	1.01	16.12	100.00	100.00	100.00	100.00	100.00	100.00	100.00	100.00	16.12	1.01	12.48	100.00	100.00	100.00	100.00	100.00	100.00	100.00	100.00
H2S	mol %	0.00	0.00	0.00	0.00	0.00	0.00	0.00	0.00	0.00	0.00	0.00	0.00	0.00	0.00	0.00	0.00	0.00	0.00	0.00	0.00	0.00	0.00
COS	mol %	0.00	0.00	0.00	0.00	0.00	0.00	0.00	0.00	0.00	0.00	0.00	0.00	0.00	0.00	0.00	0.00	0.00	0.00	0.00	0.00	0.00	0.00
CS2	mol %	0.00	0.00	0.00	0.00	0.00	0.00	0.00	0.00	0.00	0.00	0.00	0.00	0.00	0.00	0.00	0.00	0.00	0.00	0.00	0.00	0.00	0.00
SO2	mol %	0.00	0.00	0.00	0.00	0.00	0.00	0.00	0.00	0.00	0.00	0.00	0.00	0.00	0.00	0.00	0.00	0.00	0.00	0.00	0.00	0.00	0.00
S	mol %	0.00	0.00	0.00	0.00	0.00	0.00	0.00	0.00	0.00	0.00	0.00	0.00	0.00	0.00	0.00	0.00	0.00	0.00	0.00	0.00	0.00	0.00
HCN	mol %	0.00	0.00	0.00	0.00	0.00	0.00	0.00	0.00	0.00	0.00	0.00	0.00	0.00	0.00	0.00	0.00	0.00	0.00	0.00	0.00	0.00	0.00
NH3	mol %	0.00	0.00	0.00	0.00	0.00	0.00	0.00	0.00	0.00	0.00	0.00	0.00	0.00	0.00	0.00	0.00	0.00	0.00	0.00	0.00	0.00	0.00
CH3OH	mol %	0.00	0.00	0.00	0.00	0.00	0.00	0.00	0.00	0.00	0.00	0.00	0.00	0.00	0.00	0.00	0.00	0.00	0.00	0.00	0.00	0.00	0.00
Σ	mass %	100.00	100.00	100.00	100.00	100.00	100.00	100.00	100.00	100.00	100.00	100.00	100.00	100.00	100.00	100.00	100.00	100.00	100.00	100.00	100.00	100.00	100.00
H2	mass %	5.97	0.00	0.00	0.00	0.00	0.00	0.00	0.00	0.00	0.00	0.00	0.00	0.00	5.97	0.00	0.00	0.00	0.00	0.00	0.00	0.00	0.00
CO	mass %	3.52	0.00	0.00	0.00	0.00	0.00	0.00	0.00	0.00	0.00	0.00	0.00	0.00	3.52	0.00	0.00	0.00	0.00	0.00	0.00	0.00	0.00
CO2	mass %	0.72	0.05	0.99	0.00	0.00	0.00	0.00	0.00	0.00	0.00	0.00	0.99	0.05	0.72	0.00	0.00	0.00	0.00	0.00	0.00	0.00	0.00
N2	mass %	73.01	75.07	74.76	0.00	0.00	0.00	0.00	0.00	0.00	0.00	0.00	74.76	75.07	73.01	0.00	0.00	0.00	0.00	0.00	0.00	0.00	0.00
Ar	mass %	1.48	1.26	1.29	0.00	0.00	0.00	0.00	0.00	0.00	0.00	0.00	1.29	1.26	1.48	0.00	0.00	0.00	0.00	0.00	0.00	0.00	0.00
CH4	mass %	0.02	0.00	0.00	0.00	0.00	0.00	0.00	0.00	0.00	0.00	0.00	0.00	0.00	0.02	0.00	0.00	0.00	0.00	0.00	0.00	0.00	0.00
O2	mass %	0.47	23.00	12.21	0.00	0.00	0.00	0.00	0.00	0.00	0.00	0.00	12.21	23.00	0.47	0.00	0.00	0.00	0.00	0.00	0.00	0.00	0.00
H2O	mass %	14.81	0.63	10.75	100.00	100.00	100.00	100.00	100.00	100.00	100.00	100.00	10.75	0.63	14.81	100.00	100.00	100.00	100.00	100.00	100.00	100.00	100.00
H2S	mass %	0.00	0.00	0.00	0.00	0.00	0.00	0.00	0.00	0.00	0.00	0.00	0.00	0.00	0.00	0.00	0.00	0.00	0.00	0.00	0.00	0.00	0.00
COS	mass %	0.00	0.00	0.00	0.00	0.00	0.00	0.00	0.00	0.00	0.00	0.00	0.00	0.00	0.00	0.00	0.00	0.00	0.00	0.00	0.00	0.00	0.00
CS2	mass %	0.00	0.00	0.00	0.00	0.00	0.00	0.00	0.00	0.00	0.00	0.00	0.00	0.00	0.00	0.00	0.00	0.00	0.00	0.00	0.00	0.00	0.00
SO2	mass %	0.00	0.00	0.00	0.00	0.00	0.00	0.00	0.00	0.00	0.00	0.00	0.00	0.00	0.00	0.00	0.00	0.00	0.00	0.00	0.00	0.00	0.00
S	mass %	0.00	0.00	0.00	0.00	0.00	0.00	0.00	0.00	0.00	0.00	0.00	0.00	0.00	0.00	0.00	0.00	0.00	0.00	0.00	0.00	0.00	0.00
HCN	mass %	0.00	0.00	0.00	0.00	0.00	0.00	0.00	0.00	0.00	0.00	0.00	0.00	0.00	0.00	0.00	0.00	0.00	0.00	0.00	0.00	0.00	0.00
NH3	mass %	0.00	0.00	0.00	0.00	0.00	0.00	0.00	0.00	0.00	0.00	0.00	0.00	0.00	0.00	0.00	0.00	0.00	0.00	0.00	0.00	0.00	0.00
CH3OH	mass %	0.00	0.00	0.00	0.00	0.00	0.00	0.00	0.00	0.00	0.00	0.00	0.00	0.00	0.00	0.00	0.00	0.00	0.00	0.00	0.00	0.00	0.00

Appendix F6 – CHEMCAD model of the water-/steam cycle for the CC-IGCC / CoP gasifier

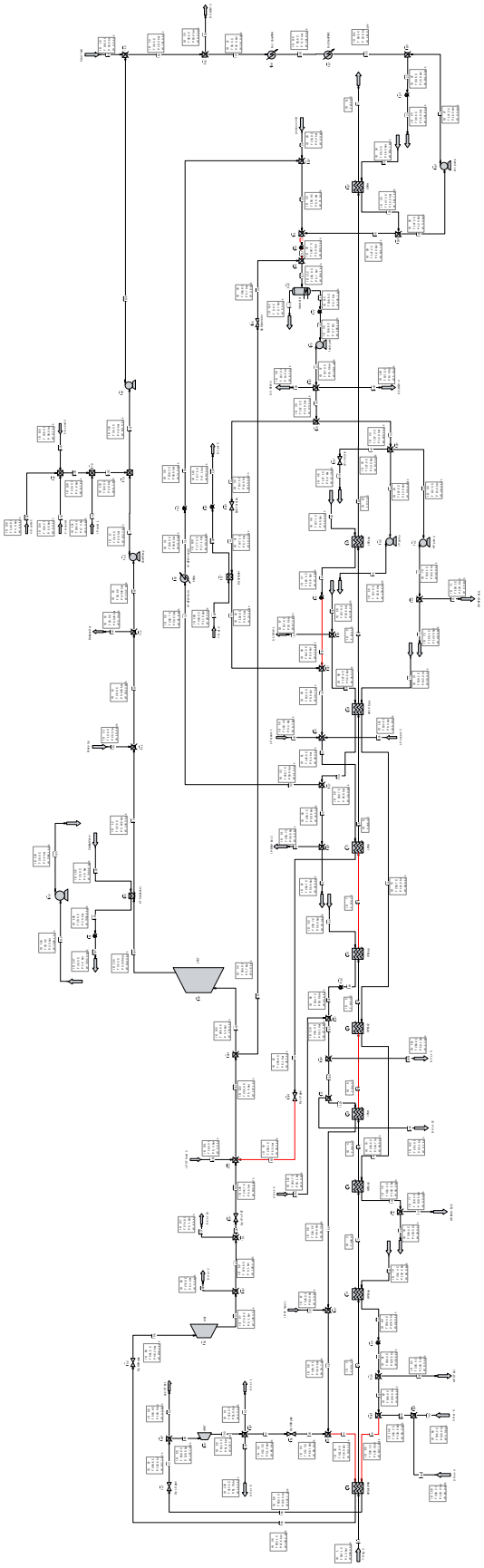

Appendix F7– Heat and material balance for the water-/steam cycle (CC-IGCC / CoP gasifier)

stream ID		3-8-gas-5	7-8-air-4	7-8-eg-2	2-8-st-5	2-8-st-6	2-8-st-4	4-8-cond-2	5-8-st-11	5-8-cond-3	IP-BFW-feed3	9-8-cw-10	10-8-mu-4	8-0-eg-3	8-1-air-5	8-?-gas-9	8-2-BFW-1	8-2-BFW-2	8-3-st-9	8-4-st-10	8-5-BFW-4	8-5-st-12	IP-BFW-Ex3	8-2-st-3	8-9-cw-9
name		GT fuel	extraction air	exhaust gas	IP steam	LP steam	HP steam	condensate	LP steam	condensate	cooling water	cooling water	make up water	exhaust gas to stack	GT extraction air	GT fuel	IP BFW	LP BFW	IP steam	LP steam	LP BFW	IP steam	IP-BFW-Ex3	IP steam	cooling water
t	°C	143.3	404.3	587.1	264.7	163.4	336.2	149.8	164.0	246.0	158.3	20.0	10.0	119.9	177.5	200.0	157.6	157.0	412.5	274.8	157.0	264.0	259.7	264.0	29.5
p	bar	32.4	17.60	1.05	50.10	6.40	139.00	4.80	6.40	38.00	49.60	4.00	20.00	1.05	17.10	32.4	52.60	14.00	51.00	6.10	14.00	50.10	50.60	50.10	2.00
m	kg/s	84.2	90.000	669.363	0.000	6.749	58.507	8.576	5.814	0.089	21.570	7.385	18.899	669.363	90.000	84.215	56.826	6.749	18.899	8.576	5.814	0.089	21.570	1.681	7.385
n	kmol/s	5.7	3.119	24.616	0.000	0.375	3.248	0.476	0.323	0.005	1.197	409.942	1.049	24.616	3.119	5.651	3.154	0.375	1.049	0.476	0.323	0.005	1.197	0.093	409.942
V	Nm³/h	455.946	251.691	1,986.251										1,986.251	251.691	455.946									
LHV	kJ/kg	8,483														8,483									
HHV	kJ/kg	10,334														10,334									
h	kJ/kg	-2,093.7	305	-838	-13,185	-13,218	-13,336	-15,350	-13,217	-14,915	-15,311	-15,897	-15,938	-1,381	65	-1,975.2	-15,314	-15,319	-12,721	-12,972	-15,319	-13,188	-14,848	-13,188	-15,858
s	J/kgK	-1,084.5	0	1	-3	-3	-4	-8	-3	-7	-7	-9	-9	0	0	-817.8	-7	-8	-3	-2	-8	-3	-7	-3	-9
M	kg/kmol	14.89	28.84	27.18	18.00	18.00	18.00	18.00	18.00	18.00	18.00	18.00	18.00	27.18	28.84	14.89	18.00	18.00	18.00	18.00	18.00	18.00	18.00	18.00	18.00
Σ	mol %	100.00	100.00	100.00	100.00	100.00	100.00	100.00	100.00	100.00	100.00	100.00	100.00	100.00	100.00	100.00	100.00	100.00	100.00	100.00	100.00	100.00	100.00	100.00	100.00
H2	mol %	45.00	0.00	0.00	0.00	0.00	0.00	0.00	0.00	0.00	0.00	0.00	0.00	0.00	0.00	45.00	0.00	0.00	0.00	0.00	0.00	0.00	0.00	0.00	0.00
CO	mol %	1.54	0.00	0.00	0.00	0.00	0.00	0.00	0.00	0.00	0.00	0.00	0.00	0.00	0.00	1.54	0.00	0.00	0.00	0.00	0.00	0.00	0.00	0.00	0.00
CO2	mol %	0.26	0.03	0.98	0.00	0.00	0.00	0.00	0.00	0.00	0.00	0.00	0.00	0.98	0.03	0.26	0.00	0.00	0.00	0.00	0.00	0.00	0.00	0.00	0.00
N2	mol %	37.70	77.32	72.35	0.00	0.00	0.00	0.00	0.00	0.00	0.00	0.00	0.00	72.35	77.32	37.70	0.00	0.00	0.00	0.00	0.00	0.00	0.00	0.00	0.00
Ar	mol %	0.61	0.91	0.89	0.00	0.00	0.00	0.00	0.00	0.00	0.00	0.00	0.00	0.89	0.91	0.61	0.00	0.00	0.00	0.00	0.00	0.00	0.00	0.00	0.00
CH4	mol %	2.34	0.00	0.00	0.00	0.00	0.00	0.00	0.00	0.00	0.00	0.00	0.00	0.00	0.00	2.34	0.00	0.00	0.00	0.00	0.00	0.00	0.00	0.00	0.00
O2	mol %	0.08	20.74	10.69	0.00	0.00	0.00	0.00	0.00	0.00	0.00	0.00	0.00	10.69	20.74	0.08	0.00	0.00	0.00	0.00	0.00	0.00	0.00	0.00	0.00
H2O	mol %	12.48	1.01	15.10	100.00	100.00	100.00	100.00	100.00	100.00	100.00	100.00	100.00	15.10	1.01	12.48	100.00	100.00	100.00	100.00	100.00	100.00	100.00	100.00	100.00
H2S	mol %	0.00	0.00	0.00	0.00	0.00	0.00	0.00	0.00	0.00	0.00	0.00	0.00	0.00	0.00	0.00	0.00	0.00	0.00	0.00	0.00	0.00	0.00	0.00	0.00
COS	mol %	0.00	0.00	0.00	0.00	0.00	0.00	0.00	0.00	0.00	0.00	0.00	0.00	0.00	0.00	0.00	0.00	0.00	0.00	0.00	0.00	0.00	0.00	0.00	0.00
CS2	mol %	0.00	0.00	0.00	0.00	0.00	0.00	0.00	0.00	0.00	0.00	0.00	0.00	0.00	0.00	0.00	0.00	0.00	0.00	0.00	0.00	0.00	0.00	0.00	0.00
SO2	mol %	0.00	0.00	0.00	0.00	0.00	0.00	0.00	0.00	0.00	0.00	0.00	0.00	0.00	0.00	0.00	0.00	0.00	0.00	0.00	0.00	0.00	0.00	0.00	0.00
S	mol %	0.00	0.00	0.00	0.00	0.00	0.00	0.00	0.00	0.00	0.00	0.00	0.00	0.00	0.00	0.00	0.00	0.00	0.00	0.00	0.00	0.00	0.00	0.00	0.00
HCN	mol %	0.00	0.00	0.00	0.00	0.00	0.00	0.00	0.00	0.00	0.00	0.00	0.00	0.00	0.00	0.00	0.00	0.00	0.00	0.00	0.00	0.00	0.00	0.00	0.00
NH3	mol %	0.00	0.00	0.00	0.00	0.00	0.00	0.00	0.00	0.00	0.00	0.00	0.00	0.00	0.00	0.00	0.00	0.00	0.00	0.00	0.00	0.00	0.00	0.00	0.00
CH3OH	mol %	0.00	0.00	0.00	0.00	0.00	0.00	0.00	0.00	0.00	0.00	0.00	0.00	0.00	0.00	0.00	0.00	0.00	0.00	0.00	0.00	0.00	0.00	0.00	0.00
Σ	mass %	100.00	100.00	100.00	100.00	100.00	100.00	100.00	100.00	100.00	100.00	100.00	100.00	100.00	100.00	100.00	100.00	100.00	100.00	100.00	100.00	100.00	100.00	100.00	100.00
H2	mass %	6.09	0.00	0.00	0.00	0.00	0.00	0.00	0.00	0.00	0.00	0.00	0.00	0.00	0.00	6.09	0.00	0.00	0.00	0.00	0.00	0.00	0.00	0.00	0.00
CO	mass %	2.90	0.00	0.00	0.00	0.00	0.00	0.00	0.00	0.00	0.00	0.00	0.00	0.00	0.00	2.90	0.00	0.00	0.00	0.00	0.00	0.00	0.00	0.00	0.00
CO2	mass %	0.76	0.05	1.58	0.00	0.00	0.00	0.00	0.00	0.00	0.00	0.00	0.00	1.58	0.05	0.76	0.00	0.00	0.00	0.00	0.00	0.00	0.00	0.00	0.00
N2	mass %	70.86	75.07	74.54	0.00	0.00	0.00	0.00	0.00	0.00	0.00	0.00	0.00	74.54	75.07	70.86	0.00	0.00	0.00	0.00	0.00	0.00	0.00	0.00	0.00
Ar	mass %	1.62	1.26	1.30	0.00	0.00	0.00	0.00	0.00	0.00	0.00	0.00	0.00	1.30	1.26	1.62	0.00	0.00	0.00	0.00	0.00	0.00	0.00	0.00	0.00
CH4	mass %	2.51	0.00	0.01	0.00	0.00	0.00	0.00	0.00	0.00	0.00	0.00	0.00	0.01	0.00	2.51	0.00	0.00	0.00	0.00	0.00	0.00	0.00	0.00	0.00
O2	mass %	0.17	23.00	12.58	0.00	0.00	0.00	0.00	0.00	0.00	0.00	0.00	0.00	12.58	23.00	0.17	0.00	0.00	0.00	0.00	0.00	0.00	0.00	0.00	0.00
H2O	mass %	15.08	0.63	10.00	100.00	100.00	100.00	100.00	100.00	100.00	100.00	100.00	100.00	10.00	0.63	15.08	100.00	100.00	100.00	100.00	100.00	100.00	100.00	100.00	100.00
H2S	mass %	0.00	0.00	0.00	0.00	0.00	0.00	0.00	0.00	0.00	0.00	0.00	0.00	0.00	0.00	0.00	0.00	0.00	0.00	0.00	0.00	0.00	0.00	0.00	0.00
COS	mass %	0.00	0.00	0.00	0.00	0.00	0.00	0.00	0.00	0.00	0.00	0.00	0.00	0.00	0.00	0.00	0.00	0.00	0.00	0.00	0.00	0.00	0.00	0.00	0.00
CS2	mass %	0.00	0.00	0.00	0.00	0.00	0.00	0.00	0.00	0.00	0.00	0.00	0.00	0.00	0.00	0.00	0.00	0.00	0.00	0.00	0.00	0.00	0.00	0.00	0.00
SO2	mass %	0.00	0.00	0.00	0.00	0.00	0.00	0.00	0.00	0.00	0.00	0.00	0.00	0.00	0.00	0.00	0.00	0.00	0.00	0.00	0.00	0.00	0.00	0.00	0.00
S	mass %	0.00	0.00	0.00	0.00	0.00	0.00	0.00	0.00	0.00	0.00	0.00	0.00	0.00	0.00	0.00	0.00	0.00	0.00	0.00	0.00	0.00	0.00	0.00	0.00
HCN	mass %	0.00	0.00	0.00	0.00	0.00	0.00	0.00	0.00	0.00	0.00	0.00	0.00	0.00	0.00	0.00	0.00	0.00	0.00	0.00	0.00	0.00	0.00	0.00	0.00
NH3	mass %	0.00	0.00	0.00	0.00	0.00	0.00	0.00	0.00	0.00	0.00	0.00	0.00	0.00	0.00	0.00	0.00	0.00	0.00	0.00	0.00	0.00	0.00	0.00	0.00
CH3OH	mass %	0.00	0.00	0.00	0.00	0.00	0.00	0.00	0.00	0.00	0.00	0.00	0.00	0.00	0.00	0.00	0.00	0.00	0.00	0.00	0.00	0.00	0.00	0.00	0.00

Appendix F8 – CHEMCAD model of the water-/steam cycle for the CC-IGCC / GE-R

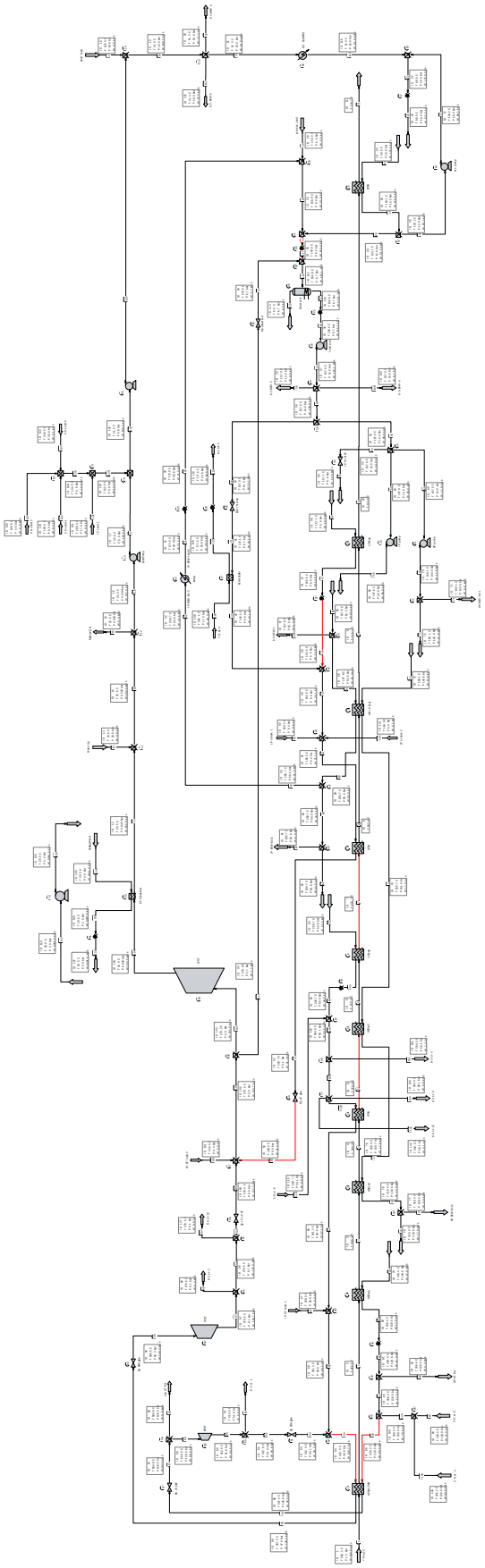

Appendix F9 – Heat and material balance for the water-/steam cycle (CC-IGCC / GE-R)

stream ID		3-8-gas-5	7-8-air-4	7-8-eg-2	2-8-cond-1	3-8-st-8	2-8-st-4	4-8-cond-2	5-8-st-11	5-8-cond-3	IP-BFW-feed3	9-8-cw-10	8-0-eg-3	8-1-air-5	8-7-gas-9	8-2-st-2	8-3-BFW-3	8-4-st-10	8-5-BFW-4	8-5-st-12	IP-BFW-Ext3	8-2-st-3	8-9-cw-9
name		GT fuel	extraction air	exhaust gas	condensate	HP steam	HP steam	condensate	LP steam	condensate	IP-BFW-feed3	cooling water	exhaust gas to stack	GT extraction air	GT fuel	LP steam	BFW	LP steam	LP BFW	IP steam	IP-BFW-Ext3	IP steam	cooling water
t	°C	6.380	401.1	592.3	100.0	336.2	336.2	149.8	164.0	246.0	172.0	20.0	118.7	177.5	200.0	278.5	41.3	278.5	157.0	264.0	259.7	264.0	41.3
p	bar	514.763	17.31	1.05	6.00	139.00	139.00	4.80	6.40	38.00	49.60	4.00	1.05	16.81	32.4	6.10	18.00	6.10	14.00	50.10	50.60	50.10	18.00
m	kg/s	32.4	90.000	646.849	5.408	27.151	49.473	8.810	6.118	0.111	21.593	8,392	646.849	90.000	93.550	5.408	27.151	8.810	6.118	0.111	21.593	2.213	47.261
n	kmol/s	157.0	3.119	24.058	0.300	1.507	2.746	0.489	0.340	0.006	1.194	465.807	24.058	3.119	6.380	0.300	1.507	0.489	0.340	0.006	1.194	0.123	2.623
V	Nm³/h	93.550	251.691	1,941.230									1,941.230	251.691	514.763								
LHV	kJ/kg	7.345													7.345								
HHV	kJ/kg	9.247													9.247								
h	kJ/kg	-2,866.8	301	-1,005	-15,562	-13,336	-13,336	-15,350	-13,217	-14,915	-15,251	-15,897	-1,564	65	-2,774.1	-12,964	-15,807	-12,964	-15,319	-13,188	-14,848	-13,188	-618
s	J/kgK	-1,082.9	0	1	-8	-4	-4	-8	-3	-7	-7	-9	0	0	-877.6	-2	-9	-2	-8	-3	-7	-3	-9
M	kg/kmol	14.65	28.84	26.88	18.00	18.00	18.00	18.00	18.00	18.00	18.00	18.00	26.88	28.84	14.65	18.00	18.00	18.00	18.00	18.00	18.00	18.00	18.00
Σ	mol %	100.00	100.00	100.00	100.00	100.00	100.00	100.00	100.00	100.00	100.00	100.00	100.00	100.00	100.00	100.00	100.00	100.00	100.00	100.00	100.00	100.00	100.00
H2	mol %	0.00	0.00	0.00	0.00	0.00	0.00	0.00	0.00	0.00	0.00	0.00	0.00	0.00	1.96	0.00	0.00	0.00	0.00	0.00	0.00	0.00	0.00
CO	mol %	1.96	0.00	0.00	0.00	0.00	0.00	0.00	0.00	0.00	0.00	0.00	0.00	0.00	1.96	0.00	0.00	0.00	0.00	0.00	0.00	0.00	0.00
CO2	mol %	0.25	0.03	0.65	0.00	0.00	0.00	0.00	0.00	0.00	0.00	0.00	0.65	0.03	0.25	0.00	0.00	0.00	0.00	0.00	0.00	0.00	0.00
N2	mol %	34.27	77.32	70.71	0.00	0.00	0.00	0.00	0.00	0.00	0.00	0.00	70.71	77.32	34.27	0.00	0.00	0.00	0.00	0.00	0.00	0.00	0.00
Ar	mol %	0.71	0.91	0.91	0.00	0.00	0.00	0.00	0.00	0.00	0.00	0.00	0.91	0.91	0.71	0.00	0.00	0.00	0.00	0.00	0.00	0.00	0.00
CH4	mol %	0.13	0.00	0.00	0.00	0.00	0.00	0.00	0.00	0.00	0.00	0.00	0.00	0.00	0.13	0.00	0.00	0.00	0.00	0.00	0.00	0.00	0.00
O2	mol %	0.07	20.74	10.25	0.00	0.00	0.00	0.00	0.00	0.00	0.00	0.00	10.25	20.74	0.07	0.00	0.00	0.00	0.00	0.00	0.00	0.00	0.00
H2O	mol %	17.61	1.01	17.48	100.00	100.00	100.00	100.00	100.00	100.00	100.00	100.00	17.48	1.01	17.61	100.00	100.00	100.00	100.00	100.00	100.00	100.00	100.00
H2S	mol %	0.00	0.00	0.00	0.00	0.00	0.00	0.00	0.00	0.00	0.00	0.00	0.00	0.00	0.00	0.00	0.00	0.00	0.00	0.00	0.00	0.00	0.00
COS	mol %	0.00	0.00	0.00	0.00	0.00	0.00	0.00	0.00	0.00	0.00	0.00	0.00	0.00	0.00	0.00	0.00	0.00	0.00	0.00	0.00	0.00	0.00
CS2	mol %	0.00	0.00	0.00	0.00	0.00	0.00	0.00	0.00	0.00	0.00	0.00	0.00	0.00	0.00	0.00	0.00	0.00	0.00	0.00	0.00	0.00	0.00
SO2	mol %	0.00	0.00	0.00	0.00	0.00	0.00	0.00	0.00	0.00	0.00	0.00	0.00	0.00	0.00	0.00	0.00	0.00	0.00	0.00	0.00	0.00	0.00
S	mol %	0.00	0.00	0.00	0.00	0.00	0.00	0.00	0.00	0.00	0.00	0.00	0.00	0.00	0.00	0.00	0.00	0.00	0.00	0.00	0.00	0.00	0.00
HCN	mol %	0.00	0.00	0.00	0.00	0.00	0.00	0.00	0.00	0.00	0.00	0.00	0.00	0.00	0.00	0.00	0.00	0.00	0.00	0.00	0.00	0.00	0.00
NH3	mol %	0.00	0.00	0.00	0.00	0.00	0.00	0.00	0.00	0.00	0.00	0.00	0.00	0.00	0.00	0.00	0.00	0.00	0.00	0.00	0.00	0.00	0.00
CH3OH	mol %	0.00	0.00	0.00	0.00	0.00	0.00	0.00	0.00	0.00	0.00	0.00	0.00	0.00	0.00	0.00	0.00	0.00	0.00	0.00	0.00	0.00	0.00
Σ	mass %	100.00	100.00	100.00	100.00	100.00	100.00	100.00	100.00	100.00	100.00	100.00	100.00	100.00	100.00	100.00	100.00	100.00	100.00	100.00	100.00	100.00	100.00
H2	mass %	6.19	0.00	0.00	0.00	0.00	0.00	0.00	0.00	0.00	0.00	0.00	0.00	0.00	6.19	0.00	0.00	0.00	0.00	0.00	0.00	0.00	0.00
CO	mass %	3.75	0.00	0.00	0.00	0.00	0.00	0.00	0.00	0.00	0.00	0.00	0.00	0.00	3.75	0.00	0.00	0.00	0.00	0.00	0.00	0.00	0.00
CO2	mass %	0.74	0.05	1.06	0.00	0.00	0.00	0.00	0.00	0.00	0.00	0.00	1.06	0.05	0.74	0.00	0.00	0.00	0.00	0.00	0.00	0.00	0.00
N2	mass %	65.46	75.07	73.68	0.00	0.00	0.00	0.00	0.00	0.00	0.00	0.00	73.68	75.07	65.46	0.00	0.00	0.00	0.00	0.00	0.00	0.00	0.00
Ar	mass %	1.93	1.26	1.35	0.00	0.00	0.00	0.00	0.00	0.00	0.00	0.00	1.35	1.26	1.93	0.00	0.00	0.00	0.00	0.00	0.00	0.00	0.00
CH4	mass %	0.15	0.00	0.00	0.00	0.00	0.00	0.00	0.00	0.00	0.00	0.00	0.00	0.00	0.15	0.00	0.00	0.00	0.00	0.00	0.00	0.00	0.00
O2	mass %	0.14	23.00	12.19	0.00	0.00	0.00	0.00	0.00	0.00	0.00	0.00	12.19	23.00	0.14	0.00	0.00	0.00	0.00	0.00	0.00	0.00	0.00
H2O	mass %	21.63	0.63	11.71	100.00	100.00	100.00	100.00	100.00	100.00	100.00	100.00	11.71	0.63	21.63	100.00	100.00	100.00	100.00	100.00	100.00	100.00	100.00
H2S	mass %	0.00	0.00	0.00	0.00	0.00	0.00	0.00	0.00	0.00	0.00	0.00	0.00	0.00	0.00	0.00	0.00	0.00	0.00	0.00	0.00	0.00	0.00
COS	mass %	0.00	0.00	0.00	0.00	0.00	0.00	0.00	0.00	0.00	0.00	0.00	0.00	0.00	0.00	0.00	0.00	0.00	0.00	0.00	0.00	0.00	0.00
CS2	mass %	0.00	0.00	0.00	0.00	0.00	0.00	0.00	0.00	0.00	0.00	0.00	0.00	0.00	0.00	0.00	0.00	0.00	0.00	0.00	0.00	0.00	0.00
SO2	mass %	0.00	0.00	0.00	0.00	0.00	0.00	0.00	0.00	0.00	0.00	0.00	0.00	0.00	0.00	0.00	0.00	0.00	0.00	0.00	0.00	0.00	0.00
S	mass %	0.00	0.00	0.00	0.00	0.00	0.00	0.00	0.00	0.00	0.00	0.00	0.00	0.00	0.00	0.00	0.00	0.00	0.00	0.00	0.00	0.00	0.00
HCN	mass %	0.00	0.00	0.00	0.00	0.00	0.00	0.00	0.00	0.00	0.00	0.00	0.00	0.00	0.00	0.00	0.00	0.00	0.00	0.00	0.00	0.00	0.00
NH3	mass %	0.00	0.00	0.00	0.00	0.00	0.00	0.00	0.00	0.00	0.00	0.00	0.00	0.00	0.00	0.00	0.00	0.00	0.00	0.00	0.00	0.00	0.00
CH3OH	mass %	0.01	0.00	0.00	0.00	0.00	0.00	0.00	0.00	0.00	0.00	0.00	0.00	0.00	0.01	0.00	0.00	0.00	0.00	0.00	0.00	0.00	0.00

Appendix G1 – Process flow diagram of the elevated pressure ASU

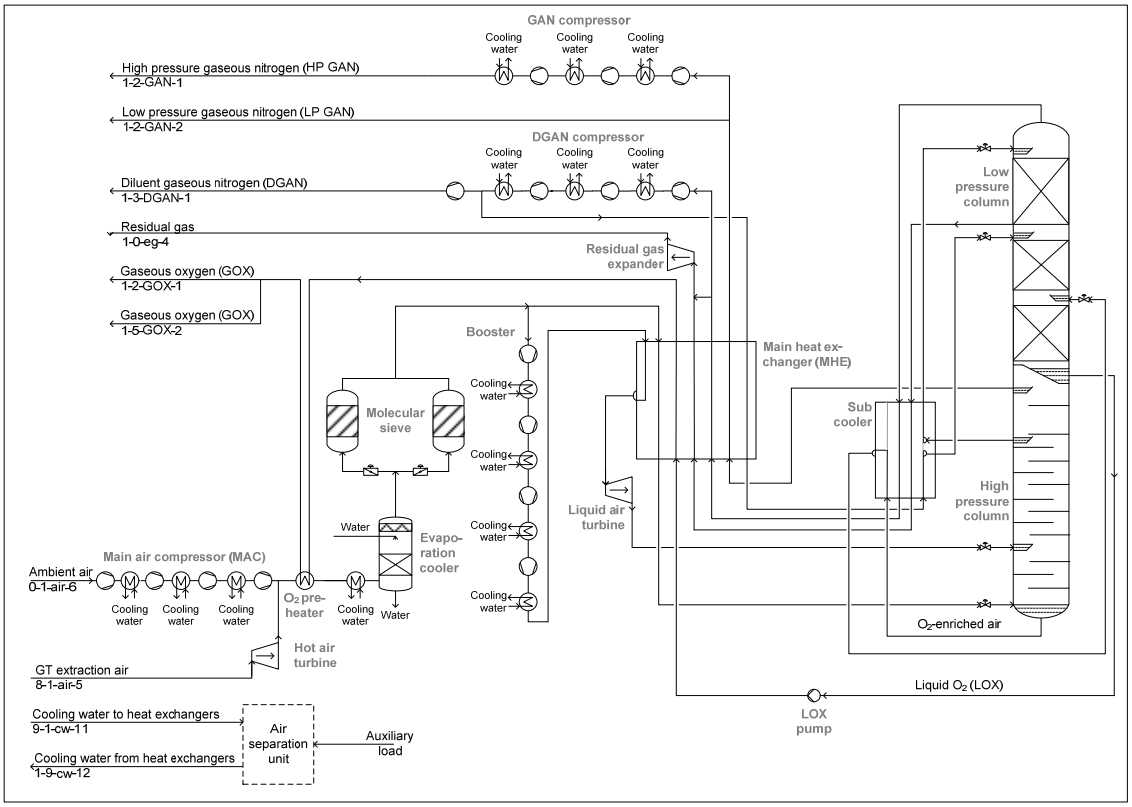

Appendix G2 – CHEMCAD model for a low pressure ASU

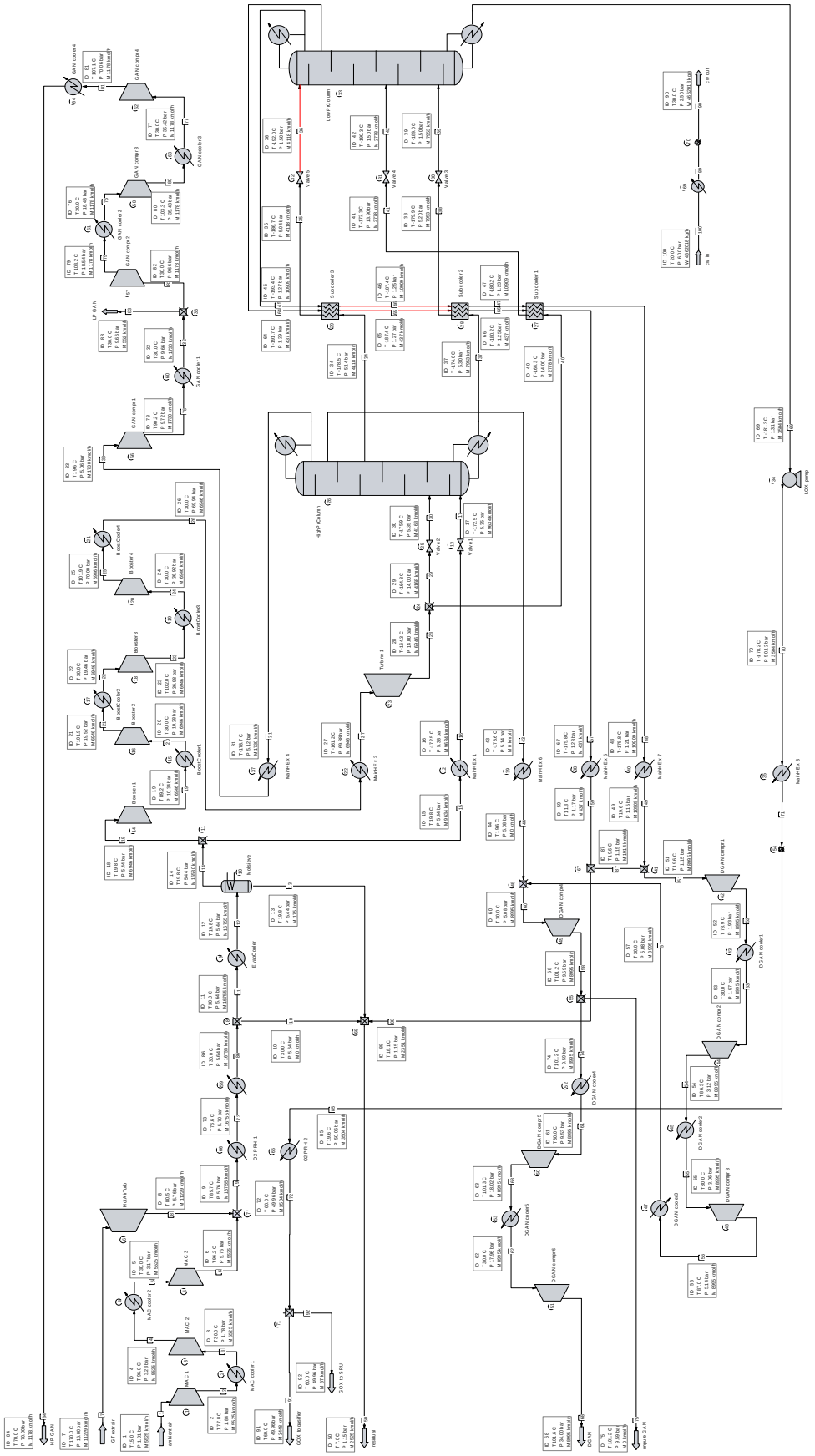

Appendix G3 – CHEMCAD model for an elevated pressure ASU

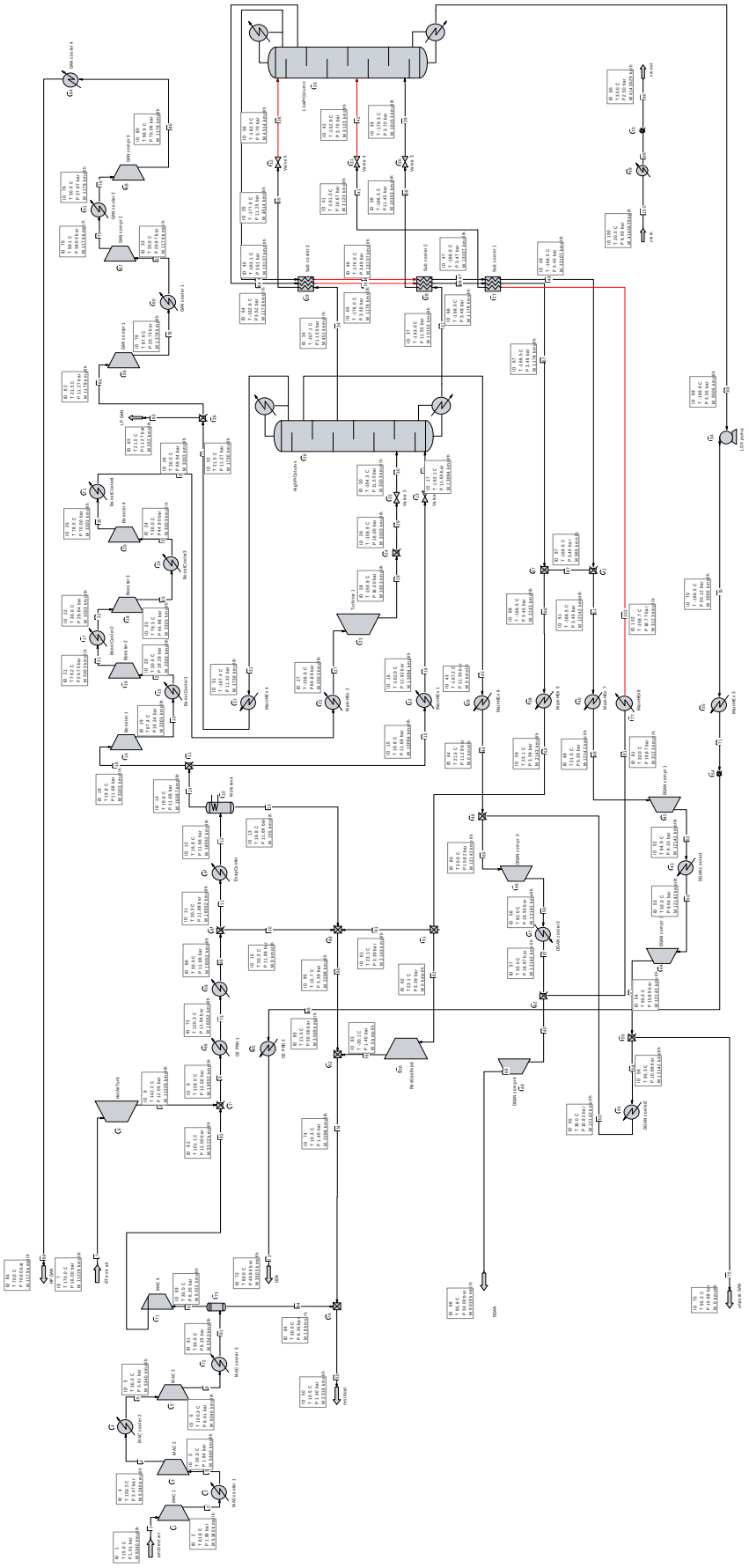

Appendix G4– Auxiliary load distribution for the ASU (effects of ASU integration)

air-int.	$K_{ASU,air}$	DGAN -int.	$K_{ASU,DGAN}$	$K_{ASU,HP\ GAN}$	$K_{ASU,LP\ GAN}$	$P_{ASU,spec.}$	$P_{MAC,spec.}$	$P_{booster,spec.}$	$P_{DGAN-compr..spec.}$	$P_{GAN-compr..spec.}$	$P_{hot\ air\ turbine,spec.}$	$P_{res.\ Gas\ exp.,\ spec.}$	$P_{residual,\ spec.}$
						[kWh/Sm³ GOX]							
LP-ASU													
0	0.00	0.00	0.0	0.30	0.16	0.569	0.335	0.199	0.000	0.036	0.000		-0.001
0	0.00	30.38	1.0	0.30	0.16	0.706	0.335	0.199	0.137	0.036	0.000		-0.001
0	0.00	60.77	2.0	0.30	0.16	0.844	0.335	0.199	0.275	0.036	0.000		-0.001
0	0.00	91.15	3.0	0.30	0.16	0.981	0.335	0.199	0.412	0.036	0.000		-0.001
25	1.19	0.00	0.0	0.30	0.16	0.447	0.251	0.199	0.000	0.036	-0.039		-0.001
25	1.19	30.38	1.0	0.30	0.16	0.584	0.251	0.199	0.137	0.036	-0.039		-0.001
25	1.19	60.77	2.0	0.30	0.16	0.721	0.251	0.199	0.275	0.036	-0.039		-0.001
25	1.19	91.15	3.0	0.30	0.16	0.859	0.251	0.199	0.412	0.036	-0.039		-0.001
50	2.38	0.00	0.0	0.30	0.16	0.324	0.167	0.199	0.000	0.036	-0.077		-0.001
50	2.38	30.39	1.0	0.30	0.16	0.462	0.167	0.199	0.137	0.036	-0.077		-0.001
50	2.38	60.77	2.0	0.30	0.16	0.599	0.167	0.199	0.275	0.036	-0.077		-0.001
50	2.38	91.16	3.0	0.30	0.16	0.737	0.167	0.199	0.412	0.036	-0.077		-0.001
75	3.56	0.00	0.0	0.30	0.16	0.202	0.084	0.199	0.000	0.036	-0.116		-0.001
75	3.56	30.39	1.0	0.30	0.16	0.340	0.084	0.199	0.137	0.036	-0.116		-0.001
75	3.56	60.77	2.0	0.30	0.16	0.477	0.084	0.199	0.275	0.036	-0.116		-0.001
75	3.56	91.16	3.0	0.30	0.16	0.614	0.084	0.199	0.412	0.036	-0.116		-0.001
100	4.75	0.00	0.0	0.30	0.16	0.080	0.000	0.199	0.000	0.036	-0.154		-0.001
100	4.75	30.39	1.0	0.30	0.16	0.217	0.000	0.199	0.137	0.036	-0.154		-0.001
100	4.75	60.77	2.0	0.30	0.16	0.355	0.000	0.199	0.275	0.036	-0.154		-0.001
100	4.75	91.16	3.0	0.30	0.16	0.492	0.000	0.199	0.412	0.036	-0.154		-0.001
EP-ASU													
0	0.00	0.00	0.0	0.30	0.16	0.628	0.547	0.118	0.000	0.022	0.000	-0.058	0.000
0	0.00	25.11	1.0	0.30	0.16	0.739	0.547	0.118	0.092	0.022	0.000	-0.040	0.000
0	0.00	50.23	2.0	0.30	0.16	0.850	0.547	0.118	0.184	0.022	0.000	-0.021	0.000
0	0.00	75.34	3.0	0.30	0.16	0.961	0.547	0.118	0.276	0.022	0.000	-0.002	0.000
25	1.36	0.00	0.0	0.30	0.16	0.478	0.410	0.118	0.000	0.022	-0.014	-0.058	0.000
25	1.36	25.11	1.0	0.30	0.16	0.589	0.410	0.118	0.092	0.022	-0.014	-0.040	0.000
25	1.36	50.23	2.0	0.30	0.16	0.699	0.410	0.118	0.184	0.022	-0.014	-0.021	0.000
25	1.36	75.34	3.0	0.30	0.16	0.810	0.410	0.118	0.276	0.022	-0.014	-0.002	0.000
50	2.72	0.00	0.0	0.30	0.16	0.327	0.273	0.118	0.000	0.022	-0.028	-0.058	0.000
50	2.72	25.11	1.0	0.30	0.16	0.438	0.273	0.118	0.092	0.022	-0.028	-0.040	0.000
50	2.72	50.23	2.0	0.30	0.16	0.549	0.273	0.118	0.184	0.022	-0.028	-0.021	0.000
50	2.72	75.34	3.0	0.30	0.16	0.660	0.273	0.118	0.276	0.022	-0.028	-0.002	0.000
75	4.08	0.00	0.0	0.30	0.16	0.177	0.137	0.118	0.000	0.022	-0.041	-0.058	0.000
75	4.08	25.11	1.0	0.30	0.16	0.288	0.137	0.118	0.092	0.022	-0.041	-0.040	0.000
75	4.08	50.23	2.0	0.30	0.16	0.398	0.137	0.118	0.184	0.022	-0.041	-0.021	0.000
75	4.08	75.34	3.0	0.30	0.16	0.509	0.137	0.118	0.276	0.022	-0.041	-0.002	0.000
100	5.44	0.00	0.0	0.30	0.16	0.026	0.000	0.118	0.000	0.022	-0.055	-0.058	0.000
100	5.44	25.11	1.0	0.30	0.16	0.137	0.000	0.118	0.092	0.022	-0.055	-0.040	0.000
100	5.44	50.23	2.0	0.30	0.16	0.248	0.000	0.118	0.184	0.022	-0.055	-0.021	0.000
100	5.44	75.34	3.0	0.30	0.16	0.359	0.000	0.118	0.276	0.022	-0.055	-0.002	0.000

Appendix G5 – Heat and material balance for the ASU (CC-IGCC / SCGP)

stream ID		0-1-air-6	8-1-air-5	9-1-cw-11	1-0-eg-4	1-2-GOX-1	1-2-GAN-1	1-2-GAN-2	1-3-DGAN-1	1-5-GOX-2	1-9-cw-12
name		ambient air	GT extraction air	cooling water	residual gas	GOX	HP GAN	LP GAN	DGAN	GOX	cooling water
t	°C	15.0	170.0	20.0		60.0	70.0	21.5	95.6	60.0	30.0
p	bar	1.013	16.000	6.000		49.960	70.000	11.265	34.000	49.960	2.500
m	kg/s	42.800	90.000	1,151	17.671	30.807	9.173	4.294	70.350	0.505	1,151
n	kmol/s	1.483	3.119	63.892	0.643	0.958	0.327	0.153	2.505	0.016	63.892
V	Nm^3/h	119,693	251,691		51,908	77,281	26,415	12,365	202,148	1,268	
h	kJ/kg	-100	57	-15,898		20	35	-7	68	20	-15,856
s	J/kgK	124	-238	-9,113		-874	-1,143	-734	-815	-874	-8,974
M	kg/kmol	28.84	28.84	18.00		32.17	28.01	28.01	28.07	32.17	18.00
Σ	mol %	100.00	100.00	100.00	100.00	100.00	100.00	100.00	100.00	100.00	100.00
H2	mol %	0.00	0.00	0.00	0.00	0.00	0.00	0.00	0.00	0.00	0.00
CO	mol %	0.00	0.00	0.00	0.00	0.00	0.00	0.00	0.00	0.00	0.00
CO2	mol %	0.03	0.03	0.00	0.24	0.00	0.00	0.00	0.00	0.00	0.00
N2	mol %	77.32	77.32	0.00	90.33	1.94	99.91	99.91	98.93	1.94	0.00
Ar	mol %	0.91	0.91	0.00	0.65	3.06	0.03	0.03	0.31	3.06	0.00
CH4	mol %	0.00	0.00	0.00	0.00	0.00	0.00	0.00	0.00	0.00	0.00
O2	mol %	20.73	20.74	0.00	1.57	95.00	0.06	0.06	0.76	95.00	0.00
H2O	mol %	1.01	1.01	100.00	7.22	0.00	0.00	0.00	0.00	0.00	100.00
H2S	mol %	0.00	0.00	0.00	0.00	0.00	0.00	0.00	0.00	0.00	0.00
COS	mol %	0.00	0.00	0.00	0.00	0.00	0.00	0.00	0.00	0.00	0.00
CS2	mol %	0.00	0.00	0.00	0.00	0.00	0.00	0.00	0.00	0.00	0.00
SO2	mol %	0.00	0.00	0.00	0.00	0.00	0.00	0.00	0.00	0.00	0.00
S	mol %	0.00	0.00	0.00	0.00	0.00	0.00	0.00	0.00	0.00	0.00
HCN	mol %	0.00	0.00	0.00	0.00	0.00	0.00	0.00	0.00	0.00	0.00
NH3	mol %	0.00	0.00	0.00	0.00	0.00	0.00	0.00	0.00	0.00	0.00
CH3OH	mol %	0.00	0.00	0.00	0.00	0.00	0.00	0.00	0.00	0.00	0.00
Σ	mass %	100.00	100.00	100.00	100.00	100.00	100.00	100.00	100.00	100.00	100.00
H2	mass %	0.00	0.00	0.00	0.00	0.00	0.00	0.00	0.00	0.00	0.00
CO	mass %	0.00	0.00	0.00	0.00	0.00	0.00	0.00	0.00	0.00	0.00
CO2	mass %	0.05	0.05	0.00	0.38	0.00	0.00	0.00	0.00	0.00	0.00
N2	mass %	75.07	75.07	0.00	92.12	1.69	99.89	99.89	98.69	1.69	0.00
Ar	mass %	1.26	1.26	0.00	0.94	3.80	0.05	0.05	0.43	3.80	0.00
CH4	mass %	0.00	0.00	0.00	0.00	0.00	0.00	0.00	0.00	0.00	0.00
O2	mass %	23.00	23.00	0.00	1.83	94.51	0.07	0.07	0.87	94.51	0.00
H2O	mass %	0.63	0.63	100.00	4.73	0.00	0.00	0.00	0.00	0.00	100.00
H2S	mass %	0.00	0.00	0.00	0.00	0.00	0.00	0.00	0.00	0.00	0.00
COS	mass %	0.00	0.00	0.00	0.00	0.00	0.00	0.00	0.00	0.00	0.00
CS2	mass %	0.00	0.00	0.00	0.00	0.00	0.00	0.00	0.00	0.00	0.00
SO2	mass %	0.00	0.00	0.00	0.00	0.00	0.00	0.00	0.00	0.00	0.00
S	mass %	0.00	0.00	0.00	0.00	0.00	0.00	0.00	0.00	0.00	0.00
HCN	mass %	0.00	0.00	0.00	0.00	0.00	0.00	0.00	0.00	0.00	0.00
NH3	mass %	0.00	0.00	0.00	0.00	0.00	0.00	0.00	0.00	0.00	0.00
CH3OH	mass %	0.00	0.00	0.00	0.00	0.00	0.00	0.00	0.00	0.00	0.00

Appendix G6 – Heat and material balance for the ASU (CC-IGCC / Siemens gasifier)

stream ID		0-1-air-6	8-1-air-5	9-1-cw-11	1-0-eg-4	1-2-GOX-1	1-2-GAN-1	1-2-GAN-2	1-3-DGAN-1	1-5-GOX-2	1-9-cw-12
name		ambient air	GT extraction air	cooling water	residual gas	GOX	HP GAN	LP GAN	DGAN	GOX	cooling water
t	°C	15.0	177.5	20.0		60.0	70.0	21.5	95.6	60.0	30.0
p	bar	1.013	16.87	6.000		49.960	70.000	11.265	34.000	49.960	2.500
m	kg/s	41.696	90.000	1,122	20.089	30.787	8.045	4.290	67.974	0.511	1,122
n	kmol/s	1.445	3.119	62.292	0.730	0.957	0.287	0.153	2.421	0.016	62.292
V	Nm³/h	116,605	251,691		58,886	77,223	23,166	12,355	195,384	1,282	
h	kJ/kg	-100	57	-15,898		22	35	-7	68	20	-15,856
s	J/kgK	124	-238	-9,113		-873	-1,144	-734	-818	-874	-8,974
M	kg/kmol	28.84	28.84	18.00		32.16	28.01	28.01	28.06	32.17	18.00
Σ	mol %	100.00	100.00	100.00	100.00	100.00	100.00	100.00	100.00	100.00	100.00
H2	mol %	0.00	0.00	0.00	0.00	0.00	0.00	0.00	0.00	0.00	0.00
CO	mol %	0.00	0.00	0.00	0.00	0.00	0.00	0.00	0.00	0.00	0.00
CO2	mol %	0.03	0.03	0.00	0.21	0.00	0.00	0.00	0.00	0.00	0.00
N2	mol %	77.32	77.32	0.00	91.86	1.94	99.92	99.92	99.12	1.90	0.00
Ar	mol %	0.91	0.91	0.00	0.58	3.06	0.03	0.03	0.28	3.10	0.00
CH4	mol %	0.00	0.00	0.00	0.00	0.00	0.00	0.00	0.00	0.00	0.00
O2	mol %	20.73	20.74	0.00	1.03	95.00	0.05	0.05	0.59	95.00	0.00
H2O	mol %	1.01	1.01	100.00	6.31	0.00	0.00	0.00	0.00	0.00	100.00
H2S	mol %	0.00	0.00	0.00	0.00	0.00	0.00	0.00	0.00	0.00	0.00
COS	mol %	0.00	0.00	0.00	0.00	0.00	0.00	0.00	0.00	0.00	0.00
CS2	mol %	0.00	0.00	0.00	0.00	0.00	0.00	0.00	0.00	0.00	0.00
SO2	mol %	0.00	0.00	0.00	0.00	0.00	0.00	0.00	0.00	0.00	0.00
S	mol %	0.00	0.00	0.00	0.00	0.00	0.00	0.00	0.00	0.00	0.00
HCN	mol %	0.00	0.00	0.00	0.00	0.00	0.00	0.00	0.00	0.00	0.00
NH3	mol %	0.00	0.00	0.00	0.00	0.00	0.00	0.00	0.00	0.00	0.00
CH3OH	mol %	0.00	0.00	0.00	0.00	0.00	0.00	0.00	0.00	0.00	0.00
Σ	mass %	100.00	100.00	100.00	100.00	100.00	100.00	100.00	100.00	100.00	100.00
H2	mass %	0.00	0.00	0.00	0.00	0.00	0.00	0.00	0.00	0.00	0.00
CO	mass %	0.00	0.00	0.00	0.00	0.00	0.00	0.00	0.00	0.00	0.00
CO2	mass %	0.05	0.05	0.00	0.33	0.00	0.00	0.00	0.00	0.00	0.00
N2	mass %	75.07	75.07	0.00	93.49	1.69	99.91	99.91	98.92	1.66	0.00
Ar	mass %	1.26	1.26	0.00	0.85	3.80	0.04	0.04	0.41	3.84	0.00
CH4	mass %	0.00	0.00	0.00	0.00	0.00	0.00	0.00	0.00	0.00	0.00
O2	mass %	23.00	23.00	0.00	1.20	94.51	0.05	0.05	0.68	94.50	0.00
H2O	mass %	0.63	0.63	100.00	4.13	0.00	0.00	0.00	0.00	0.00	100.00
H2S	mass %	0.00	0.00	0.00	0.00	0.00	0.00	0.00	0.00	0.00	0.00
COS	mass %	0.00	0.00	0.00	0.00	0.00	0.00	0.00	0.00	0.00	0.00
CS2	mass %	0.00	0.00	0.00	0.00	0.00	0.00	0.00	0.00	0.00	0.00
SO2	mass %	0.00	0.00	0.00	0.00	0.00	0.00	0.00	0.00	0.00	0.00
S	mass %	0.00	0.00	0.00	0.00	0.00	0.00	0.00	0.00	0.00	0.00
HCN	mass %	0.00	0.00	0.00	0.00	0.00	0.00	0.00	0.00	0.00	0.00
NH3	mass %	0.00	0.00	0.00	0.00	0.00	0.00	0.00	0.00	0.00	0.00
CH3OH	mass %	0.00	0.00	0.00	0.00	0.00	0.00	0.00	0.00	0.00	0.00

Appendix G7 – Heat and material balance for the ASU (CC-IGCC / CoP gasifier)

stream ID		0-1-air-6	8-1-air-5	9-1-cw-11	1-0-eg-4	1-2-GOX-1	1-2-GAN-1	1-2-GAN-2	1-3-DGAN-1	1-5-GOX-2	1-9-cw-12
name		ambient air	GT extraction air	cooling water	residual gas	GOX	HP GAN	LP GAN	DGAN	GOX	cooling water
t	°C	15.0	170.0	20.0		60.0	70.0	21.5	95.6	60.0	30.0
p	bar	1.0	16.0	6.0		50.0	70.0	11.3	34.0	50.0	2.5
m	kg/s	37.761	90.000	948	39.752	29.351	0.567	0.000	57.577	0.514	948
n	kmol/s	1.309	3.119	52.635	1.427	0.912	0.020	0.000	2.053	0.016	52.635
V	Nm³/h	105,601	251,691		115,136	73,575	1,634	0	165,656	1,290	
h	kJ/kg	-100	57	-15,898		20	35	-7	68	20	-15,856
s	J/kgK	124	-238	-9,113		-874	-1,146	-736	-827	-874	-8,974
M	kg/kmol	28.84	28.84	18.00		32.19	28.00	28.00	28.03	32.19	18.00
Σ	mol %	100.00	100.00	100.00	100.00	100.00	100.00	100.00	100.00	100.00	100.00
H2	mol %	0.00	0.00	0.00	0.00	0.00	0.00	0.00	0.00	0.00	0.00
CO	mol %	0.00	0.00	0.00	0.00	0.00	0.00	0.00	0.00	0.00	0.00
CO2	mol %	0.03	0.03	0.00	0.10	0.00	0.00	0.00	0.00	0.00	0.00
N2	mol %	77.32	77.32	0.00	94.08	1.74	100.00	100.00	99.59	1.74	0.00
Ar	mol %	0.91	0.91	0.00	0.43	3.26	0.00	0.00	0.18	3.26	0.00
CH4	mol %	0.00	0.00	0.00	0.00	0.00	0.00	0.00	0.00	0.00	0.00
O2	mol %	20.74	20.74	0.00	2.25	95.00	0.00	0.00	0.22	95.00	0.00
H2O	mol %	1.01	1.01	100.00	3.13	0.00	0.00	0.00	0.00	0.00	100.00
H2S	mol %	0.00	0.00	0.00	0.00	0.00	0.00	0.00	0.00	0.00	0.00
COS	mol %	0.00	0.00	0.00	0.00	0.00	0.00	0.00	0.00	0.00	0.00
CS2	mol %	0.00	0.00	0.00	0.00	0.00	0.00	0.00	0.00	0.00	0.00
SO2	mol %	0.00	0.00	0.00	0.00	0.00	0.00	0.00	0.00	0.00	0.00
S	mol %	0.00	0.00	0.00	0.00	0.00	0.00	0.00	0.00	0.00	0.00
HCN	mol %	0.00	0.00	0.00	0.00	0.00	0.00	0.00	0.00	0.00	0.00
NH3	mol %	0.00	0.00	0.00	0.00	0.00	0.00	0.00	0.00	0.00	0.00
CH3OH	mol %	0.00	0.00	0.00	0.00	0.00	0.00	0.00	0.00	0.00	0.00
Σ	mass %	100.00	100.00	100.00	100.00	100.00	100.00	100.00	100.00	100.00	100.00
H2	mass %	0.00	0.00	0.00	0.00	0.00	0.00	0.00	0.00	0.00	0.00
CO	mass %	0.00	0.00	0.00	0.00	0.00	0.00	0.00	0.00	0.00	0.00
CO2	mass %	0.05	0.05	0.00	0.16	0.00	0.00	0.00	0.00	0.00	0.00
N2	mass %	75.07	75.07	0.00	94.61	1.52	99.99	99.99	99.48	1.52	0.00
Ar	mass %	1.26	1.26	0.00	0.62	4.04	0.01	0.01	0.26	4.04	0.00
CH4	mass %	0.00	0.00	0.00	0.00	0.00	0.00	0.00	0.00	0.00	0.00
O2	mass %	23.00	23.00	0.00	2.59	94.44	0.00	0.00	0.25	94.44	0.00
H2O	mass %	0.63	0.63	100.00	2.02	0.00	0.00	0.00	0.00	0.00	100.00
H2S	mass %	0.00	0.00	0.00	0.00	0.00	0.00	0.00	0.00	0.00	0.00
COS	mass %	0.00	0.00	0.00	0.00	0.00	0.00	0.00	0.00	0.00	0.00
CS2	mass %	0.00	0.00	0.00	0.00	0.00	0.00	0.00	0.00	0.00	0.00
SO2	mass %	0.00	0.00	0.00	0.00	0.00	0.00	0.00	0.00	0.00	0.00
S	mass %	0.00	0.00	0.00	0.00	0.00	0.00	0.00	0.00	0.00	0.00
HCN	mass %	0.00	0.00	0.00	0.00	0.00	0.00	0.00	0.00	0.00	0.00
NH3	mass %	0.00	0.00	0.00	0.00	0.00	0.00	0.00	0.00	0.00	0.00
CH3OH	mass %	0.00	0.00	0.00	0.00	0.00	0.00	0.00	0.00	0.00	0.00

Appendix G8 – Heat and material balance for the ASU (CC-IGCC / GE-R)

stream ID		0-1-air-6	8-1-air-5	9-1-cw-11	1-0-eg-4	1-2-GOX-1	1-3-DGAN-1	1-5-GOX-2	1-9-cw-12
name		ambient air	GT extraction air	cooling water	residual gas	GOX	DGAN	GOX	cooling water
t	°C	15.0	170.0	20.0		60.0	95.6	60.0	30.0
p	bar	1.013	16.000	6.000		69.960	34.000	69.960	2.500
m	kg/s	70.861	90.000	1,222	62.473	38.229	59.600	0.551	1,222
n	kmol/s	2.456	3.119	67.853	2.246	1.187	2.125	0.017	67.853
V	Nm³/h	198,168	251,691		181,204	95,794	171,458	1,379	
h	kJ/kg	-100	57	-15,898		16	68	16	-15,856
s	J/kgK	124	-238	-9,113		-971	-827	-971	-8,974
M	kg/kmol	28.84	28.84	18.00		32.20	28.03	32.20	18.00
Σ	mol %	100.00	100.00	100.00	100.00	100.00	100.00	100.00	100.00
H2	mol %	0.00	0.00	0.00	0.00	0.00	0.00	0.00	0.00
CO	mol %	0.00	0.00	0.00	0.00	0.00	0.00	0.00	0.00
CO2	mol %	0.03	0.03	0.00	0.08	0.00	0.00	0.00	0.00
N2	mol %	77.32	77.32	0.00	96.84	1.64	99.58	1.64	0.00
Ar	mol %	0.91	0.91	0.00	0.24	3.36	0.22	3.36	0.00
CH4	mol %	0.00	0.00	0.00	0.00	0.00	0.00	0.00	0.00
O2	mol %	20.74	20.74	0.00	0.33	95.00	0.20	95.00	0.00
H2O	mol %	1.01	1.01	100.00	2.50	0.00	0.00	0.00	100.00
H2S	mol %	0.00	0.00	0.00	0.00	0.00	0.00	0.00	0.00
COS	mol %	0.00	0.00	0.00	0.00	0.00	0.00	0.00	0.00
CS2	mol %	0.00	0.00	0.00	0.00	0.00	0.00	0.00	0.00
SO2	mol %	0.00	0.00	0.00	0.00	0.00	0.00	0.00	0.00
S	mol %	0.00	0.00	0.00	0.00	0.00	0.00	0.00	0.00
HCN	mol %	0.00	0.00	0.00	0.00	0.00	0.00	0.00	0.00
NH3	mol %	0.00	0.00	0.00	0.00	0.00	0.00	0.00	0.00
CH3OH	mol %	0.00	0.00	0.00	0.00	0.00	0.00	0.00	0.00
Σ	mass %	100.00	100.00	100.00	100.00	100.00	100.00	100.00	100.00
H2	mass %	0.00	0.00	0.00	0.00	0.00	0.00	0.00	0.00
CO	mass %	0.00	0.00	0.00	0.00	0.00	0.00	0.00	0.00
CO2	mass %	0.05	0.05	0.00	0.13	0.00	0.00	0.00	0.00
N2	mass %	75.07	75.07	0.00	97.52	1.43	99.46	1.43	0.00
Ar	mass %	1.26	1.26	0.00	0.35	4.17	0.31	4.17	0.00
CH4	mass %	0.00	0.00	0.00	0.00	0.00	0.00	0.00	0.00
O2	mass %	23.00	23.00	0.00	0.38	94.40	0.23	94.40	0.00
H2O	mass %	0.63	0.63	100.00	1.62	0.00	0.00	0.00	100.00
H2S	mass %	0.00	0.00	0.00	0.00	0.00	0.00	0.00	0.00
COS	mass %	0.00	0.00	0.00	0.00	0.00	0.00	0.00	0.00
CS2	mass %	0.00	0.00	0.00	0.00	0.00	0.00	0.00	0.00
SO2	mass %	0.00	0.00	0.00	0.00	0.00	0.00	0.00	0.00
S	mass %	0.00	0.00	0.00	0.00	0.00	0.00	0.00	0.00
HCN	mass %	0.00	0.00	0.00	0.00	0.00	0.00	0.00	0.00
NH3	mass %	0.00	0.00	0.00	0.00	0.00	0.00	0.00	0.00
CH3OH	mass %	0.00	0.00	0.00	0.00	0.00	0.00	0.00	0.00

Appendix H1 – ChemCad-model for the one-reactor CO-shift cycle

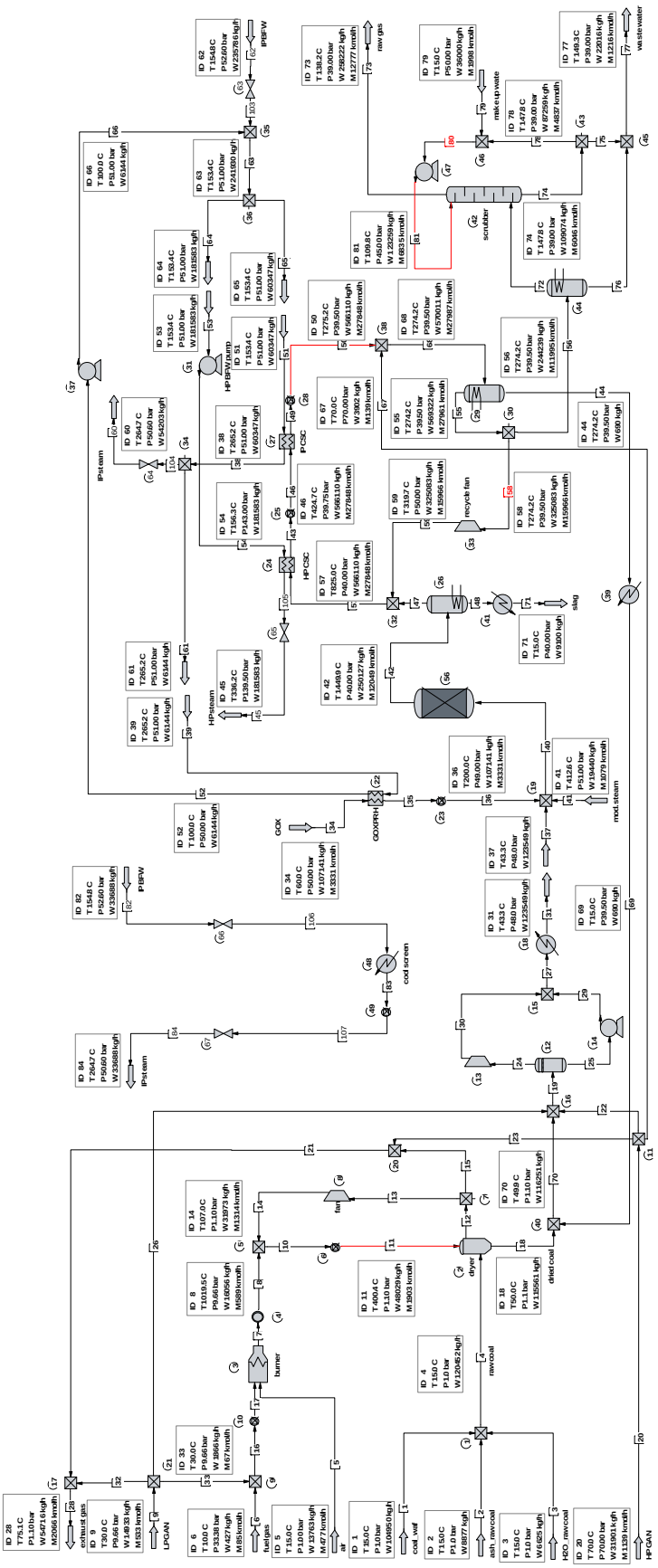

Appendix I1 – OPC-calculation for the CC-IGGC concepts with different gasifiers

The OPC for the CC-IGCC concept with Siemens gasifier (see Table 20) were used as the basis.

First, the OPC assigned to the main sub-systems were converted into specific costs by consideration of the subsequently presented simulation results:

Selected simulation results: CC-IGCC (Siemens gasifier)			
sub-system	*parameter*	*unit*	*value*
Gas generation	Coal heat input (LHV based)	MW	1,038
Gas treatment	Raw gas flow to 1st CO-shift reactor	Sm³/h	581,469
CO_2-compressor	Captured CO_2	t/h	308
Combined Cycle	Gross power output	MW	461
ASU	GOX demand	Sm³/h	77,000

so that the following specific costs were derived:

Specific investment costs: CC-IGCC (Siemens gasifier)		
sub-system	*unit*	*specific investment costs*
Gas generation	€ / kW (coal)	301
Gas treatment	€ / (Sm³ (raw gas) / h)	247
CO_2-compressor	Mio € / (t (CO_2) / h)	0.10
Combined Cycle	€ / kW (gross)	785
ASU	€ / (Sm³ (GOX) / h)	1,135

These specific costs were defined as the. Literature sources were used to estimate the investment costs necessary for the gas generation system of the three other CC-IGCC configurations. Therefore, the following information were used:

- For the gas generation part, a 35 % higher investment cost (per ton of coal capacity) is expected if the SCGP with convective syngas cooler is used instead of the same gasifier with water quench (like the Siemens-type) [21]. Consequently, the specific investment cost for the gas generation part of the CC-IGCC with SCGP adds up to 405 €/kW (coal) -> 301 €/kW (coal) times 1.35
- For the gas generation part, a 23 % lower investment cost (per ton of coal capacity) is expected if a GE-R is used instead of the SCGP [47]. Consequently, the specific investment cost for the gas generation part of the CC-IGCC with GE-R adds up to 312 €/kW (coal) -> 405 €/kW (coal) times 0.77
- For the gas generation part a 21 % lower investment cost (per ton of coal capacity) is expected if a CoP gasifier is used instead of the SCGP [47]. Consequently,

the specific investment cost for the gas generation part of the CC-IGCC with CoP gasifier adds up to 320 €/kW (coal) -> 405 €/kW (coal) times 0.79

The following table summarizes the in this way estimated investment costs for the four different gasifier types.

Investment costs for the gas geneartion part			
Gasifier type	*specific investment cost*	*Coal heat input*	*absolute investment cost*
-	€ / kW (coal)	MW	Mio €
CoP	320	1,049	335
GE-R	312	1,129	352
SCGP	405	1,035	419
Siemens	301	1,038	312

The investment costs for the other sub-systems were estimated using the individual simulation results and the above derived specific investment costs.

The absolute investment costs for the gas treatment part were estimated as follows:

Investment costs for the gas treatment part			
Gasifier type	*specific investment cost*	Raw gas flow to 1st CO-shift reactor	*absolute investment cost*
-	€ / (Sm³ (raw gas) / h)	Sm³ (raw gas) / h	Mio €
CoP	247	555,701	137
GE-R	247	586,233	145
SCGP	247	584,154	144
Siemens	247	581,469	144

The absolute investment costs for the CO_2-compressor were estimated as follows:

Investment costs for the CO_2-compressor			
Gasifier type	*specific investment cost*	Captured CO_2	*absolute investment cost*
-	Mio € / (t (CO_2) / h)	t (CO_2) / h	Mio €
CoP	0.1	296	30
GE-R	0.1	335	34
SCGP	0.1	307	31
Siemens	0.1	308	31

The absolute investment costs for the combined cycle were estimated as follows:

Investment costs for the Combined Cycle			
Gasifier type	*specific investment cost*	Gross power output	*absolute investment cost*
-	€ / kW (gross)	MW	Mio €
CoP	785	467	367
GE-R	785	496	389
SCGP	785	469	368
Siemens	785	461	362

The absolute investment costs for the ASU were estimated as follows:

Investment costs for the ASU			
Gasifier type	*specific investment cost*	GOX demand	*absolute investment cost*
-	€ / (Sm^3 (GOX) / h)	Sm^3 (GOX) / h	Mio €
CoP	1,135	74,000	84
GE-R	1,135	96,000	109
SCGP	1,135	77,000	87
Siemens	1,135	77,000	87

The direct investment costs are the sum of the investment costs for the five afore-mentioned mayor sub-systems. The costs for:

- Infrastructure and utilities,
- Main spare parts and architect engineer,
- And miscellaneous

are so adjusted that they fit to the OPC-fraction as defined in Table 21.

Appendix I2 – Payment dates and shares for the Capital Expenditures

The individual Net Present Value is calculated according to:

$$\mathrm{NPV}_{\text{year n}} = \frac{OPC\ x\ share_{year\ n}}{(1+interest\ rate)^{-year\ n}}.$$

The OPC are taken from Table 21; the interest rate is shown in Table 22. The payment shares and dates are the same as used by Gräbner et al. [21]. The following table summarizes the calculated NPV for the four CC-IGCC concepts with different gasifiers.

Date	Share	Net present value (NPV) in Mio €			
		CoP	GE-R	SCGP	Siemens
Year 0	5 %	64	69	70	62
Year 1	30 %	280	305	308	275
Year 2	40 %	616	672	677	605
Year 3	20 %	508	554	559	499
Year 4	5 %	93	102	102	91
$\Sigma\ \mathrm{NPV}_{\mathrm{CapEx}}$		1,560	1,703	1,716	1,532

Appendix I3 – Calculating the cost of electricity

The annual CapEx are calculated according to:

$$\mathrm{CapEx} = \Sigma\ \mathrm{NPV}_{\mathrm{CapEx}}\ x\ annuity.$$

The annuity is calculated according to:

$$\text{annuity} = \frac{interest\ rate\ x\ (1+\ interest\ rate)^{usefull\ live}}{(1+\ interest\ rate)^{usefull\ live-1}}.$$

The annual Operational Expenditures (OpEx) are calculated considering the data provided in Table 22 according to:

$$\text{annual OpEx} = \text{absolute costs}\ x\ annuity.$$

The following table summarizes the so calculated annual expenditures.

Cost	Unit	CoP	GE-R	SCGP	Siemens
CapEx	Mio €/a	172	188	189	169
Fuel	Mio €/a	72	77	71	71
Miscellaneous	Mio €/a	7	8	7	7
CO_2-transport	Mio €/a	17	20	18	18
CO_2-emission	Mio €/a	9	5	5	5
Labor	Mio €/a	4	4	4	4
maintenance	Mio €/a	12	13	13	11
Taxes/insurances	Mio €/a	6	6	6	6
OpEx	Mio €/a	126	133	124	122
Annual Expenditures	Mio €/a	289	315	308	286

Finally the Cost of Electricity (CoE) is calculated according to:

$$\text{CoE} = \frac{\text{annual expenditures}}{\text{Net power output x annual operating hours}}$$

Appendix I4 – OPC-calculation for the CC-IGGC concepts with different CRRs

The OPC for the concepts with different CRRs in comparison to the reference case (CC-IGCC with Siemens gasifier) are shown in the following table.

Investment cost for	Unit	Refer-ence	Case 2	Case 3	Case 4	Case 5
Gas generation	Mio €	312	312	314	313	315
Gas treatment	Mio €	144	144	144	140	140
CO_2-compressor	Mio €	31	20	20	27	20
Combined Cycle	Mio €	362	362	366	362	364
ASU	Mio €	87	87	88	88	88
Direct invest-ment costs	Mio €	936	925	932	929	927
Infrastructure and utilities	Mio €	162	160	162	161	160
	% of OPC	13	13	13	13	13
Main spare parts and AE	Mio €	37	37	37	37	37
	% of OPC	3	3	3	3	3
Miscellaneous	Mio €	112	111	112	112	111
	% of OPC	9	9	9	9	9
Overall project costs (OPC)	Mio €	1,249	1,234	1,243	1,239	1,235
	€/kW(net)	3,450	3,450	3,450	3,450	3,450

The absolute costs for the gas generation part differ only since there is a slight difference with respect to the coal flow rate between the concepts. The specific costs are identical (301 € / kW (coal)).

Case 4 and case 5 show slightly lower costs for the gas treatment part. This is caused by the saved investment costs for the second CO-shift reactor. The difference between a 2-reactor CO-shift and a 1-reactor CO-shift is amounted by NETL (2007) [46] to 2.6 %.

The absolute costs for the CO_2-compressor differ as a consequence of the different amount of captured CO_2. The specific costs 0.1 Mio € / (t (CO_2) / h) are identic.

The specific costs for other cost factors are identic between the concepts – they are shown in Appendix I1.

Appendix I5 - Reference costs for a state of the art NG CCPP

Project Cost Summary	Reference Cost	Estimated Cost	
Power Plant:			
I Specialized Equipment	109.719.000	126.177.000	EUR
II Other Equipment	7.286.000	8.379.000	EUR
III Civil	15.301.000	22.019.000	EUR
IV Mechanical	16.788.000	25.450.000	EUR
V Electrical Assembly & Wiring	3.240.000	4.904.000	EUR
VI Buildings & Structures	5.924.000	8.605.000	EUR
VII Engineering & Plant Startup	11.062.000	11.138.000	EUR
Gasification Plant	NA	NA	
Desalination Plant	NA	NA	
CO2 Capture Plant	NA	NA	
Subtotal -Contractor's Internal Cost	169.320.000	206.672.000	EUR
VIII Contractor's Soft & Miscellaneous Costs	35.690.000	47.795.000	EUR
Contractor's Price	205.010.000	254.467.000	EUR
IX Owner's Soft & Miscellaneous Costs	18.451.000	22.902.000	EUR
Total -Owner's Cost (0,7 EUR per US Dollar)	223.461.000	277.369.000	EUR
Nameplate Net Plant Output	405	405	MW
Cost per kW -Contractor's	505,7	627,7	EUR per kW
Cost per kW -Owner's	551,2	684,2	EUR per kW
* Cost estimates as of February 2012.			
** Land cost, utility connection cost, and spare parts costs are zero.			
The user may want to edit those inputs for better cost estimates.			

Appendix I6 – CHEMCAD flow sheet for the CO-shift for a GCC concept with Siemens gasifier

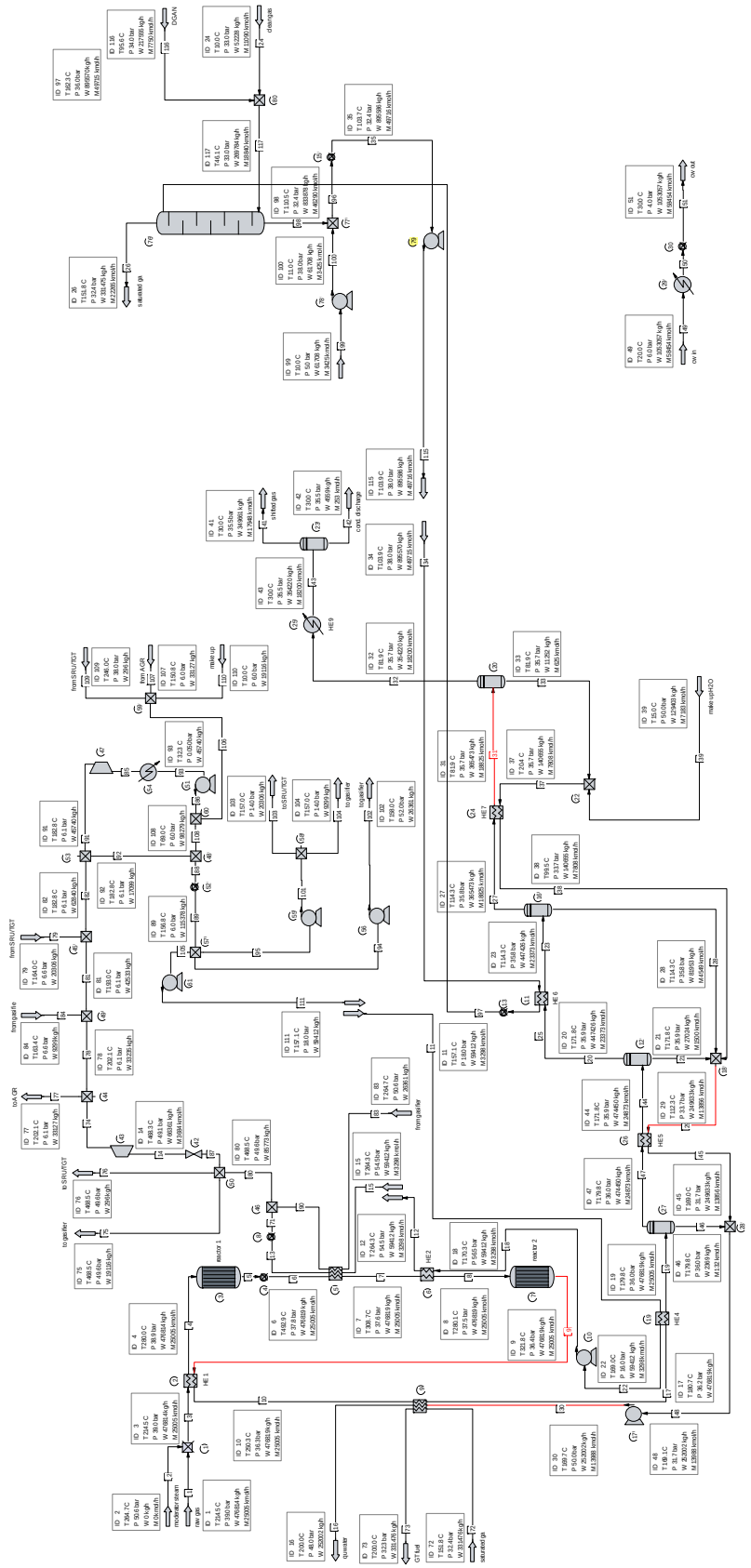

References

[1] BAEHR, H., KABELAC, S. (2009). Thermodynamik. Grundlagen und technische Anwendungen. Springer. Berlin, Heidelberg. ISBN/DOI: 3642005551.

[2] BOHMN, M., HERZOG, H., PARSONS, J., SEKAR, R. (2007). Capture-ready coal plants—Options, technologies and economics. International Journal of Greenhouse Gas Control, 1, 1, 113–120.

[3] BP (2011). BP Energy Outlokk 2030. http://www.bp.com/liveassets/bp_internet/globalbp/globalbp_uk_english/reports_and_publications/statistical_energy_review_2008/STAGING/local_assets/2010_downloads/2030_energy_outlook_booklet.pdf. last checked: 2011-04-04.

[4] CARBO, M., JANSEN, D., DIJKSTRA, J., VAN BUIJTENEN, J., VERKOOIJEN, A. (2009). Pre-combustion decarbonisation in IGCC: Gas turbine operating window at variable carbon capture ratios. Energy Procedia, 1, 1, 669–673.

[5] CHANG; ROUSSEAU; FERRELL (1987). Vapor/Liquid Equilibria of Constituents from Coal Gasification in Refrigerated Methanol.

[6] CHEN, C., RUBIN, E. (2009). CO2 control technology effects on IGCC plant performance and cost. Energy Policy, 37, 915–924.

[7] CHIESA, P., CONSONNI, S., KREUTZ, T. (2005). Co-production of hydrogen, electricity and CO from coal with commercially ready technology. Part A: Performance and emissions. International Journal of Hydrogen Energy, 30, 7, 747–767.

[8] CORMOS, C.-C. (2010). Evaluation of energy integration aspects for IGCC-based hydrogen and electricity co-production with carbon capture and storage. International Journal of Hydrogen Energy, 35, 14, 7485–7497.

[9] DESCAMPS, C., BOUALLOU, C., KANNICHE, M. (2008). Efficiency of an Integrated Gasification Combined Cycle (IGCC) power plant including CO2 removal. Energy, 33, 6, 874–881.

[10] EMUN, F., GADALLA, M., MAJOZI, T., BOER, D. (2010). Integrated gasification combined cycle (IGCC) process simulation and optimization☆. Computers & Chemical Engineering, 34, 3, 331–338.

[11] EURLINGS, J., PLOEG, J. (1999). Process Performance of the SCGP at Buggenum IGCC. Gasification Technologies Conference. San Francisco.

[12] EUROPEAN ENERGY EXCHANGE (2012). EU Emission Allowances. http://www.eex.com/de/Downloads/Marktdaten/Emissionsberechtigungen%20-%20EEX. last checked: 2012-05-14.

[13] FARINA, G., BRESSAN, L. (1999). Optimizing IGCC design. Foster Wheeler Review, no volume, 17–21.

[14] FRANK, P. (2003). Sulphur Tolerant Shift Catalyst - Sulphur Tolerant Shift Catalyst - Dealing with the Bottom of the Barrel Problem Problem.

[15] FRATZSCHER, W., MICHALEK, K., BRODJANSKIJ, V. (1986). Exergie: Theorie und Anwendung. VEB Deutscher Verlag für Grundstoffindustrie. Leipzig. ISBN/DOI: 3-342-00091-0.

[16] FREY, H., ZHU, Y. (2006). Improved System Integration for Integrated Gasification Combined Cycle (IGCC) Systems. Environmental Science & Technology, 40, 5, 1693–1699.

[17] GEOSITS, R., SCHMOE, L. (2005). IGCC - The challanges of integration. ASME Turbo Expo 2005: Power for Land, Sea and Air. Reno-Tahoe, Nevada, USA.

[18] GMEHLING, J., BREHM, A. (1996). Lehrbuch der technischen Chemie. Grundoperationen. Wiley-Vch Verlag Gmbh. ISBN/DOI: 3-527-30851-2.

[19] GRÄBNER, M. (2012). Modeling-based evaluation of coal gasification processes for high-ash coal. Dissertation. TU Bergakademie Freiberg. Freiberg.

[20] GRÄBNER, M., MORSTEIN, O. von, RAPPOLD, D., GÜNSTER, W., BEYSEL, G., MEYER, B. (2010). Constructability study on a German reference IGCC power plant with and without CO2-capture for hard coal and lignite. Energy Conversion and Management, 51, 11, 2179–2187.

[21] GRÄBNER, M.; OGRISECK, S.; OGRISECK, K.; KUSKE, E.; ABRAHAM, R.; GÜNSTER, W.; METZ, T.; KOSS, U.; JENSEN, S.; RIEGER, M.; WOLF, K.-J.; RENZENBRINK, W.; RAINER, H.; FOLKE, C.; KOROBOV, D.; BEYSEL, G.; ALEXEEV, A.; HANNEMANN, F.; KARKOWSKI, G.; HIGMAN, C.; VON MORSTEIN, O.; RAPPOLD, D.; GRAEBER, C.; RIEDL, K.; KITTEL, J.; HEIL, S.; ROST, M.; BRUNNHUBER, C.; ULBRICHT, I.; WORLITZ, F.; ROTTENBACH, T.; RAUCHFUß, H.; ROCHNER, I.; BAUERSFELD, D.; TROMPELT, M.; GUHL, S.; BRENNER, S.; MEYER, B. (2008). Schlussbericht "Verbundvorhaben COORIVA: Baubarkeitsuntersuchungen für ein IGCC-Referenzkraftwerk ab 2015 für Braun- und Steinkohle mit CO2-Rückhaltung". http://edok01.tib.uni-hannover.de/edoks/e01fb09/60863980X.pdf. last checked: 2011-04-29.

[22] HIGMAN, C., VAN DER BURGT, M. (2003). Gasification. Elsevier/Gulf Professional Pub. Boston, Mass. ISBN/DOI: 0-7506-7707-4.

[23] HOCHGESANG, G. (1970). Rectisol and Purisol - Efficient Acid Gas Removal for High Pressure Hydrogen and Syngas Production. European and Japanes Chemical Industries Symposium, Vol. 62, No. 7.

[24] HOLT, N. (2000). Evaluation of Innovative Fossil Fuel Power Plants with CO2 Removal. EPRI, Palo Alto, CA, U. S. Department of Energy — Office of Fossil Energy, Germantown, MD and U. S. Departmentof Energy/NETL, Pittsburgh, PA: 2000. 1000316.

[25] HOLT, N. (2002). Updated Cost and Performance Estimates for Fossil Fuel Power Plants with CO2-Removal. Electric Power Research Institute, Interim Report.

[26] HOLT, N. (2006). Gasification Technology Status. EPRI, Report ID: 1012224.

[27] HORLOCK, J., WATSON, D., JONES, T. (2001). Limitations on Gas Turbine Performance Imposed by Large Turbine Cooling Flows. Journal of Engineering for Gas Turbines and Power, 123, 3, 487.

[28] HORNICK, M., MCDANIEL, J. (2002). Tampa Electric Polk Power Station Integrated Gasification Combined Cycle Project – Final technical report. Work performed under cooperative agreement DE-FC-21-91MC27363 for the U.S. Department of Energy, Office of Fossil Energy, National Energy Technology Laboratory, Morgantown, West Virginia.

[29] HUANG, Y., REZVANI, S., MCILVEEN-WRIGHT, D., MINCHENER, A. (2008). Techno-economic study of CO2 capture and storage in coal fired oxygen fed entrained flow IGCC power plants. Fuel Processing Technology, 89.

[30] IEA (2010). World Energy Outlook 2010. http://www.worldenergyoutlook.org/docs/weo2010/weo2010_london_nov9.pdf. last checked: 2011-04-04.

[31] IEA GREENHOUSE GAS R&D PROGRAMME (2003). Potential for improvement in gasification combined cycle power generation with CO2 capture.

[32] INTERNATIONAL ORGANIZATION FOR STANDARDIZATION (2009). Gas Turbines - Acceptance Tests, 2314:2009.

[33] JONSSON, M.; BOLLAND, O.; BÜCKER, D.; ROST, M. (2005). Gas turbine cooling model for evaluation of novel cycles.

[34] KATZER, J. (2007). The future of coal-Options for a carbon-constrained world. Massachusetts Institute of Technology. Boston, MA. ISBN/DOI: 978-0-615-14092-6.

[35] KIM, Y., LEE, J., KIM, T., SOHN, J., JOO, Y. (2010). Performance analysis of a syngas-fed gas turbine considering the operating limitations of its components. Applied Energy, 87, 5, 1602–1611.

[36] KLARA, J., PLUNKETT, J. (2010). The potential of advanced technologies to reduce carbon capture costs in future IGCC power plants. International Journal of Greenhouse Gas Control, 4, 2, 112–118.

[37] KLOSTER, R. (1999). Thermodynamische Analyse und Optimierung von Gas-/Dampfturbinen-Kombi-Kraftwerken mit integrierter Kohlevergasung. VDI. Düsseldorf. ISBN/DOI: 3-18-340906-2.

[38] KOHL, A., NIELSEN, R. (1997). Gas purification. Gulf Pub. Houston, Tex. ISBN/DOI: 0884152200.

[39] KUNZE, C., SPLIETHOFF, H. (2010). Modelling of an IGCC plant with carbon capture for 2020. Fuel Processing Technology, 91, 8, 934–941.

[40] LECHNER, C. (2010). Stationäre Gasturbinen. Springer. Berlin, Heidelberg. ISBN/DOI: 3540927875.

[41] LEE, C., LEE, S., YUN, Y. (2007). Effect of air separation unit integration on integrated gasification combined cycle performance and NOx emission characteristics. Korean Journal of Chemical Engineering, 24, No. 2, 368–373.

[42] LEE, J., KIM, Y., CHA, K., KIM, T., SOHN, J., JOO, Y. (2009). Influence of system integration options on the performance of an integrated gasification combined cycle power plant. Applied Energy, 86, 9, 1788–1796.

[43] MARTELLI, E., KREUTZ, T., CONSONNI, S. (2009). Comparison of coal IGCC with and without CO2 capture and storage: Shell gasification with standard vs. partial water quench. Energy Procedia, 1, 1, 607–614.

[44] MAURSTAD, O. (2005). An Overview of Coal based Integrated Gasification Combined Cycle (IGCC) Technology. http://lfee.mit.edu/publications, Publication No. LFEE 2005-002 WP.

[45] NATIONAL ENERGY TECHNOLOGY LABORATORY (NETL) (2002). Evaluation of Fossil Fuel Power Plants with CO2 Recovery. Contract No. DE-AM26-99FT40465 between the National Energy Technology Center (NETL) and Concurrent Technologies Corporation (CTC).

[46] NATIONAL ENERGY TECHNOLOGY LABORATORY (NETL) (2007). Cost and Performance Baseline for Fossil Energy Plants, Volume 1: Bituminous Coal and Natural Gas to Electricity, Final Report. DOE/NETL-2007/1281.

[47] NATIONAL ENERGY TECHNOLOGY LABORATORY (NETL) (2010). Cost and performance baseline for fossil energy plants. Volume 1: Bituminous coal and natural gas to electricity.

[48] NEWMAN, S. (1985). Acid and sour gas treating processes. Latest data and methods for designing and operating today's gas treating facilities. Gulf Pub. Co. Houston. ISBN/DOI: 0872018393.

[49] ORDORICA-GARCIA, G., DOUGLAS, P., CROISET, E., ZHENG, L. (2006). Technoeconomic evaluation of IGCC power plants for CO2 avoidance. Energy Conversion and Management, 47, 15-16, 2250–2259.

[50] PARDEMANN, R. (2006). Modellierung des Betriebsverhaltens von fortschrittlichen Gasturbinen für IGCC- und Polygeneration-Kraftwerksanwendungen. Diplomarbeit. TU Bergakademie Freiberg.

[51] PRELIPCEANU, A.; KABALLO, H.-P.; KERESTECIOGLU, U. (2007). Linde Rectisol Wash Process. 2nd International Freiberg Conference on IGCC & XtL Technologies.

[52] RUBIN, E., CHEN, C., RAO, A. (2007). Cost and performance of fossil fuel power plants with CO2 capture and storage. Energy Policy, 35, 9, 4444–4454.

[53] SCHINGNITZ, M.; GÖRZ, J. (1998). Die Einstellung thermodynamischer Gleichgewichte bei der Vergasung von Rest- und Abfallstoffen durch die Noell-Flugstromvergasungstechnologie. DECHEMA Jahrestagung, 27.05.1998.

[54] SCHMALFELD, J. (2008). Die Veredlung und Umwandlung von Kohle. Technologien und Projekte 1970 bis 2000 in Deutschland. DGMK. Hamburg. ISBN/DOI: 978-3-936418-88-0.

[55] SCHREINER, B. Der Claus-Prozess. Chemie in unserer Zeit, 2008, 42, 378–392.

[56] SIEMENS AG. Siemens Gas Turbine SGT5-4000F. http://www.energy.siemens.com/hq/pool/hq/power-generation/gas-turbines/SGT5-4000F/downloads/SGT5-4000F_Brochure_2008.pdf. last checked: 2012-01-04.

[57] SMITH, I. (2009). Gas turbine technology for syngas/hydrogen in coal-based IGCC. IEA Clean Coal Centre. London. ISBN/DOI: 978-92-9029-475-7.

[58] SPLIETHOFF, H. (2010). Power generation from solid fuels. page 611-612. Springer. Heidelberg, New York. ISBN/DOI: 978-3-642-02855-7.

[59] TRAUPEL, W. (2001). Thermische Turbomaschinen. Springer. Berlin [u.a.]. ISBN/DOI: 3-540-67377-6.

[60] ULLMANN. Ullmann's encyclopedia of industrial chemistry. Gas Production (2003). Wiley-VCH. Weinheim, Germany. ISBN/DOI: 978-3-527-30673-2.

[61] VDI (2006). VDI-Wärmeatlas. Springer. Berlin ;, Heidelberg, New York. ISBN/DOI: 978-3-540-25504-8.

[62] VOß, A.; WISSEL, S.; RATH-NAGEL, S.; BLESL, M.; FAHL, U. (2008). Stromerzeugungskosten im Vergleich. http://www.ier.uni-stuttgart.de/publikationen/arbeitsberichte/Arbeitsbericht_04.pdf. last checked: 2012-05-25.

[63] WABASH. Wabash River Coal Gasification Repowering Project - Final technical report. Work performed under cooperative agreement DE-FC-21-92MC29210 for the U.S. Department of Energy, Office of Fossil Energy, National Energy Technology Laboratory, Morgantown, West Virginia (2000).

[64] WANG, Y., QIU, P., WU, S., LI, Z. (2010). Performance of an Integrated Gasification Combined Cycle System with Different System Integration Options. Energy & Fuels, 24, 3, 1925–1930.

[65] WEIß, S., MILITZER, K.-E., GRAMLICH, K. (2001). Thermische Verfahrenstechnik. Mit 54 Tabellen. [Wiley-VCH]. [Weinheim]. ISBN/DOI: 3-342-00664-1.

[66] ZUIKER, J. GE Gasification Technology Update. http://www.gasification.org/uploads/downloads/Conferences/2010/35ZUIKER.pdf. last checked: 2012-05-25.